Dissertation

Submitted to the

Combined Faculty of Natural Sciences and Mathematics

Heidelberg University, Germany

for the degree of

Doctor of Natural Sciences (Dr. rer. nat.)

Presented by

M. Sc. Benhua Wang

from Henan, China

Oral examination: September 11th, 2018

Fingerprinting Chemical Analytes with Water-Soluble Conjugated Polymer-Based Fluorescent Sensor Arrays

Referees: Prof. Dr. Uwe H. F. Bunz

Prof. Dr. A. Stephen K. Hashmi

Acknowledgement

First and foremost, I would like to express the deepest gratitude to my enthusiastic supervisor, Prof. Dr. Uwe H. F. Bunz, not only for his unwavering support and scientific mentorship throughout my research and his convincingly conveyed a spirit of adventure and creativity, but also for giving me so many wonderful opportunities. I wish to extend my sincere thanks to Dr. Kai Seehafer for his kind help and encouragement during the time of my research. His expert, sincere and valuable discussions and pieces of advice contributed to this dissertation a lot. I would also like to thank Prof. Dr. A. Stephen K. Hashmi for kindly accepting to be my second reviewer.

I take this opportunity to thank my collaborators, Prof. Dr. Andreas Herrmann (Zernike Institute for Advanced Materials, University of Groningen, Netherlands) and his Ph.D. student Chao Ma, for their kind supports on the project of amino acids discrimination, especially for the preparation of supercharged GFPs and fruitful discussions.

I also thank Shaoxiong Zhang (Fujian Agriculture and Forestry University) and Haoran Chen (Ruprecht-Karls-Universitat Heidelberg) for their assistance with tea sample collection and technical advice on the project of tea sensing.

I would like to thank Kerstin Windisch, Kerstin Brödner, Olena Tverskoy and Holger Lambert for their kind help and effective organization to provide us a smooth working circumstance. I would also like to thank all employees of the OCI for their kind help in measurements, like MS analysis, NMR spectra and elemental analysis, and also administration departments.

I would like to thank my intelligent colleagues, Jinsong Han, Dr. Markus Bender, Soh Kushida, Emanuel Smarsly, Andrea Uptmoor, Maximilian Bojanowski and Dr. Allan Bastos for their kind help and fruitful discussions during my research study. I especially thank Dr. Allan Bastos and Maximilian Bojanowski for their carefully check this dissertation. And Sebastian Hahn deserves special thanks for the many beautiful pictures in the paper. I also want to extend my thanks to the whole working group members for the friendly cooperation and general guidance that build the foundation for finishing this dissertation. I am really appreciated to work with you.

I would especially like to thank my dear friends and also colleagues, Jinsong Han, Wei Huang, Gaozhan Xie, Hao Zhang and Zeyu Li who have walked alongside me during these years. Without your company and encouragement, the road would have been a lonely place.

I am very grateful to the CSC (Chinese Scholarship Council) for their financial support of my Ph.D. research.

Finally and without hesitation, I would like to thank my beloved parents and the many friends who have always been there for me no matter where I am. Thank you for being so supportive and understanding on this journey.

Abstract

Over the past decades, conjugated polymers (CPs) have been applied to electronic and photonic devices, expanding this field in material chemistry. One recent area of interest on CPs comprises their application in the development of chemical sensors. That considered, the focus of this work was on the construction of water-soluble conjugated polymer-based chemical tongues and their application in sensing.

Initially, four water-soluble poly(*para*-phenyleneethynylene)s (PPEs) were prepared, two of which reported for the first time on the basis of this work. The two novel PPEs are negatively charged, posses benzylic side chains, and react sensitively towards 2,4-dinitrotoluene and 2,4,6-trinitrotoluene. Twelve different nitro-aromatics were successfully discriminated by a small sensor array consisting of either the two novel PPEs or additional two neutral PPEs, using linear discriminant analysis to treat the data.

A sensor array based on a combination of positively charged water-soluble PPEs, or green fluorescent protein (GFP), and three metal ions (Fe^{2+}, Co^{2+}, and Cu^{2+}) at different pH values was also reported for the first time. The array discriminates all of the 20 natural amino acids in water. The sensitivity of the array was dramatically improved by addition of further sensor elements, and an optimized eight-member sensor array that discriminates all of the 20 amino acids with 100% accuracy was created. The results show great coherence upon grouping the amino acids according to their type: hydrophobic, polar and aromatic.

Finally, two types of hypothesis-free sensor arrays, consisting of either three cationic PPEs or the same PPEs complexed with cucurbituril[8] (CB[8]) have been constructed. The PPE-CB[8] array discriminates tea-based amino acids and methylxanthine alkaloids (caffeine, theophylline and theobromine) through a displacement mechanism, while for the PPE-alone array, only caffeine, theobromine and theophylline elicited relevant fluorescence response. Both the PPE and PPE/CB[8] arrays effectivelly generated discriminating patterns for teas on the basis of differential fluorescence quenching, and allowed the differentiation of teas by brand, price, quality grades, and geographic origins.

All together, the results herein obtained represent a significant contribution to the development of the field of chemical sensors based on CPs.

Zusammenfassung

In den letzten Jahren wurden konjugierten Polymere (CPs) in organisch-elektronischen und photoelektronischen Bauteilen verwendet, einhergehend mit einem rapiden Wachstum der Materialwissenschaften. Ein neuer Interessebereich CPs umfasst ihre Anwendung in der Entwicklung chemischer Sensoren. In diesem Zusammenhang liegt der Fokus dieser Doktorarbeit auf der Entwicklung konjugierter, wasserlöslicher, Polymer-basierter, chemischer Zungen und ihre Anwendungen in der Sensorik.

Vier wasserlösliche Poly(*para*-phenylenethynylene) wurden hergestellt, von denen zwei zum ersten Mal im Rahmen dieser Arbeit veröffentlicht wurden. Diese beiden sind negativ geladen, haben benzylische Seitenketten und wechselwirken selektiv mit 2,4-Dinitrotoluol und 2,4,6-Trinitrotoluol. Zwölf verschiedene Nitroaromaten wurden erfolgreich durch ein kleines Sensorfeld, das entweder aus den zwei neuen PPEs oder zusätzlich zwei weiteren, neutralen PPEs bestand und nach der Anwendung linearer Diskriminanzanalyse unterschieden.

Ein Sensorfeld, dass auf einer Kombination aus positiv geladenem wasserlöslichem PPEs oder grün fluoreszierendem Protein (GFP) und drei Metallionen (Fe^{2+}, Co^{2+} und Cu^{2+}) bei verschiedenen pH-Werten Bestand, wurde ebenfalls im Rahmen dieser Arbeit veröffentlicht. Eine Diskriminierung aller 20 natürlichen Aminosäuren in Wasser ist mit dem einfachen Sensorfeld möglich. Durch das Hinzufügen weiterer Sensorelemente zum Feld konnten eine signifikante Verbesserung erhalten werden. Das optimierte achtgliedrige Sensorfeld kann alle 20 Aminosäuren mit einer 100% Genauigkeit unterscheiden. Die Ergebnisse werden nach Aminosäuretyp gruppiert: hydrophob, polar und aromatisch.

Schließlich wurden zwei Arten hypothesenfreier Sensorfelder aufgebaut, die entweder aus drei kationischen PPEs oder denselben drei - mit Cucurbituril[8] (CB[8]) komplexierten - PPEs bestehen. Das PPE-CB[8]-Array unterscheidet teebasierte Aminosäuren und Koffein-Typen durch eine Verdrängungsmechanismus. Beim einfachen PPE-basierten Feld haben nur Koffein, Theobromin und Theophyllin eine Fluoreszenzantwort ausgelöst. Sowohl das PPE- als auch das PPE/CB[8]-Feld erzeugen auf der Basis differentieller Fluoreszenzlöschung außerordentlich empfindliche Muster. Die zwei untersuchten chemischen Zungen erlauben eine Unterscheidung der Tees nach Marke, Preis, Qualität und geografischer Herkunft.

Insgesamt repräsentieren die hier erreichten Ergebnisse einen signifikanten Beitrag zur Entwicklung des Gebietes der chemischen Sensoren, welche auf CPs basieren.

Publications

Benhua Wang[†], Jinsong Han[†], Markus Bender, Sebastian Hahn, Kai Seehafer and Uwe H. F. Bunz, Poly(*para*-phenyleneethynylene)-Sensor Arrays Discriminate 22 Different Teas. *ACS sensors*, **2018**, 3, 504-511.

Benhua Wang, Jinsong Han, N. Maximilian Bojanowski, Markus Bender, Chao Ma, Kai Seehafer, Andreas Herrmann and Uwe H. F. Bunz, An optimized sensor array identifies all natural amino acids, *ACS sensors*, **2018**.

Benhua Wang[†], Jinsong Han[†], Markus Bender, Kai Seehafer and Uwe H. F. Bunz, Array-Based Sensing of Explosives by Water-Soluble Poly(*para*-phenylene-ethynylene)s. *Macromolecules*, **2017**, 50, 4126-4131.

Benhua Wang[†], Jinsong Han[†], Chao Ma, Markus Bender, Kai Seehafer, Andreas Herrmann and Uwe H. F. Bunz, A Simple Optoelectronic Tongue Discriminates Amino Acids. *Chemistry-A European Journal*, **2017**, 23, 12471-12474.

Jinsong Han[†], Haoran Cheng[†], Benhua Wang[†], Markus Braun, Xiaobo Fan, Markus Bender, Wei Huang, Cornelius Domhan, Walter Mier, Thomas Lindner, Kai Seehafer, Michael Wink and Uwe H. F. Bunz, Polymer/Peptide Complex-Based Sensor Array Discriminates Bacteria in Urine. *Angewandte Chemie International Edition*, **2017**, 56, 15246-15251. ([†]equal contribution)

Jinsong Han[†], Benhua Wang[†], Markus Bender, Soh Kushida, Kai Seehafer and Uwe H. F. Bunz, Poly(aryleneethynylene) tongue that identifies nonsteroidal anti-inflammatory drugs in water: A test case for combating counterfeit drugs. *ACS Applied Materials & Interfaces.* **2017**, 9, 790-797. ([†]equal contribution)

Jinsong Han[†], Benhua Wang[†], Markus Bender, Jessica Pfisterer, Wei Huang, Kai Seehafer, Mahdieh Yazdani, Vincent M. Rotello, Caren M. Rotello and Uwe H. F. Bunz, Fingerprinting antibiotics with PAE-based fluorescent sensor arrays. *Polymer Chemistry*. **2017**, 8, 2723-2732. ([†]equal contribution)

Jinsong Han[†], Benhua Wang[†], Markus Bender, Kai Seehafer and Uwe H. F. Bunz, Water-soluble poly(*p*-aryleneethynylene)s: A sensor array discriminates aromatic carboxylic acids. *ACS Applied Materials & Interfaces.* **2016**, 8, 20415-20421. ([†]equal contribution)

Jinsong Han, Benhua Wang, Markus Bender, Kai Seehafer and Uwe H. F. Bunz, Poly(*p*-phenyleneethynylene)-based tongues discriminate fruit juices. *Analyst.* **2017**, 142, 537-543.

Jinsong Han, Chao Ma, Benhua Wang, Markus Bender, Maximilian Bojanowski, Marcel Hergert, Kai Seehafer, Andreas Herrmann and Uwe H. F. Bunz, A hypothesis-free sensor array discriminates whiskies for brand, age and taste. *Chem (Cell Press)*. **2017**, 2, 817-824.

Abbreviations

ADP	adenosine diphosphate
AIDS	acquired immune deficiency syndrome
AMP	adenosine monophosphate
AO	acridine orange
ATP	adenosine triphosphate
CB[n]	cucurbit[n]uril CDNB
CDNB	2,4-dinitrochlorobenzene
CPEs	conjugated polyelectrolytes
CPs	conjugated polymers
CV	cyclic voltammetry
DNA	deoxyribonucleic acid
DNB	dinitrobenzene
DNMB	2,4-dinitroanisole
DNT	dinitrotoluene
FRET	fluorescence resonance energy transfer
GC-MS	gas chromatography-mass spectrometry
GFP	green fluorescent protein
GPC	gel permeation chromatography
HCA	hierarchical cluster analysis
HCPs	hyperbranched conjugated polymers
HPLC	high-performance liquid chromatography
HR-MS	high resolution mass spectra
ICT	intermolecular charge transfer
IDA	indicator displacement assay
LDA	linear discriminant analysis
MANOVA	multivariate analysis of variance
MS	mass spectrometry
NACs	nitroaromatic compounds
NA	nitroaniline
NB	nitrobenzene
NIR	near-infrared spectroscopy
NMR	Nuclear magnetic resonance
NP	nanoparticle
ONCB	2-nitrochlorobenzene
PA	polyacetylene
PANI	polyaniline

PCA	principal component analysis
PDI	polydispersities
PET	photo-induced electron transfer
PF	poly(fluorene)
PFP	polyfluorene-1,4-phenylene
PNP	p-nitrophenol
PPE	poly(*para*-phenyleneethynylene)
PPP	poly(*para*-phenylene)
PPV	poly(*para*-phenylenevinylene)
PPy	polypyrrole
PT	polythiophene
RT	room temperature
SDBS	sodium dodecylbenzenesulfonate
SDS	sodium dodecylsulfate
SERS	surface-enhanced Raman spectroscopy
SW	swallowtail (oligoethyleneglycol side-chains)
TLC	thin layer chromatography
TMS	Trimethylsilyl
TNT	2,4,6-trinitrotoluene
UV-Vis	ultraviolet-visible spectrophotometry
XRD	X-ray diffraction
calcd.	calculated
d	days
h	hours
min	minutes
ppm	parts per million
Φ	fluorescence quantum yields
τ	fluorescence lifetime
δ	chemical shift

Table of Contents

Abstract III

Publications V

Abbreviations VII

Table of Contents IX

Chapter 1. Introduction 1

1.1 Conjugated Polymers 2

1.1.1 Introduction of Conjugated Polymers 2

1.1.2 Synthesis of Poly(*para*-aryleneethynylene)s (PAEs) 2

1.1.3 Optical Properties of Conjugated Polymers 4

1.2 General Concepts of Conjugated Polymers Based Chemical Tongue 5

1.2.1 Introduction of Chemical Tongue 5

1.2.2 Sensory Responses of PAEs 5

1.2.3 Statistical Methods for Chemical Tongue 6

1.3 Sensing Applications of Conjugated Polymers 8

1.3.1 Sensing of Ionic Species 8

1.3.2 Sensing of Non-ionic Small Molecular Analytes 11

1.3.3 Sensing of Bio-analytes 13

1.3.4 Sensing of Complex Mixtures 16

Chapter 2. Array-Based Sensing of Explosives by Water-Soluble PPEs 17

2.1 Introduction and Construction of PPEs 18

2.1.1 Background of Explosive Detection 18

2.1.2 Mechanism for Fluorescence Based Explosive Detection 19

2.1.3 Conjugated Fluorescent Polymers for Explosive Detection 20

2.1.4 Design and Construction of PPEs 22

2.2 Results and Discussions 23

2.2.1 Synthesis of PPEs 23

2.2.2 Optical Spectroscopy and Nitroarene Discrimination and Detection 25

2.2.3 Concentration-Dependent Analysis of Explosives 27

2.2.4 Quenching Mechanism for Polymers toward Explosives 30

2.2.5 Conclusions 30

Chapter 3. Simple Optoelectronic Tongues Discriminate Amino Acids 32

3.1 Introduction of Amino Acids **33**
3.2 Sensor Arrays Discriminate Amino Acids **34**
3.3 PPE/GFP-Based Sensory for Sensing of Amino Acids **37**
3.3.1 Design and Construction of Chemical tongue 37
3.3.2 Screening Process 38
3.3.3 Identification of 20 Amino Acids in Water 43
3.3.4 Conclusions 49
3.4 Optimized Sensor Array Identifies 20 Amino Acids **50**
3.4.1 Screening and Construction of New Chemical Tongue 50
3.4.2 Results and Discussions 56
3.4.3 Conclusions 62
Chapter 4. Poly(*para*-phenyleneethynylene)-Sensor Arrays Discriminate 22 Different Teas **63**
4.1 Introduction and Construction of Chemical Tongues **64**
4.1.1 Introduction of Tea 64
4.1.2 Sensor Arrays for Tea Discrimination 65
4.1.3 Design and Construction of PPE-Based Sensor Array 68
4.2 Results and Discussions **69**
4.2.1 Complexation of PPEs by CB[8] 69
4.2.2 Screening Process 70
4.2.3 Discrimination of Tea-Based Analytes 72
4.2.4 Discrimination of Teas 73
4.2.5 Caffeine-Determination in Teas 80
4.3 Conclusions **81**
Outlook **83**
Chapter 5. Experimental Section **84**
5.1 General Remarks **85**
5.2 Synthesis Details and Analytical Data **88**
5.2.1 Synthesis of PAEs (Chapter 2) 88
5.2.2 Synthesis of PAEs (Chapter 3) 92
5.2.3 Synthesis of PAEs (Chapter 4) 93
5.2.4 Synthesis of Other PAEs 94
5.3 Linear Discriminant Analysis **98**
5.3.1 LDA Calculation of Explosives (Chapter 2) 98
5.3.2 LDA Calculation of Amino Acids (Chapter 3) 105

5.3.3 LDA Calculation of Teas (Chapter 4).....135
5.4 Determination of Binding Constants 151
5.4.1 Titration Experiments between PPE and Metal Salts (Chapter 3) 152
5.4.2 Titration Experiments between GFP and Metal Salts (Chapter 3).....153
5.4.3 Titration Experiments between PPE and Cucurbit[8] Uril (Chapter 4).....154
References 155

Chapter 1. Introduction

1.1 Conjugated Polymers

1.1.1 Introduction of Conjugated Polymers

Over the past decades, conjugated polymers (CPs) have opened up a wide variety of applications in electronic and photonic devices. One recent area of interest on CPs comprise their application in the development of chemical sensors. CPs are polyunsaturated π-conjugated compounds, in which all backbone atoms are sp or sp^2 hybridized.[1] As shown in Figure 1, CPs can be obtained with various types of backbone structures, including poly(*para*-phenyleneethynylene) (PPE), poly(*para*-phenylenevinylene) (PPV), poly(*para*-phenylene) (PPP), polyacetylene (PA), polythiophene (PT), polypyrrole (PPy), polyaniline (PANI), polyfluorene (PF) and polyfluorene-1,4-phenylene (PFP).

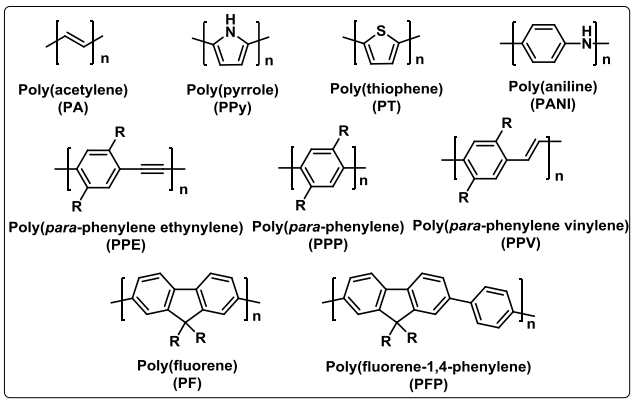

Figure 1. Molecular structures and backbones of typical conjugated polymers.

Solubility in aqueous media is essential for the sensing ability of conjugated polymers. To improve the solubility, functionalized side groups, such as oligoethyleneglycol, carboxylate, sulfonate, ammonium groups, *etc.* are incorporated as pendant groups on the conjugated backbone. Such conjugated polymers functionalized with water-soluble ionic side chains are also named "conjugated polyelectrolytes" (CPEs).[2]

1.1.2 Synthesis of Poly(*para*-aryleneethynylene)s (PAEs)

In comparison to the other conjugated polymers, PAEs (also mentioned here as PPEs) show attractive structural and chemical properties, such as facile synthesis, monomers carrying sulfonates, carboxylates and quaternary ammonium salts, functionalities can easily be introduced, high quantum yields etc.[3-4] These properties make these compounds superbly useful. Here we focus on the synthesis of poly(*para*-aryleneethynylene)s.

Main conjugated polyelectrolytes' chemical synthesis procedure includes non-catalytic and catalytic methods. Non-catalytic chemical-polymerization methods, including Wessling,[5] Gilch,[6] and Wittig[7] reactions are used, for instance, for the synthesis of PPVs. On the other hand, the most widely used

polymerization methods for poly(arylene)s are organometallic coupling methods (e.g. the Suzuki-Miyaura, Heck, Sonogashira and Yamamoto reaction).[1, 8-9]

There are several methods to prepare PAEs. The first one (Figure 2A) is the alkyne metathesis improved by Bunz *et al.* by using mixtures of $Mo(CO)_6$ and phenols at elevated temperatures.[10-11] The second one (Figure 2B) is the synthesis of semi-fluorinated PAEs reported by Watson *et al*. without Pd-catalysis but by fluoride-induced addition-elimination couplings.[12] However, both methods do not tolerate functional groups, which strongly limited their applications.

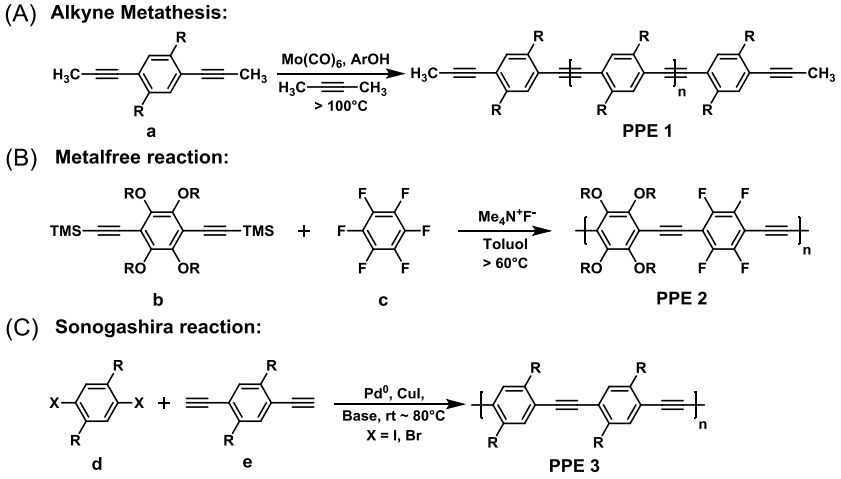

Figure 2. (A) Synthesis of PPEs by alkyne metathesis. **(B)** Synthesis of PPEs using fluoride-induced addition-elimination couplings. **(C)** Synthesis route of Sonogashira coupling reactions for PPEs.

The third one (Figure 2C) and also the most common applied to the synthesis of PAEs are palladium-catalyzed Sonogashira couplings that possess mild reaction conditions and the tolerance to functional groups.[13-14] In Sonogashira coupling reactions, the coupling of aryl diiodides with aromatic diynes using $(Ph_3P)_2PdCl_2$ as the catalyst at low concentration (0.1-0.2 mol%) and piperidine-THF as the solvent-based mixture at reaction temperatures of 20-80 ℃ are recommended.[15] Generally, higher reaction temperatures can give PAEs of higher molecular weight. In the case that the monomers are sensitive towards piperidine, triethylamine is an alternative choice.

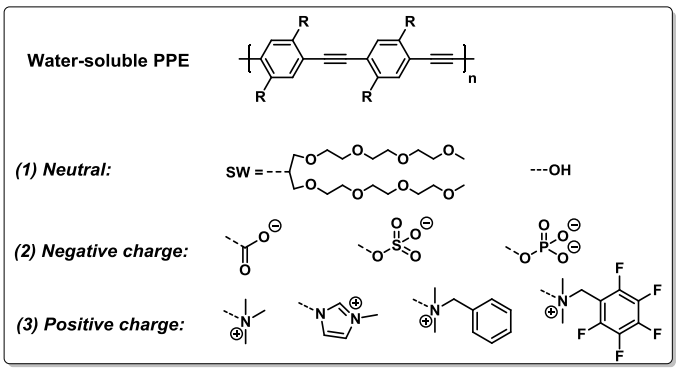

Figure 3. The construction of water-soluble conjugated polymers.

As water-soluble CPEs are important for chemical tongue sensing applications, post-modification has become a powerful tool to create a diversity of functional materials.[2, 16] Commonly used side groups

include cationic chains functionalized with quaternary amines and pyridinium, anionic chains like carboxylate (CO_2^-), phosphonate (PO_3^{2-}), sulfonate (SO_3^-) and neutral oligoethyleneglycol side-chains (swallowtail), which may help to increase water solubility, even if the conjugated polymer does not contain any ionic group (Figure 3). Thus, the solubility of PAEs in polar solvents is dependent on the ionic side chains, the hydrophilic side chains, and the hydrophobic aromatic backbones.

1.1.3 Optical Properties of Conjugated Polymers

The spectroscopy and the optical properties of the PAEs and, in particular, of the PPEs are dominated by their conformation, which is influenced by solvent, solid-state packing, temperature and other factors.[3] It was demonstrated that, in specific cases, enforced interchain interactions can lead to a red-shift in UV-vis spectra.[17] The presence of planar and twisted forms and their interconversion leads to attractive structure-property relationships. PAEs are fluorescent with emission maxima ranging from 420-600 nm, and can be either water- or organo-soluble. Generally, most PAEs are highly fluorescent materials with bright blue emission in dichloromethane, tetrahydrofuran, or chloroform. The fluorescence quantum yield decreases in polar solvents (methanol or ethanol) and drops again in water, which strongly restricted the sensory application, as most of the analytes, especially the bioanalytes are water soluble.[9, 15] This problem is settled by substitution with oligoethyleneglycol side-chains, carboxylate, ammonium and other charged groups.

Due to electronic delocalization, the development of fluorescence sensors with CPs is particularly interesting because of the enhanced sensitivity. The electronic conjugation between each repeating unit creates a semi-conductive ‘‘molecular wire effect’’, which was first described by Swager and co-workers in 1995.[18-19] Figure 4 shows how conjugated polymers amplify the molecular recognition signal by the migration of excitons along the polymer chain. In small molecules, a sensory appendage is attached to a single chromophore and only a small quenching effect would be observed. A complete fluorescence quenching would be observed as the conjugated polymers have one or several sensory appendages per repeat unit, and the signal obtained in the presence of the analyte is amplified. [20-21]

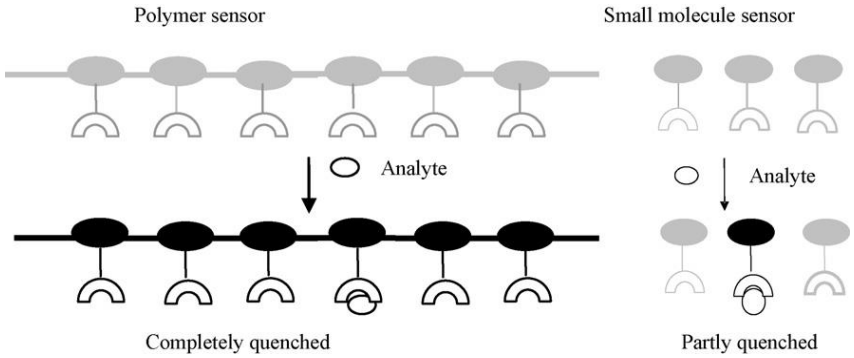

Figure 4. The schematic illustration of the “molecular wire effect” expressed by conjugated polymers. Figure reproduced with permission from ref. 21© 2009, Elsevier.

1.2 General Concepts of Conjugated Polymers Based Chemical Tongue

1.2.1 Introduction of Chemical Tongue

Taste is a chemical sense; the human taste sensing system discriminates around 10,000 different complex tastes according to the combination degrees of salty, sweet, sour, bitter, umami, and hotness, although hotness is determined by a receptor for heat and pain.[22] Similar to the human organ, researchers mimic the taste sensing elements and construct sensor arrays with various signals, such as mechanical, electronic *etc.* Chemical tongues are composed of a number of sensor or receptor elements that react with multiple types of analytes. Unlike the lock-and-key method, in which a single response is specific towards a given analyte, chemical tongues consist of the combinations of several cross-reactive sensor elements which respond selectively, but not specifically to one given analyte.[23-24]

Based on the difference of signal acquisition methods, chemical sensors can be grouped into three categories: electrical and electrochemical sensors, thermometric sensors and optical sensors.[23] We are interested in optical sensor arrays that use absorbance or fluorescence array detectors, because of the high sensitivity and precise data acquisition. The fundamental concepts of optoelectronic chemical tongues and their use were demonstrated by Anslyn, Suslick, Rotello and Bunz *et al.* The construction of the tongues and the selection of the sensor elements of these groups differ distinctly. Anslyn's group has advanced the field by developing indicator displacement assays (IDAs) based on differential sensing. Building on IDAs for a series of analytes using both organic and organometallic receptors, they successfully transitioned them into sensor arrays.[25-31] Suslick and co-workers have developed a series of colorimetric sensor arrays constructed by a large number of receptors and dyes, such as acid/base indicators, redox indicators, metal complex indicators, solvatochromic, vapochromic dyes *etc*. for the sensitive detection and discrimination of gaseous or liquid analytes.[32-37] According to Suslick, the chemical diversity of the utilized dyes is the critical ingredient for the successful discrimination. Rotello, Bunz and coworkers have developed a third concept, in which conjugated fluorescent polyelectrolytes or green fluorescent protein (GFP) were used as fluorophores. The fluorescence is quenched by positively charged gold nanoparticles functionalized with different ammonium. These electrostatic complexes work quite well when exposed to bio-analytes, including cells, bacteria, and proteins.[38-44] The secret of their success is the generation of a unique pattern and not a specific response to a given analyte.

1.2.2 Sensory Responses of PAEs

Generally, the mode of fluorescence change of PAEs towards various analytes includes fluorescence quenching, fluorescence turn-on, and ratiometric sensing.[15] Among these modes, fluorescence quenching is the most commonly used and most direct method. Upon addition of an analyte, the fluorescence of the sensory polymer decreases. This phenomenon may be caused by the mechanism of static quenching, dynamic quenching or a combination of them. The most useful and simple tool for the mathematical evaluation of the quenching process is the Stern-Volmer equation. However, sometimes such quenching data do not fit, and a more complex form of the Stern-Volmer equation has to be used (for the equation see Chapter 5.4). Because of the molecular wire effects and superquenching of PAEs, the modified Stern-Volmer equation is more useful and accurate when PAEs are employed as sensor elements.

Fluorescence turn-on is also possible in our study through analyte-introduced de-aggregation, which is based on a novel strategy using the IDA concept. The sensing principle of IDA relies on the competition between an analyte and an indicator with the same binding site on the host molecule. In our study, electrostatic complexes are constructed by using charged PAEs with oppositely charged PAEs, gold nanoparticles, metal salts or peptides.[38-40, 42-43, 45-49] These complexes are non-fluorescent, but their disruption by the addition of different analytes results in the restoration of the fluorescence. The concept is powerful and works well in water.

Ratiometric sensing is the change of the emission or absorption color of the sensor molecule upon the addition of an analyte. This concept is rarely used in PAE-based sensor array because the arenes do not contain heteroatoms, which ionic species can coordinate to. In most cases, only the planarization of the backbone (upon red shift of emission and absorption) will induce ratiometric changes. When the PAEs carry heterocyclic building blocks that contain pyridine, quinoline or bipyridine units, direct color changes by reaction with analytes or by coordination to ionic species can be observed.[15, 50]

1.2.3 Statistical Methods for Chemical Tongue

Regardless of the type of signal output, array approaches produce a large amount of data that usually cannot be easily analyzed by individual calibration curves, for the purpose of identifying and differentiating similar analytes. For the pattern recognition of similar analytes, the greater dimensionality of sensor elements, the more sophisticated statistical analysis techniques are needed. There are many statistical methods available to deal with the collected data, but most common approaches used for chemical tongues are hierarchical cluster analysis (HCA), principal component analysis (PCA), and linear discriminant analysis (LDA).[23, 51-53]

HCA is a statistical technique that clusters data points based on the cluster similarity determined by Euclidean distance. It provides a forthright dendrogram, in which, the nearest-neighbor data points are paired into a single cluster, which is then paired with other nearest-neighbor data points or clusters until all the data points and clusters are connected to each other.[23, 52] However, it is often served as an

auxiliary method for the display of cluster similarity, but not easily capable of unknown samples prediction and precise analyzing.

Both PCA and LDA are multivariate methods that decrease the dimensionality of a data set and adjust the coordinate system. PCA allows visualization of all the information contained in a dataset and helps to find out which variables contribute most to the differentiation. As ‘‘chemical tongue’’ sensor arrays always contain multiple elements, it is difficult to display all the data in 2D or 3D plots. Thus, PCA becomes a powerful tool to evaluate all the variables of the sensor array and screen the optimized elements with the best discriminative power.

LDA is one of the most used classification procedures, which has been widely used for pattern-based identification in chemical tongues. The method classifies analytes by calculating discriminant functions that maximize the variance between predetermined categories and minimize the variance within these categories.[52, 54] In addition, it is also a supervised protocol used to predict the identity of unknown samples by identifying which classes in the training set the unknowns most resemble. In the blind test, LDA converts the training matrix with multiple sensor elements into canonical scores according to their Mahalanobis distance. As seen in Figure 5, an algorithm was used in LDA to compute the Mahalanobis squared distance between the test samples and each analyte category within the corresponding training set. The test samples of the same analyte were classified within a minimal distance, as compared to the distance between categories.

Comparatively, LDA can show better distinguishing ability among sample classes than PCA, because the dimensional components are optimized to maximize differentiability. That is why we firstly use PCA for the screening of the best sensor elements based on the contribution of each element, and then distinguish the various analytes and predict the unknown samples with LDA.

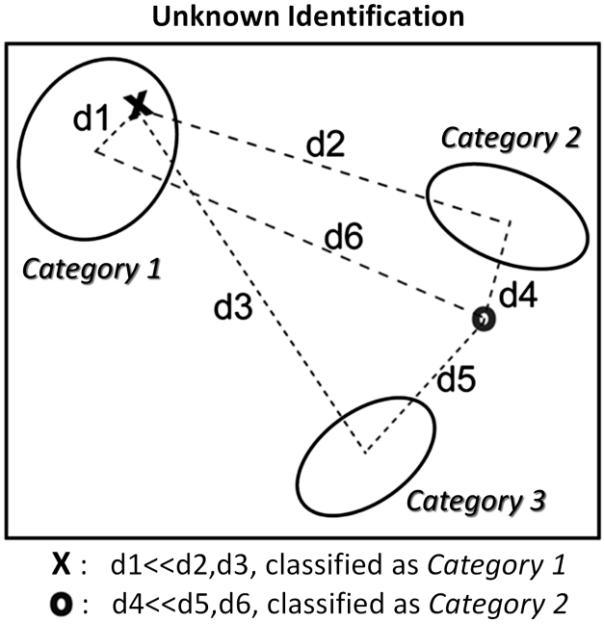

Figure 5. Schematic of unknown samples identification using LDA, where d stands for the squared Mahalanobis distance. Figure reproduced with permission from ref. 41© 2016, American Chemical Society.

1.3 Sensing Applications of Conjugated Polymers

Over the past few years, conjugated polymers have been investigated extensively as optical sensors for various analytes including metal ions, explosives, acids, amines, biomolecules, proteins, bacteria *etc.* The unique structural and optical properties of CPEs provide several advantages over traditional small molecular dyes. First, the polyelectrolyte structure of CPEs affords water solubility, which is essential for sensing analytes in aqueous solution, and the amphiphilic structure provides a platform to interact with the analytes through hydrophobic or electrostatic interactions. Second, in most cases, CPEs undergo changes in fluorescence responses, which are more sensitive towards analytes than changes in absorption spectra or color. Thus a low concentration (100 nM-10 μM) based on a per repeat unit of CPEs can be used for sensing. Third, CPE-based optical sensor arrays are less labor-intensive and less time consuming, as the analysis can be performed with a standard plate reader on a 96 well plate, which is quite fast and effective. Last but not least, CPE-based optical sensors amplify quenching, which causes superquenching when reacting to a very small amount of analytes.

1.3.1 Sensing of Ionic Species

Heavy metal pollution in water and soil sources has posed a threat to human health; their accumulation in the body could cause serious damage to the brain. Therefore, convenient detection and quantification of heavy metal ions have always been of great interest to researchers. For example, Bunz *et al.* constructed a highly selective lead ion sensor from **PPE 4** (Figure 6A) utilizing the multivalency effects, and later proved that **PPE 4** is also highly reactive towards mercury ions.[55-56] Based upon these developments, Tan and co-workers reported a PPE-based sensor array for discriminating eight different metal ions.[57] They prepared four different PPEs **PPE 4** - **PPE 7** (Figure 6A) that display an increasing number of negative charges and exposed them to different metal ions. From the fluorescence quenching behavior (Figure 6B), it is possible to see that some metal ions are quite sensitive towards the different PPEs. However, it is still not entirely clear what contributes to the different selectivity. This sensor array affords a fingerprinting technique for the identification of metal cations, as evidenced by clearly separated data clusters in 3D-LDA plots (Figure 6C).

The group of Li *et al.* investigated the reaction of cationic **PFP 1** with citrate, resulting in self-quenching of the fluorescence through induced aggregation (Figure 7).[58] These aggregates were disrupted by the addition of aluminum ions (Al^{3+}) because of the strong chelation ability of citrate with Al^{3+} and then gave a free and un-aggregated fluorescent polymer again. Other metal ions had little effect on the fluorescence recovery of **PFP 1** as they formed less strongly bound complexes with citrate.

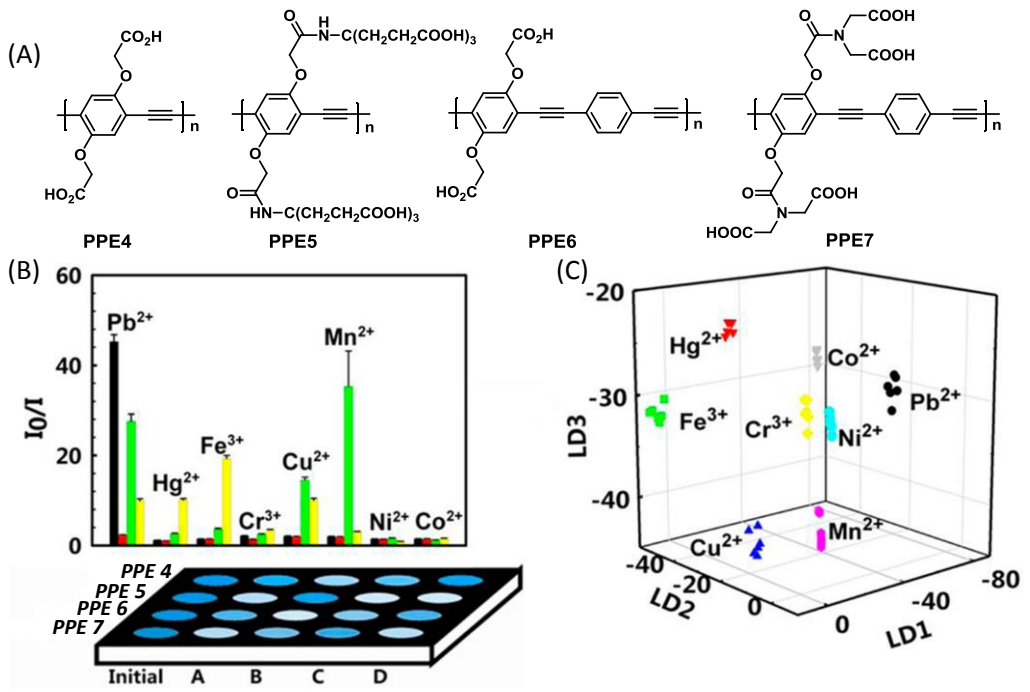

Figure 6. (A) Chemical structures of conjugated polymers **PPE 4 - PPE 7**. **(B)** Response patterns constructed based on fluorescence quenching of the four polymers by eight metal ions. **(C)** 3D canonical score plot of the fluorescence response patterns obtained by four-PPE sensor array against eight metal ions. Figure reproduced with permission from ref. 57 © 2015, American Chemical Society.

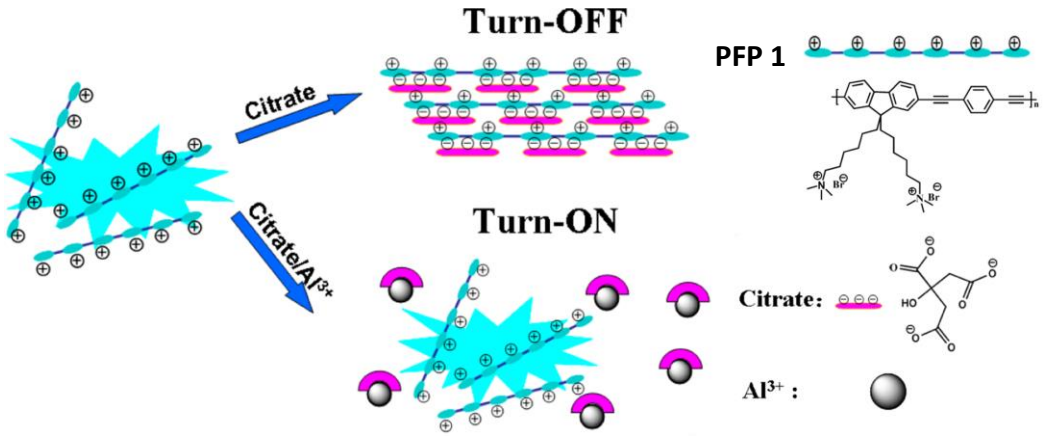

Figure 7. Schematic representation of citrate-induced aggregation of conjugated polymers for the Al^{3+} assay. Figure reproduced with permission from ref. 58 © 2013, American Chemical Society.

Identification and recognition of anions, such as amino acids, anionic surfactants, and nucleotides, which can have an anionic motif, is also of significant importance. Take anionic surfactants as the example, sodium dodecylbenzenesulfonate (SDBS) and sodium dodecyl sulfate (SDS) have a large application in pharmaceutical and food formulations that it is important to analyze them in trace quantities. Iyer and co-workers reported a water-soluble cationic conjugated polyelectrolyte **PPP 1** (Figure 8B) that is highly effective at detecting and distinguishing SDS and SDBS on the basis of different aggregation behavior via interpolymer cofacial arrangement.[59] The extended chains promote interchain packing via the SDS/CPE complex and overlap to form excimers that emit fluorescence at a longer wavelength. However, the aromatic ring from the SDBS restrict the interchain packing of the SDBS/CPE complex, which made it fail to show any excimer emission.

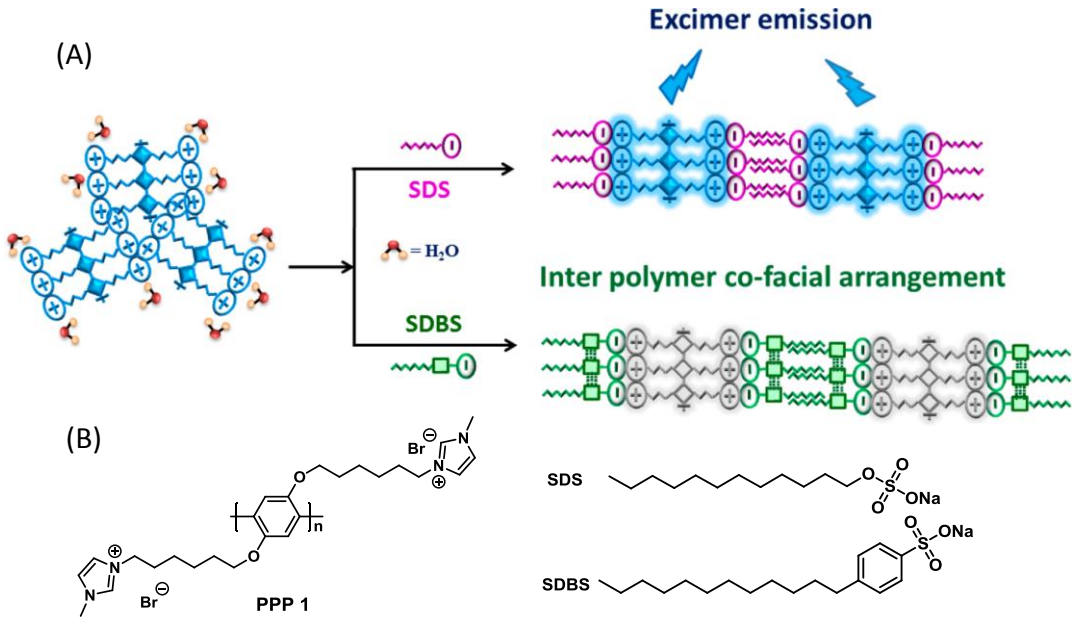

Figure 8. (A) Schematic representation of the aggregation behavior of the conjugated polymer and anionic surfactants complexes. **(B)** Structures of the cationic conjugated polymer and anionic surfactants. Figure reproduced with permission from ref. 59 © 2015, American Chemical Society.

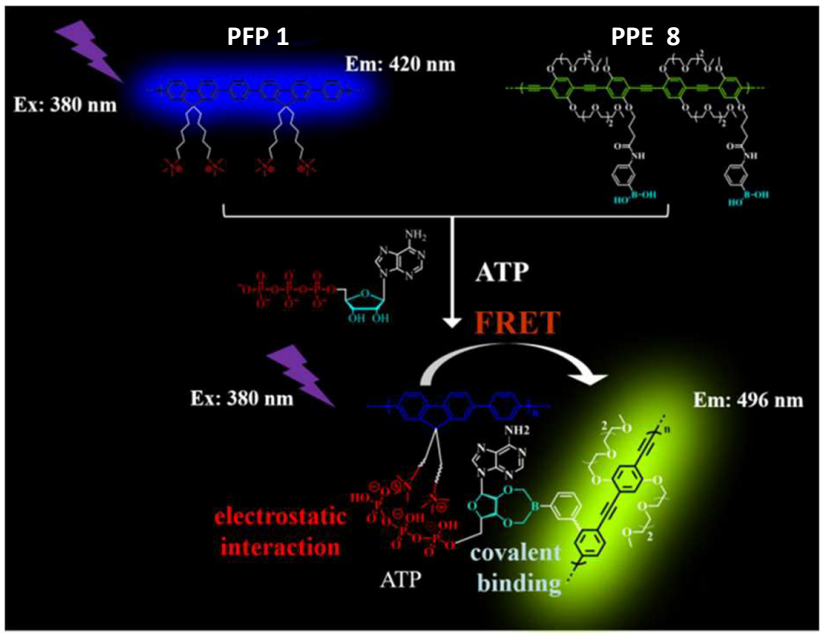

Figure 9. Mechanism of the CPE-based combination probe for sensing ATP. Figure reproduced with permission from ref. 60 © 2015, Royal Society of Chemistry.

More recently, Tang *et al.* constructed a conjugated polymers-based ratiometric combination probe for adenosine triphosphate (ATP) detection.[60] This combination system contains two conjugated polymers: a phenylboronic acid-modified **PPE 8** and a quaternary ammonium-modified **PFP 1**. The working principle of the probe is schematically represented in Figure 9. When ATP is added into the complex, **PPE 8** can recognize the ribose of ATP by covalent bonding, in the meantime, positively charged **PFP 1** can interact with the negatively charged phosphates of ATP by electrostatic interaction. Owing to the overlap between the emission spectrum of **PFP 1** and absorption spectrum of **PPE 8**, and also the shortened distance of CPEs, the efficient fluorescence resonance energy transfer (FRET) will occur. The method is highly selective, which can clearly discriminate ATP from other interferents such as

adenosine diphosphate (ADP), adenosine monophosphate (AMP), other nucleoside polyphosphates and nucleobases.

1.3.2 Sensing of Non-ionic Small Molecular Analytes

The recognition and sensing of different kinds of non-ionic small molecular analytes with conjugated polymers have also been widely investigated, including explosives, amines, hydrogen peroxide, thiol and nerve agents *etc.* Fluorescent sensing of amines in aqueous solution is challenging due to their various basicity and chemical structures of amines that may lead to poor selectivity and sensitivity. Here are some efforts that have been undertaken toward developing methods to detect amines. In 2015, He and Chen developed an ultrasensitive and reversible "fingerprint" fluorescent probe via embedding multiple reactive groups onto one conjugated polymer backbone.[61] The probe can be used for the detection of primary aliphatic amines, secondary aliphatic amines, aromatic amines and their mixtures. More recently, Fan and Zhu *et al.* designed and synthesized a fluorescent conjugated polymer **PFP 2** (Figure 10) for selective sensing of aromatic amines in aqueous solution.[62] The fluorescence of the polymer is selectively quenched by the aromatic amines, whereas the aliphatic amines enhance the fluorescence. They concluded that the high selectivity to the aromatic amines originates from the amplified π-π fluorescence quenching synergized by the amine and carboxylic acid interaction. Conjugated polymer nanoparticles functionalized with specific binding sites also offered an interesting strategy for fluorescent sensing of the biologically relevant amines, as reported by Qian *et al*.[63]

Thiols play vital roles in biological systems. Generally, alternation in the level of cellular thiols has been linked to numerous of diseases, such as cancer, liver damage, and AIDS.[64] Huang and co-workers present a water-soluble conjugated polymer with pendant disulfide linkages to PEG chains, **PF 1**, which was an efficient material for thiol detection through solubility-induced fluorescence conversion.[65] As shown in Figure 11, when the disulfide linkages were cut off by thiols, the pendant hydrophilic PEG chains would be separated and thus resulting in the decrease of the water solubility. The decreased solubility caused an aggregation of the hydrophobic conjugated backbone and increased FRET efficiency from the conjugated backbone to 1,4-dithienyl benzothiadiazole. They also successfully achieved the goal of imaging intracellular thiols in HeLa cells.

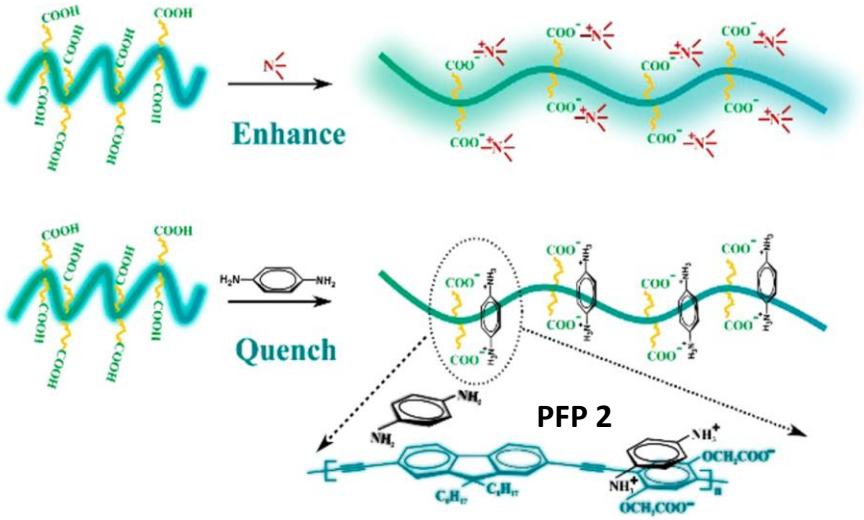

Figure 10. The proposed mechanism of the fluorescence enhancement and quenching of **PFP 2** by the amines in aqueous solution. Figure reproduced with permission from ref. 62 © 2017, American Chemical Society.

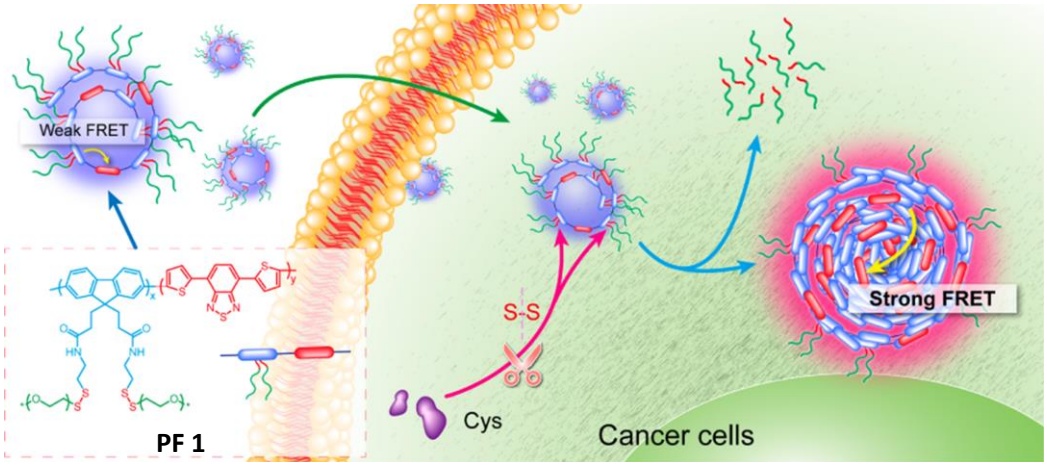

Figure 11. Schematic representation of FRET-based detection of thiol in cancer cells. Figure reproduced with permission from ref. 65 © 2015, American Chemical Society.

Recently, there has been a growing interest in the design and development of chemical sensors for hydrogen peroxide, because it relates closely to human health and disease.[66] Wang and co-workers used cationic conjugated polymer **PFP 1** and neutral peroxyfluor-1 **F1** with boronate protecting groups to detect H_2O_2.[67] The underlying principle of H_2O_2 sensing by the CP-based sensor is illustrated schematically in Figure 12. In the absence of H_2O_2, there is no electrostatic interaction between the cationic **PFP 1** and the neutral molecule **F1,** thus making **F1** well separated from the polymer and no fluorescence quenching occurs. After the addition of H_2O_2, **F1** could specifically react with H_2O_2 and generate fluorescein **F2**, which can exist as a monoanion or dianion in the pH range 5.4-9.1. The formation of the anionic fluorescein results in strong electrostatic interactions between **PFP 1** and fluorescein, and therefore efficient fluorescence quenching of the polymer can be observed. Since glucose oxidase can catalyze the oxidation of glucose to generate H_2O_2, the assay is also suitable for glucose detection.

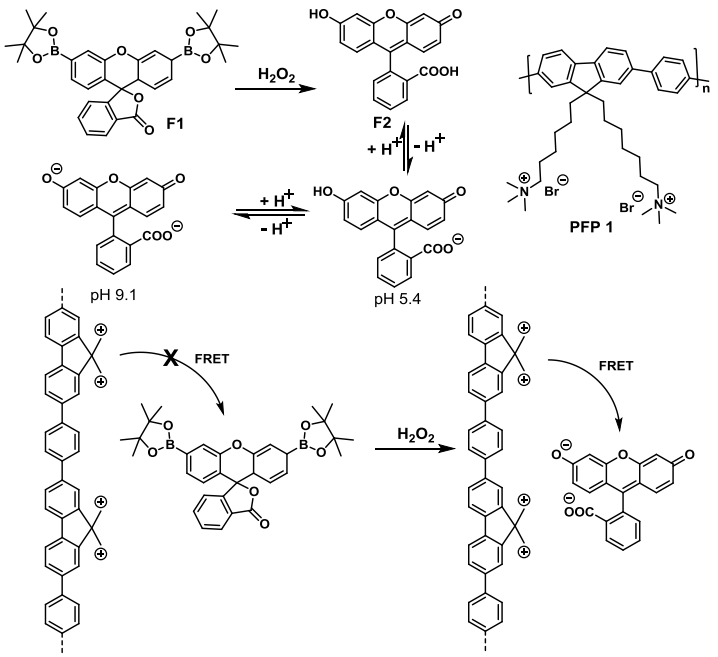

Figure 12. The chemical structures of fluorescent probe and conjugated polymer used in this study and representation of the H_2O_2 assay.

1.3.3 Sensing of Bio-analytes

The discrimination of proteins, cells, bacteria and other biological analytes in complex mixtures, such as serum, urine, and plasma, is important for the diagnosis of diseases. Traditional techniques for the detection of diseases-related biomarker generally depend on specific enzymatic or antibody/antigen interaction, which limits the scope of the analytes.[24] Recently, conjugated polymers based sensor arrays have been developed and applied successfully to distinguish a broad range of bioanalytes. Among them, nanoparticle/fluorescent polymer or fluorescent polymer/green fluorescent protein complexes constructed by Rotello and Bunz *et al.* are particularly intriguing.[39, 41, 43]

In our approach, competition binding affords various signal outputs by the displacement of a fluorophore, and generates characteristic fingerprints for pattern recognition. One representative example is a simple sensing array composed of six structurally related cationic gold nanoparticles (NP1-NP6) and an anionic PPE for protein sensing.[39] As depicted in Figure 13, the NPs act as both molecular recognition sites and quenchers for the highly fluorescent anionic PPE. The additional hydrophobic, aromatic or hydrogen-bonding units were incorporated into the terminus to further modulate NP-protein and NP-PPE association. Upon binding to the NPs, the fluorescence of **PPE 4** was quenched, and then the subsequent binding of protein analytes displaced the polymer, leading to the recovery of the fluorescence. The distinct signal response patterns can be used to differentiate seven proteins with diverse structural features at nanomolar concentrations.

One direct protein detection method was developed by Leclerc and Ho to detect human α-thrombin by a polythiophene derivative and a single-stranded DNA as an aptamer.[68] When binding to thrombin, the aptamer undergoes a conformational transition from an unfolded to a folded quadruplex structure. The

conformational change of the negatively charged oligonucleotide can be detected by the cationic polythiophene derivative, which exists in a less aggregated conformation and exhibits blue-shifted absorption and enhanced fluorescence.

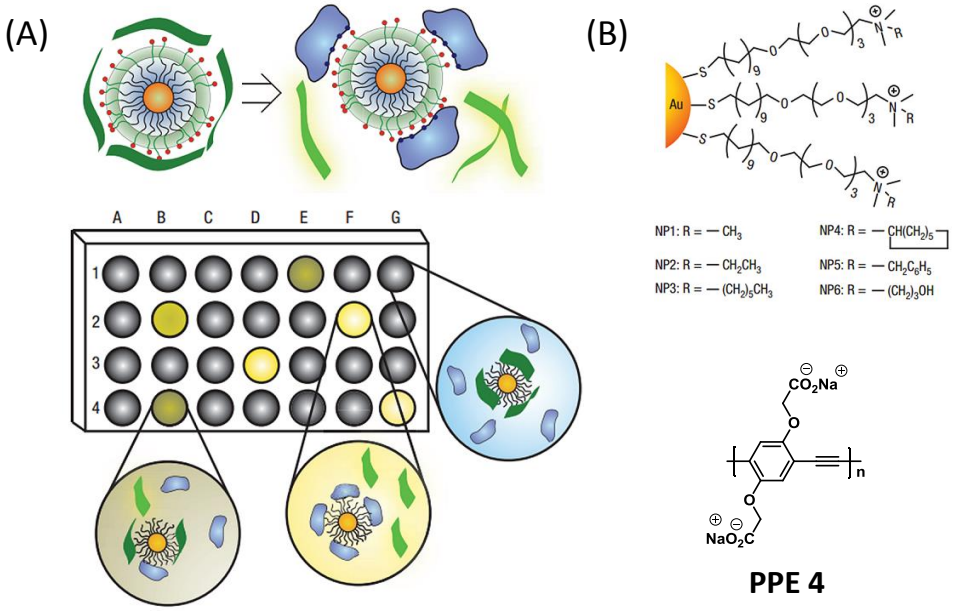

Figure 13. (A) Representation of the fluorophore displacement protein sensor array. **(B)** Chemical structure of cationic gold nanoparticles (NP1-NP6) and anionic fluorescent polymer **PPE 4**. Figure reproduced with permission from ref. 39 © 2007, Nature Publishing Group.

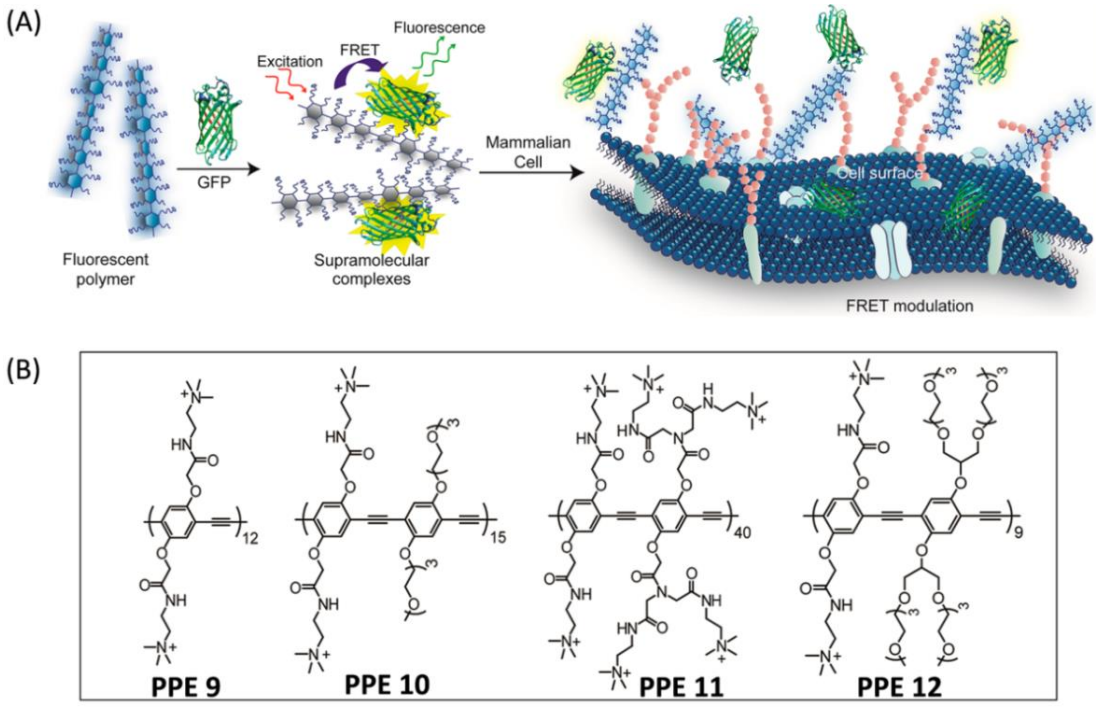

Figure 14. (A) Schematic illustration of FRET-based cell sensing using PPE-GFP complexes. **(B)** Chemical structures of the cationic PPEs. Figure reproduced with permission from ref. 41 © 2016, American Chemical Society.

More recently, we have developed a ratiometric array composed of several cationic conjugated polymers and green fluorescent protein for the detection of mammalian cells.[41] Owing to net negative charges and excellent fluorescence properties, GFP was selected as a fluorophore. Figure 14 illustrates the underlying principle, in which, the cationic PPEs and GFP form supramolecular assemblies

through electrostatic interactions and act as the donor and acceptor in the FRET processes, respectively. **PPE 9 - PPE 12** tailored with different charge densities are expected to display differential binding with GFP. Selective multivalent binding of these polymers with cell surfaces modulated the FRET signal of the PPE-GFP complexes, providing a fingerprint signature for each cell type. The sensor array allowed sensitive and reliable identification of 16 different cell types and discrimination between healthy, cancerous, and metastatic cells, with the same genetic background.

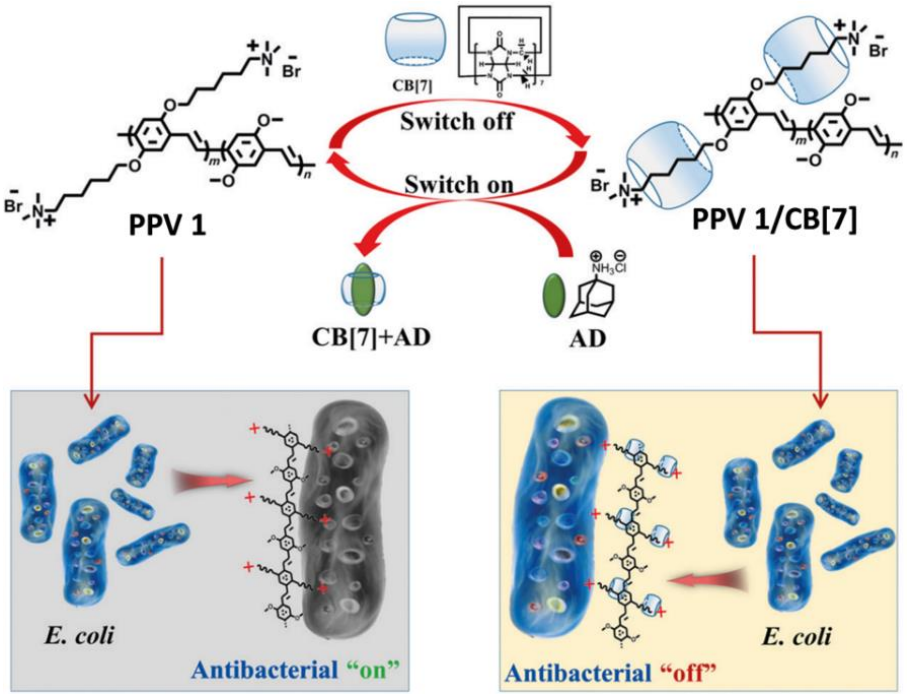

Figure 15. Supramolecular assembly of **PPV 1** with CB[7] and disassembly of **PPV 1** with CB[7] mediated by AD molecule for reversible control of the antibacterial activity of PPV. Figure reproduced with permission from ref. 69 © 2015, Wiley-VCH Verlag GmbH & Co. KGaA.

While proteins and cells are attractive classes of analytes, it is still of interest to investigate the identification of bacteria. Based on the same strategy, Rotello *et al.* developed a simple array contained an anionic PPE and three different cationic NPs.[43] The addition of negatively charged bacteria replaced the negatively charged PPE from the positively charged NPs, differentially restoring the polymer fluorescence. Thus simple constructs are able to identify three different strains of *E.coli* in minutes. Lately, our group reported a new sensor array that identifies and discriminates 14 different types of bacteria according to staining properties (Gram-positive and Gram-negative) or genetic similarity (genus, species, and strain). In the work, a negatively charged PPE formed electrostatic complexes with four positively charged antimicrobial peptides.[47] Other systems were used by Bazan *et al.*, in which, electrostatic complexes containing a cationic conjugated oligoelectrolyte and fluorescein-labeled single-stranded DNA provide a platform for identifying various types of bacteria.[70]

It is worth mentioning that conjugated polymers cannot only be used to identify bacteria, but also take part in antibacterial regulation. A supramolecular antibiotic switch that can reversibly "turn-on" and "turn-off" its antibacterial activity was described by Wang and co-workers.[69] Based on their previous study, the cationic **PPV 1** with quaternary ammonium groups as side chain was chosen as antibacterial

agent.[71] As shown in Figure 15, cationic **PPV 1** could form a noncovalent complex with cucurbit[7]uril (CB[7]) that possesses a hydrophobic cavity for encapsulating quaternary ammonium. The biocidal activity of **PPV 1** was reduced because of the encapsulation of quaternary ammonium groups. Upon adding amantadine (AD), a more stable CB[7]/AD complex was formed and released **PPV 1** through competitive replacement, thus the antibacterial activity of **PPV 1** is recovered.

1.3.4 Sensing of Complex Mixtures

Quality control and quality assurance of beverages and other complex analytes are important both to the industry and consumers. However, it is still challenging because of the similarity and complexity of their compositions. In the past decades, a variety of sensor techniques have been developed for the analyses of complex analytes, including soft drinks, coffees, beers, whiskeys, *etc.* Here two groups that work on this project should be mentioned. One specific method was formulated by Suslick *et al.*, who utilized different colorimetric indicator molecules that react with complex analytes by color change or fluorescence intensity modulation.[23, 33, 37, 72-73] Another accepted one was developed by Anslyn and co-workers, who focused on a weakened variation of the lock and key-principle. Their approach is to offer small libraries of receptors that are "filled" with dyes to be replaced by the complex analytes with differential efficiency.[24, 27, 30-31, 74-75]

Both of these approaches stressed that cross-reactivity and structural variation of the sensor elements are important, and generated a large number of exceptionally well-working tongues that may require elaborate molecular design and multistep organic synthesis. Are they necessary though? Are there any rules that guide the researchers to construct the simplest system for discriminating a given set of analytes? Bunz *et al.* have made progresses in developing minimalist sensor arrays with charged conjugated polymers which successfully discern different brands of fruit juices, teas, syrups and honeys, as well as different white wine and whiskies of various origin, age, brand, blend status and taste.[46, 76-79] These chemical tongues allow the identification and discrimination of commercially available beverages and their mixtures based upon the fluorescence turn-on or turn-off of conjugated polymers.

Chapter 2. Array-Based Sensing of Explosives by Water-Soluble PPEs

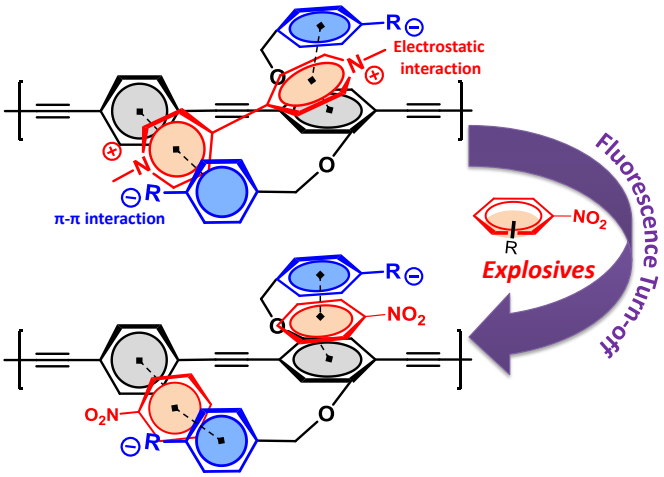

Figure 16. Schematic representation of possible interactions between the designed PPEs and quenchers. Figure reproduced with permission from ref. 80 © 2017, American Chemical Society.

In this chapter, we prepared four water-soluble poly(*para*-phenyleneethynylene)s, two of which are novel and carry benzylic side chains that are negatively charged. All of the four PPEs were employed to detect nitroaromatic compounds (NACs) in water. The two novel PPEs with the benzylic side chains react with fair sensitivity towards DNT and TNT in water. If the benzylic side groups are alkoxy-substituted, TNT is detected at concentrations down to 0.27 μM. Twelve different nitro-aromatics were successfully discriminated by a small array consisting of either two or four of the PPEs and employing linear discriminant analysis.

2.1 Introduction and Construction of PPEs

2.1.1 Background of Explosive Detection

Explosive bombs have been widely used in global terrorism, due to their ease of producing, and consequently killed tens of thousands of people as well as caused massive property damage.[81] The broad use of explosives for the military purpose has also raised concerns about environmental contaminations where they are produced and stored. Therefore, sensitive and selective detection of explosives is one of the current pressing concerns in global security.

Until now, a wide range of instrumental techniques, such as surface-enhanced Raman spectroscopy (SERS),[82] mass spectrometry (MS),[83-84] cyclic voltammetry (CV),[85-86] energy-dispersive X-ray diffraction (XRD)[87] etc., have been employed for the detection of explosives. Although these methods provide some advantages, their use is limited due to expensive instruments, cumbersome pretreatment of samples, sophisticated operation, and low sensitivity. In comparison, the fluorescence-based materials, which are cost-effective and portable, provide high-sensitivity, ultra-selectivity, as well as fast response time for explosive detection.

In recent years, a large number of emissive sensing materials have been developed for the detection of explosives in solution, vapor, and solid states by fluorescence methods.[16, 88-92] Among this, conjugated

polymers have attracted significant attention due to their strong light absorption and fluorescence emission, and high sensitivity to small perturbations through the so-called "molecular wire effect" or "super-quenching effect".[88, 93]

2.1.2 Mechanism for Fluorescence Based Explosive Detection

Among all the fluorescence-based explosives sensors, fluorescence quenching methods still dominate. There are several mechanisms responsible for fluorescence quenching, for example, photo-induced electron transfer (PET), resonance energy transfer (RET), intermolecular charge transfer (ICT), energy change, *etc.* For explosive detection, most of the researchers have used PET and FRET mechanisms as the sensing platform.

Photo-induced electron transfer contributes to the fluorescence quenching by explosives, which accounts for the most of the fluorescence-based explosive detection. Many explosives are highly nitrated organic compounds, which could bind to electron-rich fluorophores through donor-acceptor (D-A) interactions.[94] As shown in Figure 17A,[81] the excited-state of fluorophores donates an electron to the ground state of explosive compounds, thus a complex is formed between the electron donor and the electron acceptor. The energy gap between the LUMO of acceptor explosive and donor fluorophore is probably the thermodynamic driving force for this electron transfer process. For conjugated polymers, electron transfer is based on π-π stacking in the D-A system.

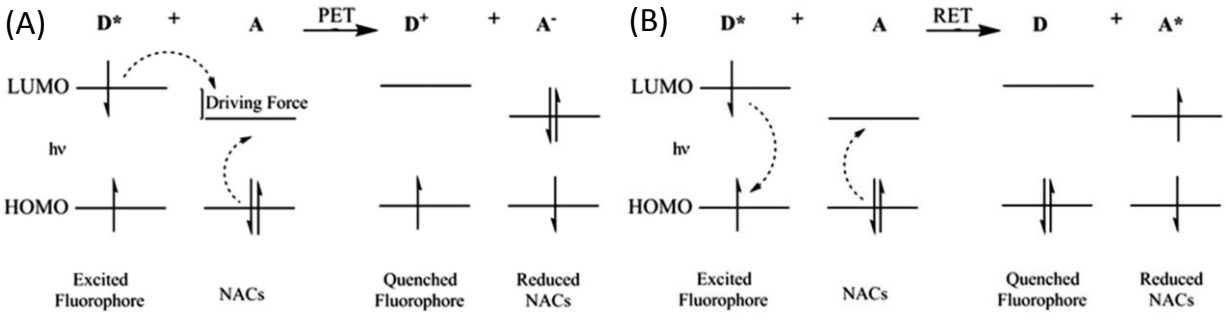

Figure 17. (A) Photoinduced electron transfer (PET) and **(B)** Resonance energy transfer (RET). Figure reproduced with permission from ref. 81 © 2015, Royal Society of Chemistry.

The energy transfer mechanism can improve sensitivity and enhance the fluorescence-quenching efficiency, therefore, it can also be used as an important tool to develop a series of explosive sensors. In Förster resonance energy transfer (FRET), an initially excited molecule (donor) returns to the ground state and, at the same time, the transferred energy causes an electron on the acceptor to go to the excited state (Figure 17B). According to FRET theory,[93, 95] the rate of energy transfer mainly depends on three aspects: (1) the distance between the donor (the fluorophore) and the acceptor (the analyte); (2) the extent of overlap between the fluorescence emission spectrum of the donor and the absorption spectrum of the acceptor; (3) the relative orientation of the donor and acceptor dipoles.

Fluorescence quenching induced by explosives can be dynamic or static, the former results from the diffusive encounter, while the latter results from complex formation.[96-97] The two quenching processes can be distinguished by time-resolved measurements of the fluorescence decays of the sensors. As a diffusion-controlled process, dynamic quenching occurs when a photo-excited fluorophore interacts with a colliding analyte molecule. Thus the average fluorescence decay lifetime will decrease as the concentration of the quencher is increased. While for static quenching, as the formation of the non-fluorophore-quencher complex is the origin of the quenching, the fluorescence lifetime will remain unchanged. Therefore, the measurement of fluorescence decay lifetime change in the presence and absence of explosive becomes the most prevalent and effective method to determine whether the quenching is a dynamic or static process.

2.1.3 Conjugated Fluorescent Polymers for Explosive Detection

Compared with small molecule fluorophores, fluorescent conjugated polymers are excellent electron donors, and their donor ability is enhanced by the delocalized π^* excited state, which facilitates exciton migration and increases the electrostatic interaction between the polymer and electron-deficient nitroaromatic analytes.[81] A pioneering work was achieved by Swager and co-workers, who introduce pentiptycene units into the PPE backbone chains and utilize the pentiptycene-derived PPE-based fluorescent polymers **PPE 13**-**PPE 16** to detect trace amount of 2,4,6-trinitrotoluene (TNT) in the air and in organic solvents.[98] The bulky rigid structure of pentiptycene could prevent self-quenching by isolating the PPE backbones, and also create a porous structure and molecular scale channels for the diffusion of explosives (Figure 18).

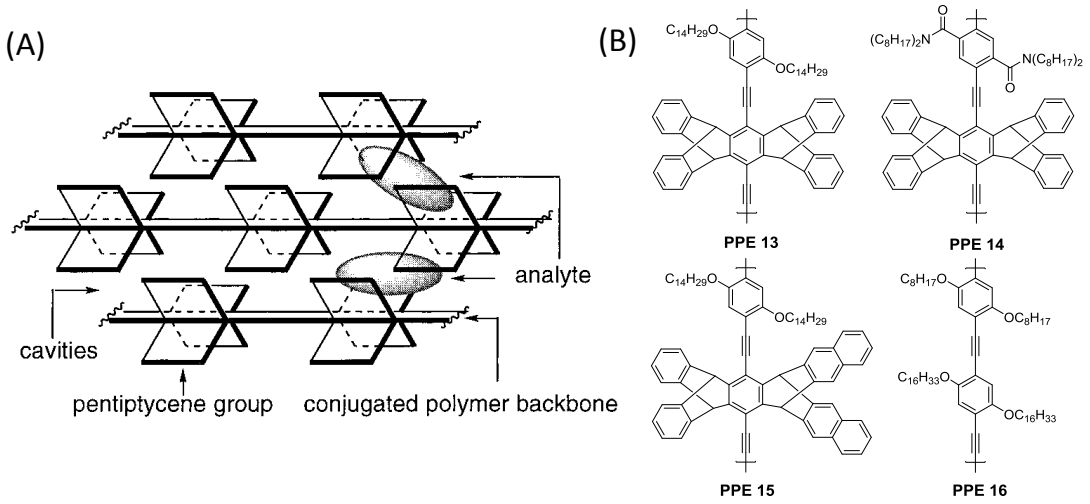

Figure 18. (A) The schematic illustration of rigid pentiptycene groups, which provide cavities for analyte binding. **(B)** The structures of pentiptycene-derived PPE-based polymers. Figure reproduced with permission from ref. 98 © 1998, American Chemical Society.

Fang's group synthesized functional PPEs bearing pyrene units within the backbones (Figure 19).[96] The solution-casted thin films from poly(pyrene-co-phenyleneethynylene)s **PPE 17** showed dramatically enhanced quenching response to TNT in the aqueous medium. Commonly nitroaromatic

compounds such as DNT, NB, and PA showed little interference to the fluorescence emission of the films. The strong quenching effect of TNT over other NACs has been ascribed to the specific π-π interactions and the matching of the LUMO energies between TNT and pyrene units in the copolymers. Furthermore, Jiang *et al.*[99] constructed a sensor array consisting of six cationic fluorescent conjugated polyelectrolytes (Figure 20). The varying binding affinity gave rise to a distinct fluorescence response via polymer-nitroaromatic interactions and fluorescence quenching, which was used to differentiate nine closely related hydrophilic nitroaromatics by linear discrimination analysis.

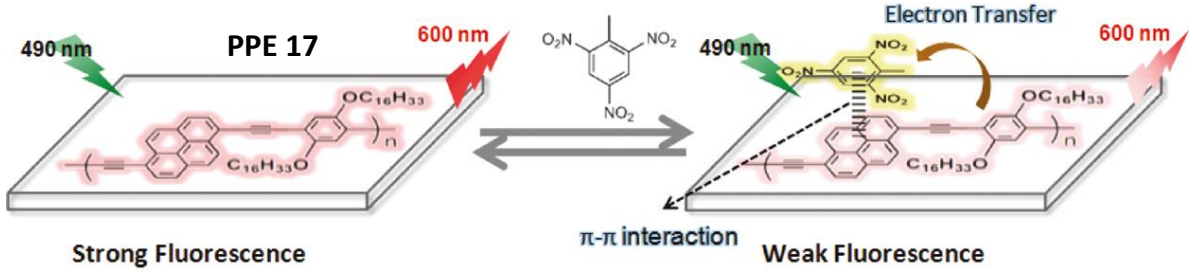

Figure 19. Schematic representation of the electron-transfer mechanism for the quenching of the fluorescence of film by TNT. Figure reproduced with permission from ref. 96 © 1998, American Chemical Society.

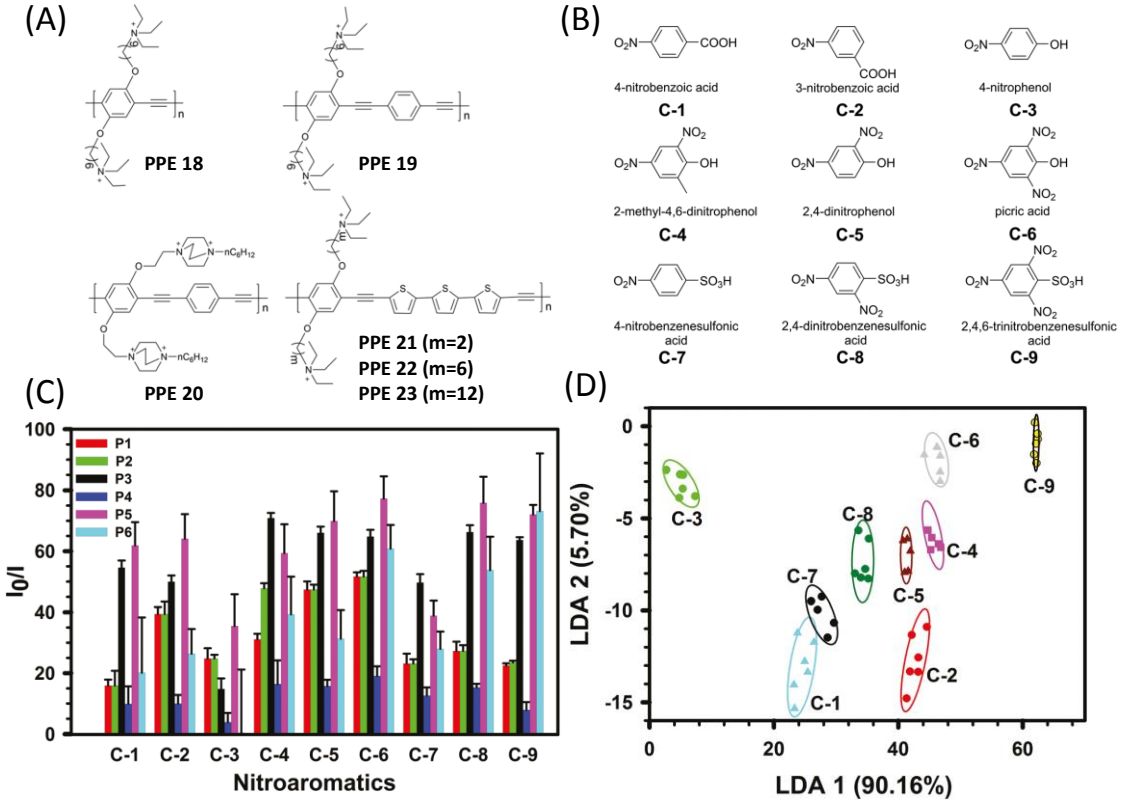

Figure 20. Structures of **(A)** six cationic conjugated polyelectrolytes (CPEs) and **(B)** nine nitroaromatics. **(C)** Fluorescence response patterns constructed based on fluorescence quenching of the six CPEs by nine nitroaromatics. **(D)** 2-D canonical score plot of the fluorescence response patterns obtained by the six CPE sensor array against nine nitroaromatics. Figure reproduced with permission from ref. 99 © 2016, Royal Society of Chemistry.

Recently, our group reported two hyperbranched conjugated polymers (HCPs) with truxene units as core (Figure 21).[100] Different fluorescence quenching responses were displayed, when tested with different nitroaromatic analytes. It was demonstrated that the quenching efficiencies are dependent upon the spectral overlap between the absorbance of the analyte and the emission of the fluorescent

polymer. The fluorescent micelles which were formed by the addition of hydrophobic HCPs into amphiphilic F-127 micelles showed an increased sensitivity compared to the sensing of nitroaromatics in organic solvents.

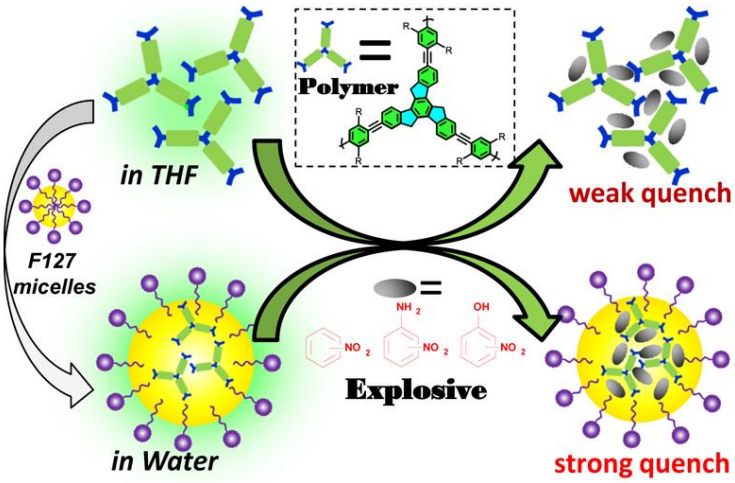

Figure 21. The schematic illustration of hyperbranched conjugated polymers and their micelle-bound conjugated polymers detect nitroaromatic analytes in THF and in water, respectively. Figure reproduced with permission from ref. 100 © 2017, American Chemical Society.

2.1.4 Design and Construction of PPEs

In this contribution, we describe new poly(*para*-phenyleneethynylene)s[80] that are useful for the sensing and discrimination of explosives and nitro-arenes in water. Ever since Swager's seminal papers on sensing of explosives employing fluorescence quenching of "porous" PPEs,[19, 101-102] this field has been an active area for novel concepts. The original applications were geared towards detecting dinitrotoluene (DNT) in the gas phase as indication for the presence of landmines.[103-104] The presence of nitroarenes in aqueous solution is also of great interest, though, as there are significant amounts of maritime ordnance present in bodies of water, particularly in current but also former areas of conflict. While these present less of a direct threat for the populace, the high toxicity of the leaching ordnance can lead to significant environmental problems.[105] Consequently, it is important to investigate and create novel sensor approaches that detect nitroarenes in aqueous solution. PPEs are highly fluorescent in organic solvents, and, when equipped with a branched oligoethylene glycol side chain, they are also fluorescent in aqueous solution, and more or less independent of the types of other substituents are present.[15, 46, 48]

Our concept here is to add a floppy, hydrophobic pocket to such water-soluble fluorescent PPEs; the pocket should modulate and enhance the PPE's binding with electron deficient species, particularly highly nitrated arenes such as TNT and DNT.

2.2 Results and Discussions

2.2.1 Synthesis of PPEs

The two new designed water-soluble conjugated polymers **P3** and **P4** featuring benzylic appendages were obtained as spongy solids with yellow/orange color and show high fluorescence (Figure 22). Starting from the commercially available **1a**/**1b**, a standard bromination reaction afforded **2a**/**2b**. Further treatment with the literature known compound diiodohydroquinone **3**[106], the key monomers **4a**/**4b** were obtained in good to excellent yields. The polymeric ethyl-ester derivatives **6a**/**6b** were synthesized through standard Sonogashira coupling between the diiodo-monomers **4a**/**4b** and the literature known dialkyne **5**[107-108] using $Pd(PPh_3)_2Cl_2$ and CuI in a mixture of THF and piperidine or Hünig's-base at room temperatures for 2 days. Interestingly enough, the ester groups are not cleaved under those conditions, but survived in the presence of the piperidine, much to our surprise.

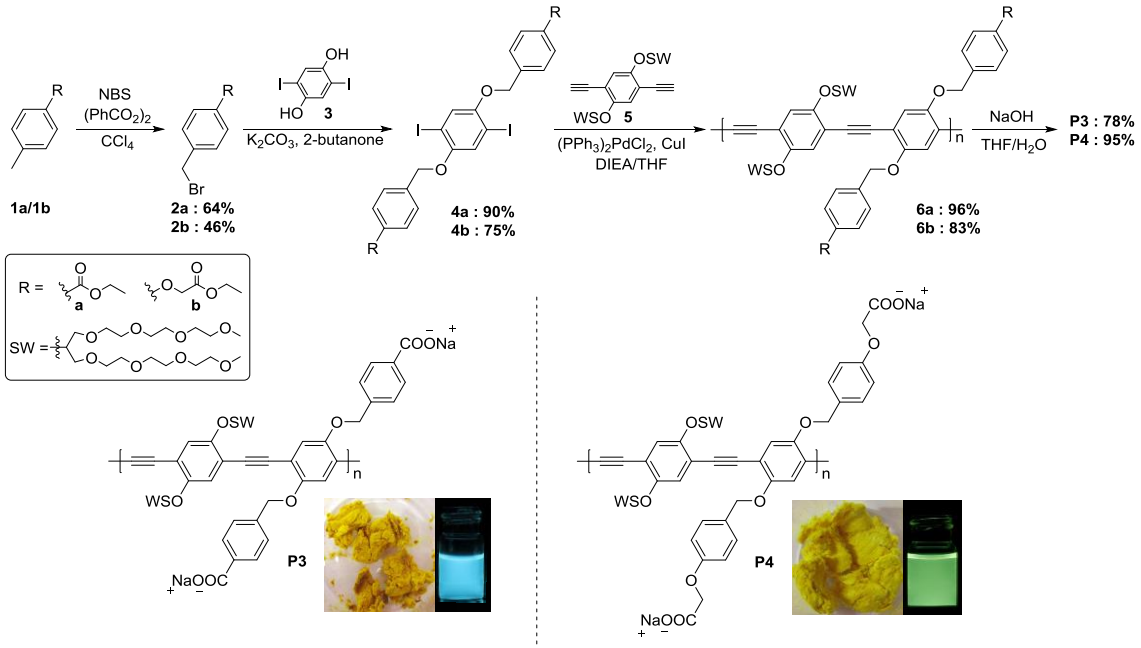

Figure 22. The synthetic route, chemical structures and photographs (left: daylight, right: in water under a hand-held black light with illumination at 365 nm) of **P3** - **P4**. Figure reproduced with permission from ref. 80 © 2017, American Chemical Society.

Saponification, dialysis, and freeze-drying of **6a**/**6b** furnished the final compounds **P3** and **P4**. To prove our design strategy (see Figure 23), two analogous polymers **P1** and **P2** were further prepared as model systems that lack the floppy pocket formed by the two benzylic arms. The number-average molecular weights (M_n) of these polymers are estimated by gel permeation chromatography in a range from 8.3 x 10^3 to 1.3 x 10^4 g/mol, with polydispersities (PDI = M_w / M_n) from 1.3 to 3.1 for all of the described PPEs. The structures and detailed properties of the four polymers are shown in Figure 23 and Table 1.

Table 1. Molecular Weights and Optical Properties of PPEs **P1** - **P4**.

PAE	M_n [g/mol]	M_w/M_n	P_n	solvent	$\lambda_{max,\ abs.}$ [nm]	$\lambda_{max,\ em.}$ [nm]	Φ	τ [ns]	
								465 nm	515 nm
P1	1.0 x10^4	2.2	12	H_2O, pH 7[a]	412	460	0.49	0.70	0.75
P2	1.1 x10^4	1.3	11	H_2O, pH 7[a]	400	462	0.09	0.92	1.53
P3[b]	1.3 x10^4	1.9	10	H_2O, pH 3[a]	448	475, 505	0.01	0.97	1.70
				H_2O, pH 7[a]	433	466, 502	0.39		
				H_2O, pH 13[a]	434	472, 506	0.38		
P4[c]	8.3 x10^3	3.1	6	H_2O, pH 3[a]	457	478, 511	0.05	0.84	1.96
				H_2O, pH 7[a]	441	480, 517	0.29		
				H_2O, pH 13[a]	441	480, 518	0.25		

[a]Buffered at pH 3 (citric acid/NaOH/NaCl), pH 7 (KH_2PO_4/Na_2HPO_4) and pH 13 (glycine/NaOH/NaCl). [b]GPC data measured on the precursor **6a**. [c]GPC data measured on the precursor **6b**.

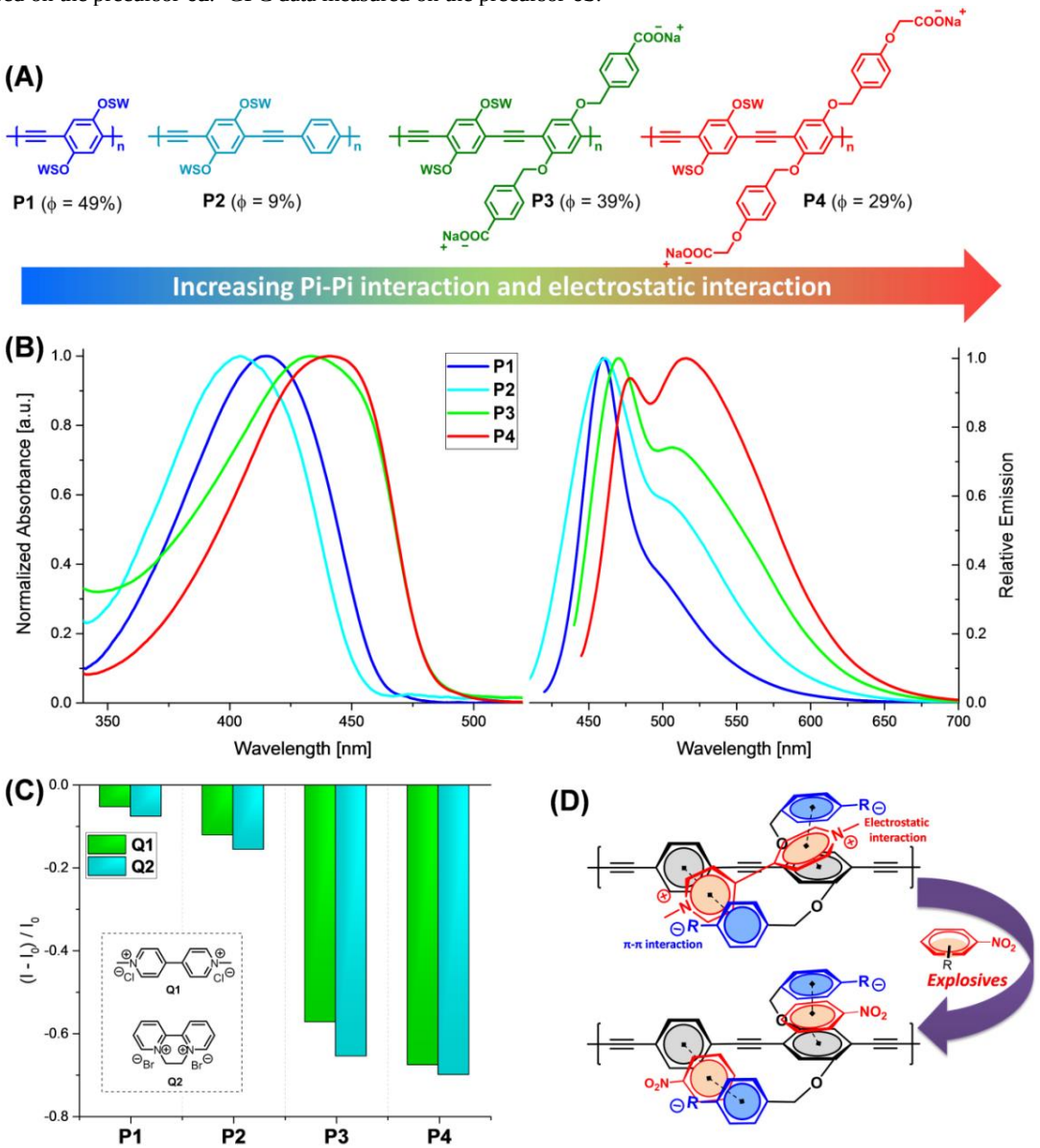

Figure 23. (A) Chemical structures and quantum yields (pH 7, buffered) of **P1** - **P4**. **(B)** Normalized absorption and fluorescence spectra of **P1** - **P4** in pH 7 buffer solution. **(C)** Fluorescence response pattern ($(I - I_0)/I_0$) obtained by **P1** - **P4** (1.3 µM, at pH 7, buffered) treated with **Q1** (Paraquat, 3.3 mM) and **Q2** (Diquat, 3.3 mM). **(D)** Schematic representation of possible interactions between the designed PPEs (**P3**, **P4**) and quenchers. Figure reproduced with permission from ref. 80 © 2017, American Chemical Society.

2.2.2 Optical Spectroscopy and Nitroarene Discrimination and Detection

Figure 23 and Table 1 show the fundamental optical properties of polymers **P1 - P4** in different buffer solutions (pH 3, pH 7 and pH 13). For **P1** - **P2** the optical properties are given only at pH 7 because **P1** and **P2** are non-ionic and show no response to the different buffer solutions. At pH 7, **P4** shows the most red-shifted absorption and emission, followed by **P3**. Both **P3** and **P4** show a strong fluorescence at pH 7 and pH 13, with quantum yields up to 25-39%. However, the fluorescence at pH 3 is mostly quenched, because the carboxylates are protonated and their neutral species are aggregated. Furthermore, polymers **P2 - P4** show a second side peak at 500-520 nm; this observation might result from the planarization of the backbone or more probably formation of excimers.[109] The fluorescence intensity of **P4** at the shoulder at 515 nm is higher than that of **P2** and **P3**, which suggests that **P4** could show stronger π-π stacking interactions than **P2** and **P3**. We carefully investigated the optical properties of the polymers **P1 - P4** and found indeed that the emissive lifetime of the feature at 515 nm is considerably higher than that of the primary peak at 450-460 nm. In **P4**, this effect is particularly distinct and the emission lifetime is almost 2 ns, while that of the primary peak is for almost all of the investigated polymers **P1 - P4** 0.7-1.0 ns (Table 1 and Figure 24). The increase in the lifetime with the red-shifted feature is probably due to excimer-formation of these polymers in water, well visible in **P4**.

To verify the effect of the aromatic side chains in **P3** and **P4**, two efficient electron-transfer quenching agents - paraquat and diquat - were selected for the first exploration of their binding capabilities.[110-111] As shown in Figure 23C, the results of fluorescence quenching response of four PPEs **P1 - P4** toward the two quenchers paraquat Q1 and diquat Q2 indicate that **P3 - P4** react strongest to the quenchers. This phenomenon is probably caused by the strong π-π stacking and an electrostatic interaction between the PPEs and the quencher (Figure 23D).

With this result in hand, we next applied PPEs **P1 - P4** to the detection of explosives. Most explosives are nitro-group-containing aromatic compounds - electron poor species. This property enables their detection through our electron rich PPEs, utilizing electron transfer and/or FRET-type mechanisms.

Figure 25C shows the thirteen analytes selected for further investigation, including twelve nitroaromatics (picric acid (PA), nitrobenzene (NB), dinitrobenzene (DNB), 2,4,6-trinitrotoluene (TNT), dinitrotoluene (DNT), nitrophenol (NP), 2-nitroaniline (2-NA), 3-nitroaniline (3-NA), 2,4-dinitrochlorobenzene (CDNB), 2,4-dinitroanisole (DNMB), 2-nitrochlorobenzene (ONCB) and p-nitrophenol (PNP)) and one control, aniline (A). Figure 25A shows the fluorescence response patterns obtained by our simple sensor array **P1 - P4** (1 μM, pH 7, buffered) treated with thirteen explosive analytes (0.5 mM).

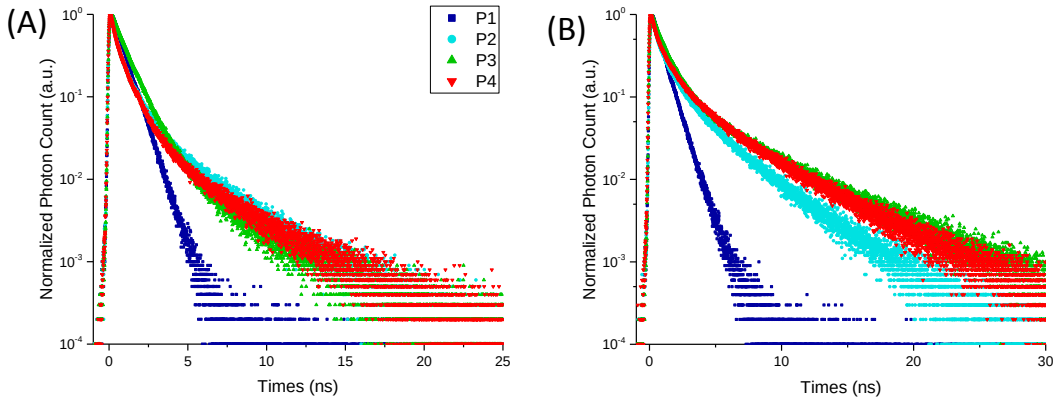

Figure 24. Fluorescence decay profiles of **P1** - **P4** at 465nm **(A)** and 515nm **(B)** in pH 7 buffer solution. Figure reproduced with permission from ref. 80 © 2017, American Chemical Society.

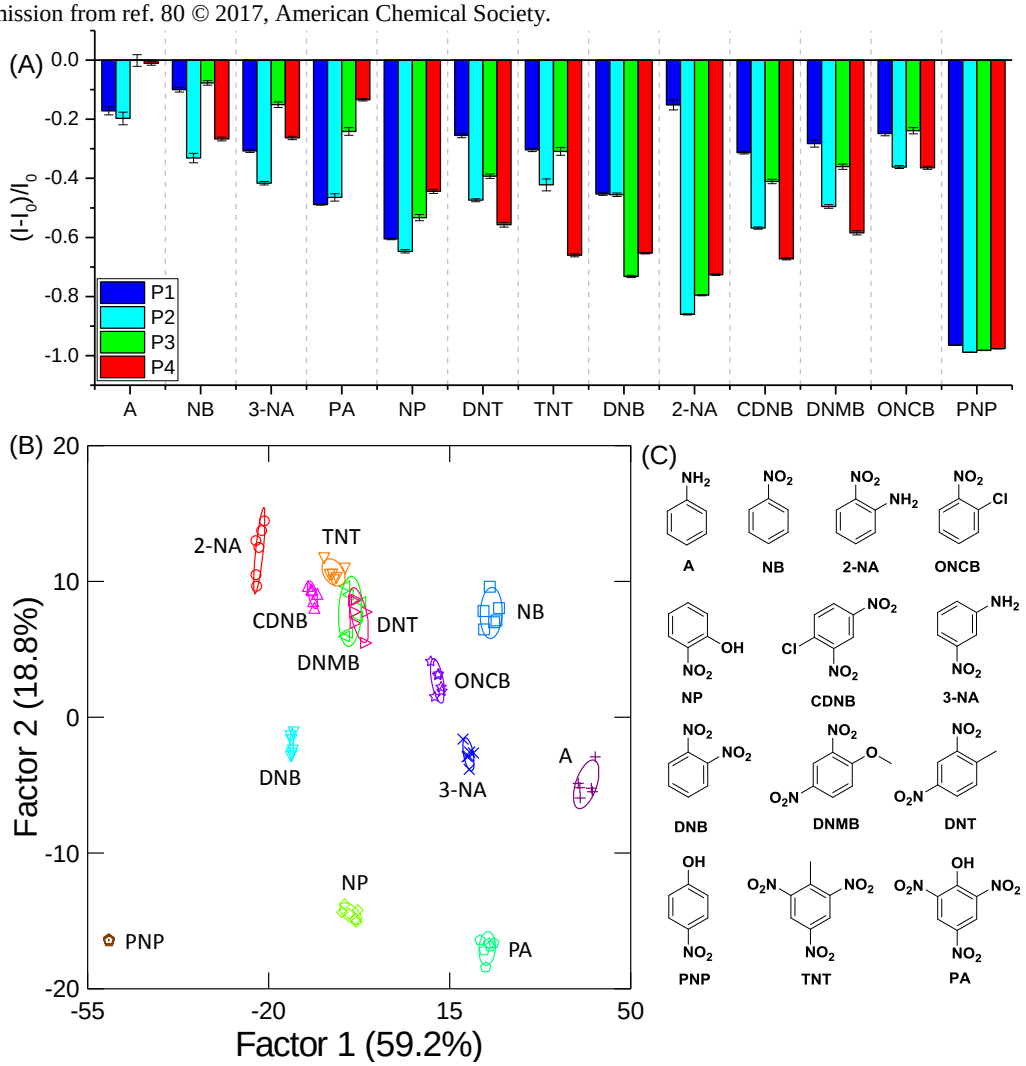

Figure 25. (A) Fluorescence response pattern ($(I-I_0)/I_0$) obtained by **P1** - **P4** (1 μM, pH 7, buffered) treated with analytes (0.5 mM). Each value is the average of six independent measurements; each error bar shows the standard error (SE) of these measurements. **(B)** 2D canonical score plot for the first two factors of fluorescence response patterns obtained with an array of the PPEs **P1** - **P4** (1 μM, pH 7, buffered) with 95% confidence ellipses. Each point represents the response pattern for a single analyte in the array. **(C)** Structures of the used analytes. Figure reproduced with permission from ref. 80 © 2017, American Chemical Society.

As expected, fluorescence quenching is only observed for the nitroaromatics, the control (aniline) shows almost no effect. The fluorescence intensity changes were recorded and later analyzed by linear discriminant analysis; the resulting data grouped according to their Mahalanobis distances, which converts the training matrix (4 polymers × 13 analytes × 6 replicates) into canonical scores. The two

main canonical factors were used to construct a 2-D discrimination plot with thirteen different groups. As illustrated in Figure 25B, the thirteen clusters are quite clear, only overlaps between DNT and DNMB were observed, which is not too surprising because of the close chemical similarity of the analytes. The jackknifed classification matrix with cross-validation reveals 99% accuracy, only one sample from DNT was misclassified as DNMB (Table 9 and Table 11). We observe that Factor 1 represents the overall quenching ability of the analytes toward the explosive quencher. These results show that the array **P1** - **P4** discriminates the nitro-aromatics. We also note that the small sensor array composed of linear polymers **P3** and **P4** alone discriminates the different explosives (Figure 26). The jackknifed classification matrix with cross-validation reveals 96% accuracy (Table 12 and Table 14).

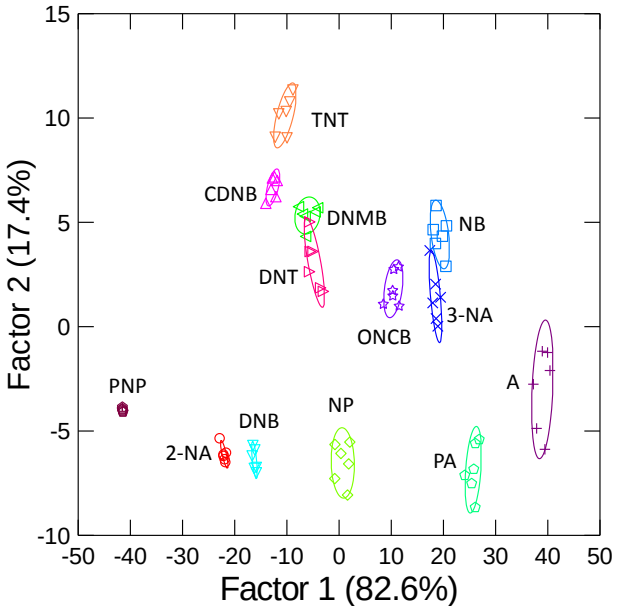

Figure 26. 2-D canonical score plot of fluorescence response patterns obtained with an array of the PPEs **P3** - **P4** (1 μM, pH 7, buffered) with 95% confidence ellipses. Each point represents the response pattern for a single analyte in the array. Figure reproduced with permission from ref. 80 © 2017, American Chemical Society.

To validate the efficiency of our sensing system, we performed blind tests with randomly chosen analytes of our training set; all samples were blind tested randomly for four times. The new cases are classified into thirteen new groups, generated through the training matrix, based on their shortest Mahalanobis distance to the respective group. 50 of the 52 unknown explosive samples were correctly identified, revealing a 96% accuracy of our system (Table 10).

2.2.3 Concentration-Dependent Analysis of Explosives

We found that the pH did not have a great effect on the sensitivity of the polymers towards the randomly chosen analytes, so we worked at pH 7 (Figure 27). To further explain the reactivity and selectivity of our tongue, we performed a quantitative comparison between polymers **P1** - **P4** and the thirteen analytes. As shown in Figure 28, all thirteen analytes show different quenching abilities upon increasing their concentration. Compare with **P1** and **P2**, the concentration-dependent curves of **P3**

and **P4** show almost no overlap. This indicates that a quantitative analysis should be possible with our PPE-tongue using **P3** and **P4** alone.

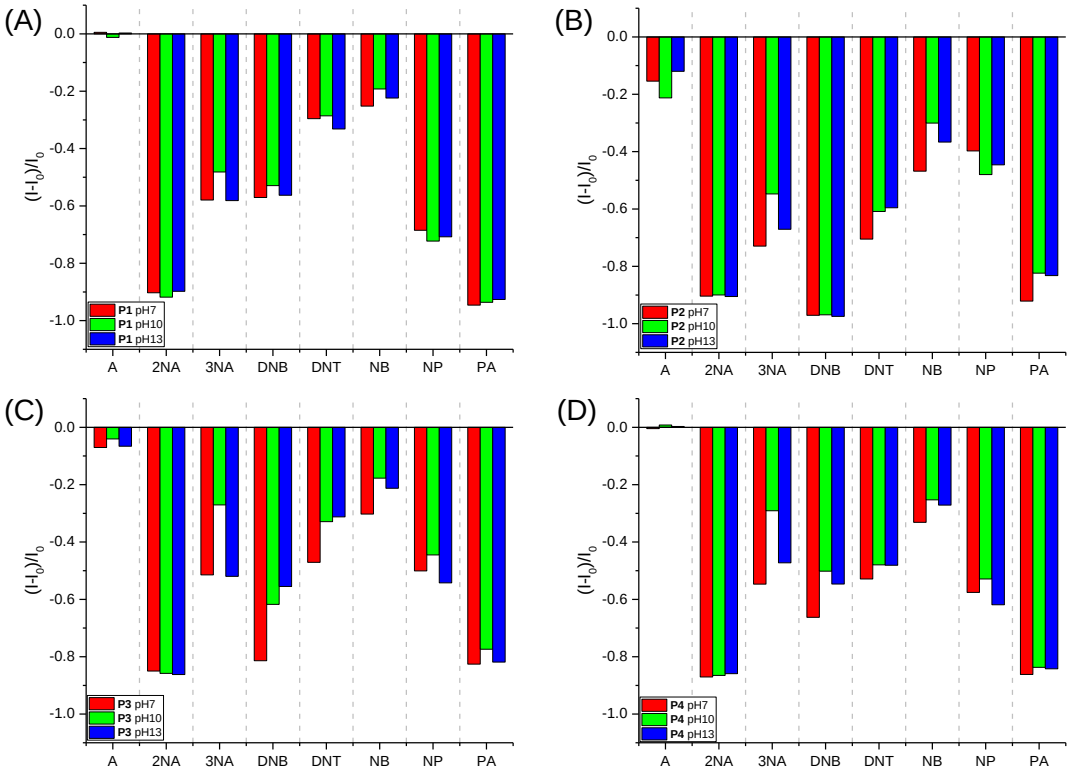

Figure 27. Fluorescence response pattern ($(I-I_0)/I_0$) obtained by **(A) P1** (1 μM), **(B) P2** (1 μM), **(C) P3** (1 μM) and **(D) P4** (1 μM) treated with analytes (0.5 mM) at different buffered solution. Figure reproduced with permission from ref. 80 © 2017, American Chemical Society.

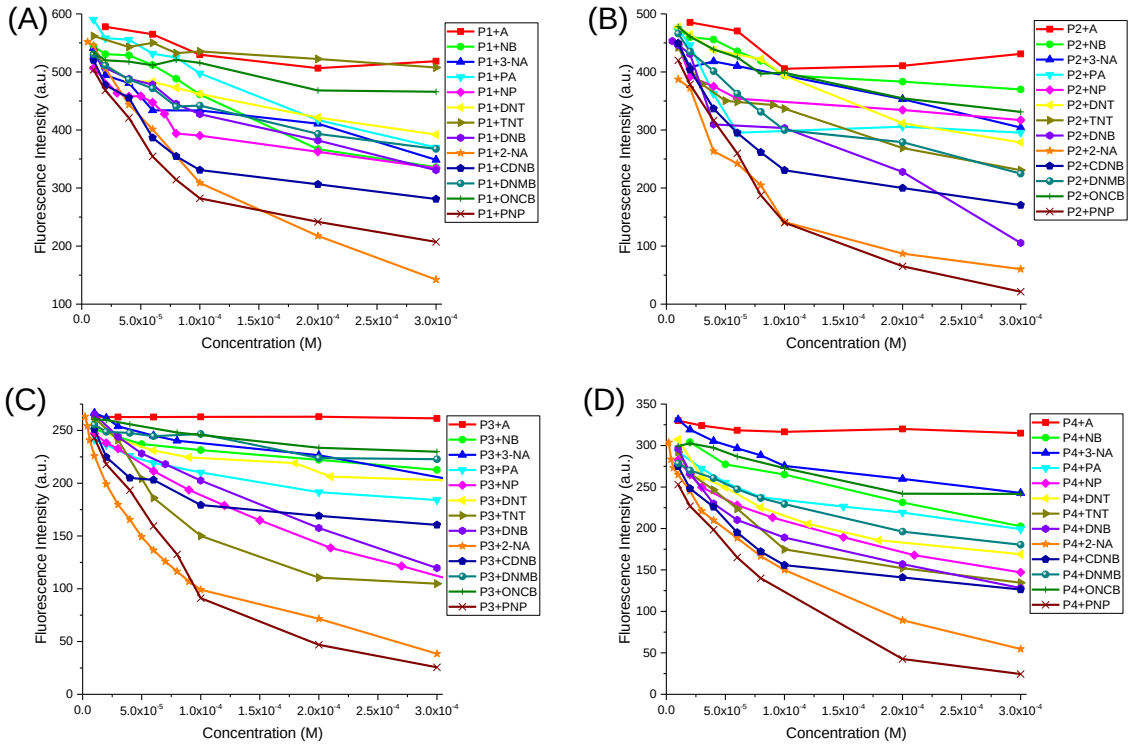

Figure 28. Fluorescence intensity change of **(A) P1** (0.5 μM), **(B) P2** (0.5 μM), **(C) P3** (0.5 μM) and **(D) P4** (0.5 μM) treated with different concentrations of the analytes at pH 7 (buffered). Figure reproduced with permission from ref. 80 © 2017, American Chemical Society.

Figure 29 and Table 2 showed the K_{sv} constants measured by a modified Stern-Volmer equation[48, 112] for the fluorescence quenching of polymers **P1 - P4** with the different nitroarenes. One can see that **P1** is particularly sensitive towards PNP, CDNB, 2-NA, and nitrophenol, while the most hydrophobic polymer, **P2**, is most sensitive towards PNP and 2-NA but not very sensitive towards TNT. Overall, **P3**, in which the benzylic group is acceptor substituted, displays on average considerably lower Stern-Volmer constants when looking at the quenching data for the nitro-arenes (see Table 2). An exception is 2-NA. We interpret this data such that for 2-NA FRET is the major quenching mechanism - independent from the electronic situation of the polymer and only dependent upon the emission spectral overlap of the FRET donor, i.e. the PPE with the UV-vis spectrum of 2-NA. In the other cases FRET may also occur but is probably not the major mechanism, as excited state electron transfer is more efficient in more acceptor substituted nitro-arenes and in more donor-substituted PPEs, here **P4**.

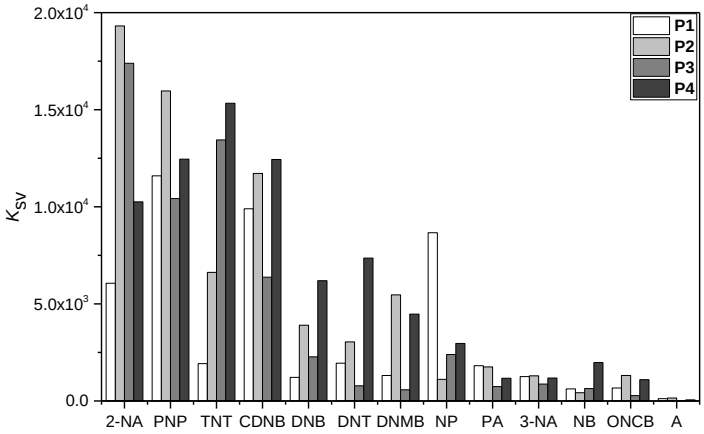

Figure 29. Stern-Volmer constants (K_{sv}) of **P1 - P4** with different analytes at pH 7 (buffered).

Table 2. K_{sv} Values and Limits of Detection (LOD) for **P1 - P4** toward each Analyte.

Analyte	K_{sv}				LOD			
	P1	**P2**	**P3**	**P4**	**P1** [mol/L]	**P2** [mol/L]	**P3** [mol/L]	**P4** [mol/L]
A	119	152	16	59	1.6×10^{-4}	1.3×10^{-4}	4.5×10^{-4}	5.4×10^{-4}
NB	6.2×10^{2}	4.26×10^{2}	6.37×10^{2}	1.98×10^{3}	3.1×10^{-5}	6.1×10^{-5}	1.2×10^{-5}	2.2×10^{-6}
3-NA	1.25×10^{3}	1.29×10^{3}	8.73×10^{2}	1.18×10^{3}	1.5×10^{-5}	1.5×10^{-5}	8.3×10^{-6}	3.3×10^{-6}
PA	1.81×10^{3}	1.75×10^{3}	7.40×10^{2}	1.17×10^{3}	1.1×10^{-5}	1.4×10^{-5}	1.0×10^{-5}	4.0×10^{-6}
NP	8.66×10^{3}	1.11×10^{3}	2.39×10^{3}	2.96×10^{3}	2.1×10^{-6}	2.2×10^{-5}	3.1×10^{-6}	1.5×10^{-6}
DNT	1.94×10^{3}	3.04×10^{3}	7.80×10^{2}	7.36×10^{3}	9.8×10^{-6}	8.5×10^{-6}	9.4×10^{-6}	5.5×10^{-7}
DNB	1.21×10^{3}	3.90×10^{3}	2.27×10^{3}	6.20×10^{3}	1.5×10^{-5}	5.3×10^{-6}	3.2×10^{-6}	6.5×10^{-7}
TNT	1.92×10^{3}	6.62×10^{3}	1.34×10^{4}	1.53×10^{4}	9.7×10^{-6}	2.4×10^{-6}	5.5×10^{-7}	2.7×10^{-7}
2-NA	6.07×10^{3}	1.93×10^{4}	1.74×10^{4}	1.03×10^{4}	3.1×10^{-6}	1.0×10^{-6}	4.2×10^{-7}	4.0×10^{-7}
CDNB	9.90×10^{3}	1.17×10^{4}	6.37×10^{3}	1.24×10^{4}	1.9×10^{-6}	1.7×10^{-6}	1.2×10^{-6}	3.3×10^{-7}
DNMB	1.31×10^{3}	5.46×10^{3}	5.76×10^{2}	4.48×10^{3}	1.4×10^{-5}	3.8×10^{-6}	1.3×10^{-5}	9.1×10^{-7}
ONCB	6.70×10^{2}	1.31×10^{3}	2.77×10^{2}	1.10×10^{3}	2.9×10^{-5}	1.6×10^{-5}	2.7×10^{-5}	3.7×10^{-6}
PNP	1.16×10^{4}	1.60×10^{4}	1.04×10^{4}	1.25×10^{4}	1.6×10^{-6}	1.3×10^{-6}	7.2×10^{-7}	3.2×10^{-7}

2.2.4 Quenching Mechanism for Polymers toward Explosives

Next, we investigated the quenching mechanism, as in principle static and dynamic quenching could be operative and even coexist. For static quenching, the fluorescence decay lifetime of the sensors will remain unchanged as the concentration of the quencher is increased. For dynamic quenching, however, the collision of the quencher with the excited fluorophores is necessary, and quenching occurs when a photo-excited sensor interacts with a colliding analyte, thus it results in a decrease in the fluorescence lifetime. We investigated the fluorescence lifetimes of our polymers in the absence and presence of the analyte 2-NA. Concentration-dependent fluorescence lifetimes of **P1** - **P4** treated with 2-NA were measured (Figure 30). We found that the excited-state fluorescence lifetime dropped only slightly with an increasing concentration of 2-NA, which indicates static quenching as the main quenching mechanism, not unexpected for the short fluorescence lifetimes observed for the conjugated polymers of the PPE-type.

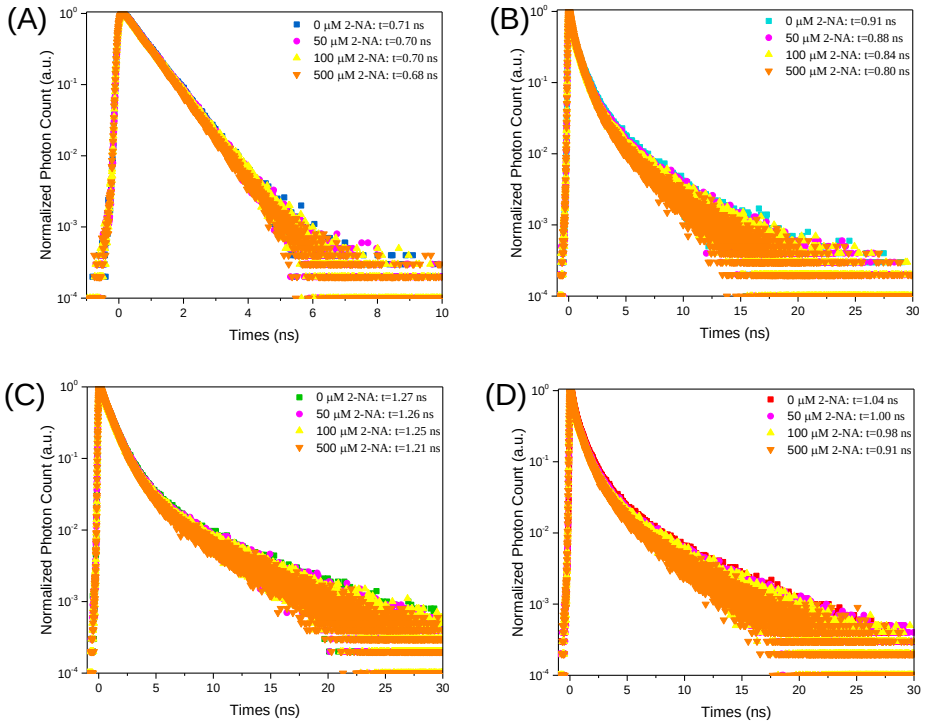

Figure 30. Fluorescence decay profiles of (**A**) **P1** at 460nm, (**B**) **P2** at 460nm, (**C**) **P3** at 475nm and (**D**) **P4** at 475nm in pH 7 buffer solution with different concentrations of 2-NA. Figure reproduced with permission from ref. 80 © 2017, American Chemical Society.

2.2.5 Conclusions

In conclusion, we have prepared two novel PPEs **P3** and **P4** with additional flexible binding pockets. These water-soluble, yet hydrophobic polymers, present fairly sensitive reactivity towards nitroarenes, particularly TNT, DNT and DNB as well as picric acid, each of which are raw materials employed in the production of land and sea mines, and therefore important analytes, leaching out of unexploded ordnance in bodies of water. A particularly nice result is that the most electron rich polymer **P4** is also

the most sensitive one, being able to detect DNT, the ubiquitous decomposition product of TNT, and present in TNT itself in sub-micromolar concentrations in water. We also note that there is differential quenching with the polymers **P1 - P4**, which allows discriminating the different nitroaromatics without any problem. Our goal was to both detect but also to discriminate the different nitroarenes, which was well possible with a small array of conjugated polyelectrolytes displaying flexible binding pockets.

Chapter 3. Simple Optoelectronic Tongues Discriminate Amino Acids

3.1 Introduction of Amino Acids

Amino acids, the building blocks for proteins and metabolites, are small molecules with functional side groups, which reflect in different roles of amino acids in physiological processes. The sensing of individual amino acids is necessary for a variety of applications, such as nutritional analysis, and the diagnosis of diseases such as pancreatitis, Alzheimer, and other biological issues.[113-115] For all these applications, the ability to easily and quickly obtain fingerprints for different amino acids is desirable.

Currently, the most used analytical procedures for amino acid determination are based on chromatographic,[116] spectroscopic,[117] or electrochemical[118] methods. However, these techniques are relatively expensive and require complicated sample pretreatment and trained personnel. Besides instrumental techniques, colorimetric and fluorimetric chemosensors have also been reported for the detection of amino acids, such as cysteine, histidine, aspartic acid, etc.[119-120] Although the detection of specific amino acids with distinctive function groups has advanced, their use to establish the identity of all 20 natural amino acids is still limited, because they cannot differentiate among the individual amino acids with high similarity in molecular configuration.

In contrast to the specific sensors for each analyte, the use of "chemical nose/tongue" strategies have emerged as an appealing powerful tool for identifying a number of analytes.[23-24, 52, 121-122] Each element of the sensor array is partially selective, and it is the overall response of the array that gives specificity for each analyte. Array-based sensors can, therefore, discriminate various analytes with high throughput and accuracy, but very few attempts have been reported for amino acids.

Recent progress in the field of amino acid sensing has focused on the use of fluorescent and colorimetric methods for the discrimination of amino acids. Specific reactions between probes and amino acids, IDA, metal complexes coordination, and other ways have been widely utilized.[119] In the specific reactions between probes and amino acids, "binding site" part (receptor) and "signaling" part (indicator) of the probe are linked through a covalent bond, and the interaction of amino acids with the binding site alters the electronic properties of the signaling part, resulting in sensing of the target analytes through color change or emission modulation. Essentially, the binding between amino acids and the receptor is labile and reversible and involves electrostatic interactions, hydrogen bonding and metal-ligand interactions, etc.[123-124]

In addition to covalently attached receptor-spacer-indicator paradigm for amino acids sensing, the indicator-displacement assay (IDA), which uses binding sites and signaling parts to create a receptor/indicator ensemble through non-covalent interactions, is currently the other primary analytical tool.[120, 125] The sensing principle of IDA relies on the competition between the analytes and indicator. When specific amino acids are added to a solution containing a host-indicator complex, the indicators will be displaced from the complex and change in their optical properties can be observed. By changing the receptor-indicator ratio or sensing conditions, the selectivity and sensitivity can be

modulated, thus making this type of supramolecular approach particularly useful for the detection of structurally similar analytes.

Metal complex coordination has widespread use in detecting amino acids because metal ions can represent the active binding site for interacting with amino acids.[126] The covalent or noncovalent interactions, such as electrostatic and hydrogen interactions, *etc*. between a metal center and amino acids is often a convenient route for achieving strong binding.[120] In this case, amino acids can capture metals from organometallic systems and thus resulting in a change in the signal's optical properties.

3.2 Sensor Arrays Discriminate Amino Acids

Sensor array based pattern recognition is a powerful tool because it can analyze a wide range of chemical structures. The use of less expensive and more commonly used instruments, such as UV-Vis spectroscopy or fluorescence spectroscopy allow easy and rapid analysis of multiple samples by using a microplate reader.

Buryak and Severin reported a chemosensor array for the colorimetric identification of 20 natural amino acids using IDA in combination with multivariate analysis.[121] UV-Vis spectra of one organometallic complex and three indicators were utilized to pattern recognition of natural amino acids through two discrimination steps and seven pH environments (Figure 31A). Using this pattern recognition approach, only Val and IIe showed some overlap; the hydroxy amino acids, such as Ser and Thr, and the aromatic amino acids, such as Phe, Tyr, and Trp, were positioned in proximity to each other (Figure 31B).

Song[127] and co-workers developed a facile sensor chip composed of one photochromic molecule with metal ions to realize identification of the full 20 natural amino acids. The metal ions can form metallic complexes with spirooxazine while amino acids compete in the metallic coordination (Figure 32A). Upon addition of amino acids, the coordination between the spirooxazine-metallic complex and amino acids promotes the formation of a new balance; different amino acids lead to diverse balances with different fluorescence. Thus, a distinct fluorescent fingerprint pattern of each amino acid is achieved (Figure 32B).

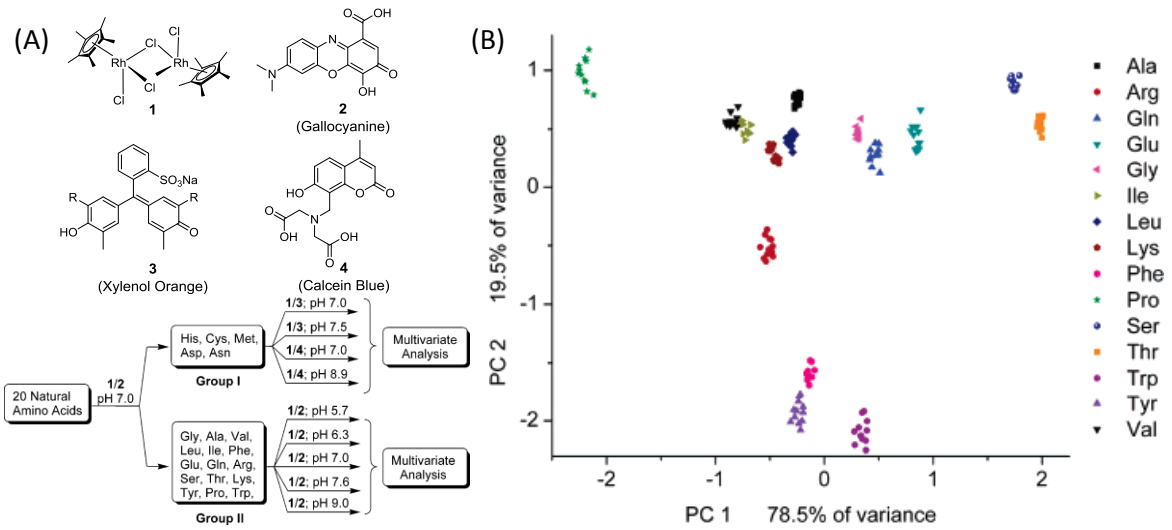

Figure 31. (A) Colorimetric identification of 20 natural amino acids using IDA arrays composed of receptor **1** and the indicators **2-4** at different pHs. **(B)** Score plot for the identification of the amino acids of group II. Figure reproduced with permission from ref. 121 © 2005, American Chemical Society.

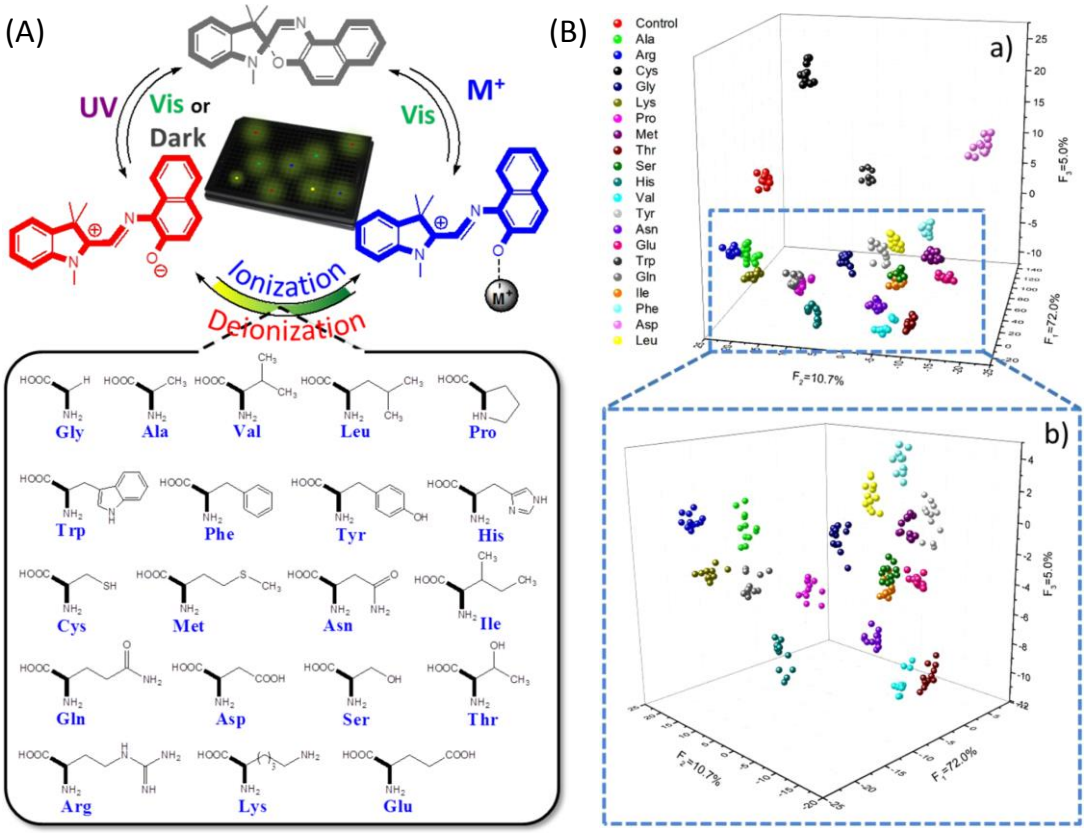

Figure 32. (A) Scheme of 20 natural amino acids identification by photochromic sensor chip composed of TNSP-Metallic complexes. **(B)** Graph of LDA result shows a clear clustering of the 20 natural amino acids and 1 PBS sample as control and the corresponding magnified image. Figure reproduced with permission from ref. 127 © 2014, American Chemical Society.

Macrocycles, such as cucurbiturils, cyclodextrins, *etc.* also played an important role in the enantioselective recognition with fluorescence of a-amino acids derivatives through host-guest interaction. A sensor array constructed by combining four fluorescent tricyclic basic dyes with cucurbiturils (Figure 33A) was reported by Baumes and Garcia *et al.*[128] Amino acids can form strong hydrogen bonds with dyes and organic capsules due to amine and carboxylate groups. As shown in Figure 33B, the chemosensor array achieved a perfect cross-selectivity for amino acids and allowed an

immediate detection and discrimination of amino acids simply by analyzing the image (color change in fluorescence images). Another promising system constructed by Aswathy and Sony using gold nanoparticles (AuNPs)-β-cyclodextrin (β-CD)-fluorescein assembly as a versatile chiroselective platform for chiral amino acids sensing had been described (Figure 34).[129] By accommodating fluorescein into the hydrophobic cavity of β-CD, energy transfer occured through the donor and quencher nearby. Upon addition of Trp, Phe and Tyr to the assembly, the FRET effect was inhibited because of the favored interaction of the phenyl ring with the β-CD receptor, which expelled fluorescein from the cavity and thus recovered the fluorescence of the quenched dye. However, this assembly is only effective for the chiro-selective optical discrimination between D, L-Trp, D, L-Phe and D, L-Tyr. Utilizing the similar mechanism, recently, Wei's group developed a novel chiral sensor array based on multi-types of host molecule modified two-dimensional MoS_2 nanosheets (MNSs).[130] Due to the combination of multiple host-guest interactions, the sensor array can obtain more information on amino acids, such as chirality, polarity, charge, and size simultaneously, and thus enable accurate discrimination of achiral Gly, 19 L-amino acids and the corresponding 19 D-enantiomers (Figure 35).

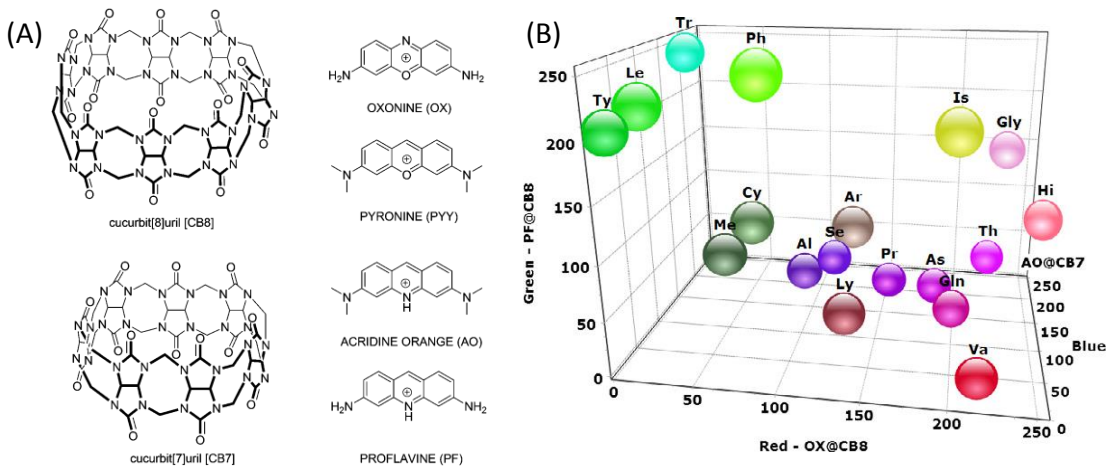

Figure 33. (A) Structures of cucurbiturils and tricyclic basic dyes oxonine, pyronine, acridine orange, and proflavine. **(B)** PCA-like representation based on three selected chemosensors. Figure reproduced with permission from ref. 128 © 2011, Elsevier.

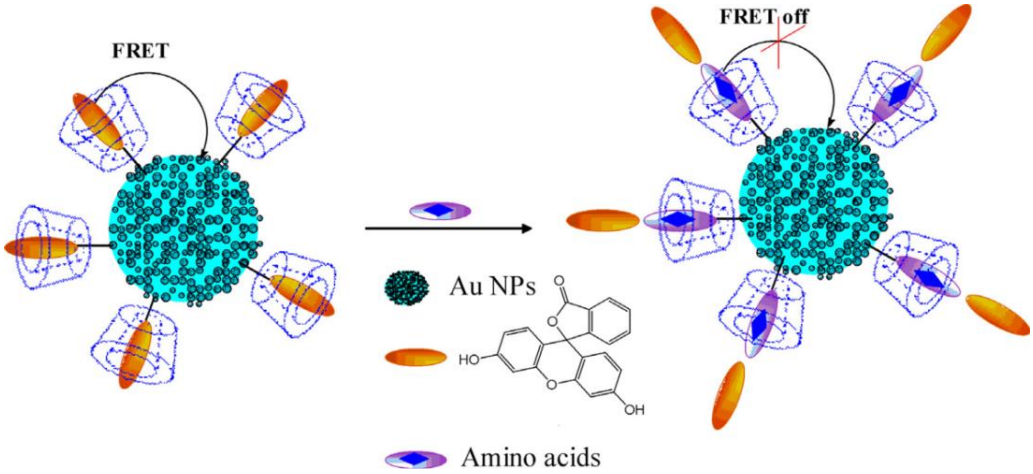

Figure 34. Schematic illustration of FRET-based amino acids sensing strategy. Figure reproduced with permission from ref. 129 © 2014, Elsevier.

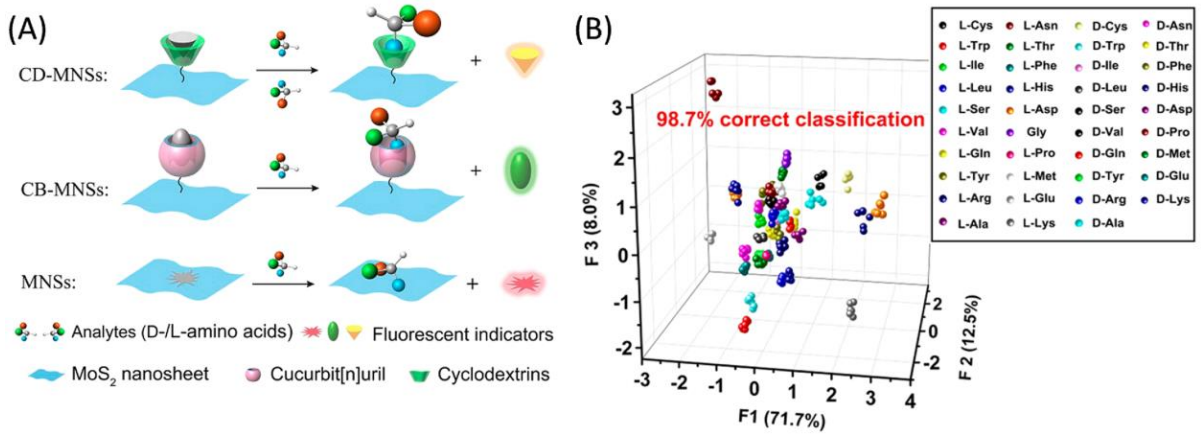

Figure 35. (A) The schematic illustration of fabrication of a chiral sensor array based on multi-types of host molecule-modified MNSs. **(B)** LDA canonical score plot for the fluorescence response of the sensors array to 39 amino acids (19 L-amino acids, 19 D-amino acids, and Gly). Figure reproduced with permission from ref. 130 © 2018, American Chemical Society.

3.3 PPE/GFP-Based Sensory for Sensing of Amino Acids

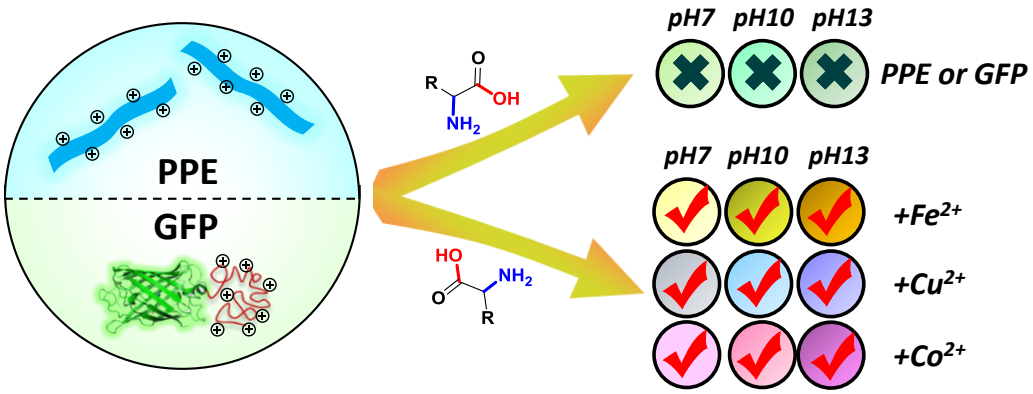

Figure 36. The systematic illustration of PPE/GFP-based sensory for the identification of amino acids in the absence and presence of metal salts. Figure reproduced with permission from ref. 49 © 2017, Wiley-VCH Verlag GmbH & Co. KGaA.

Wet-chemical discrimination of amino acids is still a challenge due to their similarity in structure. In this chapter, we report a self-assembled sensor array based on a combination of positively charged water-soluble poly(*para*-phenyleneethynylene) or green fluorescent protein (GFP, collaborated with Prof. Andreas Herrmann, from Zernike Institute for Advanced Materials, University of Groningen) and three metal ions (Fe^{2+}, $Co^{2+}$and Cu^{2+}) at three different pH-values (pH 7, 10 and 13). The array discriminates all of the 20 natural amino acids in water according to their differential fluorescence intensity modulation. The responses are analyzed by linear discriminant analysis, and sort according to the amino acid type: hydrophobic, polar, negatively charged, positively charged and aromatic amino acids all cluster very well.

3.3.1 Design and Construction of Chemical tongue

Sensing of simple but also of complex analytes by optoelectronic tongues has experienced an upswing after Anslyn,[24, 131] Suslick,[23] and Severin.[121, 132-134] They developed powerful concepts for the

discrimination of analytes employing sensor fields. The main concepts are dye displacement, a modified lock-and-key approach or arrays of chemically different dyes; both concepts are useful for colorimetric discrimination of a wide variety of analytes from, for example, red wine to coffee grounds.[33, 75, 135] Rotello, Bunz, and co-workers have employed electrostatic complexes composed of a fluorescent conjugated polymer and positively charged gold nanoparticle to discriminate proteins, bacteria, and cells.[38, 43, 45]

We recently started to examine chemical/molecular tongues composed of simple fluorescent conjugated polymers alone and with simple adjuvants (oppositely charged polymers, detergents, peptide etc.) to discriminate and identify analytes, such as carboxylic acids, nonsteroidal anti-inflammatories, fruit juices, and white wines.[46, 48, 76, 79, 112, 136-137] In all of these cases, a small to medium sized array of fluorophores discriminates the analytes. The fluorescence response (an increase or decrease of intensity) of the single elements is not useful in itself; however, the combined responses, particularly when analyzed by statistical methods, such as linear discriminant analysis,[51-52] allow the identification and discrimination of analytes-be they complex or simple.

An important question is the resolution of these tongues, that is, whether can they discriminate similar analytes. Herein, we tackle that problem and look at amino acids as suitable test bed. We find that poly(*para*-phenyleneethynylene)s (PPEs) or green fluorescent proteins (GFPs) themselves are not enough to discriminate; however, in the presence of different transition-metal ions discrimination works well (Figure 36).

3.3.2 Screening Process

In a first experiment, we treated **P5** or **GFP-K72** (Figure 37) with the 20 naturally occurring amino acids (25 mM) at three different pH values (pH 7, 10 and 13); however, we could not find strong fluorescence change of amino acids with the PPE or GFP, with exception of the aromatic ones and proline, which induced some quenching of the PPEs' fluorescence (Figure 38). In a control experiment, we also investigated the interactions of the 20 amino acids with three metal salts ($Fe(ClO_4)_2$, $Cu(ClO_4)_2$, $Co(ClO_4)_2$) in a buffer solution of different pH (pH 7, pH 10 and pH 13). We found that only cysteine and histidine gave color changes, but none of the other ones (see Figure 39).

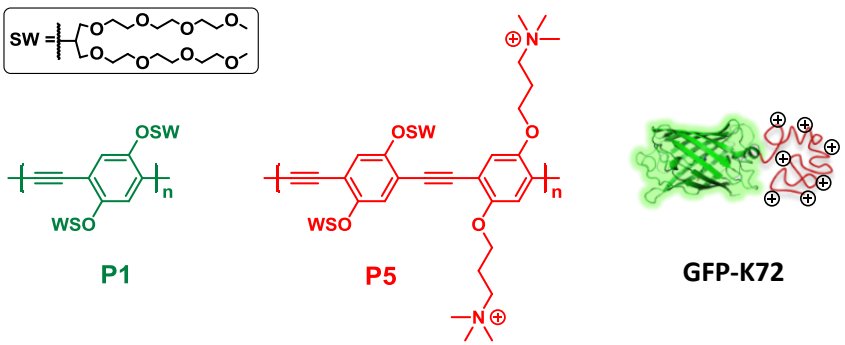

Figure 37. Structures of PPEs and GFP used for sensing. Figure reproduced with permission from ref. 49 © 2017, Wiley-VCH Verlag GmbH & Co. KGaA.

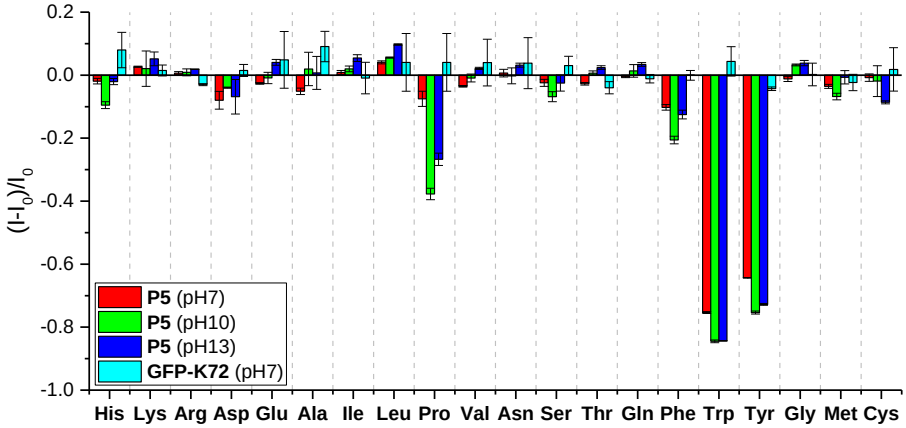

Figure 38. Fluorescence response pattern ((I - I_0) / I_0) of **P5** (1 μM) at pH 7, 10 and 13 (buffered) and **GFP-K72** (20 nM) at pH 7 (buffered) after treating with 20 natural amino acids (25 mM) (buffer solutions: pH 7 (KH_2PO_4/Na_2HPO_4), pH 10 (borax/NaOH), and pH 13 (KCl/NaOH)). Each value is the average of two independent measurements; each error bar shows the standard deviation (SD) of these measurements. Figure reproduced with permission from ref. 49 © 2017, Wiley-VCH Verlag GmbH & Co. KGaA.

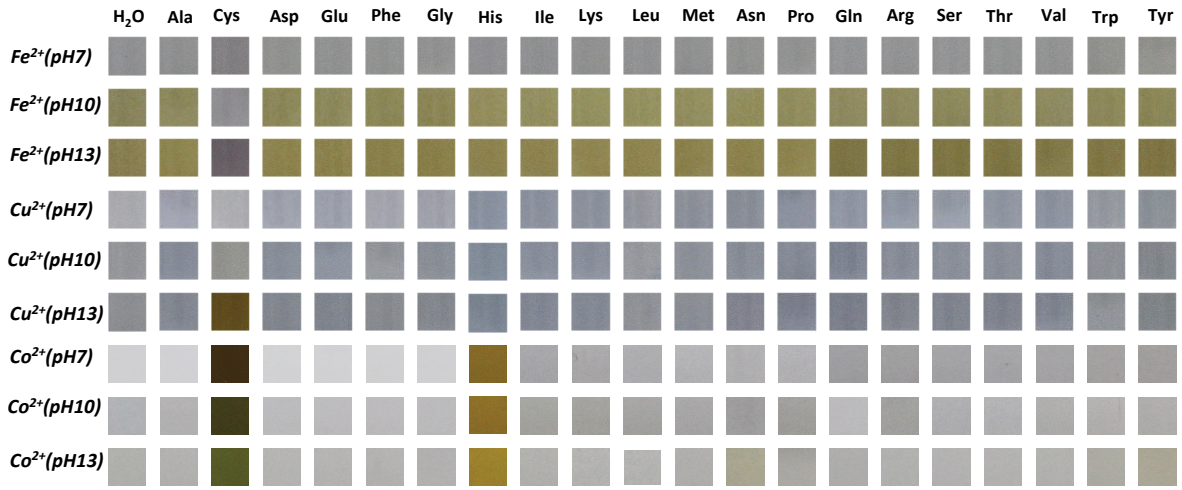

Figure 39. Photographs of **P5** (1 μM) with 20 amino acids (25 mM) in the presence of Fe^{2+}, Cu^{2+} and Co^{2+} (1 mM) at pH 7, 10 and 13 buffer solution. Figure reproduced with permission from ref. 49 © 2017, Wiley-VCH Verlag GmbH & Co. KGaA.

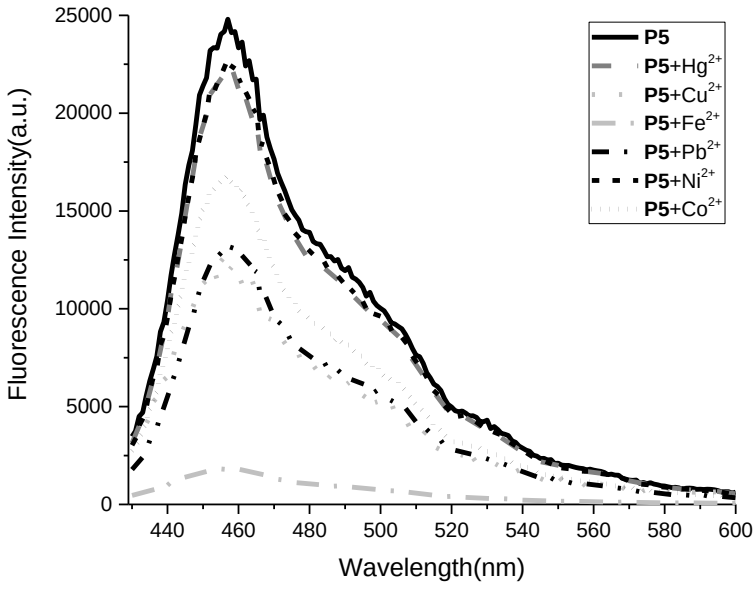

Figure 40. Fluorescence response of **P5** (1 μM) with different metal salts (1 mM) at pH 7.

It is known that transition-metal ions can quench fluorescence through energy transfer or electron transfer mechanisms due to the interaction between the complexed metal and the excited chromophore.[93, 138-142] We investigated the response of **P5** towards aqueous solutions of metal salts and found, despite the fact that the PPE is positively charged, that the metal salts lead to a significant decrease in fluorescence intensity (Figure 40). We assume that either the anions of the metal salts coordinate to the ammonium ions and/or that the metal ions are coordinated to the branched oligoethylene glycol moieties, attached to the PPE.[143-144]

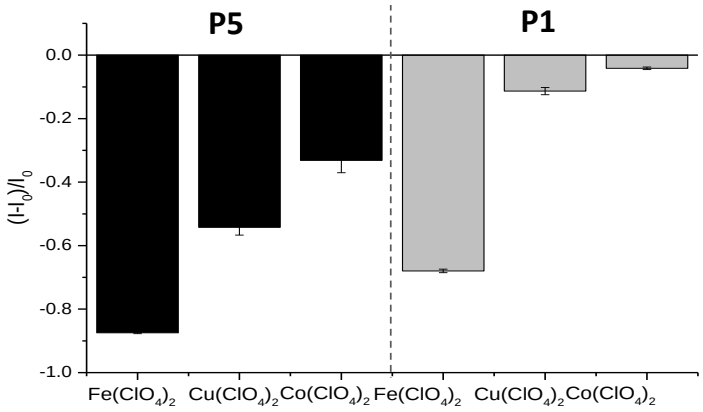

Figure 41. Fluorescence response of **P1** and **P5** (1 μM) with Fe^{2+}, Cu^{2+}, and Co^{2+} (1 mM) at pH 7 buffer solution. Each value is the average of three independent measurements; each error bar shows the standard deviation (SD) of these measurements.

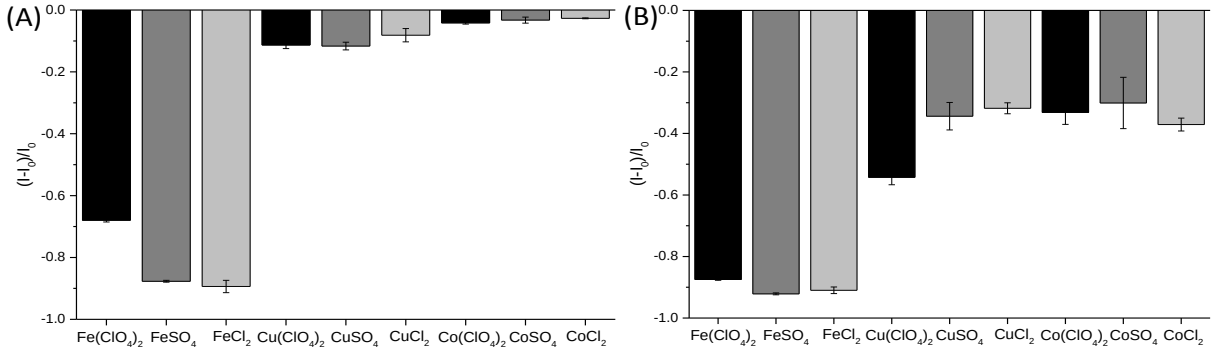

Figure 42. Fluorescence response of **(A) P1** (1 μM) and **(B) P5** (1 μM) treated with metal ions Fe^{2+}, Cu^{2+}, and Co^{2+} (1 mM) composed of different anions (ClO_4^-, Cl^-, and SO_4^{2-}) at pH 7 buffer solution. Each value is the average of three independent measurements; each error bar shows the standard deviation (SD) of these measurements.

Understanding the interactions between metal ions and polymers is important. The following studies were performed: first, we investigated the fluorescence intensity change of polymers **P5** (with hydrophilic swallowtail and positively charged side chain) and **P1** (only with hydrophilic swallowtail) toward three metal ions (Figure 41). We found that metal ions quench both of the two polymers, indicating that metal ions coordinate to the branched oligoethylene glycol moieties and contribute to the quenching. A stronger quenching of **P5** towards metal ions was observed than that of **P1**. This can be explained by the existence of oxygen and positively charged side chain with the ammonium. Oxygen may also bind to metal ions and positively charged side chain may interfere the interactions between oligoethylene glycol moieties and metal ions, leading to further quenching. Then we further investigated fluorescence response of **P1** and **P5** toward metal ions Fe^{2+}, Cu^{2+}, and Co^{2+} by changing their anions. Three different types of anions (ClO_4^-, Cl^-, and SO_4^{2-}) were selected for our study. As can

be seen in Figure 42, by changing their anions from ClO_4^- to $SO_4^{2-}$and Cl^-, negligible fluorescence intensity change was observed. Thus, we conclude that the fluorescence quenching was mostly caused by the differential binding of various metal ions to the branched oligoethylene glycol moieties.

As the combination of PPE with metal cations at certain pH values generates useful signals for the discrimination of amino acids, how can we reach the best condition (suitable PPEs, metal salts, pH values) for a discrimination of amino acids?

3.3.2.1 Screening with Individual Highly-fluorescent PAEs

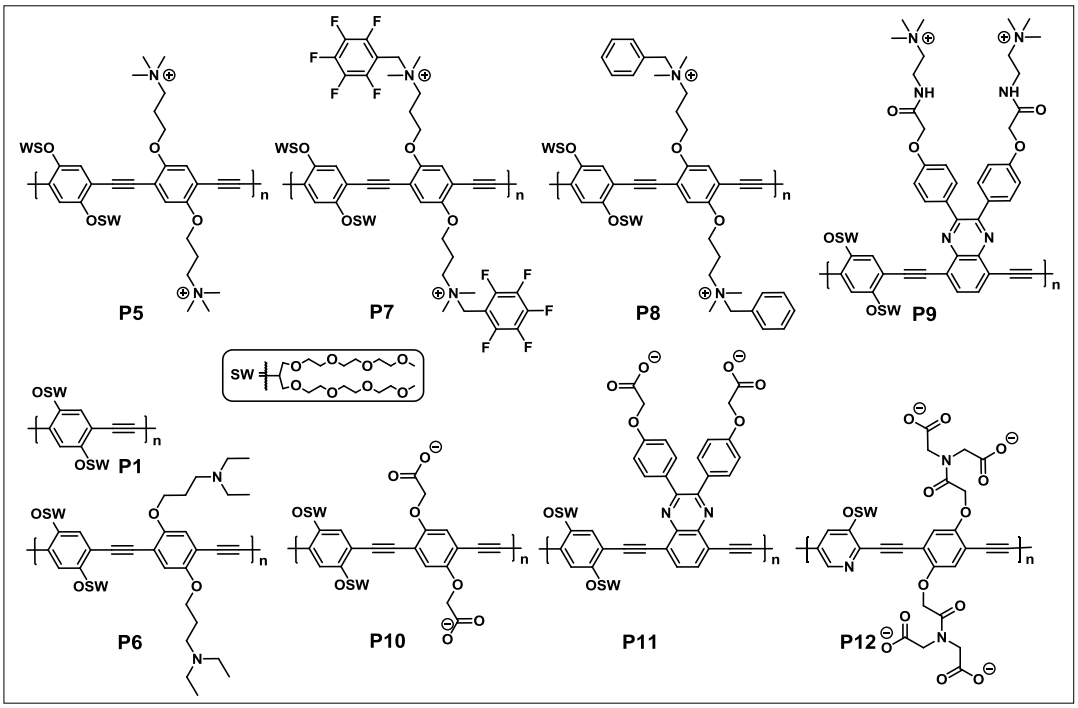

Figure 43. Structure of PAEs used for screening process.

Nine different PAEs (positively-charged **P5** and **P7**-**P9**, negatively-charged **P10**-**P12**, neutral **P1** and **P6**, Figure 43) were chosen for screening. These polymers were synthesized via the standard Sonogashira protocol. The detailed synthesis protocols and analytical data of these polymers see Chapter 5.2.2 and Table 3. The results showed that negatively-charged **P11** works poorly, and positively-charged polymers **P5** and **P7** - **P8** showed very similar response (Figure 44). For the reason that **P9**, **P11** and **P12** have low quantum yield, which may cause a big error, here we exclude the three polymers when calculating PCA. Finally, **P5** with the highest quantum yield and best distinguishing ability was selected as the sensor element.

Table 3. Detailed Analytical Data of the Used Polymers.

No.	M_n [g/mol]	M_w [g/mol]	PDI	P_n
P1	1.0×10^4	2.2×10^4	2.2	12
P5[a]	1.4×10^4	5.5×10^4	3.9	11
P6[a]	7.9×10^3	2.0×10^4	2.5	7
P7[a]	1.4×10^4	5.5×10^4	3.9	11
P8[a]	1.4×10^4	5.5×10^4	3.9	11
P9[a]	2.1×10^4	3.2×10^4	1.5	15
P10[a]	1.7×10^4	5.6×10^4	3.3	15
P11[a]	2.1×10^4	3.2×10^4	1.5	15
P12[a]	1.9×10^4	1.3×10^5	6.5	18

[a] determined by gel permeation chromtography of the corresponding organosoluble precursors.

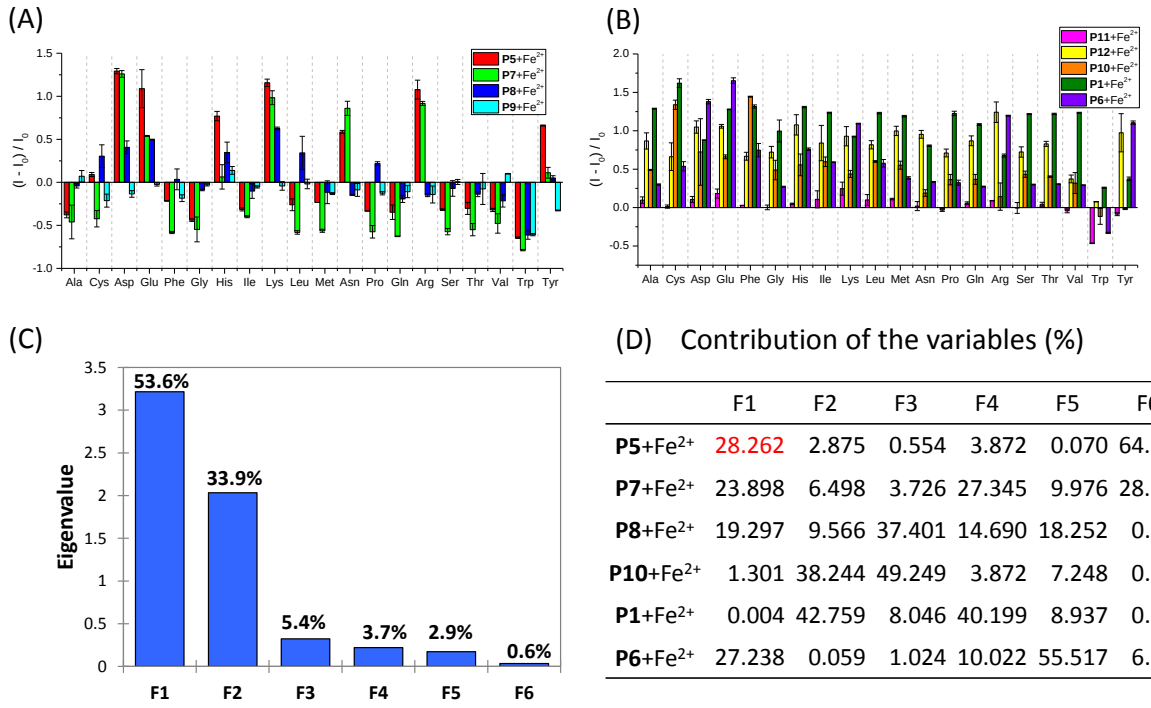

	F1	F2	F3	F4	F5	F6
P5+Fe^{2+}	28.262	2.875	0.554	3.872	0.070	64.367
P7+Fe^{2+}	23.898	6.498	3.726	27.345	9.976	28.558
P8+Fe^{2+}	19.297	9.566	37.401	14.690	18.252	0.794
P10+Fe^{2+}	1.301	38.244	49.249	3.872	7.248	0.086
P1+Fe^{2+}	0.004	42.759	8.046	40.199	8.937	0.054
P6+Fe^{2+}	27.238	0.059	1.024	10.022	55.517	6.140

Figure 44. Fluorescence response pattern ((I - I_0) / I_0) obtained by **(A)** positively charged polymers **P5** and **P7** - **P9** (1 µM, at pH 7, buffered) and **(B)** neutral and negatively charged polymers **P1**, **P6** and **P10** - **P12** (1 µM, at pH 7, buffered) in the presence of Fe^{2+} (1 mM) treated with 20 amino acids (25 mM). Each value is the average of two independent measurements. **(C)** Eigenvalue calculated from the principal component analysis, factor 1 represents 53.6% of the total variation. **(D)** The contribution of each sensor elements to the resulted six factors, **P5** contributed most to the factor 1. Figure reproduced with permission from ref. 49 © 2017, Wiley-VCH Verlag GmbH & Co. KGaA.

3.3.2.2 Screening with the Suitable Metal Salts

Amino acids Gly, Ile, Leu, Pro, Gln, Arg, Ser, Thr and Val (25 mM) were selected for the initial screening of amino acids because of their structural similarity. As shown in Figure 45, metal ions Fe^{2+}, Cu^{2+} and Co^{2+} could elicit a fluorescence response to these amino acids.

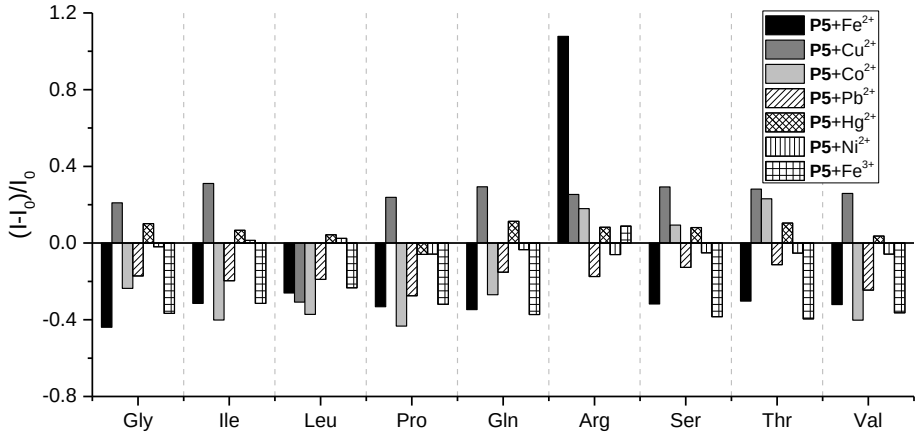

Figure 45. Fluorescence response pattern ((I - I_0) / I_0) obtained by **P5** (1 μM) with nine amino acids (25 mM) in the presence of different metal salts (1 mM). Each value is the average of three independent measurements; each error bar shows the standard deviation (SD) of these measurements.

3.3.2.3 Screening with the Suitable pH Values

We investigated and compared the fluorescence response of **P5** toward metal ions Fe^{2+} and Cu^{2+} at five different pH values (basic, neutral and basic). 8 amino acids (Gly, Lys, Leu, Met, Pro, Arg, Ser, and Thr) were randomly chosen for sensing. As can be seen in the following Figure 46, negligible fluorescence intensity changes were observed between pH 3 and 5. Although strong fluorescence turn-on can be found for Fe^{2+} at pH 5, it can't differentiate the selected 8 amino acids.

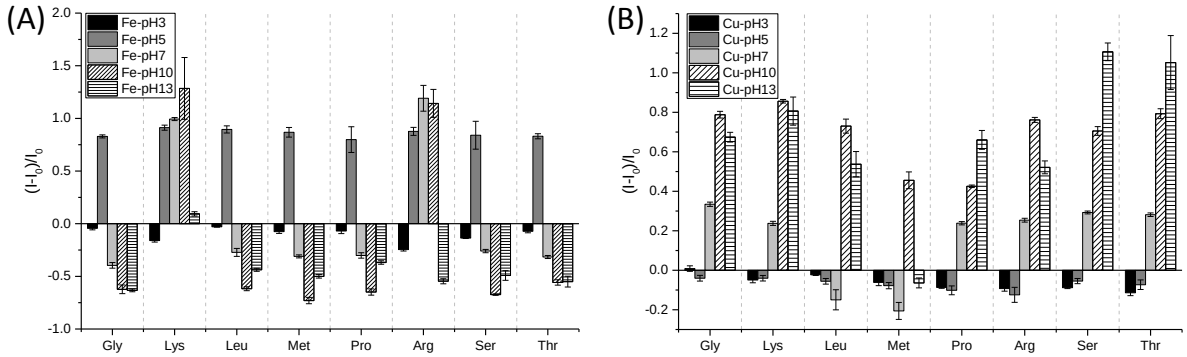

Figure 46. Fluorescence response of **P5** (1 μM) with **(A)** Fe^{2+} (1 mM) and **(B)** Cu^{2+} (1 mM) at pH 3, 5, 7, 10 and 13 (buffered). Each value is the average of two independent measurements; each error bar shows the standard deviation (SD) of these measurements. Figure reproduced with permission from ref. 49 © 2017, Wiley-VCH Verlag GmbH & Co. KGaA.

3.3.3 Identification of 20 Amino Acids in Water

Although neither the PPE nor the metal salts alone are helpful for the discrimination of amino acids, the combination of one PPE with three different metal cations at three pH values generates useful signals (Figure 47). Thus, an optoelectronic tongue was constructed by mixing **P5** and three metal ions (Fe^{2+}, Co^{2+}, and Cu^{2+}) at three different pH-values (pH 7, 10 and 13) in water. The polymer was dissolved in buffer (pH 7, pH 10 and pH 13) to make 2.5 μM of stock solutions on the basis of its molecular weight. Each polymer solution (2.5 μM, 120 μL) in buffer was respectively loaded into a well on a 96-well plate (300 μL microplate). Subsequently, 30 μL metal salts (Fe^{2+}, Cu^{2+}, and Co^{2+}) and 150 μL amino acids were added to each well. Finally, the fluorescence intensity values were

recorded on a CLARIOstar (firmware version 1.13) microplate reader. Fluorescence intensity change ((I - I_0) / I_0) was calculated and used for linear discriminant analysis. Here, I_0 and I are the fluorescence intensity of the solution (mixtures of polymer and metal salts) in the absence and presence of the amino acids, respectively.

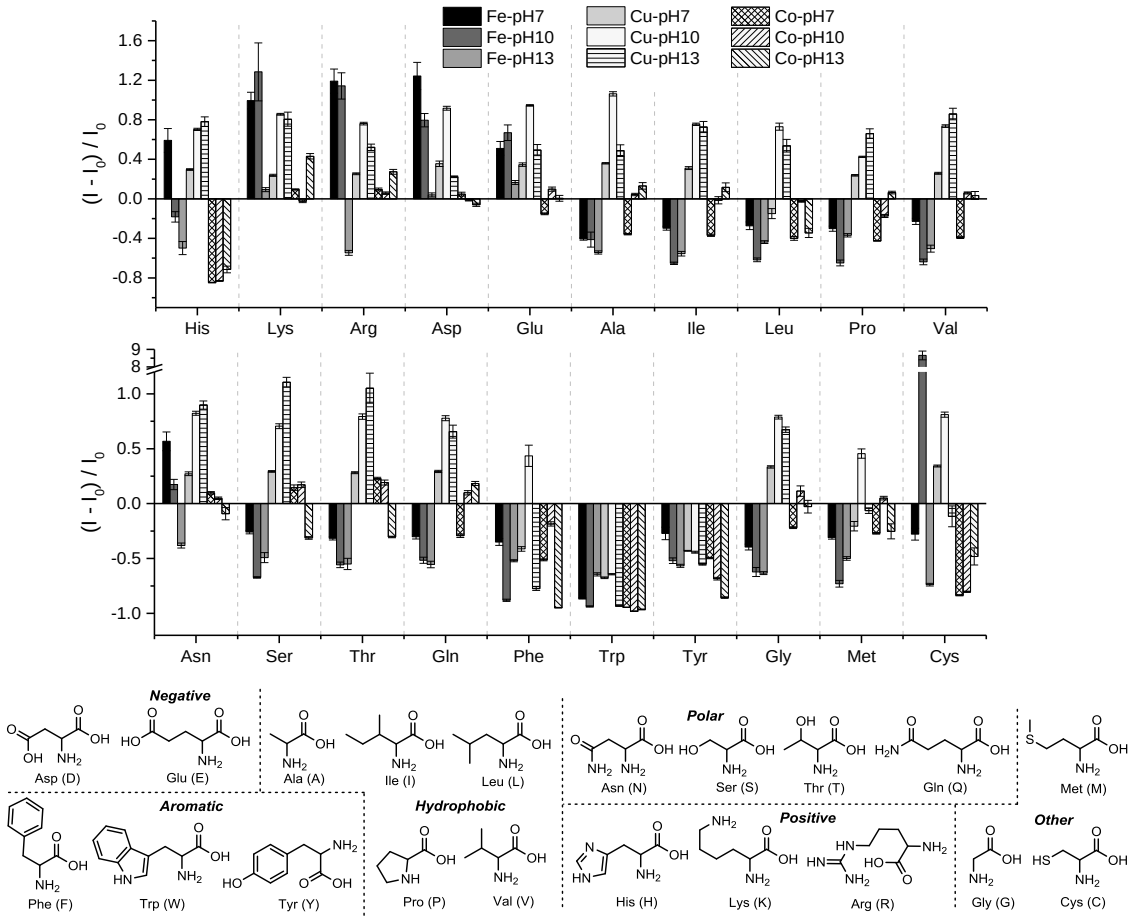

Figure 47. Fluorescence response pattern ((I - I_0) / I_0) of the **P5** (1 μM) in the presence of different metal salts (1 mM), treated with solutions of the 20 natural amino acids (25 mM) at pH 7, 10 and 13. Each value is the average of six independent measurements; each error bar shows the standard deviation (SD) of these measurements. Structures of amino acids are shown in the bottom panel. The fluorescence intensities (I_0 or I) were recorded at the peak intensity at 460 nm with an excitation at 410 nm by using a plate reader. Figure reproduced with permission from ref. 49 © 2017, Wiley-VCH Verlag GmbH & Co. KGaA.

Figure 48 shows a 3D plot of the first three canonical scores obtained by LDA, which converts the training matrix (fluorescence response patterns, 9 complexes x 20 amino acids x 6 replicates) into canonical scores according to their shortest Mahalanobis distances. Mahalanobis distance, a multi-dimensional generalization of the idea of measuring how many standard deviations away point is from the mean of the distribution, is widely used in cluster analysis and classification techniques.[145-146] It accounts for the fact that the variances in each direction are different. The larger the difference between the means of the canonical group is, the better the predictive power of the canonical discriminant function in classifying the observations. Here, all of the 20 amino acids group fall into different classes. According to the amino acid type, hydrophobic, negatively charged and aromatic amino acids all grouped very well. Only His is isolated and does not group with the positively charged amino acids Arg and Lys. A similar scenario results for the polar amino acids. Here, glutamic acid

(Gln) is not grouped with the rest of the polar amino acids Asn, Ser, and Thr. The last three "other" amino acids do not group at all. To our surprise, the closely related amino acids, such as IIe and Leu, are clearly distinguishable, which would be very difficult to achieve by a classical one sensor - one analyte approach. To investigate the influence of the cationic moiety we also looked at metal ion-complexes of the SW-PPE **P1** and find that it shows less discriminative power (Figure 49). Therefore, the cationic moiety of polymer **P5** plays a major role in the discriminating of all the amino acids.

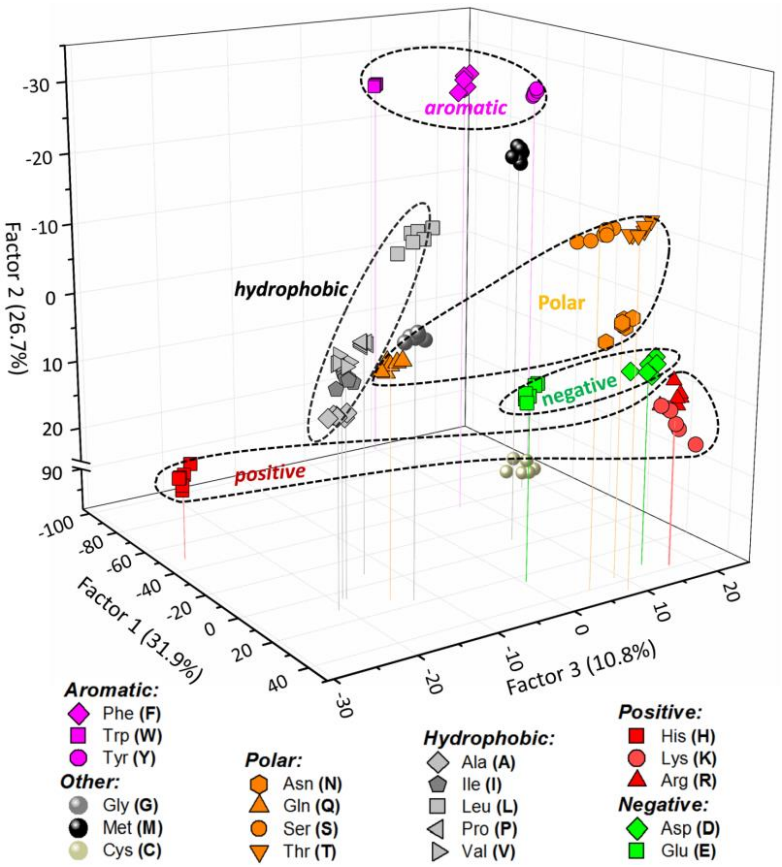

Figure 48. 3D canonical score plot for the first three factors of fluorescence response patterns obtained with an array (nine elements) of **P5** (1 µM) with 20 natural amino acids (25 mM) at pH 7, 10 and 13 and in the presence of different metal salts (Fe^{2+}, Cu^{2+} and Co^{2+}). Each point represents the response pattern for a single amino acid in the array. Figure reproduced with permission from ref. 49 © 2017, Wiley-VCH Verlag GmbH & Co. KGaA.

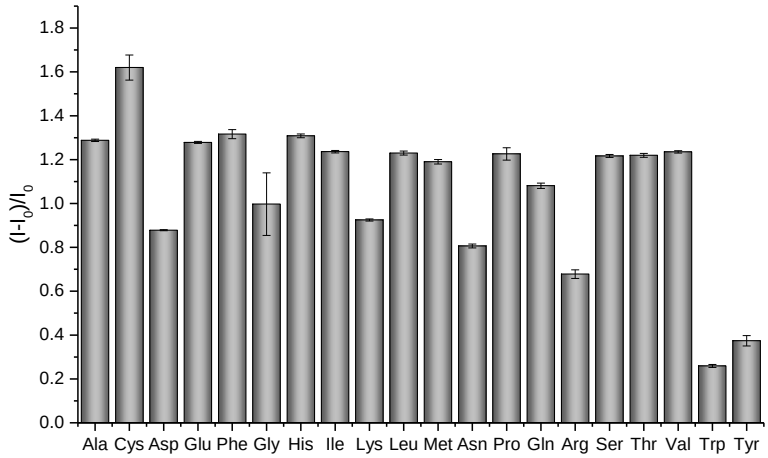

Figure 49. Fluorescence response pattern ($(I - I_0)/I_0$) of **P1** (1 µM) with 20 natural amino acids (25 mM) at pH 7 in the presence of Fe^{2+} (1 mM). Each value is the average of two independent measurements; each error bar shows the standard deviation (SD) of these measurements. Figure reproduced with permission from ref. 49 © 2017, Wiley-VCH Verlag GmbH & Co. KGaA.

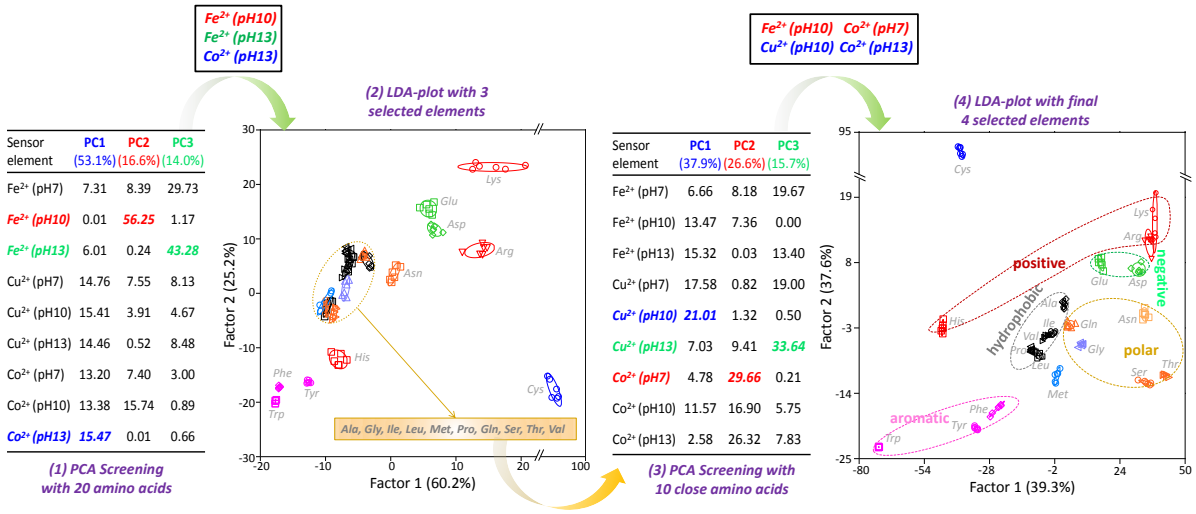

Figure 50. Two-step screening process of nine sensing elements, lead to final 4 selected elements which successfully identify 20 amino acids with cluster properties. Figure reproduced with permission from ref. 49 © 2017, Wiley-VCH Verlag GmbH & Co. KGaA.

Starting from this nine-element tongue we performed a two-stage screening process employing principal component analysis to end up with a four-element tongue identifying all of the 20 amino acids. As shown in Figure 50, data of nine sensing elements for 20 amino acids were calculated with PCA, Co^{2+} (pH 13), Fe^{2+} (pH 10) and Fe^{2+} (pH 13) contributed most. LDA-plot with the selected three elements showed 10 amino acids group together. Then, nine sensing elements with 10 overlaped amino acids were calculated with PCA again; we found that sensing elements of Cu^{2+} (pH 10), Co^{2+} (pH 7) and Cu^{2+} (pH 13) showed best discrimination power to the 10 amino acids. Finally, four elements (the first two factors of each PCA results) - Fe^{2+} (pH 10), Cu^{2+} (pH 10), Co^{2+} (pH 7) and Co^{2+} (pH 13) were selected and good discrimination results were observed in LDA.

To validate its efficiency, we performed tests with randomly chosen amino acids of our training set. The new cases are classified into groups, generated through the training matrix, based on their shortest Mahalanobis distance to the respective group. The four-element tongue identifies 77.5% of all of the amino acids when presented as unknowns (see Table 4 and Table 19). Because the discrimination of unknowns with the four-element tongue is not satisfactory, we selected a green fluorescent protein (**GFP-K72**), which is fused to an unfolded positively supercharged polypeptide by genetic engineering,[147-149] as a tongue element. Based on our recent experience, the fluorescence of GFP variants was quenched at strongly acidic or basic conditions. Thus, we investigated the GFP in the presence of metal ions (Fe^{2+}, Cu^{2+}, and Co^{2+}) at pH 7 (excitation and emission wavelengths were 480 and 514 nm, respectively); this three- elements tongue also discriminates 20 amino acids (see Figure 51). Although the discrimination of each tongue works quite well, the identification of unknowns is improved in the final combined tongue consisting of seven elements (PPE four elements, GFP three elements) (Figure 52); 69 of 80 unknown samples were correctly identified, representing an accuracy of 86.3% (Table 4 and Table 24).

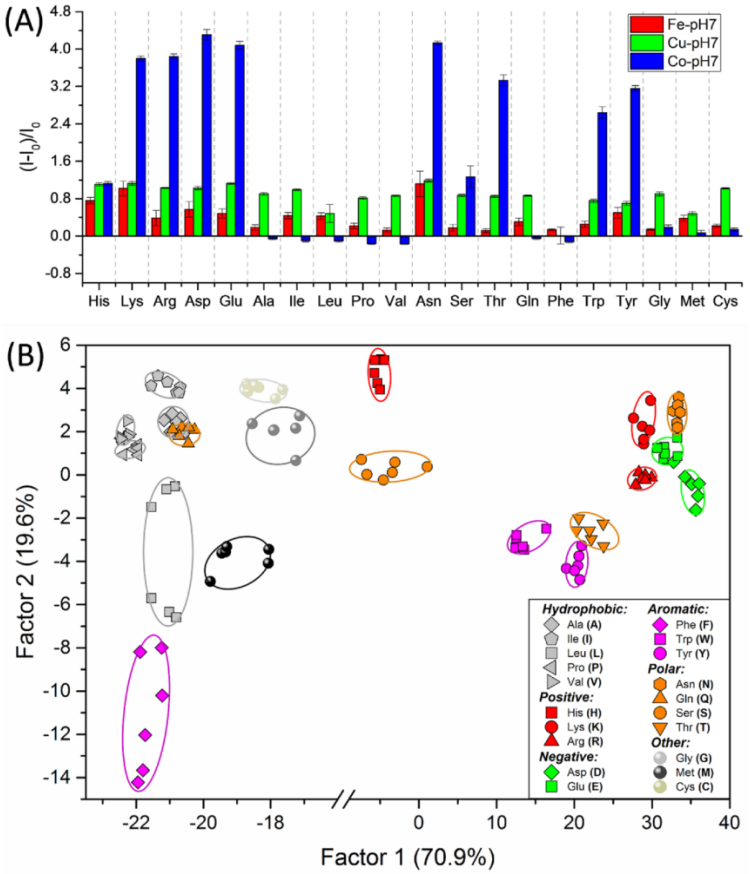

Figure 51. (A) Fluorescence response pattern ((I - I_0)/I_0) of the **GFP-K72** (20 nM) with 20 natural amino acids (25 mM) at pH 7 in the presence of different metal salts (1 mM). Each value is the average of six independent measurements; each error bar shows the standard deviation (SD) of these measurements. **(B)** 2D canonical score plot for GFP tongue (three elements) obtained by an array of **GFP-K72** (20 nM) with Fe^{2+} (pH 7), Cu^{2+} (pH 7) and Co^{2+} (pH 7), 95% confidence ellipses were shown. Figure reproduced with permission from ref. 49 © 2017, Wiley-VCH Verlag GmbH & Co. KGaA.

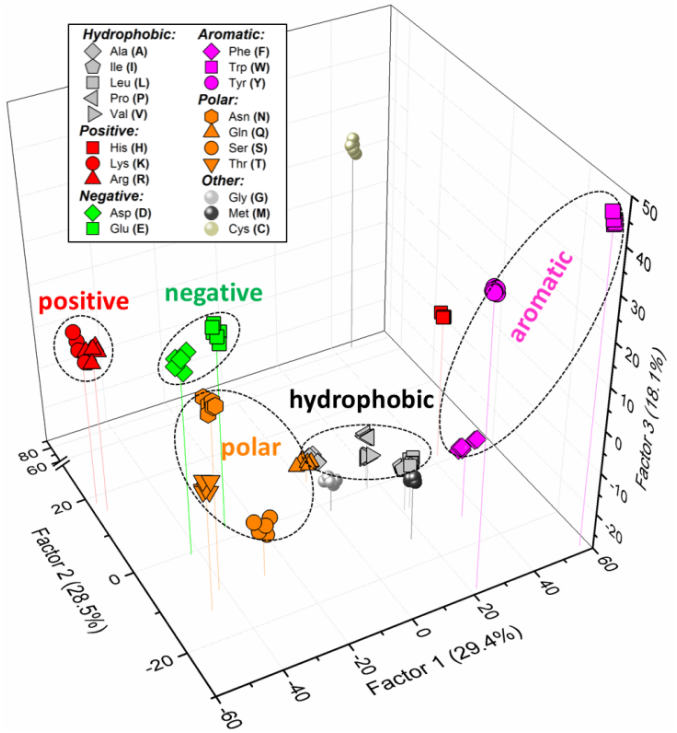

Figure 52. 3D canonical score plot for the combined tongue consisted of PPE tongue (four elements) and GFP tongue (three elements). Each point represents the response pattern for a single amino acid in the array. Figure reproduced with permission from ref. 49 © 2017, Wiley-VCH Verlag GmbH & Co. KGaA.

Table 4. Results of Unknown Detection Using an LDA Algorithm.

Amino acids	Number of samples	**4** elements tongue (PPE)		**7** elements tongue (PPE+GFP)	
		Correctly identified	Accuracy (%)	Correctly identified	Accuracy (%)
Ala	4	2	50	2	50
Cys	4	4	100	4	100
Asp	4	2	50	3	75
Glu	4	0	0	2	50
Phe	4	4	100	4	100
Gly	4	4	100	4	100
His	4	4	100	4	100
Ile	4	4	100	4	100
Lys	4	3	75	2	50
Leu	4	4	100	4	100
Met	4	4	100	4	100
Asn	4	4	100	4	100
Pro	4	3	75	3	75
Gln	4	3	75	3	75
Arg	4	1	25	3	75
Ser	4	4	100	4	100
Thr	4	1	25	4	100
Val	4	3	75	3	75
Trp	4	4	100	4	100
Tyr	4	4	100	4	100
Total	**80**	**62**	**77.5**	**69**	**86.25**

What is the mechanism of the discrimination? In this study, we employed a ternary system which consists of polymers or green fluorescent proteins, metal salts, and the amino acid. First, the fluorescence of polymers or green fluorescent proteins could be quenched by metal ions. In the presence of competitive analytes (amino acids), the metal ions might be snatched from the polymers or green fluorescent proteins because amino acids could form stable complexes with metal ions.[127, 150-152] In this case, fluorescence is either recovered or further quenched depending on the affinity of the analytes to metal ions and their abilities to impact the fluorescence of the polymers or green fluorescent proteins (Figure 53). The differential fluorescence turn-on or turn-off generates the discriminative signal that led to the identification of the amino acids.

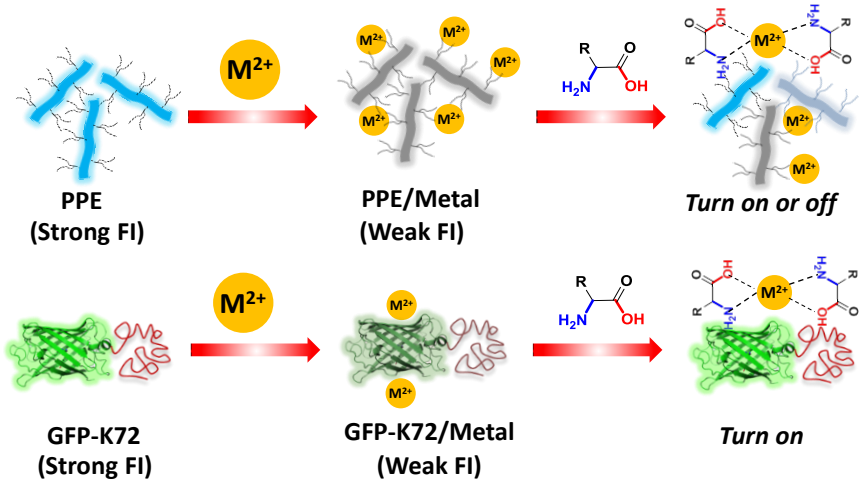

Figure 53. Schematic representation of the reactions that might happen between polymers or green fluorescent proteins, metals ions and amino acids. Figure reproduced with permission from ref. 49 © 2017, Wiley-VCH Verlag GmbH & Co. KGaA.

3.3.4 Conclusions

In conclusion, we could identify and discriminate 20 different natural amino acids by using a simple PPE tongue, GFP tongue or a combined GFP-PPE tongue, composed of a cationic PPE or a supercharged polypeptide fused to GFP and several different metal cations at different pH values. The complexes are disrupted by the metal-binding amino acids, and the differential fluorescence turn on or turn off is achieved.

3.4 Optimized Sensor Array Identifies 20 Amino Acids

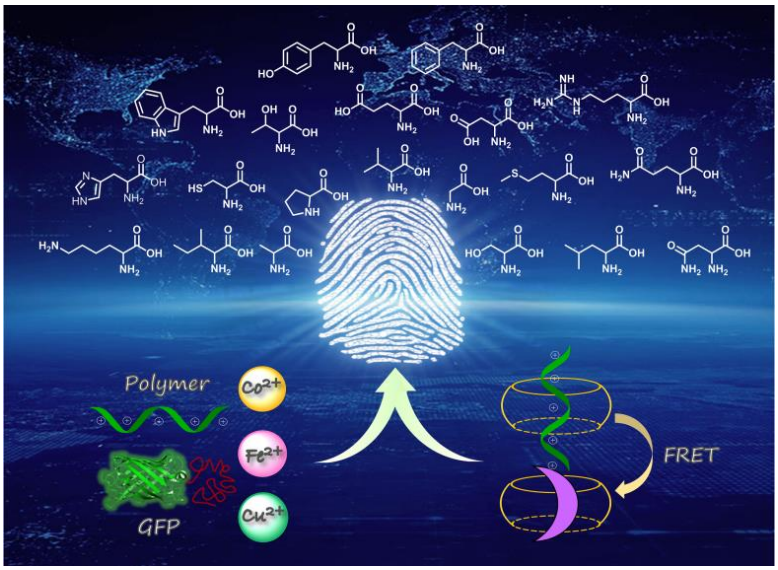

Figure 54. Schematic illustration of hypothesis-free sensor array discriminates amino acids. Figure reproduced with permission from ref. 153 © 2018, American Chemical Society.

In this section, an optimized self-assembled eight-member sensor array is reported. The optimized sensor array stems from the combination of elements of different tongues, containing poly(*para*-phenyleneethynylene)s (PPE) and a supercharged green fluorescent protein (GFP) variant. The responsivity of the sensor dyes (PPEs and GFP) is enhanced in elements that contain adjuvants, such as metal salts but also cucurbit[7]uril (CB[7]) and acridine orange; a suitable and robust eight element array discriminates all of the 20 natural amino acids in water at 25mM concentration with 100% accuracy. The results group well to the amino acid type, hydrophobic, polar and aromatic ones.

3.4.1 Screening and Construction of New Chemical Tongue

Figure 55 shows the structures of the used PPEs, the macrocyclic host cucurbiturils (CB[n], n = 7 or 8), the dye acridine orange (AO) and the green fluorescent protein variant **GFP-K72** with a high positive net charge induced by recombinant fusion of an unfolded, supercharged polypeptide chain to GFP.[49, 77] Figure 56 displays the four starting arrays. Array 1 consists of a positively charged **GFP-K72** in the presence of different metal cations at pH 7. Array 2 employs the positively charged **P5** also in the presence of the metal cations, while arrays 3 and 4 are supramolecular arrays in which cucurbituril[8] and PPEs or PPEs in the presence of acridine orange and cucurbituril[7] form complex fluorescence-responsive arrays.[49] We note that the fluorescence of **GFP-K72** or **P5** was quenched by metal ions. In arrays 3 and 4, cucurbit[n]urils (n = 7 or 8) are used for detection and recognition of amino acids as these interact with the CB host cavity.[154-156] Array 3 and its function will be discussed in detail in the following chapter.[77]

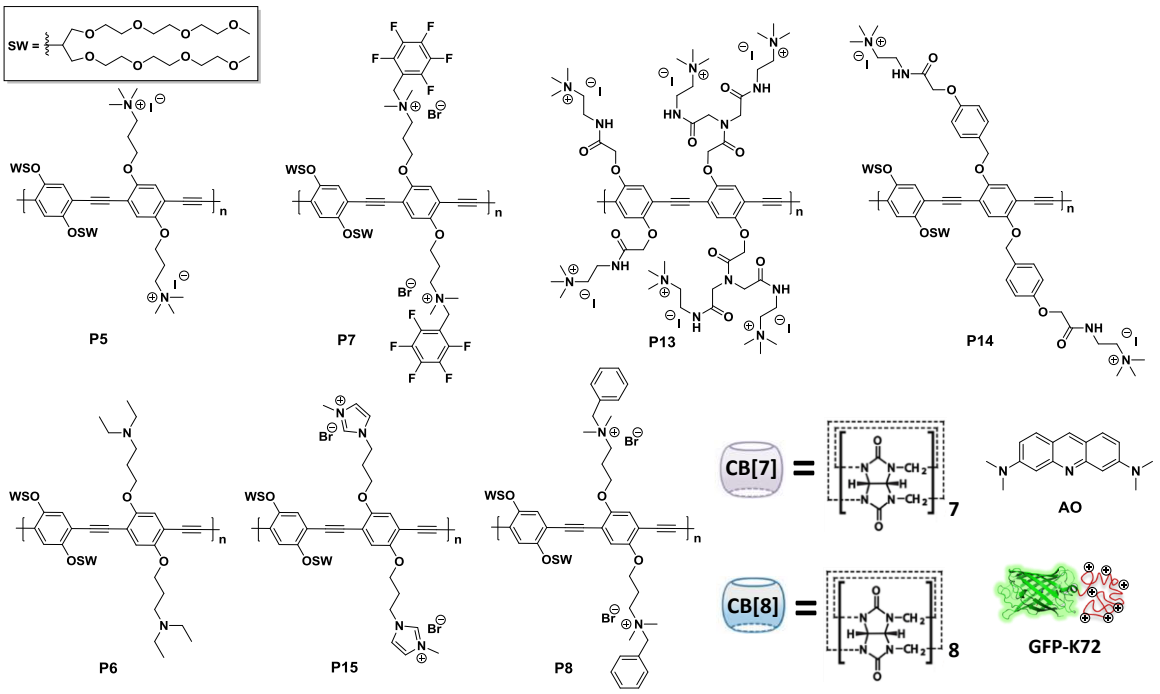

Figure 55. Chemical structures of used poly(*p*-phenyleneethynylene)s, cucurbiturils CB[7] and CB[8], the tricyclic dye acridine orange AO and the green fluorescent protein derivative **GFP-K72**. Figure reproduced with permission from ref. 153 © 2018, American Chemical Society.

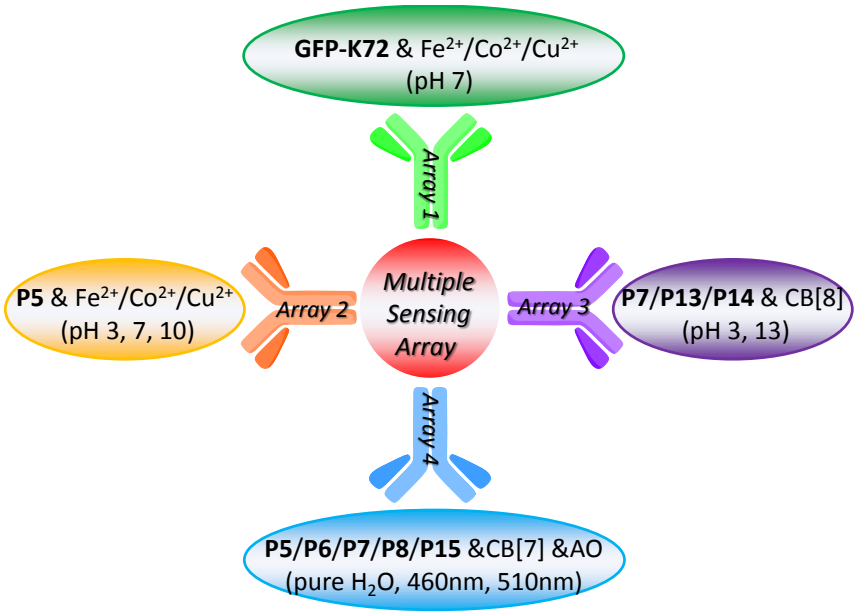

Figure 56. The fabrication of multiple sensor arrays for the discrimination of amino acids. Figure reproduced with permission from ref. 153 © 2018, American Chemical Society.

The array 3 using the larger CB[8] (vide infra) is not efficient for the discrimination of amino acids so we will not discuss it in detail. In addition to array 2, the arrays 1 and 4 impart additional selectivity to the array. Attempts to discriminate amino acids just with the cationic GFP were not very successful, but analogously to array 1, the addition of metal salts unlocked the sensitivity of the GFP towards amino acid analytes. Here we also assume that the GFP forms a non-fluorescent complex with the metal salt, which is reversed by the addition of the analytes. While the used GFP is overall positively

charged at pH 7, there will be still a significant number of negatively charged residues that coordinate to the metal salts.

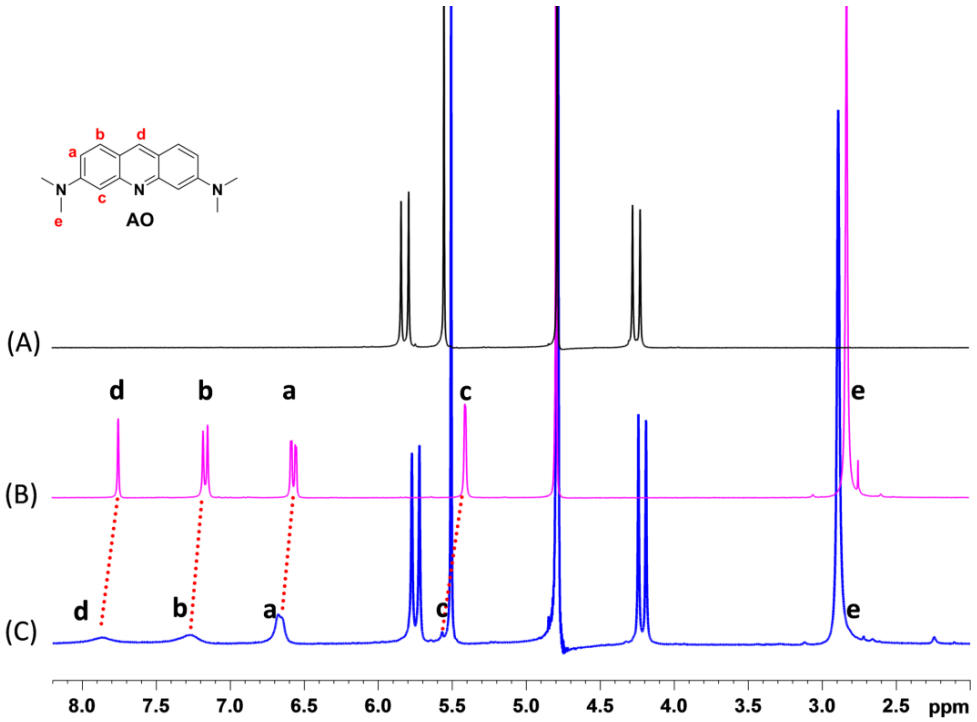

Figure 57. Partial ^{1}H-NMR spectra (300 MHz, D_2O) of pure cucurbit[7]uril (CB[7]) **(A)**, acridine orange (AO) in the absence **(B)** and the presence **(C)** of CB[7]. Figure reproduced with permission from ref. 153 © 2018, American Chemical Society.

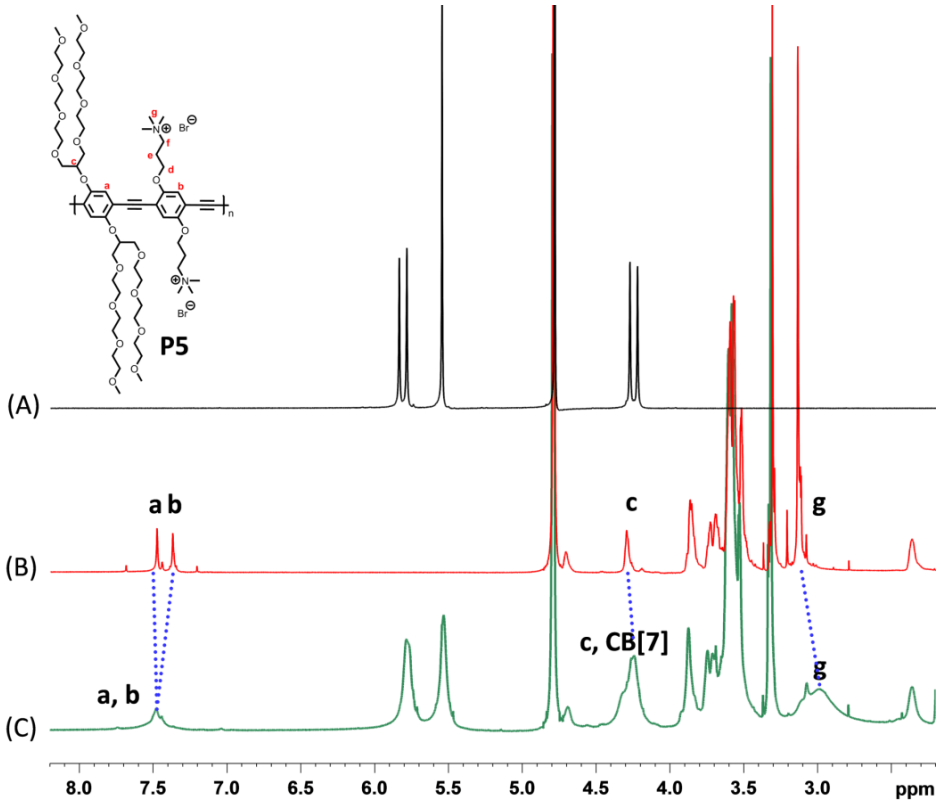

Figure 58. Partial ^{1}H-NMR spectra (600 MHz, D_2O) of pure cucurbit[7]uril (CB[7]) **(A)**, polymer **P5** in the absence **(B)** and the presence **(C)** of CB[7]. Figure reproduced with permission from ref. 153 © 2018, American Chemical Society.

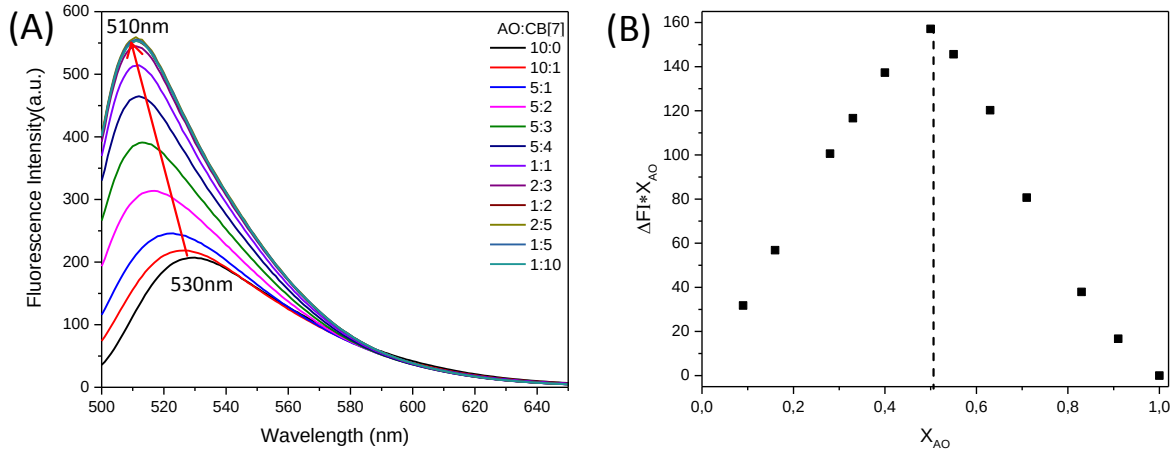

Figure 59. (A) Fluorescence spectra of the mixture of AO and CB[7] in different molar ratios. **(B)** Job plot for AO and CB[7] by plotting the difference in emission at highest intensity against the mole fraction of AO. Figure reproduced with permission from ref. 153 © 2018, American Chemical Society.

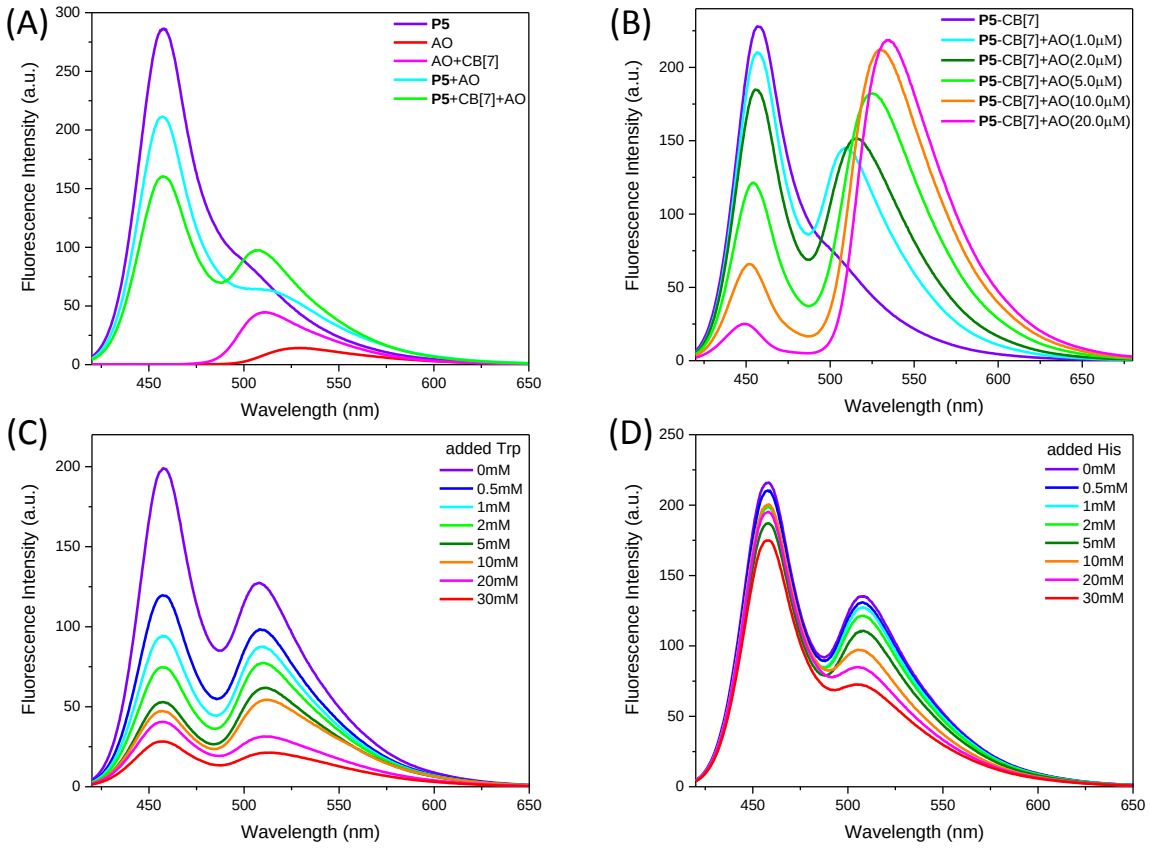

Figure 60. Fluorescence emission spectra of **(A) P5**, AO, the mixture of AO and CB[7] (1:1), **P5** and AO (1:1) and **P5** and CB[7] and AO (1:2:1), **(B) P5**-CB[7] in the presence of different concentrations of AO (from 0 to 20 μM), [**P5**] = 2 μM, [CB7] = 4 μM; The changes in fluorescence intensity of **P5**-CB[7]-AO (2.0 μM/4.0 μM/2.0 μM) upon gradual addition of (C) Trp and (D) His (from 0 to 30 mM). All spectra were performed in water upon excitation at 410 nm. Figure reproduced with permission from ref. 153 © 2018, American Chemical Society.

The most remarkable array is the ternary one (array 4), composed of acridine orange (AO), **P5** and CB[7]. Control experiments show that CB[7] enhances FRET between the AO and **P5**. Interestingly, both species bind to the cavity of CB[7], as shown by NMR titration experiments (Figure 57 and Figure 58); in the case of AO, CB[7] forms a 1:1 complex with the dye (Figure 59). AO exhibits an emission peak at 530 nm; upon addition of CB[7], a blue shift to 510 nm occurs (Figure 59 and Figure 60A).[157-158] Sensor elements were constructed through in situ assemblies of the PPEs, CB[7] and AO at

a molar ratio of 1:2:1 (based on a per repeat unit of the PPEs). Amino acids form hydrogen bonds with CB[7] and dyes due to the amine and carboxylate groups. Tryptophan (Trp) or histidine (His) displace AO or **P5** from the cavity of CB[7], shutting down the FRET and the emission of AO at 510 nm decreases (Figure 60C and Figure 60D). Figure 61 shows the proposed schematic illustration of PPE-CB[7]-AO tongue working with amino acids. Fundamentally, CB[7] acts as a FRET enhancer, but its exact mechanism is not known.

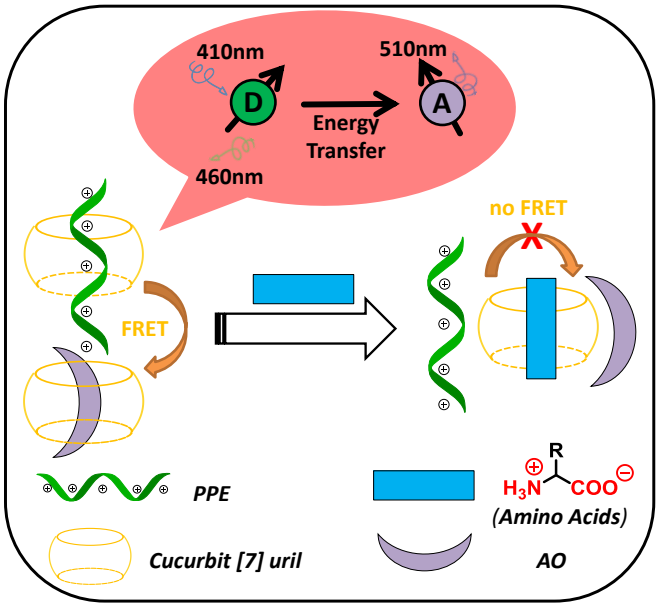

Figure 61. Proposed schematic illustration of the PPE-CB[7]-AO tongue working with amino acids. Figure reproduced with permission from ref. 153 © 2018, American Chemical Society.

As for the experimental details, first, PPEs or green fluorescent protein derivative were dissolved in buffers with desired pH values to make stock solutions. Then - according to the array - solutions of divalent metal ions or cucurbit[n]urils - with or without acridine orange were added to the stock solutions. Each complex solution (150 μL) was loaded into a well on a 96-well plate, respectively. Subsequently, 150 μL amino acids were added to each well and mixed. The different fluorescence intensities at λ_{max} were recorded on a CLARIOstar microplate reader. The Fluorescence intensity change ((I - I_0) / I_0) was calculated and used for linear discriminant analysis, where I_0 and I are the fluorescence intensity of the solution in the absence and presence of the amino acids, respectively. Similar procedures were employed to the lower concentration of amino acids.

As a control, we first treated **P5** - **P8** and **P15** (Figure 55) with the 20 naturally occurring amino acids (25 mM). The results (Figure 62) indicate that the simple PPE tongue alone is alone is useful for the discrimination of Tyr and Trp but does not discriminate the other amino acids with polar and hydrophobic residues. However, the PPE-CB[7]-AO assembly induces better sensitivity for these analytes (Figure 63). According to the two-dimensional linear discriminant analysis (Figure 65D, Table 25 and Table 26), the PPE-CB[7]-AO tongue discriminates all 20 amino acids. A more simple tongue omitting CB[7] (Figure 64) shows less discriminatory power.

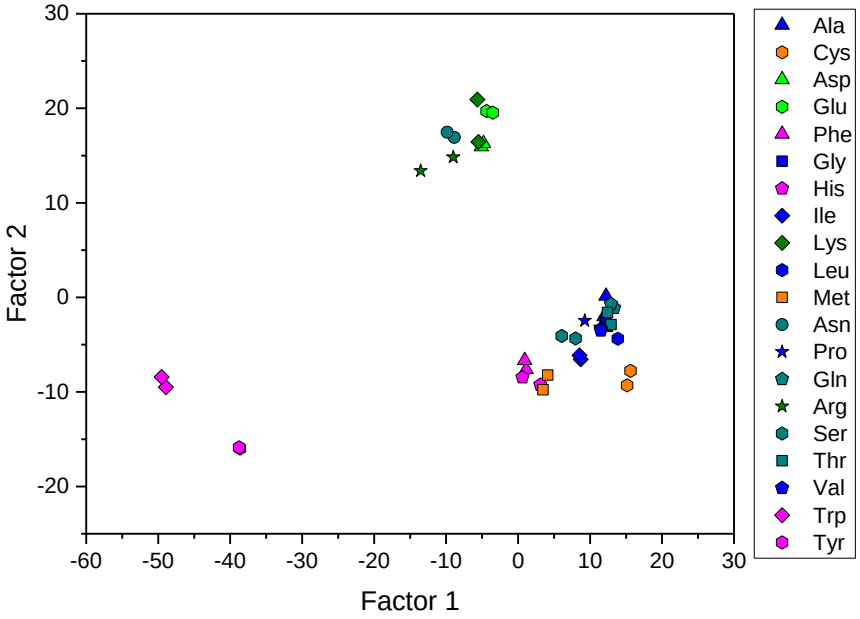

Figure 62. Two-dimensional canonical score plot for the first two factors obtained by PPE tongue treated with 20 amino acids (c = 25 mM). Each point represents the response pattern for a single amino acid to the optimized array. Figure reproduced with permission from ref. 153 © 2018, American Chemical Society.

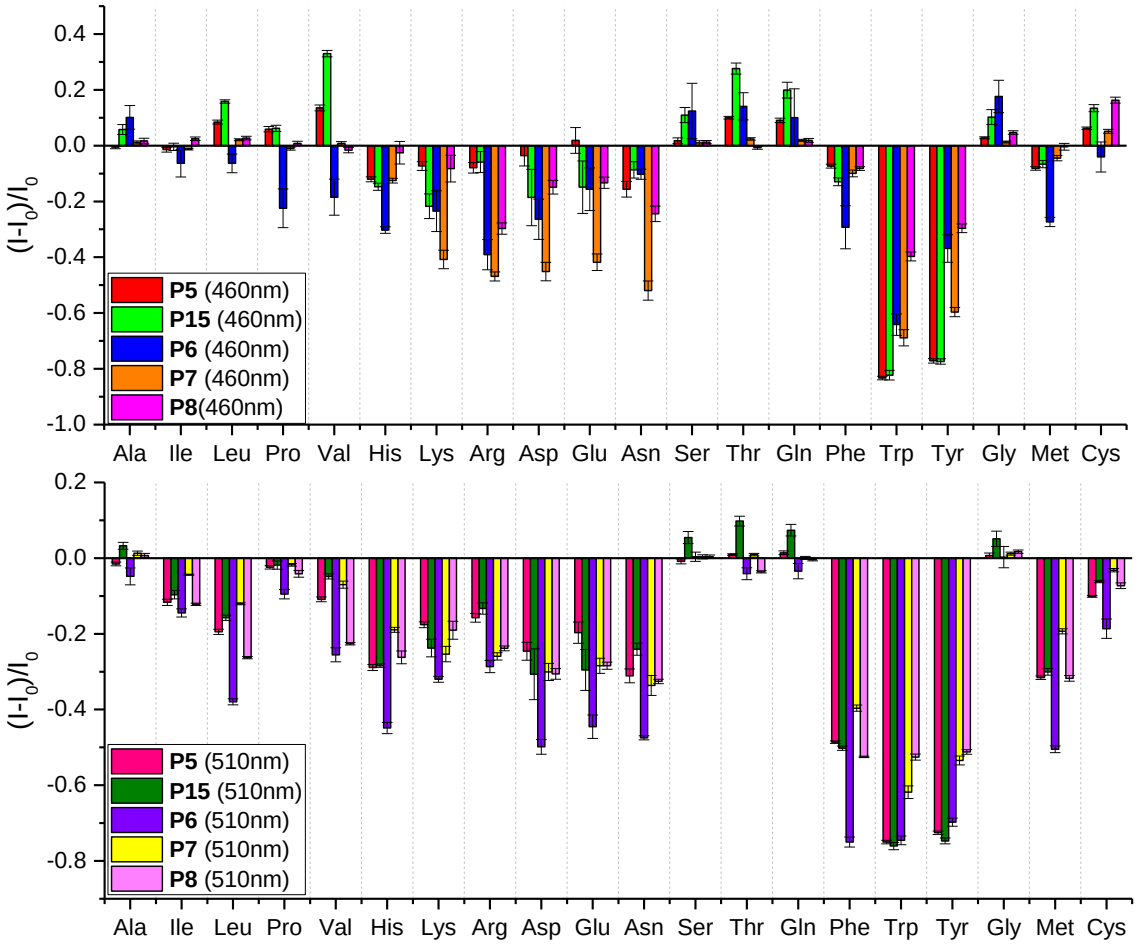

Figure 63. Fluorescence response pattern ($(I - I_0)/I_0$) obtained by PPE/CB[8]/AO tongue (2.0 μM/4.0 μM/2.0 μM) treated with amino acids (c = 25 mM) in water. Each value is the average of six independent measurements; each error bar shows the standard deviation (SD) of these measurements. Figure reproduced with permission from ref. 153 © 2018, American Chemical Society.

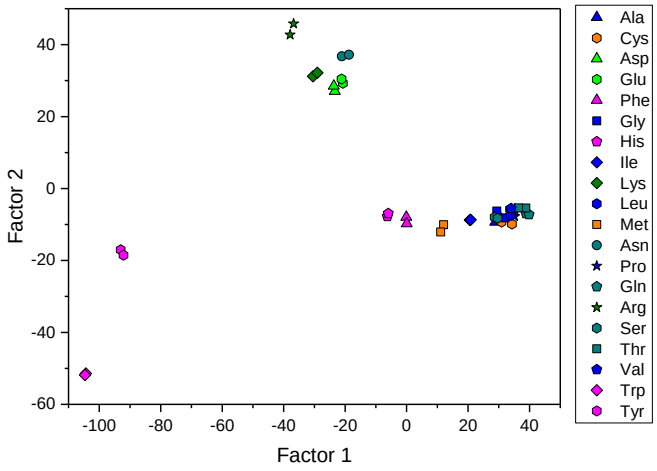

Figure 64. Two-dimensional canonical score plot for the first two factors obtained by PPE-AO (2.0 μM/2.0 μM) tongue treated with 20 amino acids (*c* = 25 mM). Each point represents the response pattern for a single amino acid to the optimized array. Figure reproduced with permission from ref. 153 © 2018, American Chemical Society.

3.4.2 Results and Discussions

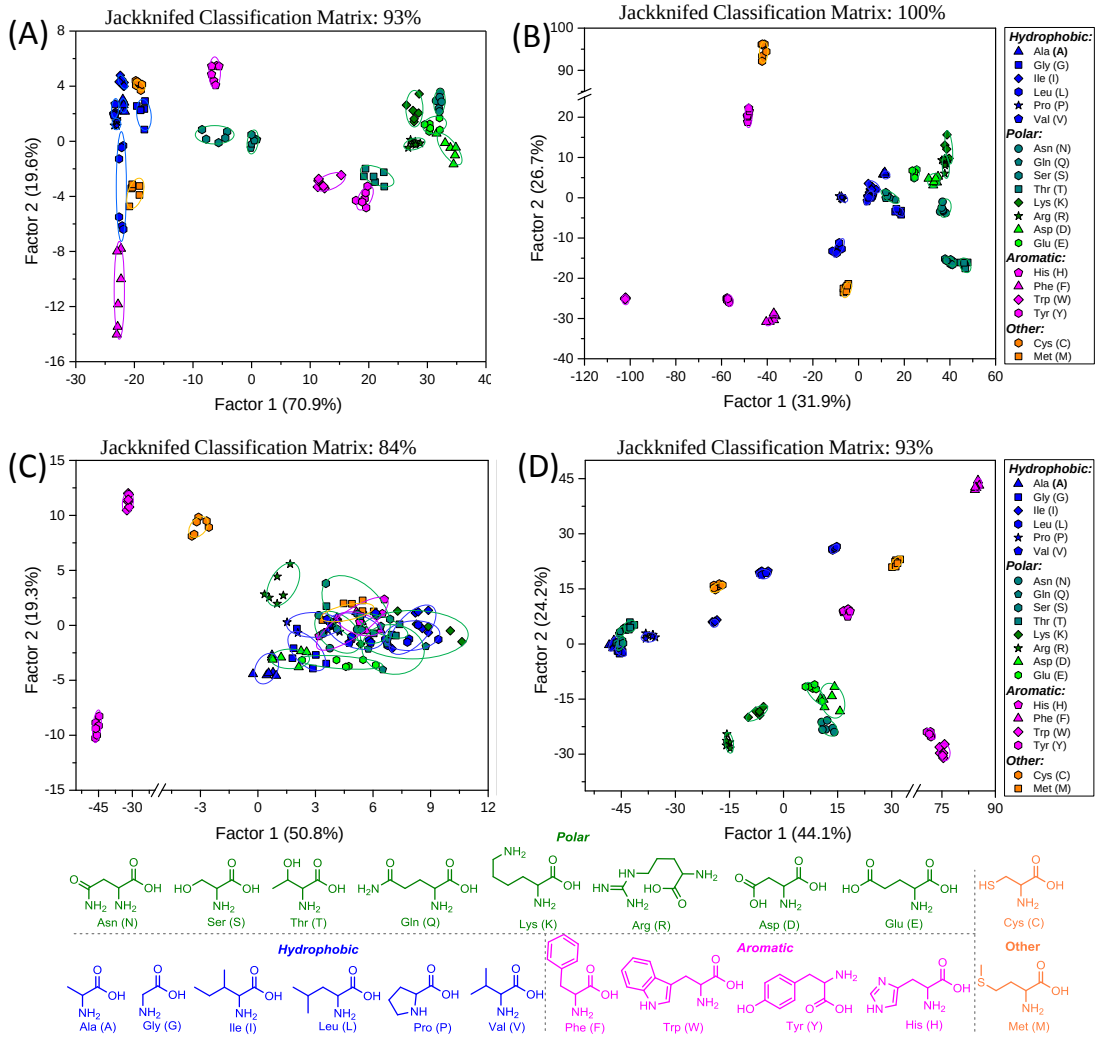

Figure 65. Two-dimensional canonical score plot for the first two factors obtained by **(A)** array 1: GFP-metal salt tongue, **(B)** array 2: PPE-metal salts tongue, **(C)** array 3: PPE-CB[8] tongue and **(D)** array 4: PPE-CB[7]-AO tongue treated with 20 amino acids (*c* = 25 mM) with 95% confidence ellipses. Each point represents the response pattern for a single amino acid to the array. Structures of amino acids are shown in the bottom panel. Figure reproduced with permission from ref. 153 © 2018, American Chemical Society.

In the next experiment, we tested all of the four tongues against the 20 amino acids. Figure 65 shows the 2D-LDA plots for the first two factors obtained by the individual sensor arrays 1-4, *i.e.* the GFP-metal salt tongue, the PPE-metal salt tongue, the PPE-CB[8] tongue and the PPE-CB[7]-AO tongue. The discrimination is fairly poor in the PPE-CB[8] sensor array, while the other arrays work quite well (Figure 65). Figure 66 shows a two-dimensional canonical score plot obtained by all the 28 sensor elements; all of the 20 amino acids are reliably discerned.

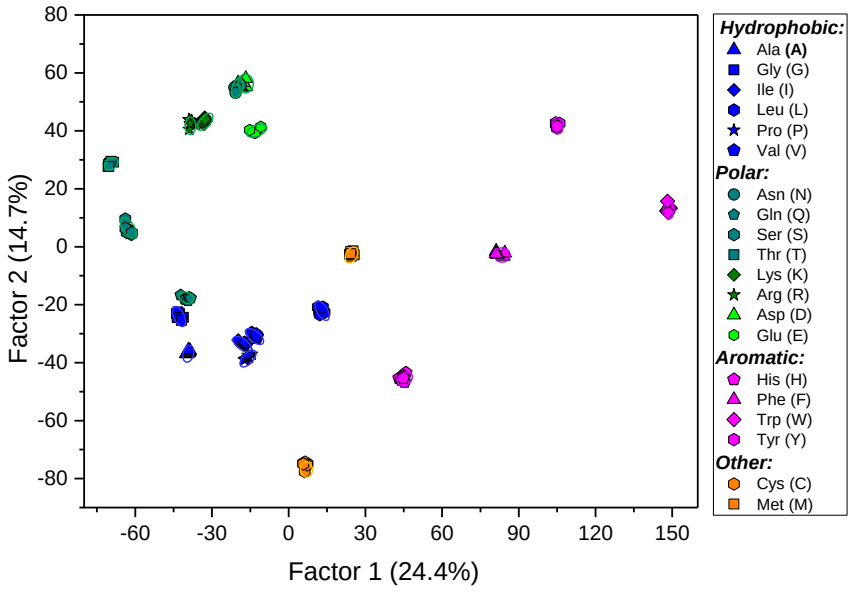

Figure 66. Two-dimensional canonical score plot for the first two factors obtained by all 28 sensor elements treated with 20 amino acids with 95% confidence ellipses. Each point represents the response pattern for a single amino acid to the array. Figure reproduced with permission from ref. 153 © 2018, American Chemical Society.

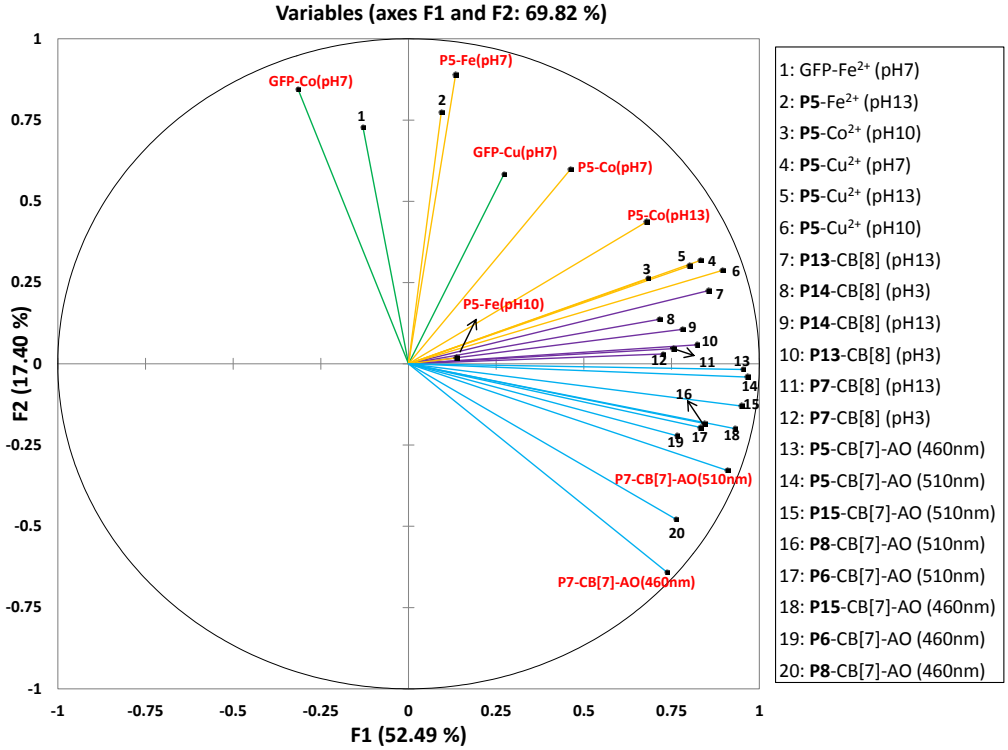

Figure 67. Loading plot of the principal component analysis plot by the four arrays, identifying the contribution of each element to an axis. The selected eight elements are labeled in red. Figure reproduced with permission from ref. 153 © 2018, American Chemical Society.

Table 5. The Screening Results by the Four Arrays.

Arrays	Selected elements
Array 1 (GFP-metal salt tongue)	GFP-Fe (pH7), GFP-Cu (pH7), GFP-Co (pH7)
Array 2 (PPE-metal salt tongue)	**P5**-Fe (pH7), **P5**-Fe (pH10), **P5**-Fe (pH13), **P5**-Co (pH7), **P5**-Co (pH13)
Array 3 (PPE-CB[8] tongue)	**P7**-CB[8] (pH3)
Array 4 (PPE-CB[7]-AO tongue)	**P5**-CB[7]-AO (460nm, 510nm) **P7**-CB[7]-AO (460nm, 510nm)

We then performed a screening process employing principal component analysis: the data of 28 sensing elements for 20 amino acids were calculated with PCA (Figure 67 and Table 27), the 13 elements showed in Table 5 contributed most to the discrimination. Then the selected 13 elements towards 20 amino acids were calculated with PCA again and we found that the sensing elements of GFP-Cu (pH7), GFP-Co (pH7), **P5**-Fe (pH7), **P5**-Fe (pH10), **P5**-Co (pH7), **P5**-Co (pH13) and **P7**-CB[7]-AO (460 nm, 510 nm) show best discrimination power to the 20 amino acids (Figure 68). These loading plots help to find the elements most useful for discrimination and allow to remove weakly performing ones.[51] Thus, excellent discrimination results with a pruned eight-element tongue (all the elements that are marked with red in Figure 67) that identifies all of the 20 amino acids after LDA. None of the high performing elements came from the PPE-CB[8] tongue; control experiments show that the addition of AO does not improve the signal of these array-elements (Figure 69).

The fluorescence modulation data of the pruned filial tongue were recorded. LDA was performed and converted the training matrix (8 factors × 20 amino acids analytes × 6 replicates) into canonical scores. The canonical scores are clustered into twenty different groups. The jackknifed classification matrix with cross-validation reveals a 100% accuracy (Table 28 and Table 29). According to the amino acid residue, hydrophobic, polar and aromatic amino acids all grouped very well (Figure 70A). By zooming into a specific part, the discrimination of hydrophobic and polar amino acids becomes quite clear (Figure 70B and Figure 70C). The testing was performed at 25 mM concentration of the amino acid. To see if we could lower the concentration we also investigated 10 mM solutions. We are still able to discriminate the amino acids, but amino acids with hydrophobic and polar residues do not group well; especially Gln, Ser, and Thr are quite close to the hydrophobic amino acids (Figure 71 and Table 30). 5 mM solutions were also investigated, however, the discrimination is not satisfactory (Figure 72).

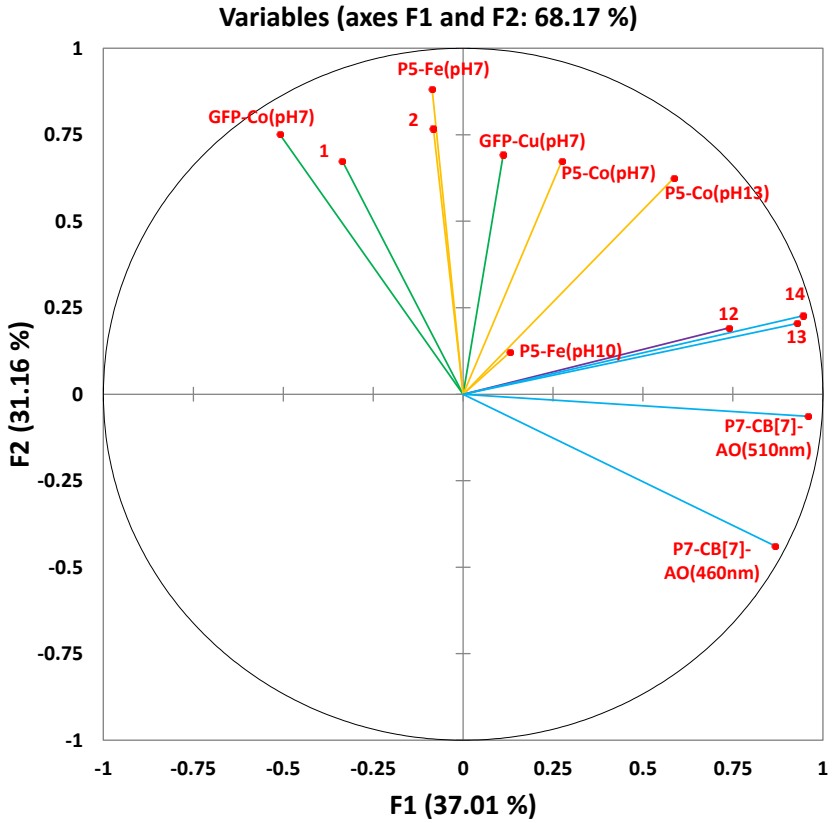

Figure 68. Loading plot of the principal component analysis plot by the 13 elements, identifying the contribution of each element to an axis. Figure reproduced with permission from ref. 153 © 2018, American Chemical Society.

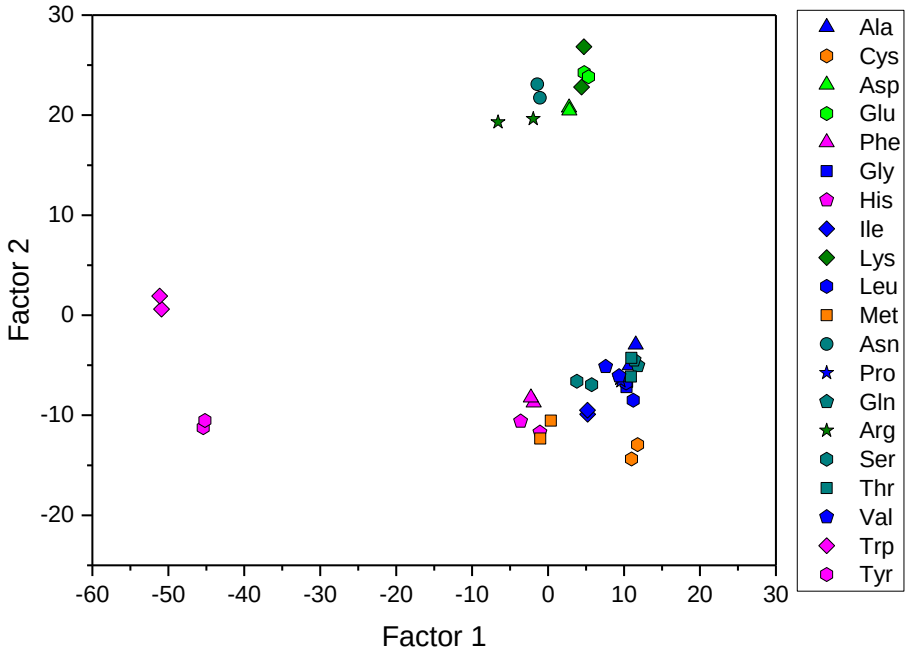

Figure 69. Two-dimensional canonical score plot for the first two factors obtained by PPE-CB[8]-AO (2.0 μM/4.0 μM/2.0 μM) tongue treated with 20 amino acids (c = 25 mM). Each point represents the response pattern for a single amino acid to the optimized array. Figure reproduced with permission from ref. 153 © 2018, American Chemical Society.

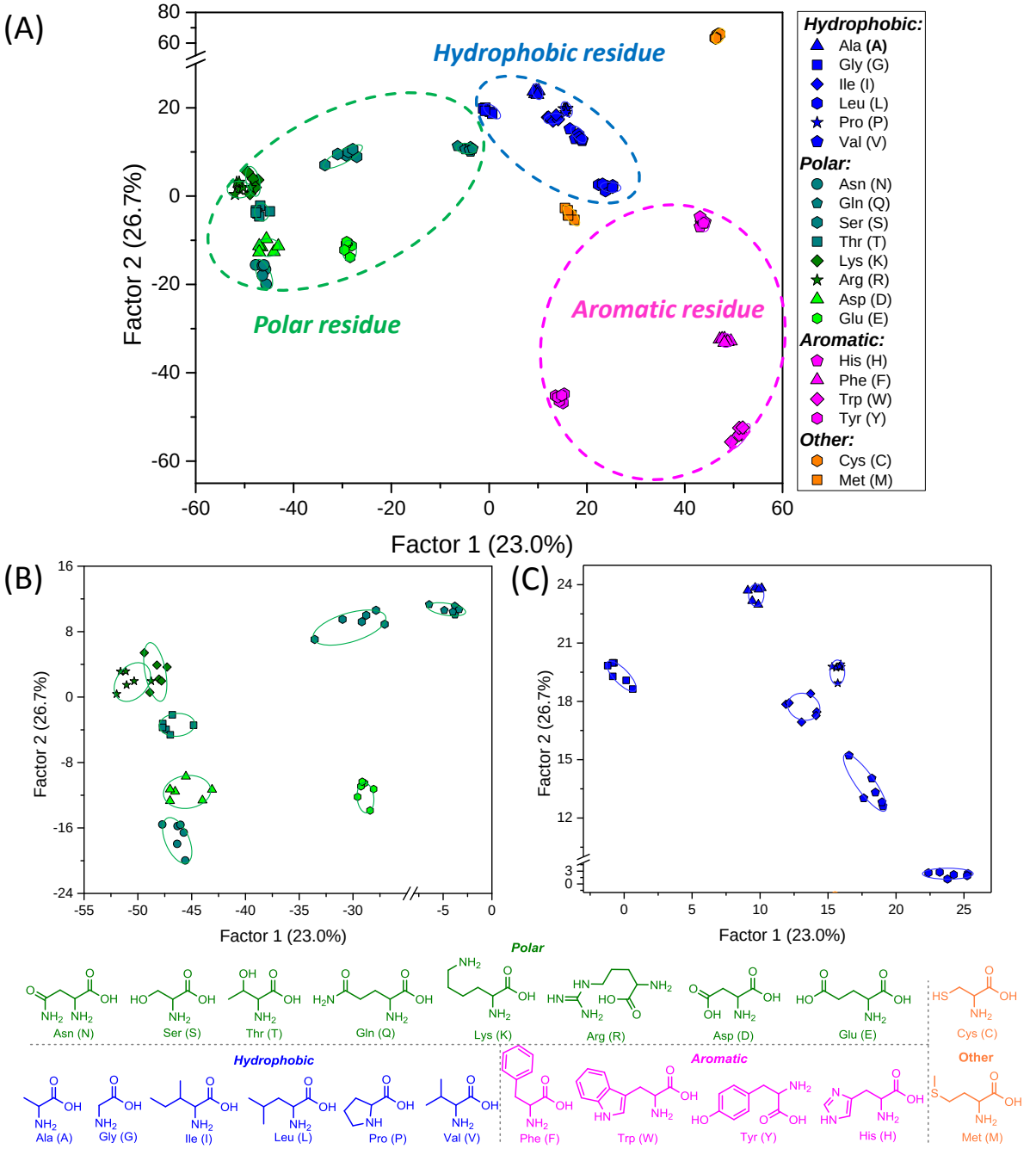

Figure 70. (A) Two-dimensional canonical score plot for the first two factors obtained by eight optimized sensor elements treated with 20 amino acids (c = 25 mM) with 95% confidence ellipses. Each point represents the response pattern for a single amino acid to the optimized array. Amino acids with hydrophobic, polar and aromatic residues are given in blue, green and pink, respectively. **(B)** and **(C)** show the detailed view of the amino acids with polar and hydrophobic residues, respectively. Figure reproduced with permission from ref. 153 © 2018, American Chemical Society.

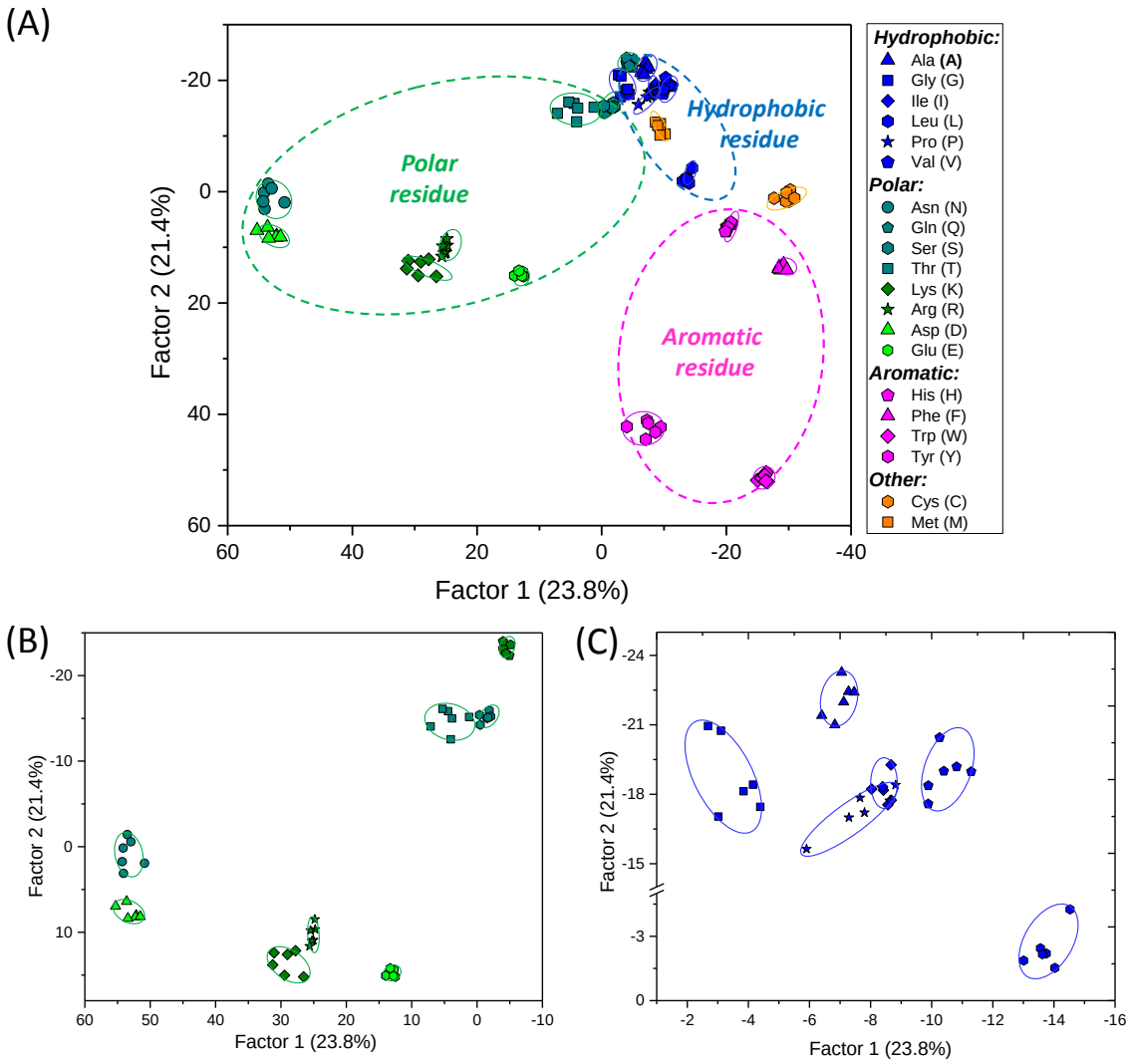

Figure 71. (A) Two-dimensional canonical score plot for the first two factors obtained by eight optimized sensor elements treated with 20 amino acids (c = 10 mM) with 95% confidence ellipses. Each point represents the response pattern for a single amino acid to the optimized array. Amino acids with hydrophobic, polar and aromatic residues are given in blue, green and pink, respectively. **(B)** and **(C)** show the detailed view of the amino acids with polar and hydrophobic residues, respectively. Figure reproduced with permission from ref. 153 © 2018, American Chemical Society.

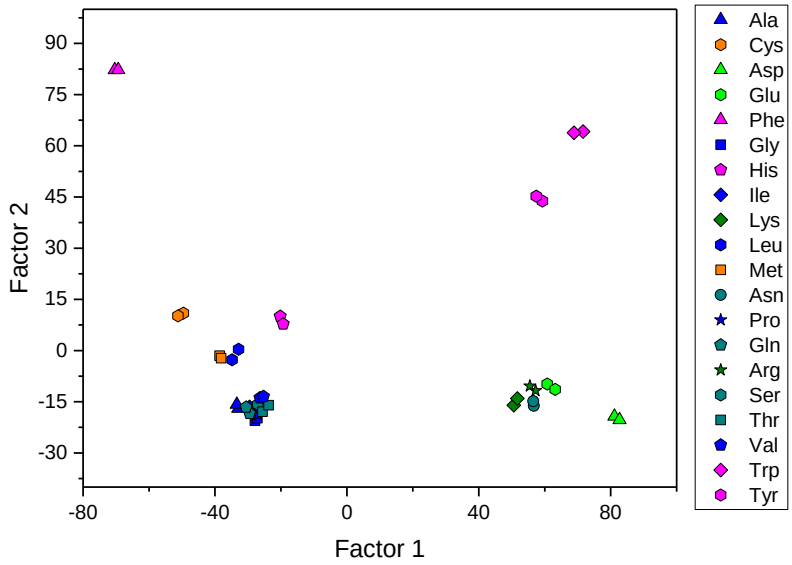

Figure 72. Two-dimensional canonical score plot for the first two factors obtained by eight optimized sensor elements treated with 20 amino acids (c = 5 mM). Each point represents the response pattern for a single amino acid to the optimized array. Figure reproduced with permission from ref. 153 © 2018, American Chemical Society.

To validate the efficiency of the optimized sensing system, we performed tests with 80 randomly chosen amino acids. The new cases are classified into groups, generated through the training matrix, based on their shortest Mahalanobis distance to the respective group.[159-160] We have used our old six-element metal salts based sensor array as a comparison and 8 of 80 unknown samples of amino acids were misclassified, representing an accuracy of 90% (Table 6 and Table 31). In stark contrast, the identification of unknowns samples is improved to 100% when employing the final 8-element tongue (Table 6 and Table 32).

Table 6. Results of Unknown Detection Using an LDA Algorithm.

Amino acids	Number of samples	**6** selected elements tongue (metals-based array)		**8** selected elements tongue (Optimized array)	
		Correctly identified	Accuracy (%)	Correctly identified	Accuracy (%)
Ala	4	3	75	4	100
Cys	4	4	100	4	100
Asp	4	3	75	4	100
Glu	4	4	100	4	100
Phe	4	4	100	4	100
Gly	4	4	100	4	100
His	4	4	100	4	100
Ile	4	3	75	4	100
Lys	4	2	50	4	100
Leu	4	2	50	4	100
Met	4	4	100	4	100
Asn	4	4	100	4	100
Pro	4	4	100	4	100
Gln	4	4	100	4	100
Arg	4	4	100	4	100
Ser	4	4	100	4	100
Thr	4	3	75	4	100
Val	4	4	100	4	100
Trp	4	4	100	4	100
Tyr	4	4	100	4	100
Total	**80**	**72**	**90**	**80**	**100**

3.4.3 Conclusions

In conclusion we have dramatically improved our PPE-based amino-acid array by addition of further sensor elements. We have investigated four different arrays, plucked the best elements from three of these arrays and created a new, much more powerful array, containing six elements of our old array and two additional elements gleaned from other tongues. Over all, this is an encouraging development, which shows that simple tongues and sensor arrays discriminate tightly related analytes.

Chapter 4. Poly(*para*-phenyleneethynylene)-Sensor Arrays Discriminate 22 Different Teas

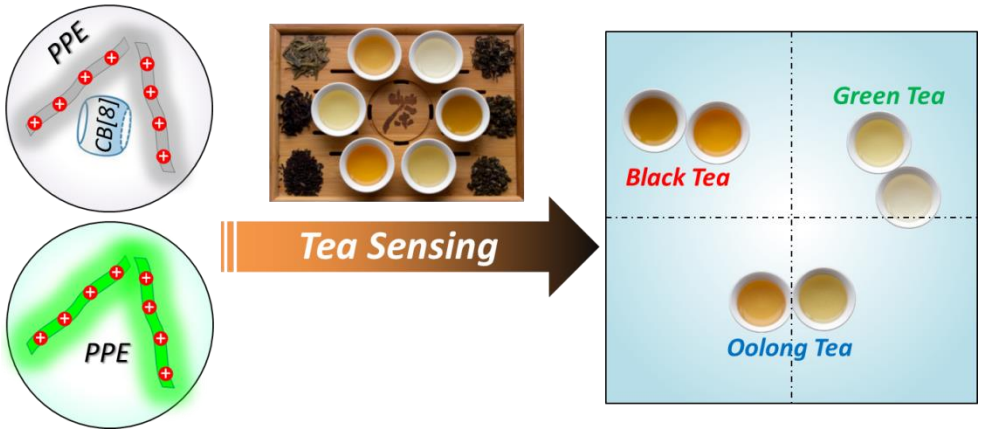

Figure 73. Schematic illustration of hypothesis-free sensor array discriminates teas. Figure reproduced with permission from ref. 77 © 2018, American Chemical Society.

In this chapter, two nine-element sensor arrays, consisting of either three cationic poly(*para*-phenylene-ethynylene)s (PPE) or the same PPEs complexed by cucurbituril[8] (CB[8]) at pH 3, 7 and 13 in water, discriminate 22 different teas and some of their small molecule components, including caffeine, theobromine and theophylline. Both arrays distinguish all of the black, green and oolong teas. The discrimination occurs by differential fluorescence modulation of the components of the sensor array and the treatment of the collected data by linear discriminant analysis. The signal is generated by either simple quenching (PPE only array) or the disruption of the PPE/CB[8] complex and quenching of the complex's or the PPEs' fluorescence through the polyphenolic colorants of the teas. Added amino acids, theobromine, theophylline, and caffeine give a fluorescence turn-on of the PPE-CB[8] array, due to the disruption of the self-assembled complex, while for the PPE-alone tongue, only caffeine, theobromine and theophylline elicited useful fluorescence response. Both tongues discriminate different teas without any problem.

4.1 Introduction and Construction of Chemical Tongues

4.1.1 Introduction of Tea

Tea is among the most popular beverages worldwide, which is of great interest due to its refreshing taste, attractive aroma, and potential health benefits. The leaves, buds, and stalks of the plant Camellia sinensis are, after fermentation and/or roasting used in infusions of hot water, "tea". According to the difference in fermentation degrees and processing techniques, unfermented versions go as green teas, lightly fermented are oolong teas and fully fermented are black teas. Black tea is consumed worldwide, while green and oolong teas are consumed mainly in Africa and Asia.[161-162] A supremely popular beverage, it is suspected of health benefits - also, its caffeine content of around 4.5% refreshes the tired mind.[163]

Teas come in many price ranges and taste variants, the price of tea is variable depending on the quality of the tea; however, no reliable tea discrimination methods can assist tea buyers in avoiding fake or

adulterate tea products. The identification of tea depends mainly on sensory evaluation, which is performed by trained tasters who evaluate tea by appearance, color, aroma, taste, as well as overall quality of the tea sample.[164] Obviously, this method would inevitably suffer from drawbacks such as personal subjectivity and poor reproducibility.[162, 165] Due to the economic impact, a large number of methods for the purpose of identifying the main compounds in teas, such as high-performance liquid chromatography (HPLC),[161] gas chromatography-mass spectrometry (GC-MS),[166-167] near-infrared spectroscopy (NIR)[168-169] have been utilized to assess tea. Even though these methods provide reliable protocols with good accuracy, the problems are that they usually suffer from shortcomings like complicated need lengthy sample pretreatment procedures, time-consuming operations, inappropriate for the implementation of bulky samples and high cost.[165, 170] Other rapid instrumental analytical techniques like electric noses and electric tongues, which are composed of an array of cross-responsive sensors, a signal collecting device and pattern recognition software for data recording and analysis also have been employed to discriminate tea grade levels.[171-173] Compared with traditional analytical approaches, this method is less expensive and more convenient to operate. However, it faces a big challenge to discriminate complex mixtures as they are easily affected by environmental conditions, particularly water.[174] Therefore, it is fundamentally interesting and important to develop effective systems for quality control and discrimination of different teas.

4.1.2 Sensor Arrays for Tea Discrimination

Given merits of cost-effective and easy to operate, analysis methods based on colorimetric artificial nose system have attracted growing attention among researchers. Nowadays, they have been widely applied to discriminate a variety of mixtures including volatile gases,[175] liquors,[176] soft drinks,[33] beers,[174] coffee aromas,[177] and *etc.* The following examples verify that colorimetric sensor arrays could serve as an effective alternative to deal with quality control and discrimination of different types and qualities of tea.

The group of Hou[162] developed an artificial chemosensor array, employing chemical-responsive dyes, such as porphyrins, metallosalophen complexes, redox metal salts and pH indicators as sensing elements to discriminate different Chinese green teas. Owing to different geographical origins and grade levels, the chemical composition of green teas varies in the number of organic compounds present and their ratios. Upon interaction with these chemical components, these sensing elements could change individual colors, thus producing a characteristic color change profile for each specific tea sample. The color change profiles of the array were used as a digital representation of a unique fingerprint for specific Chinese green teas (Figure 74). However, apart from a very good recognition ability demonstrated, here, synthesis of chromophore porphyrins limited the popularity of its application. Based on the IDA mechanism, the same group[165] chose three kinds of dye/metal ions assays including Zincon-Zn^{2+}, PV-Cu^{2+}, and Mur-Ni^{2+} in different concentrations to develop an

elegant colorimetric approach that is capable of distinguishing teas with respect to categories, quality grades, and geographical origins. After construction and deduction upon response to theanine and six other amino acids abundant in tea leaves, the sensor is capable of distinguishing 70 tea samples within four categories (Figure 75). There, the sensor's response was calculated as result of the color change (grey value or RGB value), yet, similar colorants from interfering substances can produce errors.

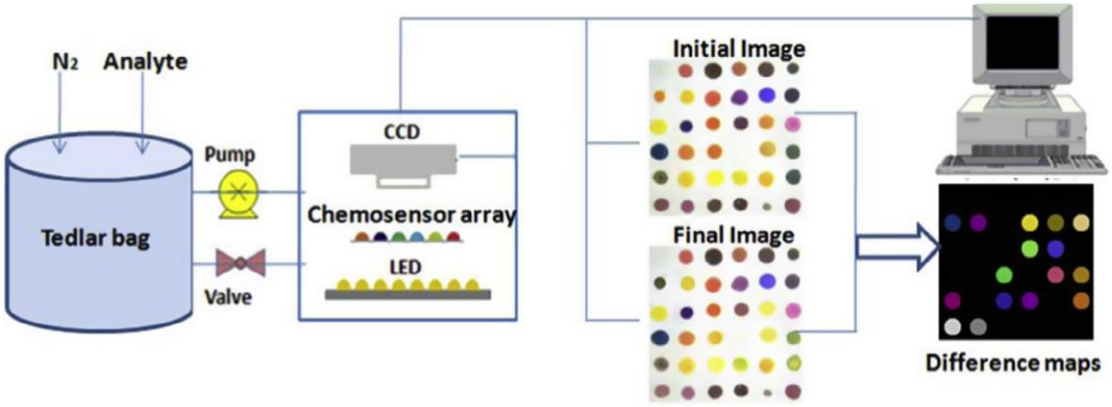

Figure 74. 6 x 6 colorimetric sensor array and schematic diagram of the detection system. Figure reproduced with permission from ref. 162 © 2014, Elsevier.

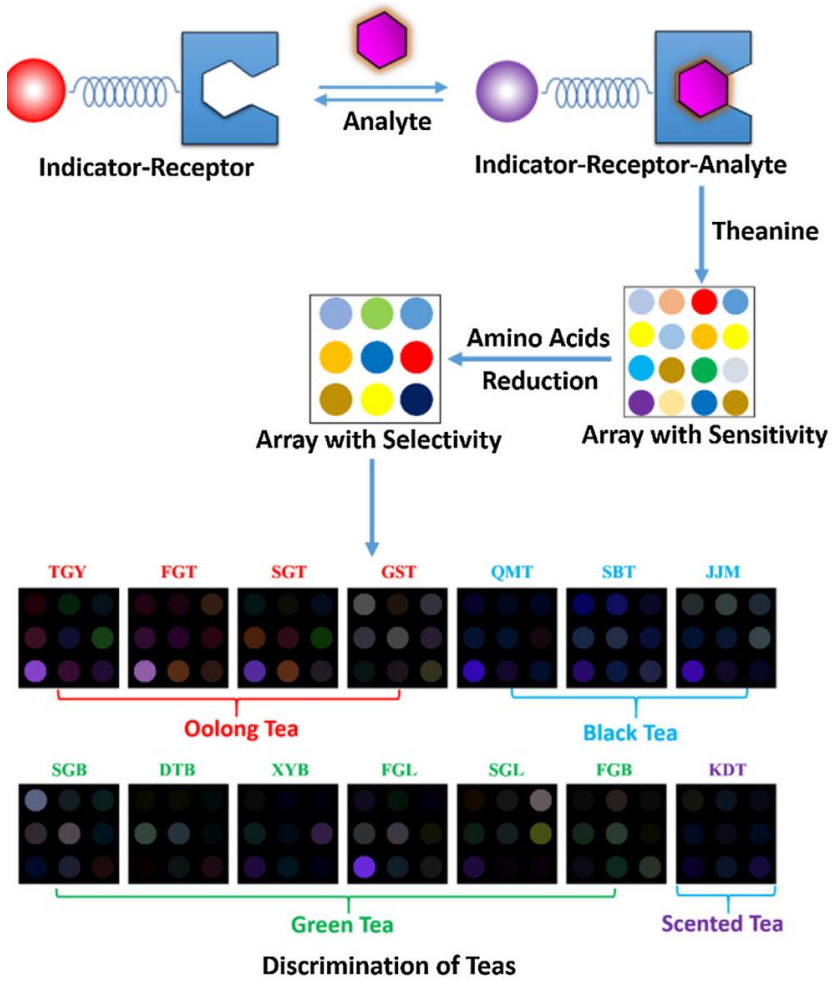

Figure 75. Proposed strategy for the discrimination of teas within different categories. Figure reproduced with permission from ref. 165 © 2017, Elsevier.

Recently, She *et al.*[178] also reported a fluorescent "turn-off" sensor based on water-soluble CdTe quantum dots (QDs) combined with chemometrics for sensitive and effective identification of 29 green teas. As presented in Figure 76, the fluorescence of N-acetyl-L-cysteine capped CdTe QDs was quenched in different degrees in light of positions and intensities of the fluorescence peaks after addition of different green teas.

Besides of colorimetric methods, arrays of host-indicator ensembles are used to discriminate black teas by Qian *et al.*[31] Also based on an IDA, they described the use of a series of simple multi-boronic acid-based receptors and pH indicators for discrimination of vicinal-diol-containing flavonoids and black tea extracts (Figure 77). By traditional UV-vis titrations, dynamic three-component sensing arrays (H-ML-PV and H-ARS-PV) were constructed and successfully differentiated individual flavonoids and black teas with high accuracy.

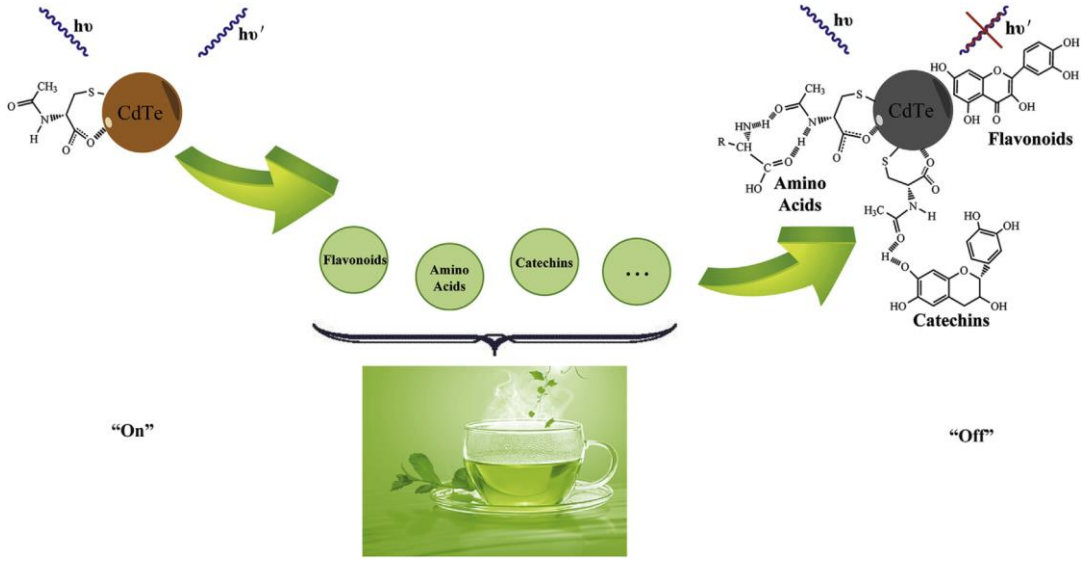

Figure 76. Schematic illustration of the NAC-capped CdTe QDs system for sensing different green teas. Figure reproduced with permission from ref. 178 © 2017, Elsevier.

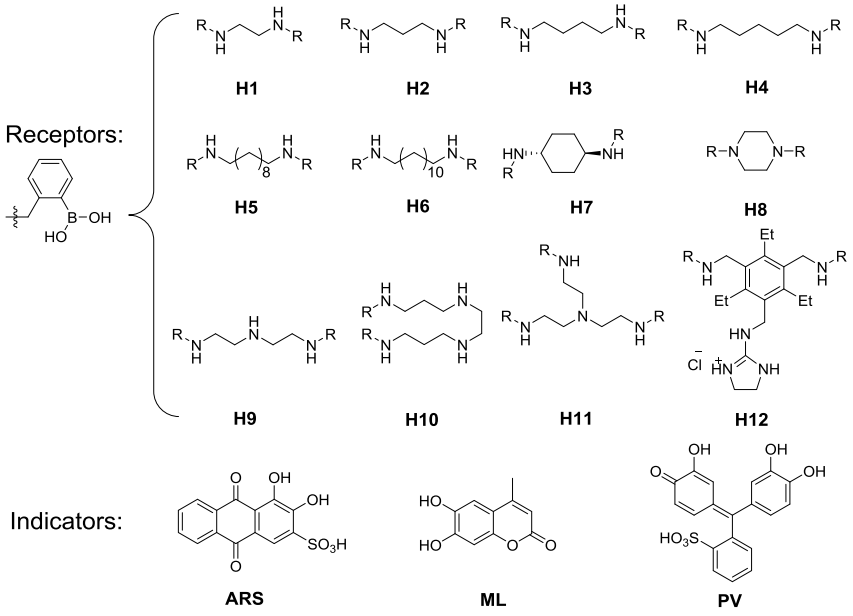

Figure 77. The structures of muti-boronic acid receptors **H1-12** and pH indicators **ARS**, **ML** and **PV**.

4.1.3 Design and Construction of PPE-Based Sensor Array

Our fluorescence-based method is sensitive and robust because the fluorescence intensity is modulated by even smallest amounts (micrograms per milliliter) of the analyte. The system in this work does not need any complicated sample preparation and is equal or superior to state-of-the-art methods with respect to speed, resolution, and efficiency of discrimination; fluorescence-based hypothesis-free array methods have to our knowledge not been employed to discriminate teas and therefore this is a fundamentally attractive proposition.

Teas are attractive analytes as they consist of at least two very different classes of component mixtures that determine their character. On the one hand, there are small molecules such as amino acids, caffeine etc. determining the taste of tea. Amino acids are primary metabolites from the nitrogen cycle of tea trees and basic constituents of proteins in tea leaves. Caffeine and the amino acids are direct small molecule targets for the discrimination and the quality control of teas. On the other hand, teas contain macromolecules including polyphenols etc. that affect the flavor, consistency and are speculated to provide potential health benefits.

We developed two different libraries for the discrimination of teas. One is poly(*para*-phenyleneethynylene (PPE) based, similar to one that has been used for detection of other analytes (white wines, whiskies, amino acids, juices, proteins, non-steroidal anti-inflammatories, etc),[45-46, 49, 76, 79, 136, 179] where hydrophobic and electrostatic interactions cause the signal generation,[79, 136] but also, a PPE-cucurbit[8]uril (CB[8]) complex, where the disruption of the complex generates a fluorescence turn-on signal. This second library employs host-guest interactions that modify the sensory response of the PPEs.[180-181] Cucurbit[n]urils (CB[n]) are macrocyclic structures formed from an acid catalyzed condensation of glycoluril and formaldehyde. CB[n] has a toroidal structure and a hydrophobic interior cavity, which provides an encapsulation site for guest molecules and carbonyl-lined portals bind charged molecules by charge-dipole or hydrogen bonding interactions.[182-185] Water-soluble CB[n] are promising hosts for binding of analytes. CB[8] is also large enough to bind two organic guests simultaneously.[186] Therefore, host-guest complexes based on CB[8] are attractive for sensing in a displacement assay using arrays.[24, 51, 122, 131]

Here we test the hypothesis that fluorescent sensor arrays discriminate different green, oolong, and black teas. We also investigate if a simple fluorescent polyelectrolyte array suffices or if a more complex cucurbituril-fluorescent polyelectrolyte complex is necessary for this type of discrimination.

4.2 Results and Discussions

4.2.1 Complexation of PPEs by CB[8]

Figure 78 shows the schematic illustration of PPE-cucurbituril[8] complexes and their fluorescence intensity modulation after addition of analytes. CB[8] simultaneously complexes two PPE chains, which aggregates the PPE-chains and decreases their fluorescence intensity. CB[8] has a large cavity, which allows the encapsulation of amino acids or xanthine. When the analytes are incubated with the PPE/CB[8] complexes, we would expect competitive binding between them, and an expected fluorescence turn on under expulsion of the PPE-chains.

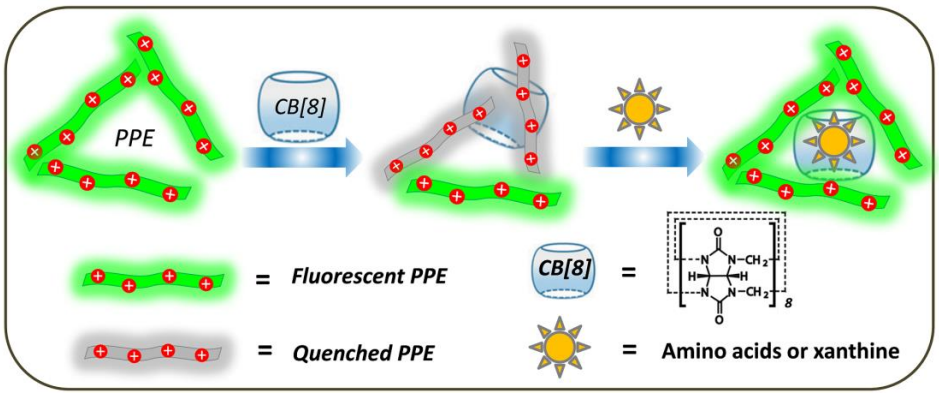

Figure 78. Schematic illustration of PPE/CB[8] tongue and fluorescence modulation after adding analytes. Figure reproduced with permission from ref. 77 © 2018, American Chemical Society.

Upon mixing of CB[8] and **P7** (for the structure see Figure 80) quenching is observed; while addition of CB[7] does not affect the fluorescence intensity of **P7**, even though the concentration of CB[7] is 8 times higher than that of CB[8] (Figure 79A). The reversibility of the **P7**/CB[8] complexation was investigated by addition of CB[8]-binders methyl viologen (MV^{2+}) and adamantylamine (AD).[181, 187-188] Upon adding MV^{2+} or AD, stable CB[8]/MV^{2+} or CB[8]/AD complexes are formed, the PPE chains are released, and fluorescence restored (Figure 79B). Therefore, PPE/CB[8] complexes might serve as a sensitive probe for strongly binding guests.

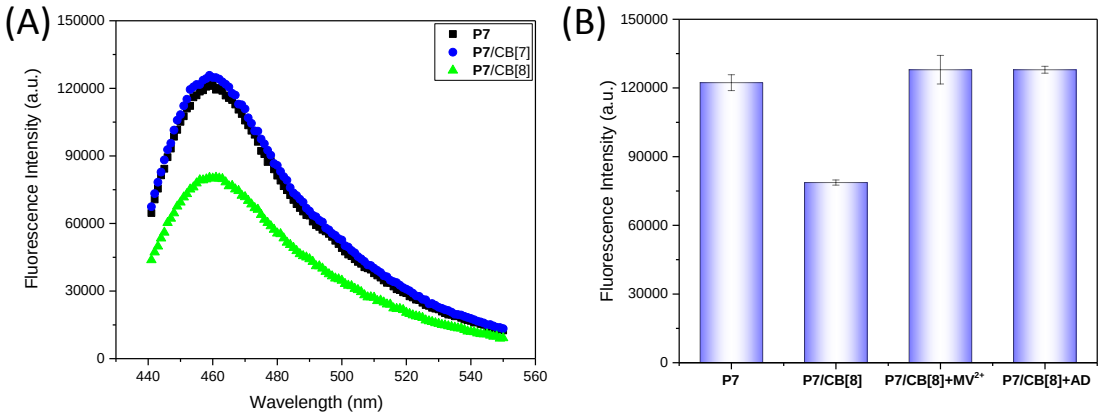

Figure 79. (A) Fluorescence intensity properties of **P7** (1 µM, black square), **P7**/CB[7] (1 µM/50 µM, blue circle) and **P7**/CB[8] (1 µM/6 µM, green triangle). **(B)** Fluorescence response pattern obtained by **P7**, **P7**/CB[8], **P7**/CB[8] + MV^{2+} and **P7**/CB[8] + AD (MV^{2+}: methyl viologen, AD: adamantylamine). Each value is from the average of two independent measurements. Figure reproduced with permission from ref. 77 © 2018, American Chemical Society.

4.2.2 Screening Process

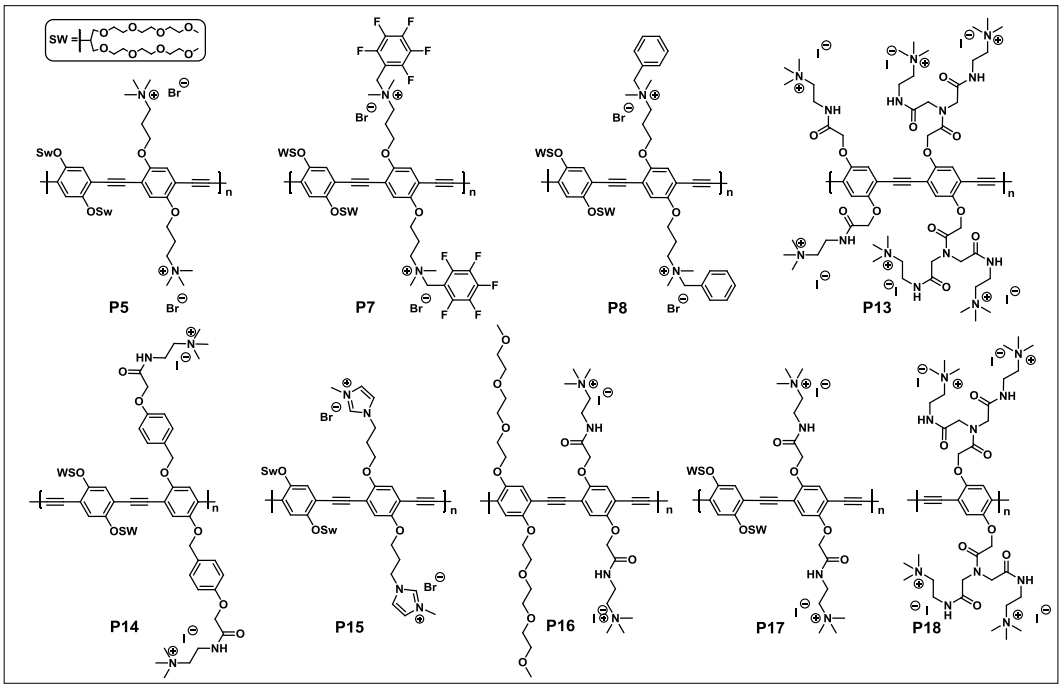

Figure 80. Structures of PPEs used for the screening process.

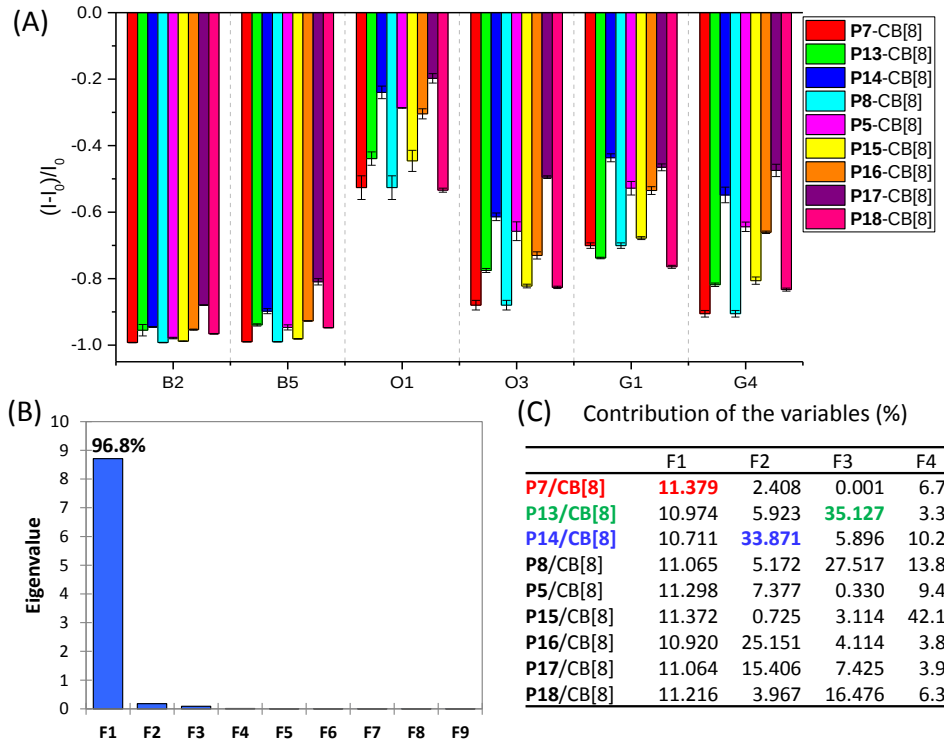

	F1	F2	F3	F4
P7/CB[8]	11.379	2.408	0.001	6.732
P13/CB[8]	10.974	5.923	35.127	3.328
P14/CB[8]	10.711	33.871	5.896	10.293
P8/CB[8]	11.065	5.172	27.517	13.875
P5/CB[8]	11.298	7.377	0.330	9.430
P15/CB[8]	11.372	0.725	3.114	42.153
P16/CB[8]	10.920	25.151	4.114	3.838
P17/CB[8]	11.064	15.406	7.425	3.957
P18/CB[8]	11.216	3.967	16.476	6.392

Figure 81. (A) Fluorescence response pattern ((I - I_0) / I_0) obtained by the 9 positively charged PPEs (1.2 μM) in the presence of CB[8] (9.0 μM) treated with 6 randomly chosen teas. Each value is the average of two independent measurements. **(B)** Eigenvalue calculated from the principal component analysis, factor 1 represent 96.8% of the total variation. **(C)** The contribution of each sensor elements to the resulted six factors (F1-F4). Figure reproduced with permission from ref. 77 © 2018, American Chemical Society.

A library of 9 positively charged PPEs (see Figure 80) were selected for screening. According to principal component analysis, three polymers, **P7** (positive charge), **P13** (higher positive charge) and **P14** (positive charge), were selected as they displayed the highest discriminative power for teas

(Figure 81). Figure 82A shows that the fluorescence of **P7**/CB[8] was almost fully quenched when the concentration of tea was over 0.5 mg/mL. The most suitable concentration was 0.1 mg/mL for the discrimination. Then 25 mg of tea samples were infused with 10 mL distilled boiling water for 5 min, 10 min, 30 min and 60 min, respectively. Then the tea leaves were removed by filtration and the tea infusions were cooled down to room temperature. Afterward, the tea infusions were diluted to 0.1 mg/mL when loaded into a well on a 96-well plate. Figure 82B shows that the fluorescence wasn't further quenched when the infusion time was prolonged. Suitable infusion time was 5 min. Acidic, neutral and basic pH conditions were further investigated. As shown in Figure 83, this sensor system is much more sensitive at pH 7 (concentration of tea infusion: 0.01 mg/mL) than at pH 3 and 13 (concentration of tea infusion: 0.1 mg/mL). Finally, screening arrived at a suitable tongue consisting of 18 elements, **P7**, **P13**, **P14** and **P7**/CB[8], **P13**/CB[8], **P14**/CB[8] at pH 3, 7 and 13 (Figure 84, grey and purple circles).

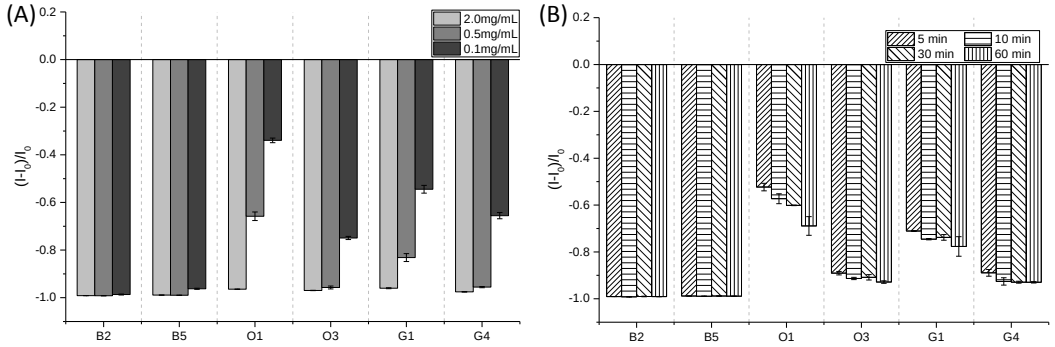

Figure 82. Fluorescence response pattern ((I - I_0) / I_0) obtained by **P7**/CB[8] (1.2 μM/9.0 μM) treated with **(A)** different concentration of 6 randomly chosen teas and **(B)** 6 randomly chosen teas at different infusion time. Each value is the average of two independent measurements.

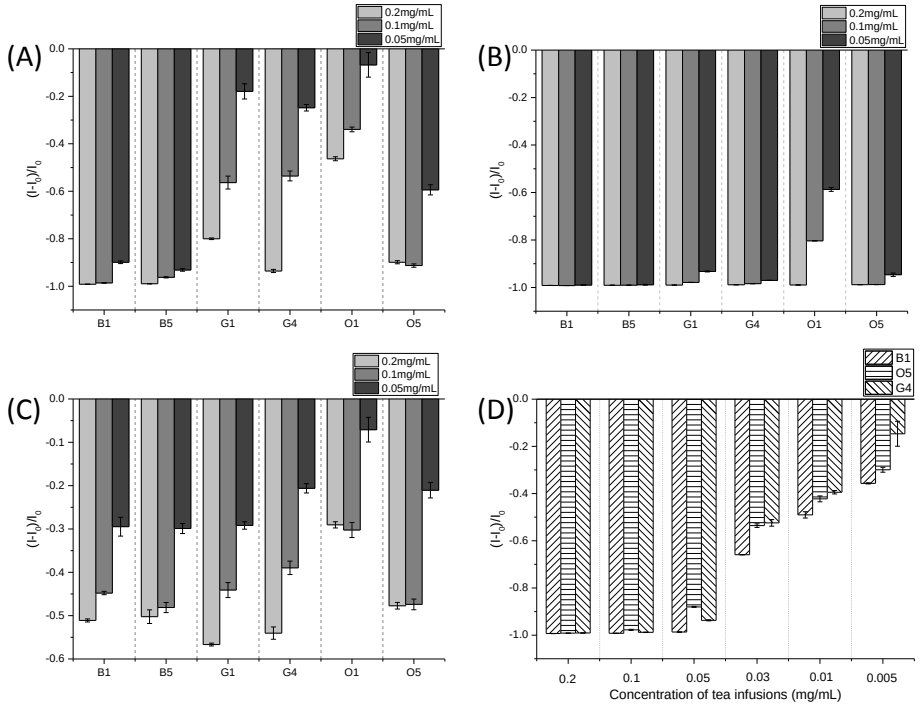

Figure 83. Fluorescence response pattern ((I - I_0) / I_0) obtained by **P7**/CB[8] (1.2 μM/9.0 μM) treated with teas at **(A)** pH 3, **(B)** pH 7, **(C)** pH 13 buffer solution and **(D)** different concentration at pH 7 buffer solution. Each value is the average of two independent measurements.

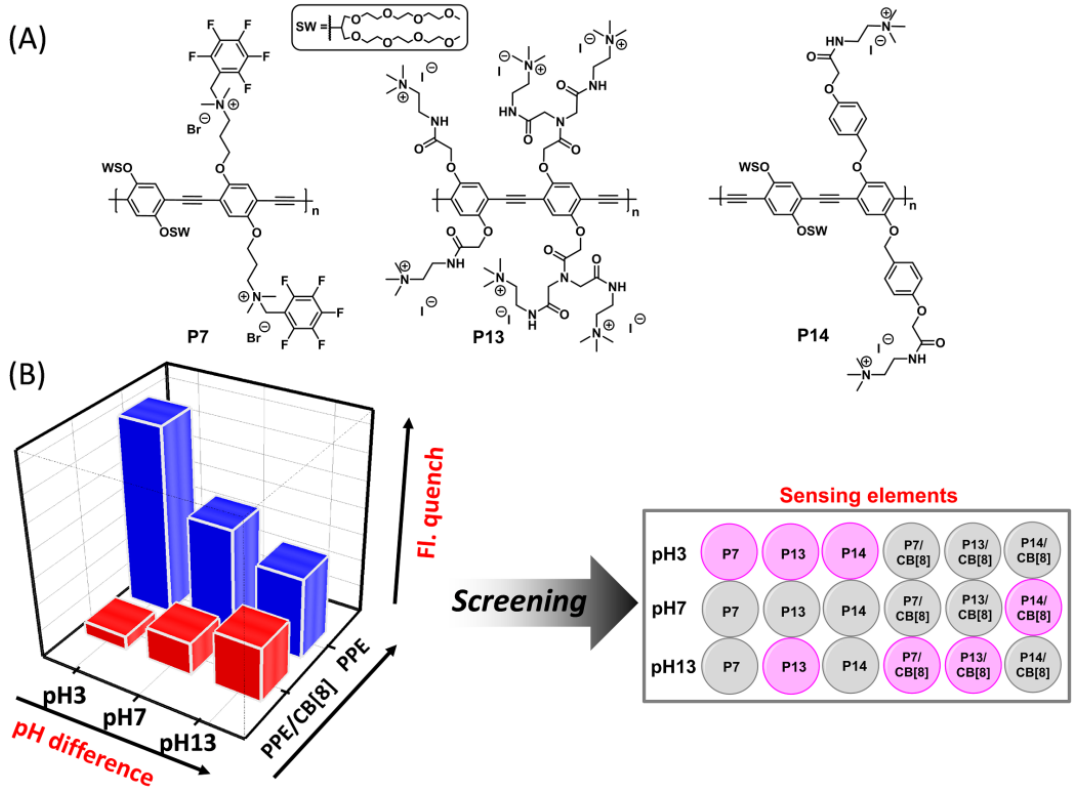

Figure 84. (A) Chemical structures of the used poly(*p*-phenyleneethynylene)s. **(B)** Systematic evaluation and selection of the successful tongue elements for sensing. Figure reproduced with permission from ref. 77 © 2018, American Chemical Society.

4.2.3 Discrimination of Tea-Based Analytes

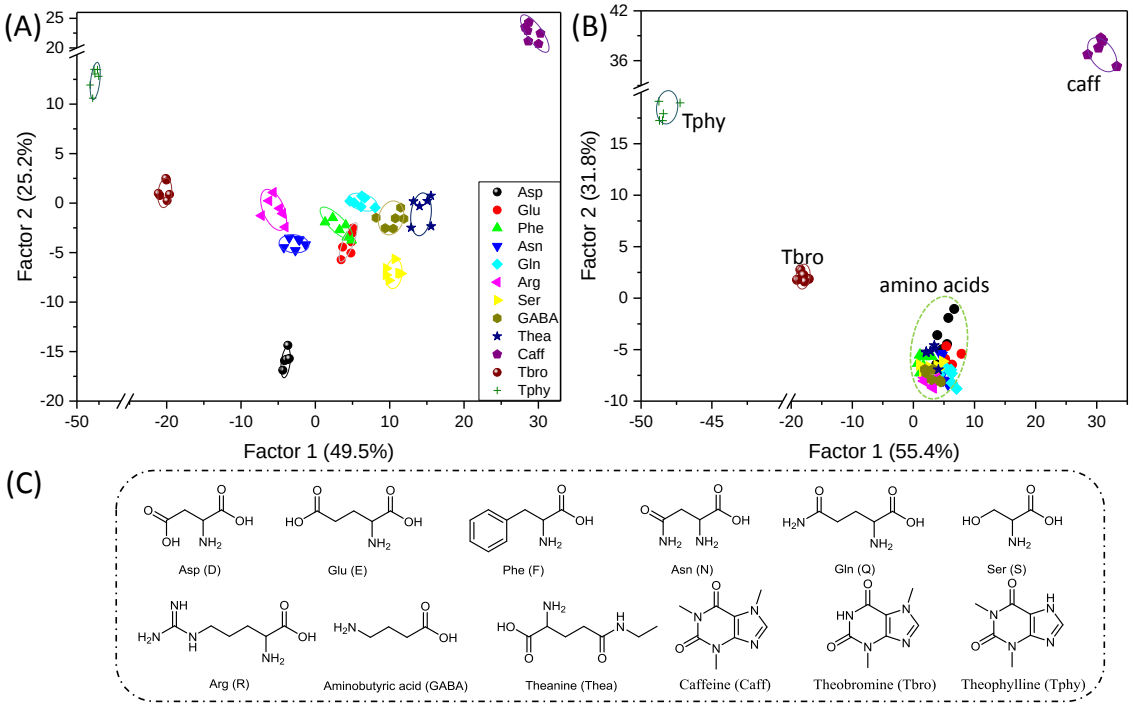

Figure 85. 2D canonical score plot for the first two factors obtained by **(A)** PPE/CB[8] tongue (1.2 µM/9.0 µM, at pH 3 and 13, buffered) and **(B)** PPE-only-tongue (1.2 µM, at pH 3 and 13, buffered) treated with tea-related analytes (c = 10 mM) with 95% confidence ellipses. Each point represents the response pattern for a single analyte to the array. **(C)** Structures of key components in tea leaves. Figure reproduced with permission from ref. 77 © 2018, American Chemical Society.

Amino acids are one of the three key components (polyphenols, amino acids, and caffeine) that determine the characteristic flavor and taste of tea.[189-190] More than 26 different amino acids have been found in tea, including the 20 basic amino acids and 6 non-proteinogenic amino acids. Theanine, aspartic acid, glutamic acid, phenylalanine, asparagine, glutamine, arginine, serine andγ-aminobutyric acid contribute most to the total amino acid content in tea.[165, 191-192] Theobromine and theophylline are also found in tea, but in smaller amounts.[193] In the following experiments we treated the two different libraries (PPE-CB[8]-array and PPE-only-array) with the 12 analytes (9 amino acids and three xanthine types, Figure 85C). The results indicated that the simple PPE tongue alone is useful for the discrimination of caffeine, theobromine, and theophylline but does not discriminate the other key components (amino acids, Figure 85B and Figure 86B) well; however, the addition of CB[8] to the PPEs imbues selectivity toward all of these small molecule analytes (Figure 85A and Figure 86A). According to the 2D-LDA, the PPE/CB[8] tongue discriminates all of these compounds (Figure 85A, Table 33 and Table 34). 46 of 48 unknown samples were correctly identified, representing an accuracy of 96% (Table 35).

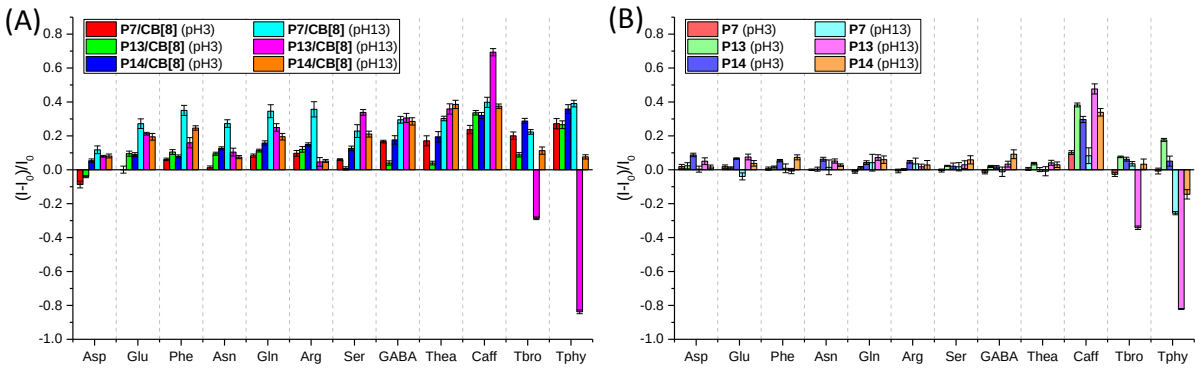

Figure 86. Fluorescence response pattern ($(I - I_0)/I_0$) obtained by **(A)** PPE/CB[8] tongue (1.2 μM/9.0 μM, at pH 3 and 13, buffered) and **(B)** PPE tongue (1.2 μM, at pH 3 and 13, buffered) treated with tea-related analytes (c = 10 mM). Each value is the average of six independent measurements; each error bar shows the standard deviation (SD) of these measurements. Figure reproduced with permission from ref. 77 © 2018, American Chemical Society.

4.2.4 Discrimination of Teas

The two investigated tongues allow differentiation of teas by brand, price, quality grades, and geographic origins. Table 7 and Figure 87 display the detailed information and appearance of the teas selected for the study. PPEs and the PPE-CB[8] complexes were dissolved in different pH buffer (pH 3, 7 and 13) to give 2.0 μM and 2.0 μM-15.0 μM of stock solutions on the basis of their molecular weights. Each PPE or complex solution (180 μL) in buffer was respectively loaded into a well on a 96-well plate (300 μL microplate). Subsequently, 120 μL tea infusions were added to each well and mixed. Finally, the fluorescence intensities (I_0 or I) were recorded at the peak 460 nm with an excitation at 410 nm by using a microplate reader. Figure 88 shows the fluorescence response patterns of PPE/CB[8] tongue and PPE tongue treated with 22 kinds of teas, respectively.

Table 7. Detailed Information on the Investigated Teas (8 Black Teas B1-B8, 6 Green Teas G1-G6, and 8 Oolong Teas O1-O8) Used in This Study.

Abbr.	Category	Fermentation	Company	Brand name	Geographical origin
B1	Black tea	Fermented	Teekanne	Earl Grey	-
B2	Black tea	Fermented	Teekanne	Assam	Assam, India
B3	Black tea	Fermented	Teekanne	Ostfriesen Gold	-
B4	Black tea	Fermented	Teekanne	Darjeeling	Darjeeling, India
B5	Black tea	Fermented	Meßmer	Darjeeling	Darjeeling, India
B6	Black tea	Fermented	Tee Gschwendner	Flugtee Nepal	Nepal
B7	Black tea	Fermented	Tee Gschwendner	Flugtee Nordindien	India
B8	Black tea	Fermented	Tee Gschwendner	Flugtee Darjeeling	Darjeeling, India
G1[a]	Green tea	Non-fermented	-	Longjing	Hangzhou, China
G2[a]	Green tea	Non-fermented	-	Longjing	Hangzhou, China
G3	Green tea	Non-fermented	Teekanne	Grüner Tee	China
G4	Green tea	Non-fermented	Meßmer	Grüner Tee	China
G5	Green tea	Non-fermented	-	Linglong	Guidong, China
G6	Green tea	Non-fermented	-	Biluochun	Dongting, China
O1[a]	Oolong tea	Semi-fermented	-	Tieguanyin	Anxi, China
O2[a]	Oolong tea	Semi-fermented	-	Tieguanyin	Anxi, China
O3	Oolong tea	Semi-fermented	-	Huangguanyin	Wuyishan, China
O4	Oolong tea	Semi-fermented	-	Tieluohan	Wuyishan, China
O5[a]	Oolong tea	Semi-fermented	-	Rougui	Wuyishan, China
O6[a]	Oolong tea	Semi-fermented	-	Rougui	Wuyishan, China
O7	Oolong tea	Semi-fermented	-	Shuixian	Wuyishan, China
O8[a]	Oolong tea	Semi-fermented	-	Rougui	Wuyishan, China

[a] Tea samples (G1, G2; O1, O2 and O5, O6, O8) are obtained from different manufacturers in China. "-" means not known.

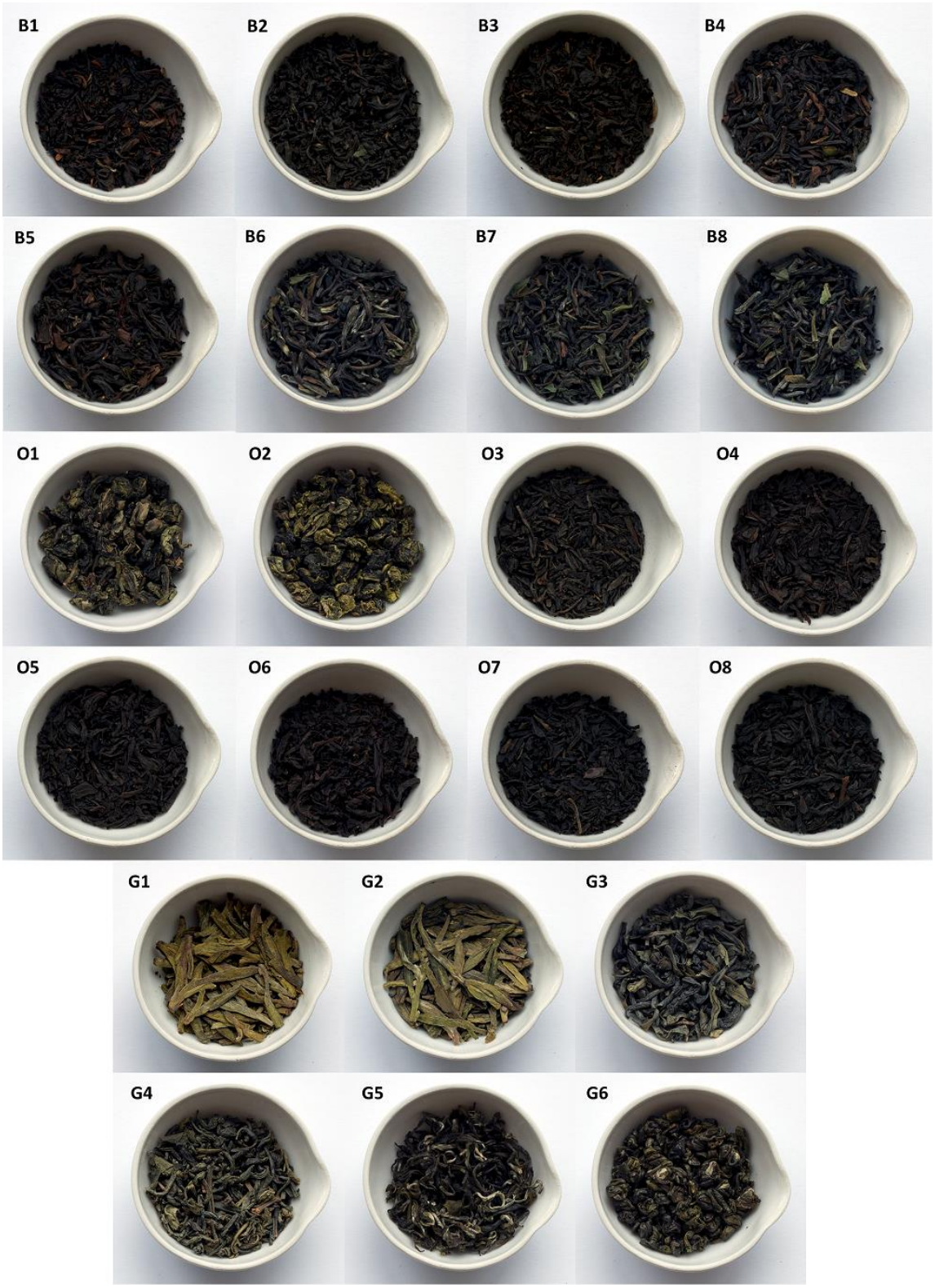

Figure 87. The appearance of the investigated teas (black teas B1-B8, green teas G1-G6 and oolong teas O1-O8). Figure reproduced with permission from ref. 77 © 2018, American Chemical Society.

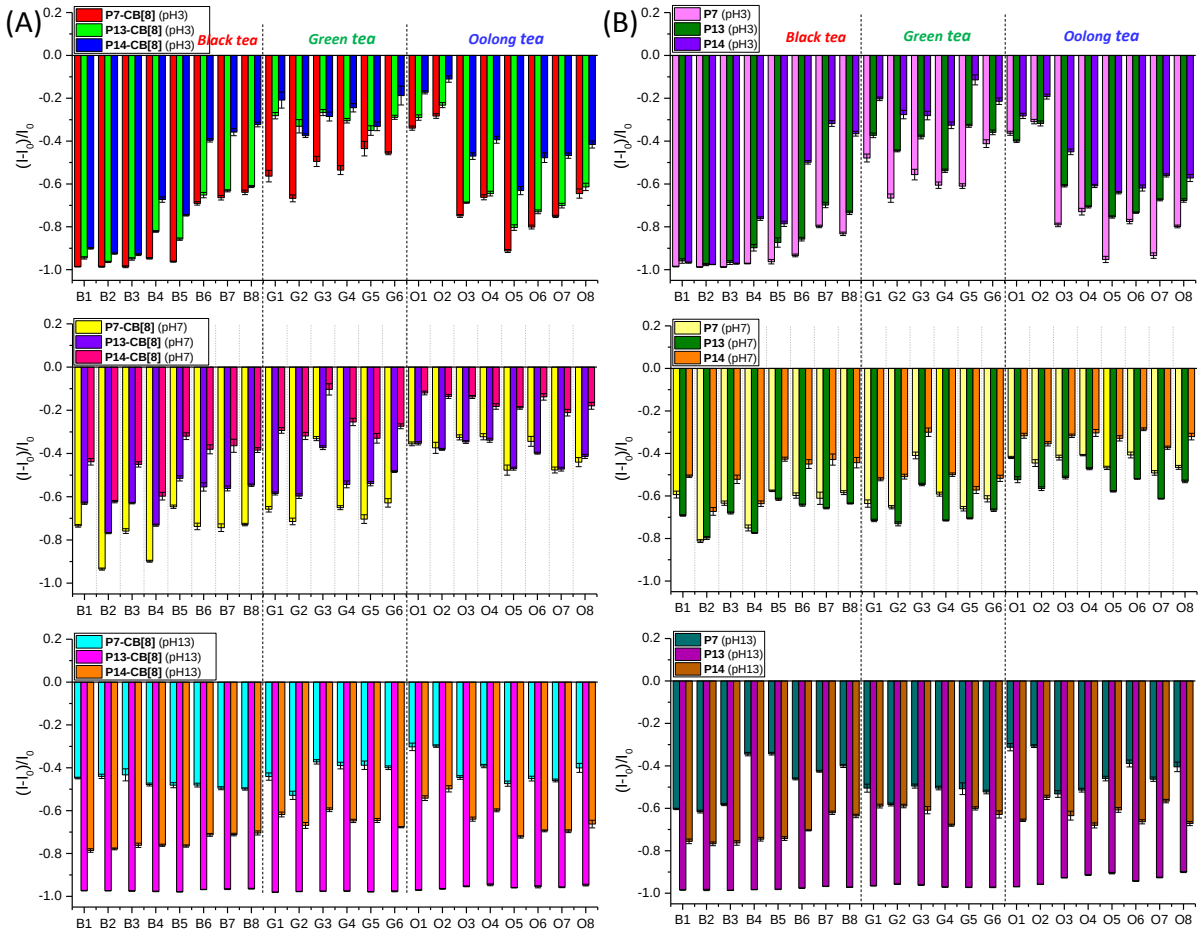

Figure 88. Fluorescence response patterns ($(I - I_0)/I_0$) obtained by **(A)** PPE/CB[8] tongue (1.2 μM/9.0 μM, at pH 3, 7 and 13, buffered) and **(B)** PPE tongue (1.2 μM, at pH 3, 7 and 13, buffered) treated with 22 kinds of teas (0.1 mg/mL at pH 3 and 13, 0.01 mg/mL at pH 7, respectively). Each value is the average of six independent measurements; each error bar shows the standard deviation (SD) of these measurements. Figure reproduced with permission from ref. 77 © 2018, American Chemical Society.

The quality grade of the tea products determines their value, of which the price may vary from cents to multiple of dollars per gram, and therefore, it is attractive to be able to perform simple quality control.[171] In the LDA plot of the data of the PPE-CB[8]-array (Figure 89A) black tea samples B1, B2, and B3 cluster together; B6, B7, and B8, high-quality Darjeeling teas, expensive, are of the same type but from a different producer and also group. Eight oolong tea samples, produced in two different districts (Anxi and Wuyishan, Fujian, China) were further analyzed. Oolong tea samples from Anxi (O1 and O2) are located in the upper right corner of the score plot, while Wuyishan teas (O3-O8) are located in the left region of the scatter plot (Figure 89A); the three quality grades, first grade (O5, O6), second grade (O3, O4), and third grade (O7, O8) are well discriminated. In Figure 89B, the PPE tongue was employed. Overall, the discriminative power is similar to that of the PPE/CB[8] tongue and in some better for black teas. The six Wuyishan teas of three different quality grades also cluster well. Figure 89C shows the 2D score plot of the first two canonical scores obtained by the combination of both tongues. As expected, the overall resolution of the combined array has increased; however, the system does not distinguish between the black teas B7 and B8 when only looking at two scores.

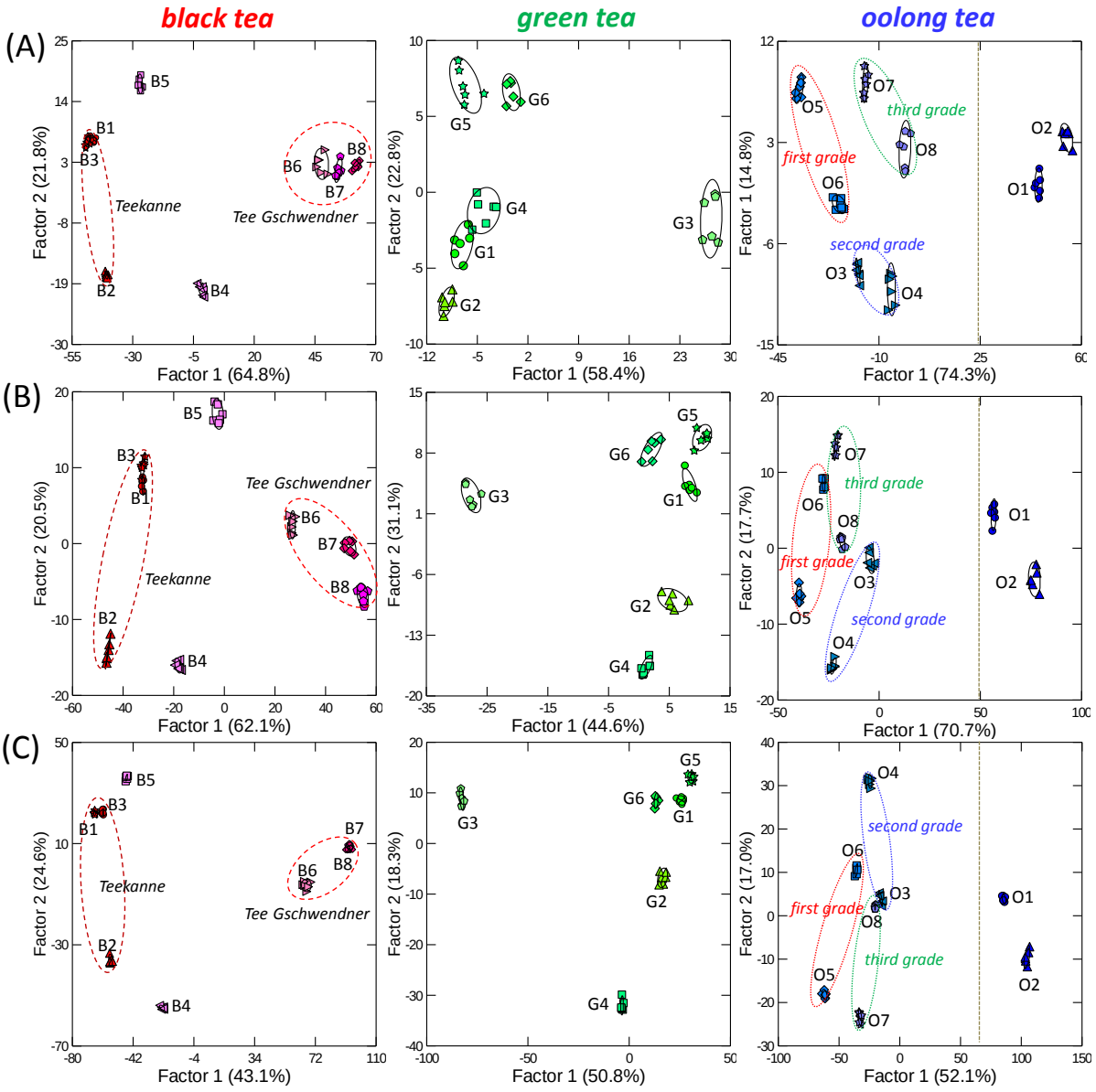

Figure 89. Two-dimensional canonical score plot obtained by an array of **(A)** PPE/CB[8] tongue (1.2 μM/9.0 μM, at pH 3, 7 and 13, buffered); **(B)** single PPE-tongue (1.2 μM, at pH 3, 7 and 13, buffered); **(C)** combined tongue of PPE/CB[8] tongue and single PPE-tongue treated with different black teas, green teas and oolong teas (0.1 mg/mL at pH 3 and 13, 0.01 mg/mL at pH 7, respectively) with 95% confidence ellipses. Each point represents the response pattern for a single analyte to the array. The vertical line in oolong tea denotes geography. O1 and O2 share the brand (Tieguanyin) and grow in the same district, but were obtained from different manufacturers. Figure reproduced with permission from ref. 77 © 2018, American Chemical Society.

The 2D plots of the first two canonical scores obtained by the PPE/CB[8] tongue and the simple PPE-tongue for all teas convert the training matrix 2 × (9 factors × 22 teas × 6 replicates) into canonical scores according to their shortest Mahalanobis distances (Figure 90, Table 36 and Table 37). Both tongues discriminate 85 of 88 unknown samples, representing an accuracy of 96% (Table 8). The two arrays have similar power in discrimination but show somewhat different, complementary selectivity. The complex tongue discriminates oolong teas better, while the PPE-tongue itself is better at discriminating black and green teas. Although the PPE/CB[8] tongue shows excellent discrimination of the small key compounds in tea, the PPE tongue alone is also very powerful, because it displays strong discriminative power for xanthine-type structures (caffeine, theobromine, and theophylline).

After combining the two tongues, the result looks similar to the result gathered from the simple PPE tongue, but with improved discrimination results (Figure 90C). The combined tongue identifies 87 of 88 unknown samples, improving the accuracy to a 99% (Table 8).

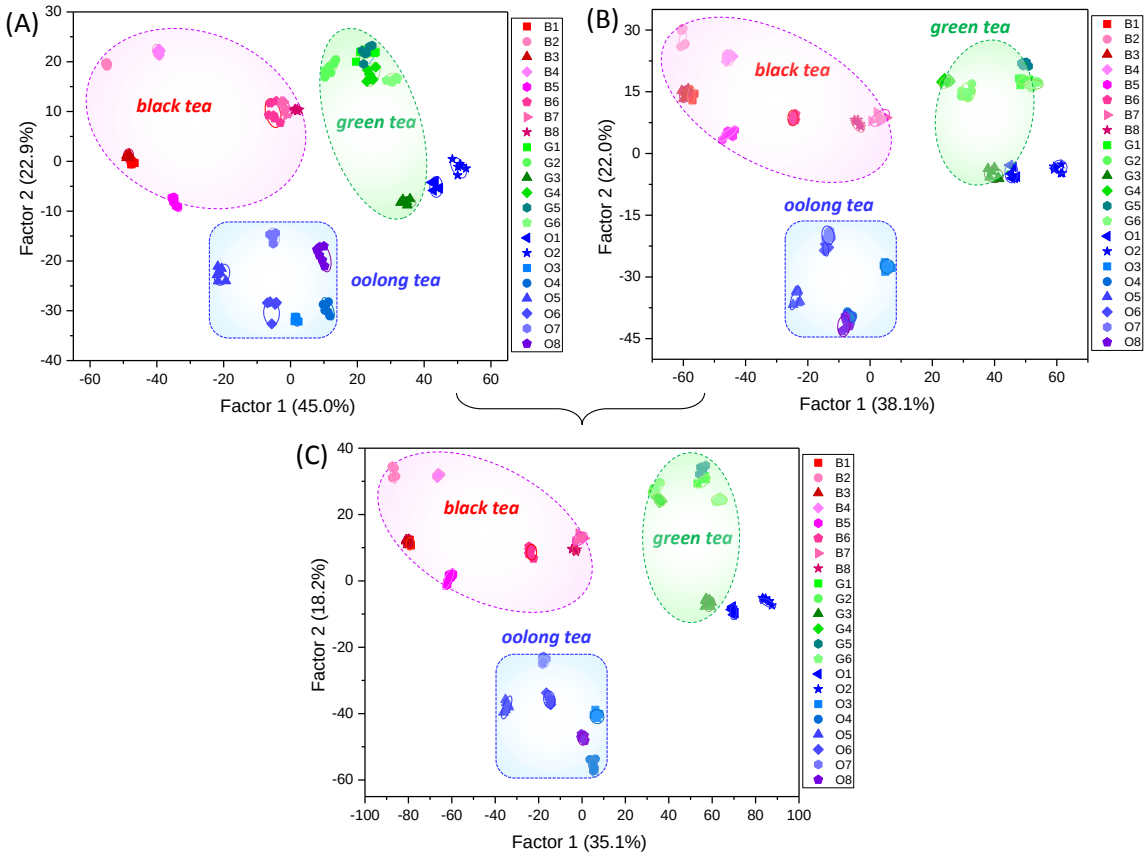

Figure 90. Two-dimensional canonical score plot for the first two factors obtained with an array of **(A)** PPE/CB[8] tongue (1.2 µM/9.0 µM, at pH 3, 7 and 13, buffered); **(B)** PPE tongue (1.2 µM, at pH pH 3, 7 and 13, buffered); and **(C)** combined tongue of the PPE/CB[8] tongue and the PPE-only-tongue treated with 22 kinds of teas with 95% confidence ellipses. Each point represents the response pattern for a single analyte to the array. Figure reproduced with permission from ref. 77 © 2018, American Chemical Society.

Table 8. Jackknifed Classification Matrix and Unknown Sample Identification Obtained From LDA.

Tongue	Tea samples	Jackknifed classification matrix			Unknown samples identification		
		Number of samples	Correctly classified	Accuracy (%)	Number of samples	Correctly classified	Accuracy (%)
PPE-CB[8] tongue	black tea	48	47	98	32	29	91
	green tea	36	35	97	24	24	100
	oolong tea	48	48	100	32	32	100
	all teas	132	132	100	88	85	96
PPE tongue	black tea	48	48	100	32	31	97
	green tea	36	36	100	24	24	100
	oolong tea	48	48	100	32	32	100
	all teas	132	132	100	88	85	96
Combined tongue	black tea	48	48	100	32	30	94
	green tea	36	36	100	24	24	100
	oolong tea	48	48	100	32	32	100
	all teas	132	132	100	88	87	99

Starting from this 18-element tongue, we performed a three-stage pruning process, using principal component analysis to reduce the number of elements without losing discriminative power. First, the data of 18 sensing elements for 22 teas were calculated with PCA, **P14**/CB[8] (pH 7), **P7**/CB[8] (pH 13), and **P13**/CB[8] (pH 13) contributed most. The LDA-plot with the selected three elements shows oolong teas O3-O8 group together (Figure 91A). Then, the left 15 elements toward the 6 lying close oolong teas were calculated with PCA again and we found that the sensing elements of **P7** (pH 3), **P13** (pH 3) and **P13** (pH 13) show best discrimination power to the 6 oolong teas. However, the black teas are still very close to each other (Figure 91B). The left 12 elements toward 8 lying close black teas were calculated with PCA and **P14** (pH 3) show best discrimination power. Thus, a seven element array (Figure 84, purple circles) was selected and identified all of the 22 teas (Figure 92).

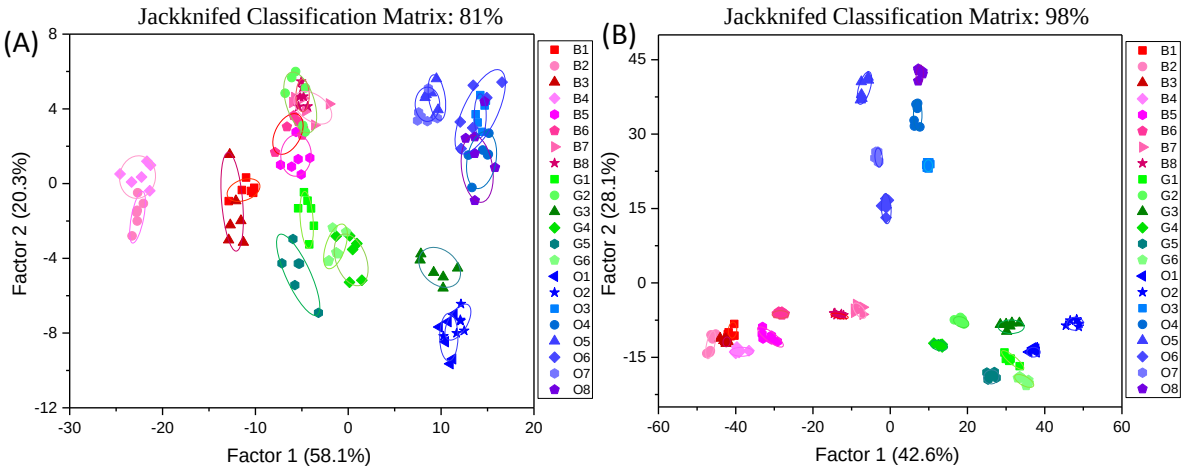

Figure 91. Two-dimensional canonical score plot obtained by an array of **(A)** three elements (**P14**/CB[8] (pH 7), **P7**/CB[8] (pH 13), and **P13**/CB[8] (pH 13)) and **(B)** six elements (**P14**/CB[8] (pH 7), **P7**/CB[8] (pH 13), **P13**/CB[8] (pH 13), and **P7** (pH 3), **P13** (pH 3), **P13** (pH 13)). Figure reproduced with permission from ref. 77 © 2018, American Chemical Society.

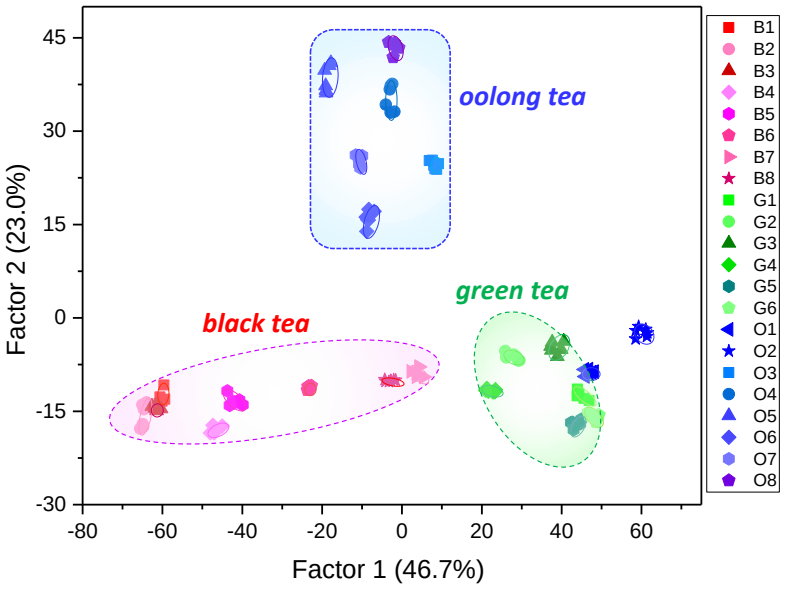

Figure 92. Two-dimensional canonical score plot for the optimized tongue obtained by an array of seven elements (**P14**/CB[8] (pH 7), **P7**/CB[8] (pH 13), **P13**/CB[8] (pH 13), **P7** (pH 3), **P13** (pH 3), **P14** (pH 3) and **P13** (pH 13). Figure reproduced with permission from ref. 77 © 2018, American Chemical Society.

The oolong teas O1 and O2 localize in all score plots, regardless of the employed array quite close to green teas. We inspected the leaves of all teas and find that oolong tea leaves have an appearance that is similar to that of black teas. The leaves of O1, O2, however, resemble those of green teas and show a similar light appearance (Figure 87), whereas the leaves of O3-O8 are much darker. It seems that O1 and O2 were fermented much less, rendering them more similar to the green teas.

4.2.5 Caffeine-Determination in Teas

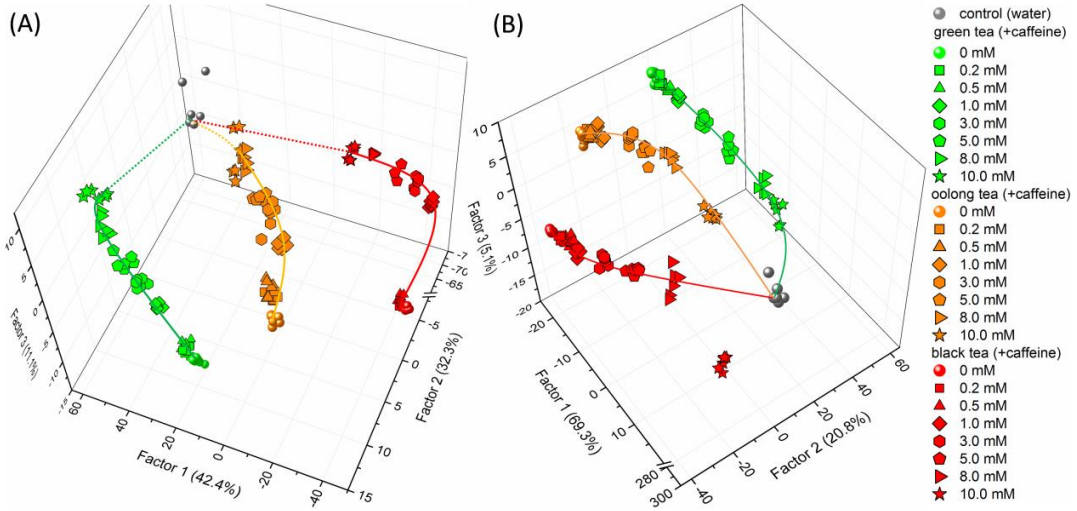

Figure 93. Three-dimensional canonical score plot obtained with an array of **(A)** PPE/CB[8] (1.2 µM/9.0 µM) and **(B)** PPE-only-tongue (1.2 µM) treated with different concentrations of caffeine (0-10 mM) in three kinds of tea infusions. Figure reproduced with permission from ref. 77 © 2018, American Chemical Society.

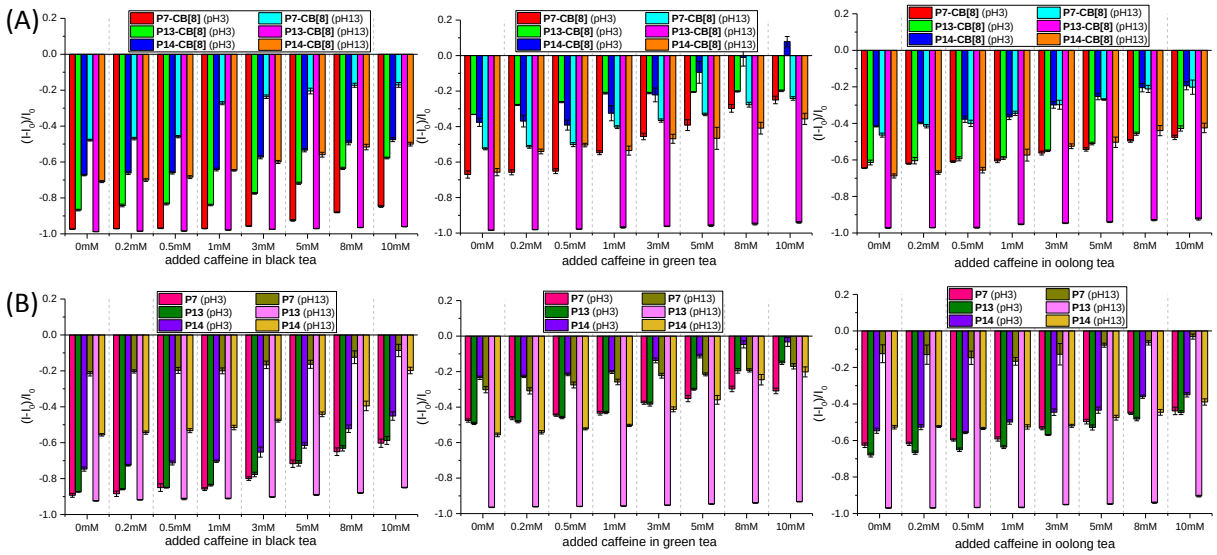

Figure 94. Fluorescence response patterns ($(I - I_0)/I_0$) obtained by **(A)** PPE/CB[8] tongue (1.2 µM/9.0 µM, at pH 3 and 13, buffered) and **(B)** PPE tongue (1.2 µM, at pH 3 and 13, buffered) treated with different concentrations of caffeine (0-10 mM) in black tea, green tea and oolong tea infusions. Figure reproduced with permission from ref. 77 © 2018, American Chemical Society.

Based on the successful discrimination of teas with such a sensor array, we carried out a semi-quantitative assay to identify caffeine at various concentrations (from 0.2 mM to 10 mM) in three different tea infusions employing the complex tongue. The fluorescence modulation data were

recorded and an LDA with canonical scores was calculated (training matrix, 6 factors × 8 concentrations ×6 replicates). The first three canonical factors represent 86% of the total variation. The jackknifed classification matrix with cross-validation reveals 96% accuracy (Table 38). As shown in Figure 93A, the concentration is almost linearly mapped in the LDA plot, and added caffeine could be discriminated and also scaled with the concentration in the presence of different teas. By spiking caffeine in tea, the fluorescence intensity gradually increases with increasing caffeine concentration (Figure 94A and Figure 95), giving insights into the detection mechanism. CB[8] has a large cavity, which allows the encapsulation of caffeine; competitive binding between caffeine and CB[8] displaces the PPEs from the cavity and restores fluorescence. We can readily observe this using the simple PPE-tongue (Figure 93B and Figure 94B), which shows that different concentration (> 3 mM) of added caffeine could also be discriminated. When X is used as the log value of the concentration of caffeine in the teas and Y stands for the fluorescence response, fitted curves plots could be obtained. According to the fitting formula shown in Figure 95, it may possible to determine the concentration of caffeine in teas. We find that the complex tongue is a bit more sensitive, but overall the simple PPE-based array is useful too.

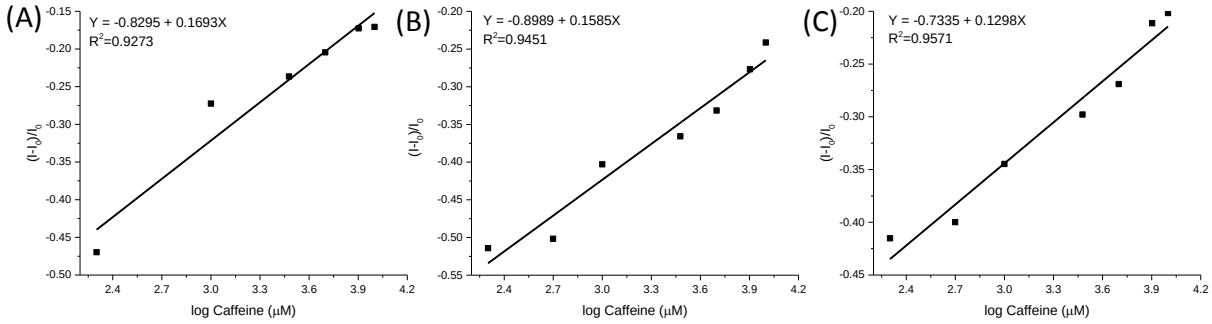

Figure 95. The linear relationship between fluorescence response ($(I - I_0) / I_0$) vs log concentration of caffeine obtained by **P7**/CB[8] (1.2 μM/9.0 μM) in **(A)** black tea, **(B)** green tea and **(C)** oolong tea infusions. Figure reproduced with permission from ref. 77 © 2018, American Chemical Society.

4.3 Conclusions

In conclusion, we have created a library consisting of positively charged PPEs complexed with CB[8] at different pH values. This array discriminates tea-based amino acids and caffeine-types by a displacement array. When CB[8] is omitted, with PPEs alone, caffeine, theobromine, and theophylline in tea infusions are also discriminated. Both the PPE and PPE/CB[8] array generate exquisitely sensitive patterns for teas on the basis of differential fluorescence quenching and order tea samples with respect to brand, price, quality grades and geographic origins. A combined tongue of both arrays is even more powerful; 99% of all of the investigated teas are discriminated. PCA based culling reveals that a seven-element tongue suffices to discriminate the teas. Over all, the fairly simple PPE-based sensor arrays do an excellent job for quality control and differentiation of teas. So in some ways, it is not absolutely necessary to employ additional supramolecular binders such as CB[8], but an effective pruned tongue contains both simple PPEs but also CB[8]-complexed elements, giving

testament to the function of the commercially available adjuvant CB[8]. Overall, the simple environmentally friendly setup makes these sensor arrays attractive for applicative tasks in quality control and the detection and discrimination of fraud/fake teas. On a more fundamental level, this contribution shows that teasing out of information from very simple arrays should be re-framed as an emergent phenomenon, in which almost trivially constructed arrays discriminate almost any analyte. This concept-particularly when executed with water-soluble conjugated polymers such as the PPEs seems to be universally applicable as long as it is not necessary to identify and quantify trace components. Our recent contributions support this notion.

Outlook

In the future, the structure of PPEs can be further modified to increase the selectivity and sensitivity of the array. Hence, it might be possible to effectively detect and discriminate analytes that are structurally more similar or analytes within complex mixtures. For example, the pockets of the polymers can be enlarged, and hydrophobicity can be increased to some extent for a more effective binding of explosives and landmines, without decreasing the solubility of the PPEs in water.

Future researches should also aim at identifying and discriminating phenylthiohydantoin-amino acid derivatives that can be formed through Edman degradation. If assays can be performed with high precision, it might be an attractive way to investigate and discriminate degradation products of polypeptides, which form a large part of the human proteome. Equally important is the identification of peptide hormones, which, in principle, can also be performed using hypothesis free sensor arrays like the ones herein described.

In this work, we have only dealt with a small part of chemical tongue sensing. The key for the successful discrimination of similar analytes is the combination of several interactions, e.g. electrostatic interactions, π-π stacking, hydrophobic interactions, hydrogen bonding etc. However, a better comprehension of how and to which extent these interactions contribute to the discrimination is still needed. Further efforts should be concentrated, therefore, on the exactly working mechanisms between the analytes and the conjugated polymers, or with their complexes. The underlying observables, such as wavelength, pressure, temperature and change of solvents are important, and also need to be investigated in future researches.

Chapter 5. Experimental Section

5.1 General Remarks

Chemicals were either purchased from the chemical store at the Organisch-Chemisches Institute of the University of Heidelberg or from commercial laboratory suppliers. Metal salts $Fe(ClO_4)_2 \cdot xH_2O$, $Cu(ClO_4)_2 \cdot 6H_2O$, $Co(ClO_4)_2 \cdot 6H_2O$, $FeSO_4 \cdot 7H_2O$, $CuSO_4$, $CoSO_4 \cdot 7H_2O$, $FeCl_2 \cdot 4H_2O$, $CuCl_2$ and $CoCl_2 \cdot 6H_2O$ were purchased from Sigma-Aldrich®. Cucurbit [7] uril hydrate and Cucurbit [8] uril hydrate were purchased from abcr GmbH®. Reagents were used without further purification unless otherwise noted.

Solvents were purchased from the store of the Theoretikum or chemical store at the Organisch-Chemisches Institute of the University of Heidelberg and if necessary distilled prior use. All of the other absolute solvents were dried by an MB SPS-800 using drying columns. Buffer solutions of pH 1 (HCl/KCl), pH 2 (KHPh/HCl), pH 3 (citric acid/NaOH/NaCl), pH 4 (citric acid/NaOH/NaCl), pH 5 (citric acid/NaOH), pH 6 (citric acid/NaOH), pH 7 (KH_2PO_4/Na_2HPO_4), pH 8 (borax/HCl), pH 9 KHPh/NaOH), pH 10 (borax/NaOH), pH 11 (boric acid/NaOH/KCl), pH 12 (Na_2HPO_4/NaOH), pH 13 (NaOH/KCl) were purchased from Sigma-Aldrich®.

Tea samples within three categories were purchased from local supermarkets in Germany and China. Upon test, tea samples were crashed into powders. A 25 mg powder was weighed into 10 mL boiled water for 5 min. Then the solutions were separated and diluted to the desired concentration as final tea infusions.

Analytical thin layer chromatography (TLC) was performed on Macherey & Nagel Polygram® SIL G/UV254 pre-coated plastic sheets. Components were visualized by observation under UV light (254 nm or 365 nm).

Flash column chromatography was carried out using silica gel S (0.032 mm-0.062 mm), purchased from Sigma Aldrich, according to G. Nill, unless otherwise stated.[194] As noted, Celite® 545, coarse, (Fluka) was used for filtration.

GC/MS chromatograms were recorded using a HP 5890 Series II Plus model, coupled with a HP 5972 Mass Selective Detector. As the capillary column, a HP 1 Crosslinked Methyl Silicone (25 m x 0.2 mm x 0.33 μm) was employed, with helium as carrier gas. The acquired data were analyzed using ACD/Labs Spectrus Processor 2012.

Ultrahigh pressure liquid chromatography (UPLC-MS) was performed on a Waters Acquity system. The mass spectra were recorded with a SQD2 mass detector. The acquired data were analyzed using ACD/Labs Spectrus Processor 2012.

Gel Permeation Chromatography (GPC): Number-average molecular weight (M_n), weight-average molecular weight (M_w) and polydispersities (PDI, M_w/M_n) were determined by GPC versus polystyrene standards. Measurements were carried out at room temperature in chloroform or THF with

PSS-SDV columns (8.0 mm x 30.0 mm, 5 µm particles, 10^2-, 10^3- and 10^5-Å pore size) on a Jasco PU-2050 GPC unit equipped with a Jasco UV-2075 UV-detector and a Jasco RI-2031 RI-detector. Data processing was done using PSS WinGPC Unity software.

Dialysis was realized using an appropriate length of the commercially available regenerated cellulose tubular membranes (ZelluTrans Roth® or Cellu Sep®) with the following specifications: molecular weight cut-off-3500 g/mol, flat width-46 mm, wall thickness-28 µm, vol/cm-6.74 mL/cm, and diameter in dry state-29.3 mm. Unless stated otherwise the equipped tubular membranes were put into excess (~ 10 L) of deionized water and stirred for 5 d by changing the surrounding solvent once every day. The dialyzed solution was freeze-dried afterward.

^{1}H NMR spectra were recorded at room temperature on the following spectrometers: Bruker Avance III 300 (300 MHz), Bruker Avance III 400 (400 MHz) and Bruker Avance III 600 (600 MHz). The data were interpreted in first-order spectra. The spectra were recorded in $CDCl_3$, D_2O or MeOD as indicated in each case. Chemical shifts are reported in δ units relative to the solvent residual peak ($CHCl_3$ in $CDCl_3$ at δ_H = 7.26 ppm, HDO in D_2O at δ_H = 4.79 ppm, HCD_2OD in MeOD at δ_H = 3.21 ppm) or TMS (δ_H = 0.00 ppm).[195] The following abbreviations are used to indicate the signal multiplicity: s (singlet), d (doublet), t (triplet), q (quartet), quin (quintet), sext (sextet), dd (doublet of doublet), dt (doublet of triplet), ddd (doublet of doublet of doublet), etc., bs (broad signal), m (multiplet). Coupling constants (*J*) are given in Hz and refer to H, H-couplings.

^{13}C NMR spectra were recorded at room temperature on the following spectrometers: Bruker Avance III 300 (75 MHz), Bruker Avance III 400 (100 MHz) and Bruker Avance III 600 (150 MHz). The spectra were recorded in $CDCl_3$ or D_2O as indicated in each case. Chemical shifts are reported in δ units relative to the solvent signal: $CDCl_3$ [δ_C = 77.16 ppm (central line of the triplet)] or TMS (δ_C = 0.00 ppm).[195] All NMR spectra were integrated and processed using Bruker's TopSpin™ Software.

High resolution mass spectra (HR-MS) were either recorded on the JEOL JMS-700 (EI^+), Bruker ApexQehybrid 9.4 T FT-ICR-MS (ESI^+, $DART^+$) or a Finnigan LCQ (ESI^+) mass spectrometer at the Organisch-Chemisches Institut der Universität Heidelberg.

Elemental analyses were carried out at the Organisch-Chemisches Institut der Universität Heidelberg.

IR spectra were recorded on a JASCO FT/IR-4100. Substances were applied as a film, solid or in solution. The obtained data were processed with the software JASCO Spectra Manager™ II.

A**bsorption spectra** were recorded on a JASCO UV-VIS V-660 or JASCO UV-VIS V-670 and processed with the software JASCO Spectra Manager™ II. ASCII-files were exported and visualized by Origin.

Fluorescence spectra were recorded on a Jasco FP6500 spectrometer. Raw data were processed using JASCO Spectra Manager™ II. ASCII-files were exported and visualized with Origin.

Photographs of solutions were taken with a Canon EOS 7D camera equipped with an EF-S 60mm F/2.8 Macro lens. Solid state photographs were taken using a Samsung Galaxy S7.

Fluorescence quantum yields (Φ) were obtained by the absolute method using an emission spectrometer equipped with an Ulbricht sphere. The system was calibrated with a primary light source.[196] The procedure from Würth[197] was used for substances with emission intensities ≥ 5000 counts, whereas the procedure of DeRose[196] was used < 5000 counts, applying a filter ND 2.0. Given Φ for each sample are average values of at least three independent measurements.

Fluorescence lifetimes (τ) were acquired by an exponential fit according to the least mean square with commercially available software HORIBA Scientific Decay Data Analyses 6 (DAS6) version 6.4.4. The luminescence decays were recorded with a HORIBA Scientific Fluorocube single photon counting system operated with HORIBA Scientific Data Station version 2.2.

Yields of polymers were determined on the basis of the formula weight of their shortest repeating unit. Negatively charged polymers were treated as the free acid, whereas for positively charged polymers the counter ion was taken into calculation.

Fluorescence response patterns were recorded using a CLARIOstar (firmware version 1.13) plate reader from BMG Labtech using the corresponding software (software version 5.20 R5). Data were analyzed with CLARIOstar MARS Data Analysis Software (software version 3.10 R5) from BMG Labtech. The polymers were dissolved in water to prepare stock solutions on the basis of their molecular weights. The resulting solutions were loaded into a 96-well plate (300 µL microplate). The analyte was then added and the solutions were adjusted with buffer to the desired concentrations. The excitation wavelength was set according to the absorption wavelength of the used polymer or complex. The specific response for each analyte was measured six times and the peak values were obtained. These acquired data were used as the observables for the subsequent linear discriminant analysis.

Linear discriminant analysis (LDA) was carried out using the classical linear discriminant analysis method in SYSTAT (version 13.0). In LDA, all variables were used in the model (complete mode) and the tolerance was set as 0.001. The fluorescence response patterns were transformed into canonical patterns. The Mahalanobis distances of each individual pattern to the centroid of each group in a multidimensional space were calculated and the assignment of the case was based on the shortest Mahalanobis distance.

Principal component analysis (PCA) is a mathematical transformation used to extract variance between entries in a data matrix by reducing the redundancy in the dimensionality of the data. It takes the data points for all analytes and generates a set of orthogonal eigenvectors (principal components, PCs) for maximum variance.[51] PCA was carried out using XLSTAT (version 2016).

5.2 Synthesis Details and Analytical Data

5.2.1 Synthesis of PAEs (Chapter 2)

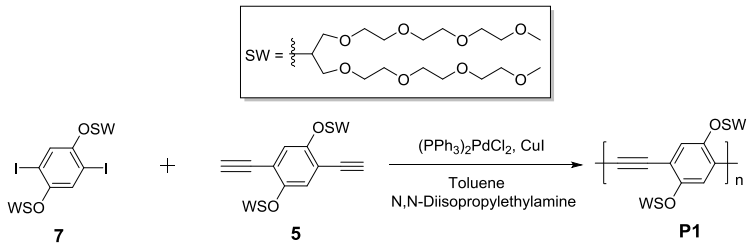

Compound **5** and **7** were synthesized according to the literature.[108]

Synthesis of P1. Monomer **7** (180 mg, 164.41 µmol) and monomer **5** (146.50 mg, 164.41 µmol) were dissolved in degassed Toluene/N,N-Diisopropylethylamine (1.2 mL/1.2 mL). $Pd(PPh_3)_2Cl_2$ (0.46 mg, 0.66 µmol) and CuI (0.25 mg, 1.32 µmol) were added and the mixture was stirred under nitrogen at 60 °C for 2 d. $CHCl_3$ was added to the mixture, and then washed with water, NaCl saturated solution and NH_4Cl saturated solution. The combined organic layers were dried over $MgSO_4$, filtered and concentrated under vacuum. The crude product was dissolved in $CHCl_3$ and slowly added to an excess of n-hexane to give **P1** as a sticky orange oil (128 mg, 90 %). The M_n was estimated to be 1.0 x 10^4 with a PDI of 2.2. ^{1}H NMR (300 MHz, $CDCl_3$): δ = 7.12-7.15 (m, 2 H), 4.50-4.52 (m, 2 H), 3.50-3.77 (m, 56 H), 3.34-3.36 (m, 12 H) ppm. Due to low solubility, ^{13}C NMR spectrum could not be obtained. IR (cm^{-1}): ν 2867, 2361, 2342, 1507, 1489, 1473, 1457, 1418, 1350, 1251, 1200, 1102, 1040, 947, 850.

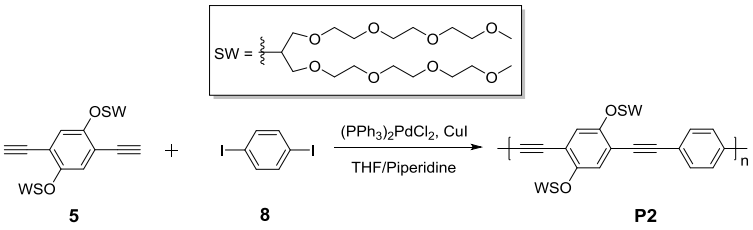

Compound **8** was purchased by Sigma-Aldrich®.

Synthesis of P2. Monomer **5** (216.07 mg, 242.49 µmol) and monomer **8** (80 mg, 242.49 µmol) were dissolved in degassed THF / piperidine (1.3 mL/1.3 mL). $Pd(PPh_3)_2Cl_2$ (0.51 mg, 0.73 µmol) and CuI (0.28 mg, 1.45 µmol) were added and the mixture was stirred under nitrogen at 60 °C for 2 d. $CHCl_3$ was added to the mixture, and then washed with water, NaCl saturated solution and NH_4Cl saturated solution. The combined organic layers were dried over $MgSO_4$, filtered and concentrated under vacuum. The crude product was dissolved in $CHCl_3$ and slowly added to an excess of n-hexane to give **P2** as a sticky orange oil (130 mg, 56 %). The M_n was estimated to be 1.1 x 10^4 with a PDI of 1.3. ^{1}H NMR (300 MHz, $CDCl_3$): δ = 7.40-7.50 (m, 2 H), 7.12-7.17 (m, 4 H), 4.44-4.50 (m, 2 H), 3.44-3.75 (m, 56 H), 3.27-3.33 (m, 12 H) ppm. Due to low solubility, ^{13}C NMR spectrum could not be obtained. IR (cm^{-1}): ν 2867, 2361, 2328, 1508, 1489, 1460, 1406, 1350, 1280, 1245, 1200, 1100, 950, 845, 548.

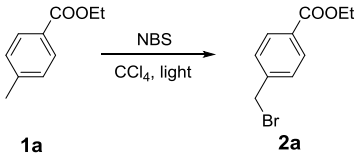

Compound **1a** was purchased by Sigma-Aldrich®.

Synthesis of 2a. Ethyl 4-methylbenzoate **1a** (10 g, 60.90 mmol) and N-Bromosuccinimide (11.38 g, 63.94 mmol) were dissolved in 100 mL HPLC-grade acetonitrile. The mixture was stirred under a strong light for 12 h. After the solvent was removed, water and CH_2Cl_2 were added; the aqueous layer was separated and extracted with CH_2Cl_2. The combined organic layers were dried over $MgSO_4$, filtered and concentrated under reduced pressure. The crude product was recrystallized from ethanol to afford **2a** as a colorless solid (9.54 g, 64.4 %). ^{1}H NMR (300 MHz, $CDCl_3$): δ = 8.02 (d, *J* = 8.4 Hz, 2 H), 7.45 (d, *J* = 8.4 Hz, 2 H), 4.50 (s, 2 H), 4.38 (q, *J* = 7.1 Hz, 2 H), 1.39 (t, *J* = 7.1 Hz, 3 H) ppm. ^{13}C NMR (75 MHz, $CDCl_3$): δ = 166.04, 142.50, 130.46, 130.04, 128.98, 61.10, 32.26, 14.32 ppm.

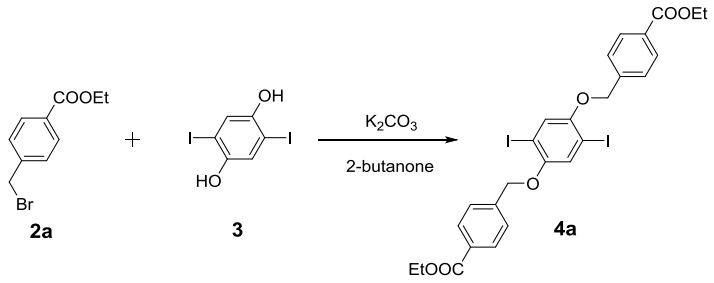

Compound **3** was synthesized according to the literature.[18]

Synthesis of 4a. Compound **2a** (3.99 g, 16.40 mmol), **3** (2.89 g, 8.00 mmol) and K_2CO_3 (11.06 g, 80.00 mmol) were dissolved in degassed butanone (160 mL). The mixture was stirred at ambient temperature for 2 d. Removed the salts by filtration and the filtrate was concentrated under reduced pressure. Then water and CH_2Cl_2 were added, the aqueous layer was extracted with CH_2Cl_2. The combined organic layers were dried over $MgSO_4$, filtered and concentrated under vacuum. The crude product was purified by recrystallization two times from toluene to afford **4a** (5.20 g, 90 %) as a white solid. ^{1}H NMR (300 MHz, $CDCl_3$): δ = 8.08 (d, *J* = 8.3 Hz, 4 H), 7.56 (d, *J* = 8.3 Hz, 4 H), 7.25 (d, *J* = 1.5 Hz, 2 H), 5.11 (s, 4 H), 4.38 (q, *J* = 7.1 Hz, 4 H), 1.40 (t, *J* = 7.1 Hz, 6 H) ppm. ^{13}C NMR (75 MHz, $CDCl_3$): δ = 166.32, 152.64, 141.08, 130.21, 129.88, 126.81, 123.40, 86.36, 71.33, 61.03, 14.34 ppm. IR (cm^{-1}): ν 2978, 2901, 1713, 1613, 1481, 1439, 1354, 1267, 1221, 1105, 1065, 1029, 844, 750, 688, 473. HR-MS (DART$^+$): *m/z* calcd. for $C_{26}H_{24}I_2O_6$ 703.9662 $[M+NH_4]^+$; found 704.0005. $C_{26}H_{24}I_2O_6$: calcd. C 45.50, H 3.53; found C 45.60, H 3.70.

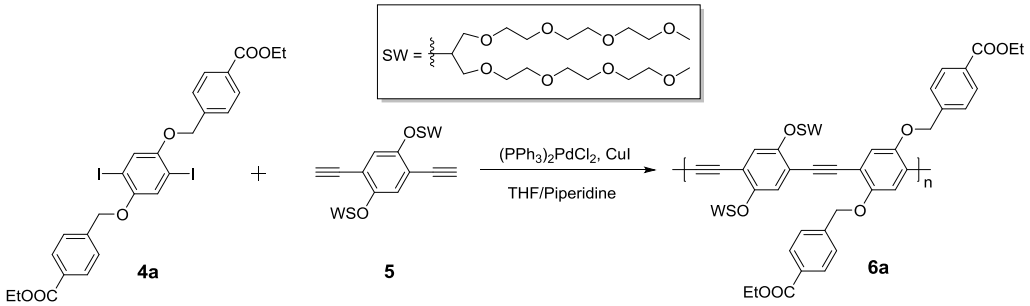

Synthesis of 6a. Monomer **4a** (150 mg, 218.56 µmol) and monomer **5** (194.75 mg, 218.56 µmol) were dissolved in degassed THF / piperidine (1.8 mL/1.3 mL). $Pd(PPh_3)_2Cl_2$ (0.47 mg, 0.67 µmol) and CuI (0.26 mg, 1.36 µmol) were then added and the mixture was stirred under nitrogen at room temperature for 2 d. $CHCl_3$ was added to the mixture, and then washed with water, NaCl saturated solution and NH_4Cl saturated solution. The combined organic layers were dried over $MgSO_4$, filtered and concentrated under vacuum. The crude product was dissolved in $CHCl_3$ and slowly added to an excess of n-hexane to give **6a** as sticky, dark orange oil (280 mg, 96 %). The M_n was estimated to be 1.3 x 10^4 with a PDI of 1.9. ^{1}H NMR (600 MHz, $CDCl_3$): δ = 8.04-8.06 (m, 4 H), 7.58-7.60 (m, 4 H), 7.09-7.19(m, 4 H), 5.16-5.27 (m, 4 H), 4.48-4.49 (m, 2 H), 4.34-4.37 (m, 4 H), 3.46-3.66 (m, 56 H), 3.31-3.33 (m, 12 H), 1.36-1.39 (m, 6 H) ppm. ^{13}C NMR (150 MHz, $CDCl_3$): δ = 165.18, 152.57, 152.21, 141.02, 128.94, 128.88, 125.72, 119.80, 117.13, 114.86, 113.75, 78.73, 70.84, 70.05, 69.50, 69.46, 69.43, 69.42, 59.96, 57.96, 13.37 ppm. IR (cm^{-1}): ν 2916, 2869, 2361, 2342, 1715, 1508, 1489, 1460, 1413, 1364, 1274, 1200, 1100, 1019, 851, 760.

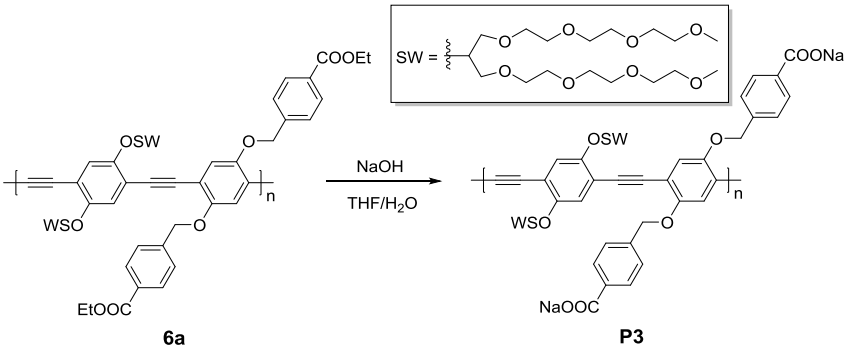

Synthesis of P3. NaOH (60.54 mg, 1.51 mmol) was added to a solution of polymer **6a** (200 mg, 0.15 mmol) in THF / H_2O (10 mL/10 mL) and the mixture was stirred at 70 ℃ for 2 d. After reducing the solvent in vacuo, the residue was dissolved in H_2O and adjusted the pH to 7 by HCl solution and then dialyzed against DI H_2O for 3 d. After freeze-drying, a spongy, yellow solid (156 mg, 78 %) was obtained. The M_n and PDI result from polymer **6a**. ^{1}H NMR (600 MHz, D_2O): δ = 7.79-8.19 (m, 4 H), 7.33-7.73 (m, 4 H), 6.67-7.00 (m, 4 H), 4.99-5.16 (m, 4 H), 3.23-3.39 (m, 58 H), 3.06-3.14 (m, 12 H) ppm. Due to low solubility, ^{13}C NMR spectrum could not be obtained. IR (cm^{-1}): ν 2868, 2361, 1715, 1508, 1489, 1460, 1412, 1270, 1198, 1091, 1034, 948, 847, 756, 635, 519.

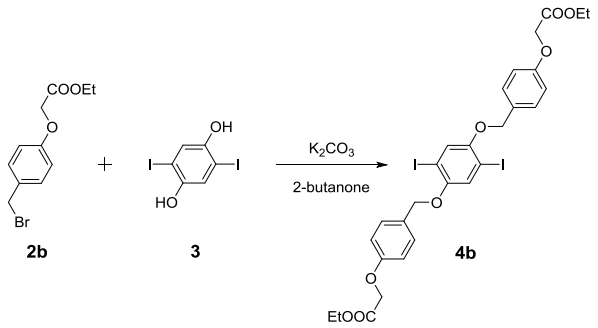

Compound **2b** was synthesized according to the literature.[198]

Synthesis of 4b. 2b (2.00 g, 7.32 mmol), **3** (1.29 g, 3.57 mmol) and K_2CO_3 (4.94 g, 35.72 mmol) were dissolved in degassed butanone (50 mL). The mixture was stirred at ambient temperature for 2 d. Removed the salts by filtration and the filtrate was concentrated under reduced pressure. Then water and CH_2Cl_2 were added, the aqueous layer was extracted with CH_2Cl_2. The combined organic layers were dried over $MgSO_4$, filtered and concentrated under vacuum. The crude product was purified by recrystallization from toluene to afford **4b** (2.0 g, 75%) as a white solid. ^{1}H NMR (300 MHz, $CDCl_3$): δ = 7.40 (d, *J* = 8.7 Hz, 4 H), 7.26 (s, 2 H), 6.93 (d, *J* = 8.7 Hz, 4 H), 4.98 (s, 4 H), 4.63 (s, 4 H), 4.28 (q, *J* = 7.1 Hz, 4 H), 1.30 (t, *J* = 7.1 Hz, 6 H) ppm. ^{13}C NMR (100 MHz, CDCl3): δ = 166.85, 157.74, 141.08, 129.42, 128.97, 123.75, 114.78, 86.65, 71.81, 65.33, 61.42, 14.18 ppm. IR (cm^{-1}): ν 2989, 2897, 1753, 1514, 1488, 1456, 1425, 1384, 1353, 1258, 1197, 1178, 1081, 1063, 1026, 849, 817, 781, 592, 514, 439. HR-MS (DART$^+$): *m*/*z* calcd. for $C_{28}H_{28}I_2O_8$ 763.9874 $[M+NH_4]^+$; found 764.0231.

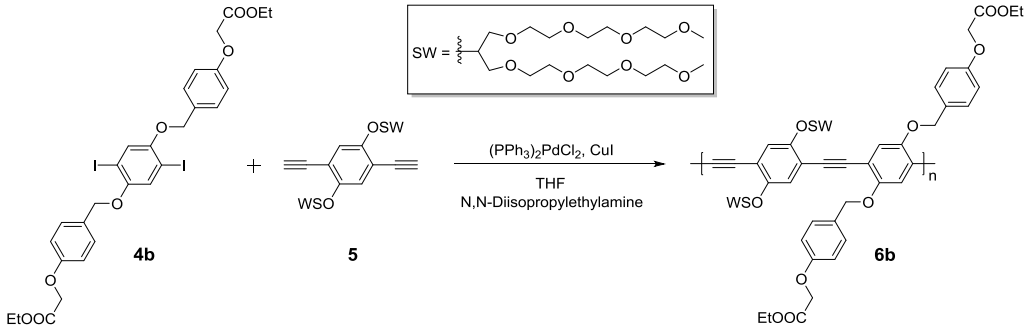

Synthesis of 6b. Monomer **4b** (150 mg, 200.98 µmol) and monomer **5** (179.09 mg, 200.98 µmol) were dissolved in degassed THF / N,N-Diisopropylethylamine (1.8 mL/1.3 mL). $Pd(PPh_3)_2Cl_2$ (0.42 mg, 0.60 µmol) and CuI (0.23 mg, 1.21 µmol) were added and the mixture was stirred under nitrogen at room temperature for 2 d. $CHCl_3$ were added to the mixture, and then washed with water, NaCl saturated solution and NH_4Cl saturated solution. The combined organic layers were dried over $MgSO_4$, filtered and concentrated under vacuum. The crude product was dissolved in $CHCl_3$ and slowly added to an excess of n-hexane to give **6b** as sticky, dark orange oil (230 mg, 83 %). The M_n was estimated to be 8.3 x 10^3 with a PDI of 3.0. ^{1}H NMR (600 MHz, $CDCl_3$): δ = 7.37-7.45 (m, 4 H), 7.13-7.18 (m, 2 H), 7.02-7.07 (m, 2 H), 6.90-6.94 (m, 4 H), 5.02-5.12 (m, 4 H), 4.60-4.62 (m, 4 H), 4.47-4.48 (m, 2 H), 4.23-4.27 (m, 4 H), 3.46-3.68 (m, 56 H), 3.31-3.34 (m, 12 H), 1.24-1.30 (m, 6 H) ppm. ^{13}C NMR (150 MHz, $CDCl_3$): δ = 169.10, 157.92, 153.78, 153.69, 130.32, 129.22, 121.33, 118.72, 117.18,

116.25, 115.07, 72.20, 72.16, 71.36, 70.88, 70.82, 70.77, 70.33, 65.67, 61.60, 59.31, 59.27, 14.50 ppm. IR (cm^{-1}): ν 2869, 2361, 1755, 1509, 1489, 1460, 1417, 1385, 1352, 1197, 1101, 1028, 950, 850, 820, 515.

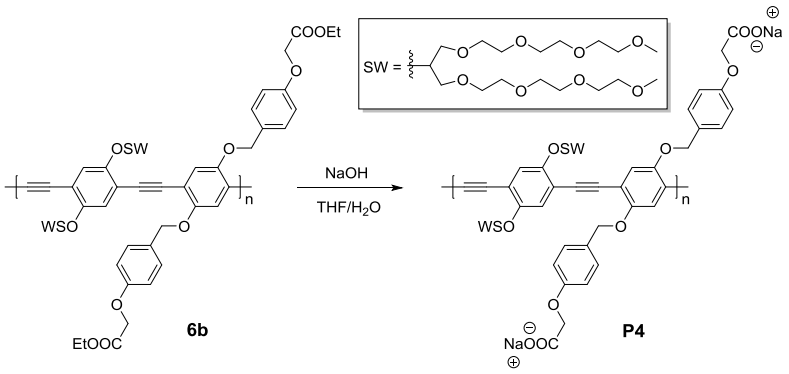

Synthesis of P4. NaOH (46.36 mg, 1.16 mmol) was added to a solution of polymer **6b** (180 mg, 115.89 μmol) in THF / H_2O (10 mL/10 mL) and the mixture was stirred at 70 ℃ for 2 d. After reducing the solvent in vacuo, the residue was dissolved in H_2O and adjusted the pH to 7 by HCl solution and then dialyzed against DI H_2O for 3 d. After freeze-drying, a spongy, yellow solid (170 mg, 95 %) was obtained. The M_n and PDI result from polymer **6b**. ^{1}H NMR (600 MHz, D_2O): δ = 7.28-7.42 (m, 4 H), 6.80-7.04 (m, 8 H), 4.82-5.08 (m, 4 H), 4.44-4.57 (m, 6 H), 3.20-3.71 (m, 68 H) ppm. ^{13}C NMR spectrum could not be obtained. IR (cm^{-1}): ν 3441, 3355, 2872, 1611, 1512, 1487, 1456, 1415, 1351, 1200, 1075, 1028, 951, 848, 821, 461.

5.2.2 Synthesis of PAEs (Chapter 3)

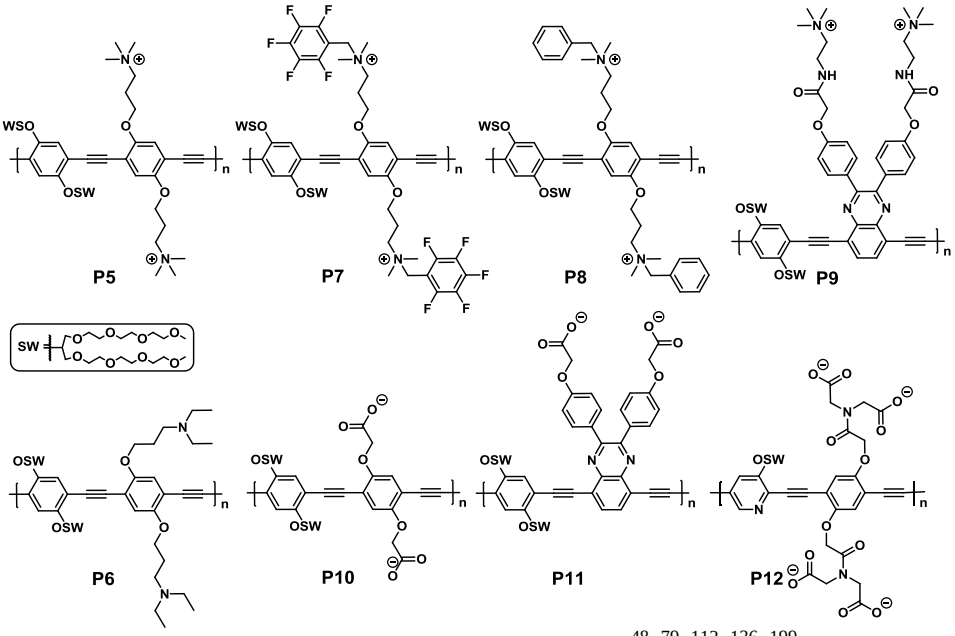

The synthesis of **P5**-**P7** and **P9**-**P12** were reported previously.[48, 79, 112, 136, 199] The synthesis of **P8** is reported here.

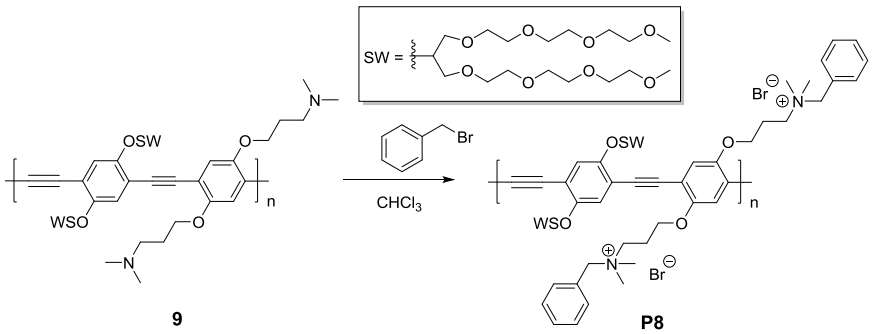

Synthesis of P8. Polymer **9** (180 mg, 157.89 μmol) was dissolved in degassed $CHCl_3$ (5 mL). Benzyl bromide (780 mg, 4.56 mmol) was added and reacted at 55 °C for 7 d. After evaporation of the solvents, the polymer was dissolved in small amount of MeOH and precipitated in n-hexane for two times, and then dialyzed against DI water for another 7 d. After freeze-drying, yellow solid (182 mg, 77%) was obtained. The M_n and PDI result from polymer **9**, which was 1.48 x 10^4 g/mol and 3.8, respectively. ^{1}H NMR (300 MHz, MeOD) δ = 7.26-7.59 (m, 10 H), 4.57-4.68 (m, 2 H), 4.27-4.33 (m, 4 H), 3.52-3.71 (m, 60 H), 3.32-3.34 (m, 24 H), 3.12-3.19 (m, 4 H) ppm. Due to low solubility, ^{13}C NMR spectrum could not be obtained. IR (cm^{-1}): ν 2873, 2815, 1730, 1650, 1524, 1477, 1378, 1349, 1258, 1199, 1106, 1091, 1032, 948, 850, 782, 677, 585.

5.2.3 Synthesis of PAEs (Chapter 4)

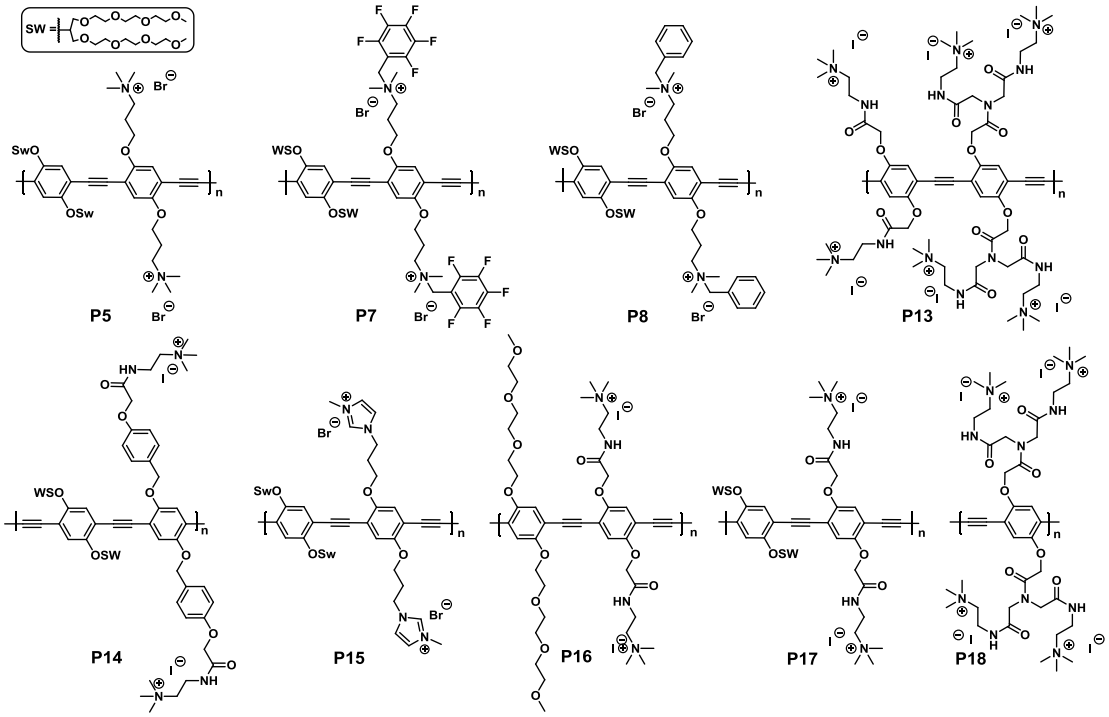

The synthesis of **P13** and **P15-P18** were reported previously.[41, 76, 112, 136] The synthesis of **P14** is reported here.

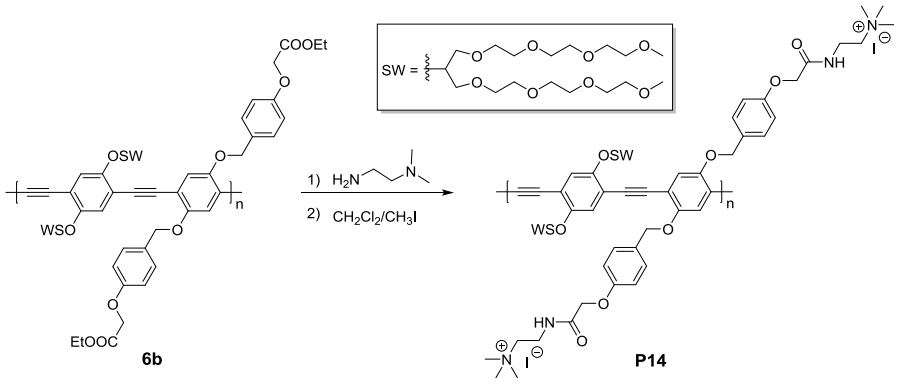

Synthesis of P14. Polymer **6b** (75 mg, 54.3 µmol) was dissolved in N, N'-dimethyl-ethylenediamine (20 mL) and stirred at 70 °C for 24 h. The reaction mixture was evaporated to dryness and washed with copious amounts of *n*-hexane. The crude product was dissolved in CH_2Cl_2 (20 mL). After addition of CH_3I (10 mL), the reaction mixture was stirred overnight at ambient temperature. All volatiles were removed under reduced pressure. The residue was dissolved in H_2O and dialyzed against DI H_2O for 3 d. After freeze-drying, a spongy, yellow solid (75 mg, 92%) was obtained. The M_n and PDI result from polymer **6b**, which was 8.3 x 10^3 g/mol and 3.0, respectively. ^{1}H NMR (600 MHz, D_2O): δ = 6.99-7.47 (m, 12 H), 5.20-5.21 (m, 2 H), 4.56-4.67 (m, 4 H), 3.36-3.61 (m, 68 H), 3.13-3.27 (m, 30 H) ppm. IR (cm^{-1}): ν 3455, 2870, 2361, 1738, 1671, 1611, 1534, 1510, 1488, 1416, 1351, 1201, 1091, 954, 847, 584, 518, 451. Due to low solubility, ^{13}C NMR spectrum could not be obtained.

5.2.4 Synthesis of Other PAEs

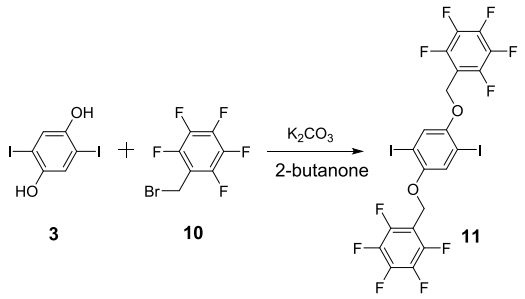

Compound **10** was purchased by Sigma-Aldrich®.

Synthesis of 11. Compound **3** (434.3 mg, 1.2 mmol), **10** (783.97 g, 3.00 mmol) and K_2CO_3 (1.66 g, 12.00 mmol) were dissolved in degassed butanone (12.00 mL). The mixture was stirred at ambient temperature for 10 hours. Poured the mixtures into ice water (100 mL) and stirred for a few minutes and then collected the formed solids by filtration. The crude product was purified by recrystallization two times from ethyl acetate to afford **11** (780 mg, 90%) as a colorless solid. ^{1}H NMR (300 MHz, $CDCl_3$): δ = 7.37 (s, 2 H), 5.10 (s, 4 H) ppm. ^{13}C NMR (75 MHz, $CDCl_3$): δ = 153.18, 124.76, 115.00, 86.97, 60.02 ppm. IR (cm^{-1}): ν 1656, 1501, 1483, 1460, 1429, 1382, 1351, 1313, 1289, 1231, 1196, 1133, 1045, 999, 971, 933, 857, 826, 661, 633, 607, 571, 478, 435. HR-MS ($DART^+$): *m*/*z* calcd. for

$C_{20}H_6F_{10}I_2O_2$ 721.8297 $[M]^+$; found 721.8288. $C_{20}H_6F_{10}I_2O_2$ (722.06): calcd. C 33.27, H 0.84; found C 33.33, H 0.99.

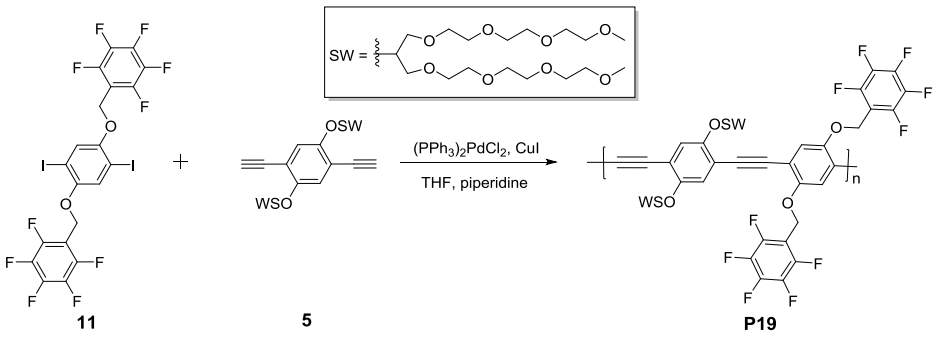

Synthesis of P19. Monomer **11** (300.00 mg, 415.48 µmol) and monomer **5** (370.22 mg, 415.48 µmol) were dissolved in degassed THF / piperidine (2.6 mL/2.6 mL). $Pd(PPh_3)_2Cl_2$ (0.87 mg, 1.25 µmol) and CuI (0.47 mg, 2.49 µmol) were added and the mixture was stirred under nitrogen at 48°C for 4 d. $CHCl_3$ was added to the mixture, and then washed with water, NaCl saturated solution and NH_4Cl saturated solution. The combined organic layers were dried over $MgSO_4$, filtered and concentrated under vacuum. The crude product was dissolved in $CHCl_3$ and slowly added to an excess of n-hexane to give **P19** as a sticky, dark red oil (485.32 mg, 84%). The M_n was estimated to be 1.3 x 10^4 with a PDI of 2.1. ^{1}H NMR (300 MHz, $CDCl_3$): δ = 7.10-7.11 (m, 4 H), 5.02-5.16 (m, 4 H), 4.46-4.47 (m, 2 H), 3.41-3.68 (m, 56 H), 3.27-3.28 (m, 12 H) ppm. Due to low solubility, ^{13}C NMR spectrum could not be obtained. IR (cm^{-1}): ν 2919, 2863, 2360, 2342, 1652, 1508, 1488, 1418, 1382, 1362, 1278, 1200, 1109, 1046, 977, 937, 901, 852.

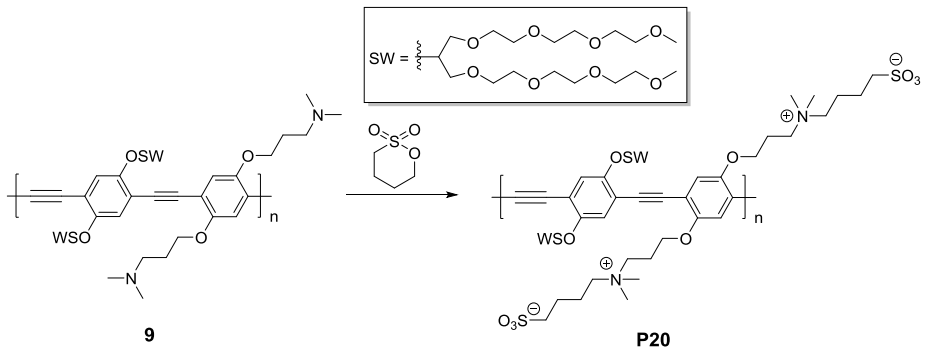

Synthesis of P20. Polymer **9** (114.00 mg, 100.00 µmol) was dissolved in butanesultone (5 mL) and stirred at 90 °C for 5 d. After reducing the solvent in vacuum, the residue was diluted with H_2O, purified by dialysis for 3 d. After freeze-drying, a spongy, yellow solid (100 mg, 69 %) was obtained. The M_n and PDI result from polymer **9**, which is 1.48 x 10^4 g/mol and 3.8, respectively. ^{1}H NMR (600 MHz, $CDCl_3$): δ = 7.43-7.45 (m, 2 H), 6.95-7.02 (m, 2 H), 5.11-5.17 (m, 2 H), 4.42-4.64 (m, 8 H), 3.33-3.72 (m, 76 H), 3.07-3.18 (m, 24 H) ppm. Due to low solubility, ^{13}C NMR spectrum could not be obtained. IR (cm^{-1}): ν 3453, 2869, 2358, 1738, 1617, 1455, 1365, 1200, 1094, 1031, 946, 849, 600, 526.

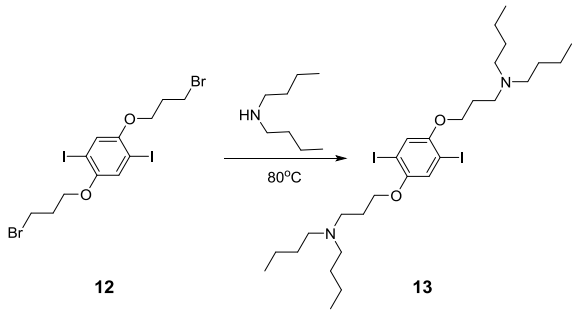

Compound **12** was synthesized according to the literature.[200]

Synthesis of 13. 12 (1.50 g, 2.48 mmol) was dissolved in dibutylamine (10 mL) and stirred at 80 °C for 2 d. Water and CH_2Cl_2 were added into the mixture and then the aqueous layer was separated and extracted with CH_2Cl_2 twice. The combined organic layers were dried over MgSO4, filtered and concentrated under vacuum. The crude product was purified by flash chromatography on silica gel [petroleum ether/ethyl acetate (10/1)] to give compound **13** (1.50 g, 86%) as colorless solid. ^{1}H NMR (300 MHz, $CDCl_3$): δ = 7.18 (s, 2 H), 3.96-4.00 (t, *J* = 7.1 Hz, 4 H), 2.62-2.66 (t, *J* = 7.1 Hz, 4 H), 2.40-2.44 (t, *J* = 7.1 Hz, 8 H), 1.89-1.93 (t, *J* = 7.1 Hz, 4 H), 1.38-1.45 (m, 8 H), 1.25-1.33 (m, 8 H), 0.87-0.91 (t, *J* = 7.1 Hz, 12 H) ppm. ^{13}C NMR (100 MHz, $CDCl_3$): δ = 152.75, 122.60, 86.16, 68.40, 54.09, 50.41, 29.39, 27.03, 20.76, 14.11 ppm. IR (cm^{-1}): ν 2954, 2925, 2870, 2858, 2798, 1485, 1446, 1374, 1359, 1344, 1267, 1213, 1181, 1167, 1088, 1050, 987, 958, 937, 850, 841, 792, 750, 730, 457, 435. HR-MS (DART$^+$): m/z calcd. for $C_{28}H_{50}I_2N_2O_2$ 701.1962 $[M+H]^+$; found 701.2014.

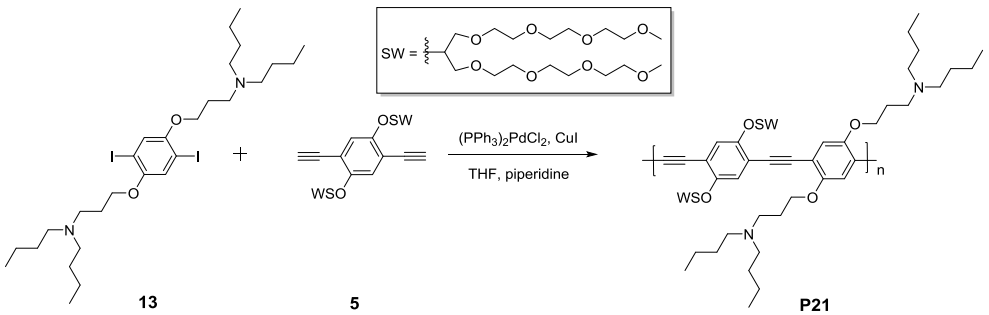

Synthesis of P21. Monomer **13** (300 mg, 428.25 μmol) and monomer **5** (381.59 mg, 428.25 μmol) were dissolved in degassed THF / piperidine (1.5 mL/1.5 mL). $Pd(PPh_3)_2Cl_2$ (0.90 mg, 1.28 μmol) and CuI (0.49 mg, 2.57 μmol) were added and the mixture was stirred under nitrogen at 60 °C for 3 d. $CHCl_3$ was added to the mixture, and then washed with water, NaCl saturated solution and NH_4Cl saturated solution. The combined organic layers were dried over $MgSO_4$, filtered and concentrated under vacuum. The crude product was dissolved in $CHCl_3$ and slowly added to an excess of n-hexane to give **P21** as a sticky, yellow solid (166 mg, 30 %). ^{1}H NMR (600 MHz, $CDCl_3$): δ = 7.12 (s, 2 H), 6.96 (s, 2 H), 4.44 (s, 2 H), 4.07 (s, 4 H), 3.44-3.73 (m, 56 H), 3.29 (s, 12 H), 1.51 (m, 20H), 0.80-0.82 (m, 12 H) ppm. Due to low solubility, ^{13}C NMR spectrum could not be obtained. IR (cm^{-1}): ν 2869, 1670, 1489, 1463, 1420, 1376, 1351, 1270, 1200, 1097, 948, 850.

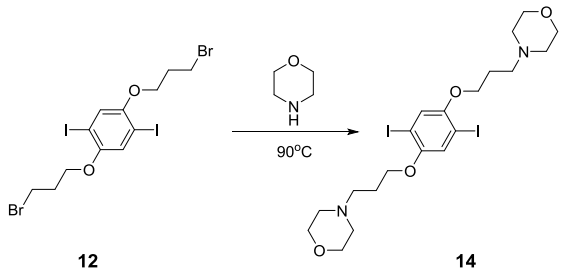

Synthesis of 14. 12 (1.50 g, 2.48 mmol) was dissolved in degassed morpholine (15 mL) and stirred at 90 °C for 2 d. Water and CH_2Cl_2 were added to the mixture and then the aqueous layer was separated and extracted with CH_2Cl_2 twice. The combined organic layers were dried over MgSO4, filtered and concentrated under vacuum. The crude product was purified by flash chromatography on silica gel [petroleum ether/ethyl acetate (10/1)] to give compound **14** (1.40 g, 92%) as colorless solid. ^{1}H NMR (300 MHz, $CDCl_3$): δ = 7.20 (s, 2 H), 3.99-4.03 (t, J = 7.1 Hz, 4 H), 3.72-3.75 (t, J = 7.1 Hz, 8 H), 2.56-2.60 (t, J = 7.1 Hz, 4 H), 2.47-2.50 (t, J = 7.1 Hz, 8 H), 1.96-2.01 (m, 4 H) ppm. ^{13}C NMR (75 MHz, $CDCl_3$): δ = 152.79, 122.85, 86.32, 68.25, 66.72, 55.45, 53.64, 26.06 ppm. IR (cm^{-1}): ν 2949, 2917, 2875, 2848, 2820, 2772, 1487, 1469, 1457, 1392, 1352, 1266, 1210, 1141, 1117, 1053, 1038, 1023, 959, 917, 865, 859, 817, 801, 752, 612, 438. HR-MS (DART$^+$): m/z calcd. for $C_{20}H_{30}I_2N_2O_4$ 617.0295 $[M+H]^+$; found 617.0343.

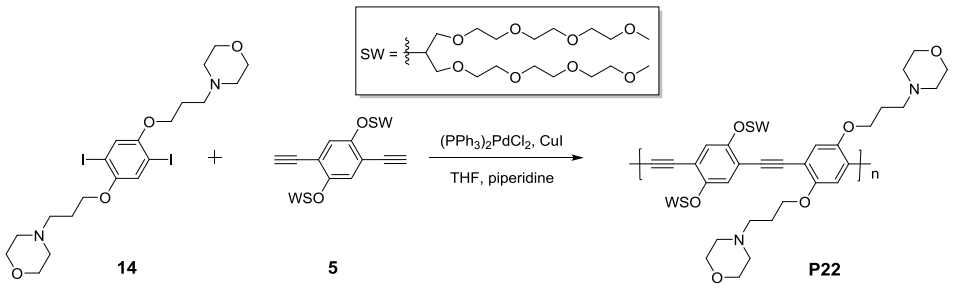

Synthesis of P22. Monomer **14** (150 mg, 243.40 μmol) and monomer **5** (216.88 mg, 243.40 μmol) were dissolved in degassed THF / piperidine (1.5 mL/1.5 mL). $Pd(PPh_3)_2Cl_2$ (0.85 mg, 1.22 μmol) and CuI (0.46 mg, 2.43 μmol) were added and the mixture was stirred under nitrogen at 90 °C for 3 d. $CHCl_3$ was added to the mixture, and then washed with water, NaCl saturated solution and NH_4Cl saturated solution. The combined organic layers were dried over $MgSO_4$, filtered and concentrated under vacuum. The crude product was dissolved in $CHCl_3$ and slowly added to an excess of n-hexane to give **P22** as sticky, dark orange oil (238 mg, 78 %). The M_n was estimated to be 1.0 x 10^4 g/mol with a PDI of 2.8. ^{1}H NMR (300 MHz, $CDCl_3$): δ = 7.12 s, 2 H), 6.97 (s, 2 H), 4.46-4.48 (m, 2 H), 4.06 (m, 4 H), 3.43-3.72 (m, 56 H), 3.28 (m, 12 H), 2.38-2.49 (m, 12 H), 1.96 (m, 4 H), 1.57 (m, 8 H) ppm. Due to low solubility, ^{13}C NMR spectrum could not be obtained. IR (cm^{-1}): ν 2867, 2814, 1489, 1457, 1420, 1351, 1261, 1200, 1096, 1031, 952, 861, 801, 541.

5.3 Linear Discriminant Analysis

5.3.1 LDA Calculation of Explosives (Chapter 2)

Table 9. Training matrix of fluorescence response pattern from water-soluble PPEs **P1**-**P4** (1 µM, at pH 7, buffered) against 13 nitroaromaitic analytes at a concentration of 0.5 mM. LDA was carried out as described above resulting in the four factors of the canonical scores and group generation. The jackknifed classification matrix with cross-validation reveals an accuracy of 99%.

Analytes	Fluorescence Response Pattern				Results LDA				
Nitroaromaitc	**P1**	**P2**	**P3**	**P4**	Factor 1	Factor 2	Factor 3	Factor 4	Group
A	-0.20	-0.14	-0.02	-0.01	40.17	-5.19	-0.18	3.67	3
A	-0.15	-0.14	-0.06	0.03	42.60	-5.49	3.01	4.83	3
A	-0.16	-0.26	-0.05	0.01	39.86	-4.87	4.32	1.23	3
A	-0.19	-0.17	0.05	0.01	42.40	-5.23	-0.46	1.20	3
A	-0.12	-0.21	0.04	0.02	43.16	-2.92	2.34	0.36	3
A	-0.21	-0.26	0.04	0.00	40.25	-5.95	0.70	-1.31	3
2-NA	-0.10	-0.86	-0.79	-0.72	-20.71	14.42	15.13	-1.47	1
2-NA	-0.15	-0.85	-0.79	-0.74	-22.36	12.97	13.47	-1.43	1
2-NA	-0.15	-0.86	-0.80	-0.73	-21.76	12.47	14.22	-1.38	1
2-NA	-0.19	-0.86	-0.80	-0.73	-22.35	10.45	13.39	-1.50	1
2-NA	-0.11	-0.87	-0.80	-0.72	-21.26	13.71	15.23	-1.55	1
2-NA	-0.21	-0.86	-0.80	-0.72	-22.22	9.61	13.36	-1.47	1
3-NA	-0.29	-0.42	-0.17	-0.26	18.85	-2.57	0.22	-2.13	2
3-NA	-0.32	-0.41	-0.14	-0.27	18.64	-2.87	-1.71	-2.65	2
3-NA	-0.31	-0.39	-0.16	-0.27	18.39	-2.91	-1.41	-1.39	2
3-NA	-0.31	-0.43	-0.18	-0.25	18.78	-3.84	0.18	-2.29	2
3-NA	-0.30	-0.42	-0.14	-0.25	19.60	-2.64	-0.60	-2.89	2
3-NA	-0.31	-0.42	-0.12	-0.29	17.58	-1.61	-2.55	-3.67	2
DNB	-0.45	-0.46	-0.72	-0.66	-15.78	-1.40	0.23	9.06	5
DNB	-0.44	-0.45	-0.72	-0.65	-15.17	-1.12	0.40	9.47	5
DNB	-0.45	-0.43	-0.73	-0.66	-15.62	-1.68	-0.05	10.28	5
DNB	-0.46	-0.48	-0.74	-0.65	-15.50	-2.68	1.23	9.19	5
DNB	-0.47	-0.45	-0.74	-0.65	-15.69	-2.89	0.36	9.93	5
DNB	-0.46	-0.46	-0.74	-0.65	-15.33	-2.45	0.84	9.45	5
DNT	-0.25	-0.47	-0.41	-0.57	-3.28	7.77	-0.72	1.46	7
DNT	-0.23	-0.46	-0.40	-0.54	-1.04	7.74	0.31	1.49	7
DNT	-0.28	-0.47	-0.40	-0.53	-1.16	5.47	-0.47	1.34	7
DNT	-0.28	-0.49	-0.38	-0.56	-3.18	6.93	-1.44	0.03	7
DNT	-0.24	-0.46	-0.39	-0.57	-2.95	8.64	-1.26	1.03	7
DNT	-0.26	-0.49	-0.36	-0.58	-3.48	8.60	-2.07	-0.57	6
NB	-0.08	-0.32	-0.06	-0.28	22.75	9.61	-0.89	-1.99	8
NB	-0.09	-0.31	-0.05	-0.25	24.55	8.04	-0.62	-1.56	8
NB	-0.09	-0.38	-0.10	-0.25	23.59	6.99	2.03	-2.59	8
NB	-0.11	-0.27	-0.07	-0.26	24.06	7.13	-1.65	0.28	8
NB	-0.13	-0.35	-0.10	-0.28	21.65	6.47	-0.22	-1.79	8
NB	-0.11	-0.35	-0.09	-0.28	21.54	7.82	-0.26	-2.05	8
NP	-0.61	-0.66	-0.52	-0.43	-3.21	-14.89	2.15	-1.40	9
NP	-0.60	-0.64	-0.56	-0.43	-3.08	-15.07	2.96	0.19	9

NP	-0.60	-0.67	-0.57	-0.46	-5.78	-14.36	2.76	-0.66	9
NP	-0.60	-0.65	-0.50	-0.43	-2.78	-14.21	1.33	-1.68	9
NP	-0.61	-0.64	-0.53	-0.45	-4.45	-14.48	1.27	-0.80	9
NP	-0.61	-0.63	-0.53	-0.47	-5.32	-13.77	0.77	-0.41	9
PA	-0.48	-0.46	-0.27	-0.15	20.86	-16.41	2.29	-0.57	11
PA	-0.50	-0.51	-0.28	-0.12	21.96	-18.42	4.07	-1.67	11
PA	-0.49	-0.49	-0.26	-0.13	21.69	-17.18	3.13	-1.59	11
PA	-0.49	-0.46	-0.21	-0.14	22.62	-16.67	1.22	-2.05	11
PA	-0.49	-0.45	-0.20	-0.13	23.55	-16.63	0.87	-1.82	11
PA	-0.49	-0.42	-0.24	-0.13	22.82	-16.88	1.39	-0.03	11
TNT	-0.30	-0.36	-0.26	-0.65	-5.27	10.95	-10.00	0.71	13
TNT	-0.30	-0.40	-0.33	-0.65	-6.86	10.25	-7.54	0.89	13
TNT	-0.31	-0.48	-0.28	-0.65	-7.38	10.10	-7.54	-2.63	13
TNT	-0.31	-0.46	-0.30	-0.66	-7.68	10.51	-7.48	-1.52	13
TNT	-0.28	-0.45	-0.35	-0.68	-9.25	11.71	-6.34	-0.04	13
TNT	-0.32	-0.38	-0.32	-0.68	-8.19	10.48	-9.34	1.47	13
CDNB	-0.30	-0.55	-0.44	-0.69	-12.40	9.66	-2.74	-0.93	4
CDNB	-0.31	-0.58	-0.42	-0.68	-11.78	9.41	-2.82	-2.26	4
CDNB	-0.33	-0.57	-0.40	-0.67	-11.36	8.55	-3.74	-2.66	4
CDNB	-0.31	-0.56	-0.39	-0.66	-10.57	9.08	-3.44	-2.36	4
CDNB	-0.31	-0.58	-0.40	-0.68	-11.61	9.35	-3.27	-2.69	4
CDNB	-0.33	-0.57	-0.41	-0.66	-11.16	8.06	-3.03	-2.23	4
DNMB	-0.26	-0.51	-0.33	-0.56	-2.29	8.49	-2.01	-2.03	6
DNMB	-0.26	-0.48	-0.37	-0.61	-5.36	9.64	-2.79	-0.23	6
DNMB	-0.28	-0.49	-0.34	-0.57	-2.87	7.41	-2.78	-1.27	6
DNMB	-0.33	-0.52	-0.37	-0.59	-5.42	5.95	-3.22	-1.38	6
DNMB	-0.26	-0.48	-0.37	-0.60	-4.70	9.04	-2.66	-0.15	6
DNMB	-0.31	-0.49	-0.39	-0.58	-4.83	6.23	-2.79	0.09	6
ONCB	-0.22	-0.35	-0.28	-0.38	11.34	4.11	-0.72	2.48	10
ONCB	-0.24	-0.35	-0.24	-0.37	12.82	3.19	-1.44	1.69	10
ONCB	-0.25	-0.37	-0.24	-0.35	13.51	1.93	-0.59	0.97	10
ONCB	-0.25	-0.37	-0.22	-0.37	12.70	3.10	-1.97	0.44	10
ONCB	-0.26	-0.37	-0.20	-0.36	13.33	2.22	-2.33	0.12	10
ONCB	-0.27	-0.37	-0.25	-0.36	12.11	1.51	-1.45	0.95	10
PNP	-0.97	-0.99	-0.98	-0.98	-50.84	-16.51	-2.68	-2.28	12
PNP	-0.97	-0.99	-0.98	-0.98	-50.92	-16.43	-2.92	-2.29	12
PNP	-0.96	-0.99	-0.98	-0.98	-50.93	-16.36	-2.78	-2.23	12
PNP	-0.96	-0.99	-0.98	-0.98	-50.82	-16.40	-2.66	-2.20	12
PNP	-0.96	-0.99	-0.98	-0.98	-50.89	-16.41	-2.70	-2.29	12
PNP	-0.96	-0.99	-0.98	-0.98	-50.92	-16.36	-2.80	-2.26	12

Table 10. Detection and identification of 52 unknown samples using LDA training matrix from PPEs **P1**-**P4** (1 µM, at pH 7, buffered). All unknown samples could be assigned to the corresponding group defined by the training matrix according to their shortest Mahalanobis distance. 50 of the 52 unknown explosive samples were correctly identified, reveals 96 % accuracy.

Sample	Fluorescence Response Pattern				Results LDA					Analyte	
#	**P1**	**P2**	**P3**	**P4**	Factor 1	Factor 2	Factor 3	Factor 4	Group	Identification	Verification
1	-0.59	-0.66	-0.49	-0.47	-4.82	-12.38	0.70	-2.59	9	NP	NP

2	-0.23	-0.48	-0.40	-0.61	-3.30	8.02	-1.39	-0.29	7	DNT	DNT
3	-0.09	-0.31	-0.10	-0.32	19.69	9.94	-1.57	-0.50	8	NB	NB
4	-0.47	-0.46	-0.73	-0.66	-16.27	-2.69	-0.13	9.57	5	DNB	DNB
5	-0.24	-0.47	-0.38	-0.54	-1.54	6.07	-2.33	-0.82	7	DNT	DNT
6	-0.08	-0.27	-0.10	-0.34	19.07	11.14	-2.65	0.62	8	NB	NB
7	-0.46	-0.44	-0.74	-0.67	-16.49	-1.75	-0.21	10.13	5	DNB	DNB
8	-0.34	-0.44	-0.30	-0.66	-7.83	9.13	-8.52	-1.04	13	TNT	TNT
9	-0.26	-0.46	-0.38	-0.60	-4.61	8.68	-2.61	-0.62	6	DNMB	DNT
10	-0.27	-0.46	-0.38	-0.60	-3.36	7.46	-1.04	0.26	7	DNT	DNT
11	-0.12	-0.33	-0.08	-0.28	21.81	7.13	-1.07	-1.56	8	NB	NB
12	-0.33	-0.57	-0.42	-0.65	-10.65	7.48	-2.66	-1.94	4	CDNB	CDNB
13	-0.51	-0.41	-0.29	-0.17	19.81	-16.83	0.89	1.31	11	PA	PA
14	-0.33	-0.57	-0.39	-0.66	-10.81	8.32	-3.86	-2.87	4	CDNB	CDNB
15	-0.14	-0.87	-0.79	-0.72	-21.64	12.69	14.48	-1.70	1	2-NA	2-NA
16	-0.32	-0.32	-0.13	-0.28	18.86	-2.19	-3.95	-0.19	2	3-NA	3-NA
17	-0.13	-0.30	0.00	0.00	40.18	-3.10	4.27	-1.59	3	A	A
18	-0.50	-0.34	-0.29	-0.13	23.21	-18.06	1.12	4.00	11	PA	PA
19	-0.31	-0.44	-0.27	-0.65	-6.52	10.35	-8.62	-1.64	13	TNT	TNT
20	-0.26	-0.34	-0.25	-0.34	14.09	1.28	-0.95	2.07	10	ONCB	ONCB
21	-0.10	-0.32	-0.06	-0.25	24.74	7.26	-0.40	-1.49	8	NB	NB
22	-0.47	-0.45	-0.74	-0.68	-17.14	-1.94	-0.52	9.82	5	DNB	DNB
23	-0.32	-0.44	-0.12	-0.26	18.65	-3.17	-1.49	-4.11	2	3-NA	3-NA
24	-0.60	-0.59	-0.50	-0.45	-3.26	-13.47	-0.34	0.11	9	NP	NP
25	-0.23	-0.32	-0.27	-0.36	13.31	3.05	-0.67	3.09	10	ONCB	ONCB
26	-0.61	-0.67	-0.49	-0.46	-4.88	-13.41	0.51	-2.51	9	NP	NP
27	-0.23	-0.35	-0.26	-0.36	12.92	3.21	-0.82	1.99	10	ONCB	ONCB
28	-0.96	-0.99	-0.98	-0.98	-51.00	-16.31	-2.80	-2.30	12	PNP	PNP
29	-0.10	-0.25	-0.07	0.00	39.78	-2.42	5.49	1.64	3	A	A
30	-0.23	-0.36	-0.23	-0.38	12.12	4.40	-1.72	0.81	10	ONCB	ONCB
31	-0.97	-0.99	-0.99	-0.98	-51.16	-16.41	-2.81	-2.19	12	PNP	PNP
32	-0.27	-0.49	-0.37	-0.59	-4.95	9.01	-2.95	0.74	6	DNMB	DNMB
33	-0.61	-0.65	-0.50	-0.44	-3.52	-14.18	1.08	-1.90	9	NP	NP
34	-0.48	-0.47	-0.29	-0.17	19.62	-16.20	2.76	-0.08	11	PA	PA
35	-0.48	-0.37	-0.23	-0.15	22.41	-15.78	-0.34	1.45	11	PA	PA
36	-0.09	-0.86	-0.80	-0.73	-21.32	14.71	15.52	-1.37	1	2-NA	2-NA
37	-0.97	-0.99	-0.99	-0.98	-50.97	-16.56	-2.70	-2.19	12	PNP	PNP
38	-0.19	-0.86	-0.80	-0.73	-22.51	11.04	13.17	-1.38	1	2-NA	2-NA
39	-0.32	-0.44	-0.13	-0.26	18.96	-3.03	-1.24	-3.67	2	3-NA	3-NA
40	-0.96	-0.99	-0.98	-0.98	-51.06	-16.32	-2.78	-2.19	12	PNP	PNP
41	-0.20	-0.20	0.01	-0.02	39.54	-5.00	0.13	1.10	3	A	A
42	-0.33	-0.41	-0.16	-0.28	17.34	-3.12	-1.67	-1.99	2	3-NA	3-NA
43	-0.46	-0.47	-0.73	-0.66	-15.92	-2.01	0.63	9.18	5	DNB	DNB
44	-0.29	-0.49	-0.34	-0.54	-0.96	7.61	-0.53	0.58	7	DNT	DNMB
45	-0.32	-0.49	-0.36	-0.65	-8.74	8.62	-5.60	-0.86	13	TNT	TNT
46	-0.26	-0.49	-0.39	-0.57	-5.03	8.68	-3.38	0.71	6	DNMB	DNMB
47	-0.29	-0.57	-0.38	-0.65	-9.66	9.72	-3.02	-2.88	4	CDNB	CDNB
48	-0.26	-0.49	-0.38	-0.57	-5.51	10.53	-1.83	0.67	6	DNMB	DNMB

49	-0.11	-0.28	0.01	-0.01	39.90	-1.04	3.53	-1.42	3	A	A
50	-0.34	-0.46	-0.36	-0.68	-10.38	9.41	-7.43	-0.40	13	TNT	TNT
51	-0.33	-0.58	-0.42	-0.66	-11.25	7.73	-2.86	-2.38	4	CDNB	CDNB
52	-0.18	-0.82	-0.79	-0.72	-21.37	11.02	12.53	-0.30	1	2-NA	2-NA

Table 11. Jackknifed classification matrix from water-soluble PPEs sensor array **P1-P4** (1 μM, at pH 7, buffered) against 13 nitroaromaitic analytes at a concentration of 0.5 mM.

	2-NA	**3-NA**	**A**	**CDNB**	**DNB**	**DNMB**	**DNT**	**NB**	**NP**	**ONCB**	**PA**	**PNP**	**TNT**	**%correct**
2-NA	6	0	0	0	0	0	0	0	0	0	0	0	0	100
3-NA	0	6	0	0	0	0	0	0	0	0	0	0	0	100
A	0	0	6	0	0	0	0	0	0	0	0	0	0	100
CDNB	0	0	0	6	0	0	0	0	0	0	0	0	0	100
DNB	0	0	0	0	6	0	0	0	0	0	0	0	0	100
DNMB	0	0	0	0	0	6	0	0	0	0	0	0	0	100
DNT	0	0	0	0	0	1	5	0	0	0	0	0	0	83
NB	0	0	0	0	0	0	0	6	0	0	0	0	0	100
NP	0	0	0	0	0	0	0	0	6	0	0	0	0	100
ONCB	0	0	0	0	0	0	0	0	0	6	0	0	0	100
PA	0	0	0	0	0	0	0	0	0	0	6	0	0	100
PNP	0	0	0	0	0	0	0	0	0	0	0	6	0	100
TNT	0	0	0	0	0	0	0	0	0	0	0	0	6	100
Total	6	6	6	6	6	7	5	6	6	6	6	6	6	**99**

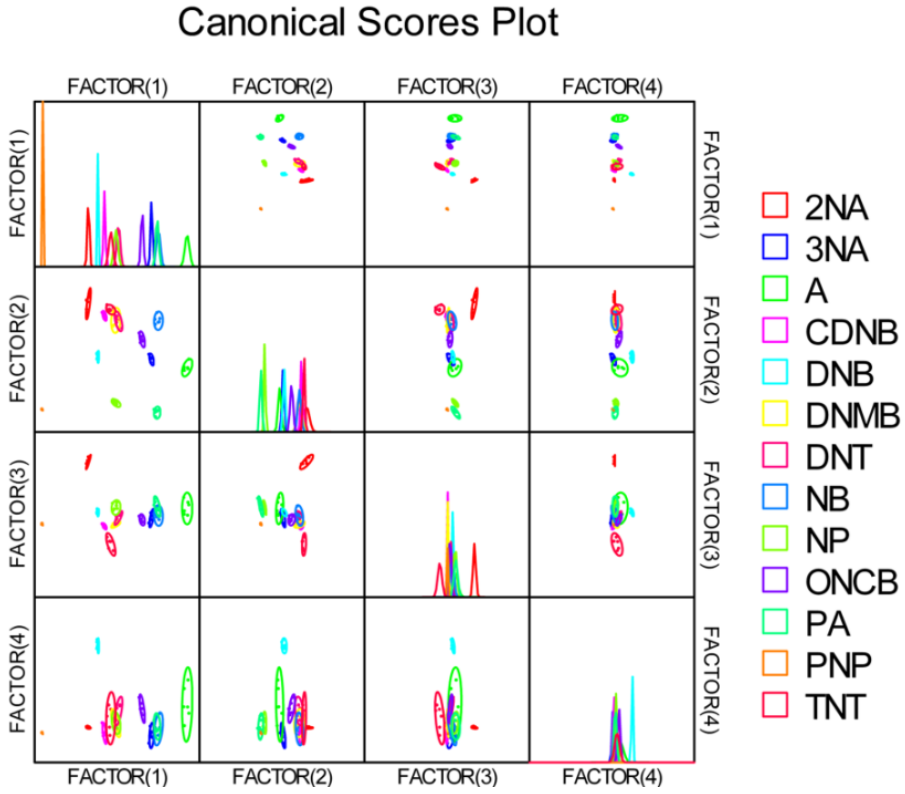

Figure 96. Correlations of canonical fluorescence response patterns from PPEs sensor array **P1-P4** (1 μM, at pH 7, buffered) against 13 aromatic analytes. The 95% confidence ellipses for the individual acids are also shown.

Table 12. Training matrix of fluorescence response pattern from water-soluble PPEs **P3-P4** (1 μM, at pH 7, buffered) against 13 nitroaromaitic analytes at a concentration of 0.5 mM. LDA was carried out as described above resulting in the two factors of the canonical scores and group generation. The jackknifed classification matrix with cross-validation reveals an accuracy of 96%.

Analytes	Fluorescence Response Pattern		Results LDA		
Nitroaromaitc	**P3**	**P4**	Factor 1	Factor 2	Group
A	-0.02	-0.01	37.23	-2.76	3
A	-0.06	0.03	39.45	-5.88	3
A	-0.05	0.01	37.86	-4.87	3
A	0.05	0.01	39.95	-1.24	3
A	0.04	0.02	40.41	-2.10	3
A	0.04	0.00	38.95	-1.18	3
2-NA	-0.79	-0.72	-21.57	-6.06	1
2-NA	-0.79	-0.74	-22.80	-5.37	1
2-NA	-0.80	-0.73	-22.07	-6.15	1
2-NA	-0.80	-0.73	-22.06	-6.22	1
2-NA	-0.80	-0.72	-21.84	-6.37	1
2-NA	-0.80	-0.72	-21.71	-6.52	1
3-NA	-0.17	-0.26	18.59	0.39	2
3-NA	-0.14	-0.27	18.49	2.04	2
3-NA	-0.16	-0.27	17.95	1.14	2
3-NA	-0.18	-0.25	18.93	0.02	2
3-NA	-0.14	-0.25	19.45	1.41	2
3-NA	-0.12	-0.29	17.38	3.65	8
DNB	-0.72	-0.66	-16.53	-5.69	5
DNB	-0.72	-0.65	-16.15	-5.91	5
DNB	-0.73	-0.66	-16.66	-6.19	5
DNB	-0.74	-0.65	-15.87	-7.00	5
DNB	-0.74	-0.65	-16.25	-6.79	5
DNB	-0.74	-0.65	-15.88	-6.74	5
DNT	-0.41	-0.57	-5.66	2.64	7
DNT	-0.40	-0.54	-3.54	1.86	7
DNT	-0.40	-0.53	-3.02	1.69	7
DNT	-0.38	-0.56	-4.99	3.61	7
DNT	-0.39	-0.57	-5.54	3.60	7
DNT	-0.36	-0.58	-5.62	5.02	6
NB	-0.06	-0.28	18.58	5.81	8
NB	-0.05	-0.25	20.57	4.83	8
NB	-0.10	-0.25	20.47	2.89	8
NB	-0.07	-0.26	19.80	4.34	8
NB	-0.10	-0.28	18.46	3.99	8
NB	-0.09	-0.28	18.04	4.65	8
NP	-0.52	-0.43	1.84	-6.57	9
NP	-0.56	-0.43	1.62	-8.07	9
NP	-0.57	-0.46	-0.83	-7.28	9
NP	-0.50	-0.43	2.05	-5.53	9
NP	-0.53	-0.45	0.35	-6.07	9
NP	-0.53	-0.47	-0.79	-5.64	9

PA	-0.27	-0.15	24.09	-7.12	11
PA	-0.28	-0.12	26.09	-8.66	11
PA	-0.26	-0.13	25.41	-7.51	11
PA	-0.21	-0.14	26.10	-5.59	11
PA	-0.20	-0.13	26.85	-5.41	11
PA	-0.24	-0.13	25.81	-6.83	11
TNT	-0.26	-0.65	-8.85	11.34	13
TNT	-0.33	-0.65	-9.98	9.05	13
TNT	-0.28	-0.65	-9.45	10.77	13
TNT	-0.30	-0.66	-10.14	10.31	13
TNT	-0.35	-0.68	-12.24	9.08	13
TNT	-0.32	-0.68	-11.56	10.20	13
CDNB	-0.44	-0.69	-14.04	5.91	4
CDNB	-0.42	-0.68	-13.04	6.58	4
CDNB	-0.40	-0.67	-12.37	7.18	4
CDNB	-0.39	-0.66	-11.86	7.01	4
CDNB	-0.40	-0.68	-12.78	7.13	4
CDNB	-0.41	-0.66	-12.11	6.23	4
DNMB	-0.33	-0.56	-4.10	5.70	6
DNMB	-0.37	-0.61	-7.79	5.75	6
DNMB	-0.34	-0.57	-4.59	5.50	6
DNMB	-0.37	-0.59	-6.51	5.29	6
DNMB	-0.37	-0.60	-7.02	5.40	6
DNMB	-0.39	-0.58	-6.41	4.33	6
ONCB	-0.28	-0.38	8.48	1.08	10
ONCB	-0.24	-0.37	10.26	1.74	10
ONCB	-0.24	-0.35	11.51	0.99	10
ONCB	-0.22	-0.37	10.48	2.75	10
ONCB	-0.20	-0.36	11.38	2.87	10
ONCB	-0.25	-0.36	10.29	1.48	10
PNP	-0.98	-0.98	-41.42	-4.07	12
PNP	-0.98	-0.98	-41.53	-3.85	12
PNP	-0.98	-0.98	-41.56	-3.97	12
PNP	-0.98	-0.98	-41.45	-4.09	12
PNP	-0.98	-0.98	-41.49	-4.02	12
PNP	-0.98	-0.98	-41.54	-3.93	12

Table 13. Detection and identification of 52 unknown samples using LDA training matrix from PPEs sensor array **P3**-**P4** (1 µM, at pH 7, buffered). All unknown samples could be assigned to the corresponding group defined by the training matrix according to their shortest Mahalanobis distance. 50 of the 52 unknown explosive samples were correctly identified, reveals a 96 % accuracy.

Sample	Fluorescence Response Pattern		Results LDA			Analyte	
#	**P3**	**P4**	Factor 1	Factor 2	Group	Identification	Verification
1	-0.08	-0.28	18.29	4.78	8	NB	NB
2	-0.16	-0.28	17.19	1.54	2	3-NA	3-NA
3	-0.10	-0.32	15.23	5.63	8	NB	NB
4	-0.74	-0.67	-17.40	-6.05	5	DNB	DNB
5	-0.40	-0.61	-5.32	4.14	7	DNT	DNT

6	-0.13	-0.28	17.66	2.77	2	3-NA	3-NA
7	-0.06	-0.25	20.97	4.34	8	NB	NB
8	-0.73	-0.66	-16.77	-6.16	5	DNB	DNB
9	-0.49	-0.47	-0.13	-3.94	9	NP	NP
10	-0.74	-0.68	-17.88	-5.73	5	DNB	DNB
11	-0.50	-0.44	1.41	-5.23	9	NP	NP
12	-0.38	-0.60	-6.71	5.47	6	DNMB	DNT
13	-0.12	-0.26	19.00	2.50	2	3-NA	3-NA
14	-0.36	-0.68	-12.60	9.22	13	TNT	TNT
15	-0.79	-0.72	-21.92	-6.11	1	2-NA	2-NA
16	-0.38	-0.57	-8.35	4.87	6	DNMB	DNMB
17	-0.80	-0.73	-22.22	-6.32	1	2-NA	2-NA
18	-0.36	-0.65	-10.62	7.79	13	TNT	TNT
19	-0.38	-0.60	-5.34	3.38	7	DNT	DNT
20	-0.50	-0.45	0.79	-4.89	9	NP	NP
21	-0.23	-0.38	9.50	2.83	10	ONCB	ONCB
22	-0.38	-0.54	-3.08	4.45	7	DNT	DNT
23	-0.39	-0.66	-11.75	7.31	4	CDNB	CDNB
24	-0.37	-0.59	-7.51	5.15	6	DNMB	DNMB
25	-0.80	-0.73	-22.42	-5.89	1	2-NA	2-NA
26	-0.13	-0.26	19.14	2.13	2	3-NA	3-NA
27	-0.34	-0.54	-3.25	2.93	7	DNT	DNMB
28	-0.29	-0.17	22.79	-7.69	11	PA	PA
29	-0.42	-0.65	-11.53	5.59	4	CDNB	CDNB
30	-0.23	-0.15	24.58	-5.85	11	PA	PA
31	-0.27	-0.36	10.42	0.38	10	ONCB	ONCB
32	-0.73	-0.66	-16.48	-6.29	5	DNB	DNB
33	-0.49	-0.46	0.07	-4.22	9	NP	NP
34	-0.42	-0.66	-12.04	6.05	4	CDNB	CDNB
35	-0.38	-0.65	-11.03	7.21	4	CDNB	CDNB
36	-0.29	-0.13	25.37	-9.12	11	PA	PA
37	-0.25	-0.34	11.90	0.48	10	ONCB	ONCB
38	-0.30	-0.66	-10.09	10.35	13	TNT	TNT
39	0.00	0.00	38.42	-2.73	3	A	A
40	-0.98	-0.98	-41.62	-3.90	12	PNP	PNP
41	-0.07	0.00	37.05	-5.09	3	A	A
42	-0.27	-0.65	-9.08	11.22	13	TNT	TNT
43	-0.39	-0.57	-7.51	5.37	6	DNMB	DNMB
44	-0.99	-0.98	-41.78	-3.98	12	PNP	PNP
45	-0.10	-0.34	13.93	6.32	8	NB	NB
46	-0.26	-0.36	10.30	1.10	10	ONCB	ONCB
47	-0.99	-0.98	-41.55	-4.12	12	PNP	PNP
48	0.01	-0.02	37.33	-1.62	3	A	A
49	-0.79	-0.72	-21.72	-5.93	1	2-NA	2-NA
50	0.01	-0.01	37.47	-1.48	3	A	A
51	-0.98	-0.98	-41.70	-3.97	12	PNP	PNP
52	-0.29	-0.17	22.62	-7.18	11	PA	PA

Table 14. Jackknifed classification matrix from water-soluble PPEs sensor array **P3**-**P4** (1 μM, at pH 7, buffered) against 13 nitroaromaitic analytes at a concentration of 0.5 mM.

	2-NA	**3-NA**	**A**	**CDNB**	**DNB**	**DNMB**	**DNT**	**NB**	**NP**	**ONCB**	**PA**	**PNP**	**TNT**	**%correct**
2-NA	6	0	0	0	0	0	0	0	0	0	0	0	0	100
3-NA	0	5	0	0	0	0	0	1	0	0	0	0	0	83
A	0	0	6	0	0	0	0	0	0	0	0	0	0	100
CDNB	0	0	0	6	0	0	0	0	0	0	0	0	0	100
DNB	0	0	0	0	6	0	0	0	0	0	0	0	0	100
DNMB	0	0	0	0	0	6	0	0	0	0	0	0	0	100
DNT	0	0	0	0	0	1	5	0	0	0	0	0	0	83
NB	0	0	0	0	0	0	0	6	0	0	0	0	0	100
NP	0	0	0	0	0	0	0	0	6	0	0	0	0	100
ONCB	0	0	0	0	0	0	0	0	0	6	0	0	0	100
PA	0	0	0	0	0	0	0	0	0	0	6	0	0	100
PNP	0	0	0	0	0	0	0	0	0	0	0	6	0	100
TNT	0	0	0	1	0	0	0	0	0	0	0	0	5	83
Total	6	5	6	7	6	7	5	7	6	6	6	6	5	**96**

5.3.2 LDA Calculation of Amino Acids (Chapter 3)

Table 15. Training matrix of fluorescence response pattern from an array of **P5**-Fe^{2+}, **P5**-Cu^{2+}, **P5**-Co^{2+} (each at pH 7, 10 and 13, buffered) against 20 amino acids. LDA was carried out as described above resulting in the nine factors of the canonical scores and group generation.

Analyte	Fluorescence response pattern									Results LDA (the first three scores)			
Amino acids	Fe^{2+} (pH7)	Fe^{2+} (pH10)	Fe^{2+} (pH13)	Cu^{2+} (pH7)	Cu^{2+} (pH10)	Cu^{2+} (pH13)	Co^{2+} (pH7)	Co^{2+} (pH10)	Co^{2+} (pH13)	Factor 1	Factor 2	Factor 3	Group
A	-0.41	-0.40	-0.52	0.36	1.05	0.54	-0.36	0.06	0.15	11.61	6.05	-20.95	1
A	-0.39	-0.50	-0.53	0.35	1.06	0.48	-0.36	0.03	0.17	10.74	5.79	-21.20	1
A	-0.41	-0.51	-0.54	0.37	1.06	0.56	-0.36	0.04	0.15	11.73	5.91	-22.09	1
A	-0.39	-0.39	-0.56	0.36	1.07	0.44	-0.37	0.06	0.12	10.95	5.94	-20.90	1
A	-0.41	-0.35	-0.56	0.36	1.04	0.50	-0.35	0.05	0.09	11.70	5.70	-19.79	1
A	-0.42	-0.33	-0.55	0.36	1.10	0.40	-0.35	0.04	0.10	11.44	6.32	-20.00	1
C	-0.19	8.87	-0.73	0.34	0.82	-0.03	-0.83	-0.80	-0.55	-41.19	96.20	18.26	2
C	-0.24	8.93	-0.72	0.35	0.78	-0.14	-0.84	-0.80	-0.55	-42.40	96.08	19.36	2
C	-0.31	8.62	-0.75	0.33	0.79	-0.11	-0.83	-0.81	-0.54	-42.15	93.38	18.12	2
C	-0.32	8.78	-0.74	0.35	0.81	-0.13	-0.84	-0.81	-0.47	-42.12	96.23	17.47	2
C	-0.31	8.31	-0.74	0.33	0.83	-0.28	-0.84	-0.80	-0.38	-42.24	92.15	16.12	2
C	-0.31	8.42	-0.75	0.35	0.83	-0.01	-0.83	-0.80	-0.40	-40.37	94.44	14.61	2
D	1.40	0.73	0.06	0.30	0.93	0.24	0.05	-0.02	-0.04	32.67	3.11	15.26	3
D	1.27	0.77	0.03	0.36	0.91	0.23	0.07	-0.02	-0.05	34.34	3.84	14.93	3
D	1.12	0.79	0.07	0.36	0.90	0.21	0.01	-0.01	-0.05	30.66	4.76	12.36	3
D	1.10	0.93	0.03	0.38	0.94	0.22	0.06	0.00	-0.07	34.77	5.26	14.15	3
D	1.16	0.78	0.04	0.36	0.89	0.23	0.05	-0.02	-0.06	32.99	3.89	14.24	3
D	1.41	0.78	0.02	0.38	0.94	0.22	0.05	-0.01	-0.08	33.81	4.83	13.81	3
E	0.49	0.66	0.14	0.35	0.93	0.45	-0.16	0.12	0.02	24.30	5.88	-0.13	4
E	0.49	0.71	0.16	0.32	0.94	0.47	-0.15	0.12	-0.03	24.32	4.84	1.46	4
E	0.43	0.73	0.20	0.36	0.95	0.54	-0.15	0.11	0.03	25.45	7.02	-0.23	4
E	0.53	0.62	0.17	0.36	0.94	0.47	-0.15	0.08	0.03	24.47	6.33	0.34	4
E	0.64	0.54	0.17	0.35	0.94	0.45	-0.14	0.08	0.01	24.62	4.98	1.00	4
E	0.48	0.75	0.15	0.33	0.96	0.58	-0.16	0.09	-0.03	23.55	6.76	0.06	4
F	-0.29	-0.87	-0.52	-0.42	0.50	-0.76	-0.50	-0.18	-0.94	-36.24	-29.42	7.04	5
F	-0.36	-0.89	-0.53	-0.44	0.49	-0.76	-0.51	-0.16	-0.95	-37.05	-30.37	6.82	5
F	-0.34	-0.89	-0.53	-0.42	0.36	-0.76	-0.52	-0.16	-0.95	-38.89	-30.76	7.33	5

F	-0.38	-0.88	-0.52	-0.41	0.27	-0.77	-0.52	-0.20	-0.95	-40.45	-30.82	8.51	5
F	-0.36	-0.87	-0.51	-0.42	0.52	-0.78	-0.50	-0.20	-0.95	-36.93	-29.16	6.86	5
F	-0.36	-0.89	-0.51	-0.38	0.48	-0.81	-0.51	-0.20	-0.94	-37.13	-28.68	6.11	5
G	-0.37	-0.61	-0.61	0.33	0.76	0.65	-0.22	0.18	0.03	18.64	-4.21	-12.67	6
G	-0.39	-0.68	-0.63	0.35	0.80	0.66	-0.23	0.15	0.03	18.60	-3.22	-14.26	6
G	-0.40	-0.64	-0.64	0.33	0.78	0.67	-0.21	0.13	0.01	18.16	-3.71	-12.48	6
G	-0.42	-0.63	-0.65	0.33	0.80	0.70	-0.22	0.09	-0.05	17.14	-3.33	-12.61	6
G	-0.43	-0.63	-0.62	0.35	0.79	0.66	-0.23	0.09	-0.09	16.03	-3.48	-13.02	6
G	-0.36	-0.55	-0.64	0.32	0.80	0.71	-0.21	0.05	-0.09	16.55	-2.75	-11.27	6
H	0.68	-0.21	-0.47	0.31	0.71	0.84	-0.85	-0.82	-0.75	-48.14	20.48	-28.40	7
H	0.66	-0.25	-0.38	0.28	0.70	0.77	-0.84	-0.83	-0.75	-48.58	18.83	-26.84	7
H	0.45	-0.18	-0.55	0.29	0.69	0.72	-0.84	-0.83	-0.71	-48.71	20.19	-27.65	7
H	0.45	-0.19	-0.55	0.30	0.70	0.75	-0.85	-0.83	-0.72	-48.58	20.44	-28.17	7
H	0.73	-0.18	-0.49	0.30	0.70	0.84	-0.85	-0.83	-0.67	-47.81	21.53	-28.05	7
H	0.58	-0.09	-0.54	0.30	0.72	0.77	-0.85	-0.83	-0.68	-48.10	22.25	-28.01	7
I	-0.26	-0.64	-0.57	0.32	0.75	0.69	-0.36	-0.04	0.13	5.87	2.81	-17.70	8
I	-0.30	-0.67	-0.56	0.31	0.77	0.70	-0.36	0.03	0.17	7.66	2.07	-18.69	8
I	-0.31	-0.64	-0.57	0.29	0.76	0.76	-0.38	0.00	0.06	4.71	1.36	-18.68	8
I	-0.29	-0.66	-0.57	0.32	0.77	0.67	-0.37	-0.03	0.08	5.10	2.17	-18.19	8
I	-0.33	-0.66	-0.51	0.32	0.75	0.82	-0.38	-0.06	0.11	4.27	3.54	-19.45	8
I	-0.29	-0.63	-0.54	0.30	0.74	0.73	-0.38	0.02	0.15	5.73	2.01	-18.62	8
K	1.14	1.74	0.07	0.22	0.86	0.75	0.10	-0.03	0.47	38.72	15.63	19.63	9
K	0.94	1.50	0.10	0.24	0.87	0.75	0.08	-0.03	0.41	37.78	13.05	17.38	9
K	0.92	1.33	0.08	0.25	0.86	0.74	0.10	-0.03	0.44	38.60	12.07	16.68	9
K	0.94	1.02	0.10	0.24	0.85	0.82	0.10	-0.04	0.45	38.77	9.57	15.38	9
K	1.04	1.12	0.13	0.24	0.86	0.89	0.10	-0.01	0.40	39.63	9.78	15.48	9
K	0.98	1.00	0.08	0.23	0.84	0.90	0.09	-0.01	0.41	38.60	9.03	14.50	9
L	-0.27	-0.63	-0.45	-0.14	0.74	0.63	-0.39	-0.03	-0.36	-8.45	-12.42	-6.83	10
L	-0.27	-0.64	-0.42	-0.11	0.71	0.47	-0.38	-0.03	-0.33	-7.39	-12.70	-5.66	10
L	-0.33	-0.62	-0.45	-0.15	0.72	0.58	-0.40	-0.03	-0.41	-9.57	-13.61	-5.95	10
L	-0.23	-0.61	-0.42	-0.09	0.79	0.50	-0.42	-0.01	-0.38	-8.50	-11.16	-8.82	10
L	-0.23	-0.62	-0.45	-0.23	0.73	0.57	-0.43	-0.01	-0.29	-11.42	-13.26	-6.38	10
L	-0.30	-0.58	-0.43	-0.19	0.69	0.47	-0.39	-0.03	-0.30	-9.63	-13.77	-4.00	10
M	-0.30	-0.74	-0.51	-0.25	0.48	-0.09	-0.28	0.07	-0.26	-6.60	-23.53	6.43	11
M	-0.30	-0.70	-0.49	-0.23	0.50	-0.10	-0.27	0.03	-0.30	-6.59	-22.57	7.05	11
M	-0.31	-0.77	-0.48	-0.16	0.44	-0.04	-0.27	0.04	-0.30	-5.62	-22.27	5.51	11
M	-0.33	-0.70	-0.49	-0.17	0.41	-0.07	-0.26	0.06	-0.19	-4.48	-21.39	6.29	11
M	-0.30	-0.75	-0.52	-0.18	0.41	-0.04	-0.26	0.06	-0.32	-5.39	-23.23	6.52	11
M	-0.32	-0.72	-0.52	-0.25	0.49	-0.05	-0.27	0.06	-0.15	-4.95	-21.84	6.31	11
N	0.61	0.17	-0.41	0.27	0.84	0.88	0.12	0.06	-0.14	38.19	-3.77	10.18	12
N	0.65	0.14	-0.39	0.27	0.80	0.90	0.10	0.03	-0.13	35.74	-3.44	9.70	12
N	0.42	0.22	-0.36	0.28	0.82	0.92	0.10	0.06	-0.14	37.03	-3.26	9.10	12
N	0.63	0.14	-0.38	0.26	0.84	0.88	0.10	0.05	-0.08	36.89	-3.00	9.12	12
N	0.57	0.24	-0.36	0.25	0.83	0.85	0.09	0.05	-0.05	36.42	-2.44	9.73	12
N	0.53	0.13	-0.40	0.30	0.81	0.95	0.08	0.04	0.00	36.79	-1.00	7.03	12
P	-0.27	-0.65	-0.38	0.23	0.43	0.62	-0.42	-0.17	0.08	-7.53	-0.11	-12.95	13
P	-0.32	-0.68	-0.38	0.24	0.43	0.64	-0.42	-0.17	0.07	-7.28	-0.19	-13.56	13
P	-0.30	-0.67	-0.38	0.25	0.42	0.67	-0.43	-0.15	0.05	-6.93	-0.40	-13.73	13
P	-0.28	-0.64	-0.37	0.25	0.43	0.67	-0.43	-0.18	0.04	-7.53	0.41	-13.52	13
P	-0.32	-0.59	-0.35	0.23	0.42	0.61	-0.43	-0.19	0.07	-8.35	0.39	-12.55	13
P	-0.33	-0.67	-0.34	0.24	0.42	0.74	-0.42	-0.18	0.07	-7.25	0.09	-13.63	13
Q	-0.28	-0.49	-0.51	0.28	0.81	0.71	-0.27	0.14	0.19	16.00	-0.47	-13.91	14
Q	-0.28	-0.54	-0.57	0.29	0.75	0.69	-0.28	0.09	0.19	13.63	0.01	-14.05	14
Q	-0.33	-0.52	-0.53	0.31	0.78	0.72	-0.30	0.09	0.17	12.71	0.91	-15.84	14
Q	-0.30	-0.54	-0.56	0.28	0.78	0.63	-0.30	0.09	0.16	11.84	-0.12	-14.84	14
Q	-0.33	-0.53	-0.59	0.30	0.75	0.60	-0.29	0.10	0.21	12.66	0.39	-14.65	14
Q	-0.30	-0.47	-0.57	0.30	0.80	0.59	-0.31	0.08	0.19	11.92	1.37	-15.00	14
R	1.13	1.22	-0.54	0.26	0.77	0.56	0.10	0.07	0.23	38.53	8.49	16.75	15

R	1.09	1.25	-0.53	0.25	0.76	0.47	0.10	0.07	0.28	37.93	8.64	17.49	15
R	1.20	1.15	-0.57	0.26	0.78	0.54	0.07	0.06	0.26	36.49	9.33	14.94	15
R	1.06	1.16	-0.52	0.25	0.75	0.49	0.10	0.06	0.31	37.85	8.06	17.40	15
R	1.27	0.88	-0.58	0.24	0.76	0.52	0.11	0.04	0.27	37.71	6.01	16.43	15
R	1.39	1.20	-0.53	0.26	0.75	0.54	0.09	0.04	0.28	37.66	9.67	17.13	15
S	-0.25	-0.68	-0.53	0.30	0.71	1.12	0.17	0.18	-0.30	41.93	-16.00	5.23	16
S	-0.27	-0.67	-0.51	0.30	0.73	1.07	0.10	0.19	-0.33	37.88	-15.20	2.51	16
S	-0.24	-0.68	-0.48	0.30	0.73	1.17	0.14	0.19	-0.31	40.30	-15.39	3.59	16
S	-0.27	-0.68	-0.55	0.29	0.70	1.05	0.15	0.18	-0.32	40.32	-16.49	5.56	16
S	-0.25	-0.68	-0.43	0.29	0.68	1.14	0.17	0.17	-0.30	41.08	-16.62	6.33	16
S	-0.28	-0.66	-0.45	0.28	0.69	1.09	0.15	0.12	-0.31	38.46	-15.63	5.83	16
T	-0.29	-0.53	-0.48	0.28	0.79	1.26	0.23	0.20	-0.31	47.79	-16.07	7.69	17
T	-0.33	-0.53	-0.50	0.28	0.78	1.00	0.23	0.15	-0.30	44.64	-16.09	9.43	17
T	-0.31	-0.56	-0.54	0.27	0.78	1.07	0.23	0.20	-0.30	46.55	-16.96	8.87	17
T	-0.31	-0.55	-0.59	0.28	0.77	1.15	0.22	0.20	-0.30	46.17	-16.06	7.38	17
T	-0.34	-0.59	-0.59	0.28	0.79	0.88	0.24	0.20	-0.30	46.75	-17.56	9.67	17
T	-0.32	-0.59	-0.60	0.30	0.84	0.96	0.22	0.20	-0.31	46.19	-16.18	6.99	17
V	-0.20	-0.59	-0.45	0.27	0.73	0.97	-0.38	0.07	0.04	6.21	0.48	-18.62	18
V	-0.19	-0.64	-0.46	0.26	0.73	0.83	-0.38	0.06	0.07	5.60	0.03	-18.13	18
V	-0.28	-0.63	-0.53	0.25	0.73	0.81	-0.40	0.05	0.07	4.09	0.28	-18.69	18
V	-0.23	-0.65	-0.52	0.25	0.73	0.89	-0.40	0.07	-0.03	3.77	-0.84	-19.03	18
V	-0.24	-0.68	-0.53	0.25	0.76	0.83	-0.40	0.04	0.04	4.01	0.25	-19.39	18
V	-0.24	-0.63	-0.52	0.27	0.74	0.82	-0.40	0.07	0.01	4.54	0.06	-19.28	18
W	-0.86	-0.94	-0.66	-0.68	-0.64	-0.93	-0.94	-0.98	-0.97	-102.16	-25.09	9.94	19
W	-0.86	-0.94	-0.64	-0.67	-0.65	-0.93	-0.94	-0.98	-0.96	-102.12	-24.94	9.92	19
W	-0.87	-0.94	-0.63	-0.67	-0.64	-0.93	-0.95	-0.98	-0.97	-102.12	-25.03	9.88	19
W	-0.86	-0.93	-0.63	-0.68	-0.65	-0.93	-0.95	-0.98	-0.96	-102.30	-25.12	10.20	19
W	-0.87	-0.94	-0.64	-0.67	-0.64	-0.93	-0.95	-0.98	-0.96	-102.03	-24.79	9.74	19
W	-0.86	-0.94	-0.66	-0.68	-0.64	-0.93	-0.94	-0.98	-0.97	-102.15	-25.20	10.16	19
Y	-0.27	-0.51	-0.57	-0.43	-0.46	-0.54	-0.50	-0.69	-0.86	-57.79	-25.08	22.25	20
Y	-0.22	-0.51	-0.54	-0.42	-0.44	-0.56	-0.50	-0.69	-0.86	-57.53	-24.87	22.09	20
Y	-0.27	-0.55	-0.56	-0.43	-0.45	-0.54	-0.49	-0.68	-0.84	-56.63	-25.65	22.50	20
Y	-0.34	-0.54	-0.58	-0.43	-0.44	-0.57	-0.49	-0.70	-0.86	-57.55	-25.51	22.30	20
Y	-0.33	-0.54	-0.58	-0.44	-0.43	-0.55	-0.49	-0.67	-0.85	-56.73	-26.02	22.41	20
Y	-0.20	-0.48	-0.57	-0.43	-0.44	-0.55	-0.50	-0.67	-0.86	-57.30	-25.09	22.22	20

Table 16. LDA jackknifed classification matrix table obtained from an array of **P5**-Fe^{2+}, **P5**-Cu^{2+}, **P5**-Co^{2+} (each at pH 7, 10 and 13, buffered) against 20 amino acids. The jackknifed classification matrix with cross-validation reveals a 100% accuracy.

	A	C	D	E	F	G	H	I	K	L	M	N	P	Q	R	S	T	V	W	Y	%correct
A	6	0	0	0	0	0	0	0	0	0	0	0	0	0	0	0	0	0	0	0	100
C	0	6	0	0	0	0	0	0	0	0	0	0	0	0	0	0	0	0	0	0	100
D	0	0	6	0	0	0	0	0	0	0	0	0	0	0	0	0	0	0	0	0	100
E	0	0	0	6	0	0	0	0	0	0	0	0	0	0	0	0	0	0	0	0	100
F	0	0	0	0	6	0	0	0	0	0	0	0	0	0	0	0	0	0	0	0	100
G	0	0	0	0	0	6	0	0	0	0	0	0	0	0	0	0	0	0	0	0	100
H	0	0	0	0	0	0	6	0	0	0	0	0	0	0	0	0	0	0	0	0	100
I	0	0	0	0	0	0	0	6	0	0	0	0	0	0	0	0	0	0	0	0	100
K	0	0	0	0	0	0	0	0	6	0	0	0	0	0	0	0	0	0	0	0	100
L	0	0	0	0	0	0	0	0	0	6	0	0	0	0	0	0	0	0	0	0	100
M	0	0	0	0	0	0	0	0	0	0	6	0	0	0	0	0	0	0	0	0	100
N	0	0	0	0	0	0	0	0	0	0	0	6	0	0	0	0	0	0	0	0	100
P	0	0	0	0	0	0	0	0	0	0	0	0	6	0	0	0	0	0	0	0	100
Q	0	0	0	0	0	0	0	0	0	0	0	0	0	6	0	0	0	0	0	0	100
R	0	0	0	0	0	0	0	0	0	0	0	0	0	0	6	0	0	0	0	0	100
S	0	0	0	0	0	0	0	0	0	0	0	0	0	0	0	6	0	0	0	0	100
T	0	0	0	0	0	0	0	0	0	0	0	0	0	0	0	0	6	0	0	0	100

V	0	0	0	0	0	0	0	0	0	0	0	0	0	0	0	0	6	0	0	100
W	0	0	0	0	0	0	0	0	0	0	0	0	0	0	0	0	0	6	0	100
Y	0	0	0	0	0	0	0	0	0	0	0	0	0	0	0	0	0	0	6	100
Total	6	6	6	6	6	6	6	6	6	6	6	6	6	6	6	6	6	6	6	**100**

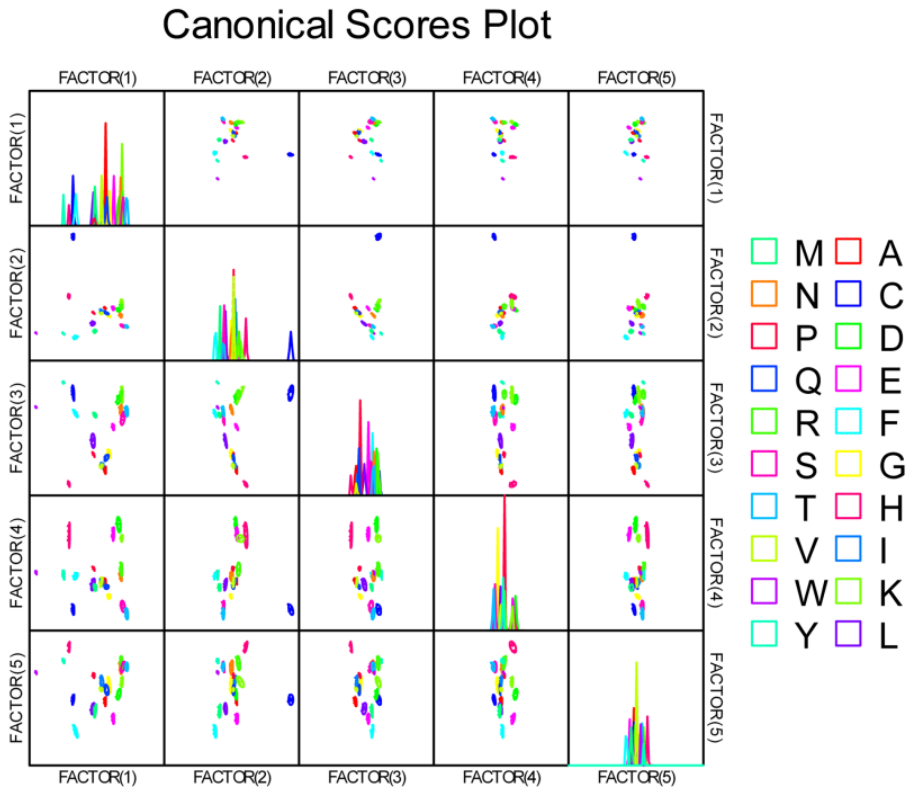

Figure 97. Correlations of canonical fluorescence response patterns from **P5**-Fe^{2+}, **P5**-Cu^{2+}, **P5**-Co^{2+} (each at pH 7, 10 and 13, buffered) against 20 amino acids. The 95% confidence ellipses for the individual acids are shown.

Table 17. Training matrix of fluorescence response pattern from an array of **P5**-Fe^{2+} (pH 10, buffered), **P5**-Cu^{2+} (pH 10, buffered), **P5**-Co^{2+} (pH 7 and 13, buffered) against 20 amino acids. LDA was carried out as described above resulting in the four factors of the canonical scores and group generation.

Analyte	Fluorescence response pattern				Results LDA				
Amino acids	Fe^{2+} (pH10)	Cu^{2+} (pH10)	Co^{2+} (pH7)	Co^{2+} (pH13)	Factor 1	Factor 2	Factor 3	Factor 4	Group
A	-0.40	1.05	-0.36	0.15	1.56	1.22	-18.86	1.72	1
A	-0.50	1.06	-0.36	0.17	1.59	0.53	-19.69	1.88	1
A	-0.51	1.06	-0.36	0.15	1.75	0.20	-19.59	1.34	1
A	-0.39	1.07	-0.37	0.12	1.09	1.36	-19.36	0.67	1
A	-0.35	1.04	-0.35	0.09	2.06	1.00	-17.49	0.23	1
A	-0.33	1.10	-0.35	0.10	2.45	1.87	-19.34	-0.50	1
C	8.87	0.82	-0.83	-0.55	-39.53	88.17	9.47	-5.19	2
C	8.93	0.78	-0.84	-0.55	-40.40	88.47	10.65	-4.23	2
C	8.62	0.79	-0.83	-0.54	-39.43	85.47	9.71	-4.31	2
C	8.78	0.81	-0.84	-0.47	-39.78	87.96	8.36	-3.05	2
C	8.31	0.83	-0.84	-0.38	-38.86	84.15	5.77	-1.42	2
C	8.42	0.83	-0.83	-0.40	-38.64	85.13	6.22	-1.78	2
D	0.73	0.93	0.05	-0.04	32.03	6.41	3.08	-3.04	3
D	0.77	0.91	0.07	-0.05	33.05	6.39	4.23	-3.33	3
D	0.79	0.90	0.01	-0.05	28.46	7.03	2.69	-2.79	3
D	0.93	0.94	0.06	-0.07	32.47	8.12	3.96	-3.92	3
D	0.78	0.89	0.05	-0.06	31.36	6.40	4.46	-2.86	3
D	0.78	0.94	0.05	-0.08	31.62	6.68	3.31	-4.29	3

E	0.66	0.93	-0.16	0.02	15.58	8.02	-4.75	-0.50	4
E	0.71	0.94	-0.15	-0.03	16.42	8.01	-3.98	-1.83	4
E	0.73	0.95	-0.15	0.03	16.59	8.85	-4.72	-0.45	4
E	0.62	0.94	-0.15	0.03	16.81	7.62	-4.69	-0.48	4
E	0.54	0.94	-0.14	0.01	17.34	6.58	-4.54	-1.21	4
E	0.75	0.96	-0.16	-0.03	15.40	8.65	-4.61	-2.12	4
F	-0.87	0.50	-0.50	-0.94	-23.38	-16.07	-0.40	-14.30	5
F	-0.89	0.49	-0.51	-0.95	-24.38	-16.32	-0.44	-14.18	5
F	-0.89	0.36	-0.52	-0.95	-26.92	-17.32	2.54	-12.03	5
F	-0.88	0.27	-0.52	-0.95	-27.72	-17.96	4.88	-10.58	5
F	-0.87	0.52	-0.50	-0.95	-23.50	-15.90	-0.93	-14.64	5
F	-0.89	0.48	-0.51	-0.94	-24.51	-16.37	-0.25	-13.86	5
G	-0.61	0.76	-0.22	0.03	8.14	-5.43	-6.41	2.45	6
G	-0.68	0.80	-0.23	0.03	8.32	-5.66	-8.04	1.85	6
G	-0.64	0.78	-0.21	0.01	9.02	-5.74	-6.55	1.73	6
G	-0.63	0.80	-0.22	-0.05	8.68	-5.97	-6.59	0.05	6
G	-0.63	0.79	-0.23	-0.09	7.19	-6.27	-6.35	-0.69	6
G	-0.55	0.80	-0.21	-0.09	9.12	-5.67	-5.68	-1.08	6
H	-0.21	0.71	-0.85	-0.75	-47.29	-3.47	-16.62	-10.75	7
H	-0.25	0.70	-0.84	-0.75	-46.66	-3.95	-16.31	-10.65	7
H	-0.18	0.69	-0.84	-0.71	-46.64	-3.04	-16.39	-9.61	7
H	-0.19	0.70	-0.85	-0.72	-46.83	-3.07	-16.56	-9.76	7
H	-0.18	0.70	-0.85	-0.67	-46.63	-2.55	-17.03	-8.75	7
H	-0.09	0.72	-0.85	-0.68	-46.49	-1.52	-17.34	-9.34	7
I	-0.64	0.75	-0.36	0.13	-1.85	-3.96	-11.42	5.87	8
I	-0.67	0.77	-0.36	0.17	-1.53	-3.57	-12.58	6.59	8
I	-0.64	0.76	-0.38	0.06	-4.13	-4.30	-11.74	4.24	18
I	-0.66	0.77	-0.37	0.08	-2.81	-4.28	-11.82	4.38	8
I	-0.66	0.75	-0.38	0.11	-3.89	-4.10	-12.04	5.70	8
I	-0.63	0.74	-0.38	0.15	-3.43	-3.56	-12.08	6.69	8
K	1.74	0.86	0.10	0.47	38.46	19.68	4.93	9.96	9
K	1.50	0.87	0.08	0.41	37.14	16.88	4.23	8.39	9
K	1.33	0.86	0.10	0.44	38.16	15.39	3.82	9.02	9
K	1.02	0.85	0.10	0.45	38.42	12.27	3.33	9.36	9
K	1.12	0.86	0.10	0.40	38.09	12.93	3.68	8.11	9
K	1.00	0.84	0.09	0.41	37.25	11.83	3.33	8.67	9
L	-0.63	0.74	-0.39	-0.36	-8.26	-7.67	-7.86	-5.13	10
L	-0.64	0.71	-0.38	-0.33	-6.97	-7.81	-7.00	-4.09	10
L	-0.62	0.72	-0.40	-0.41	-8.94	-8.12	-6.89	-5.97	10
L	-0.61	0.79	-0.42	-0.38	-9.64	-6.98	-9.90	-6.31	10
L	-0.62	0.73	-0.43	-0.29	-10.48	-6.80	-9.35	-3.13	10
L	-0.58	0.69	-0.39	-0.30	-7.92	-7.22	-6.69	-3.02	10
M	-0.74	0.48	-0.28	-0.26	-1.76	-10.93	1.10	0.60	11
M	-0.70	0.50	-0.27	-0.30	-0.86	-10.77	1.52	-0.56	11
M	-0.77	0.44	-0.27	-0.30	-1.71	-12.09	3.01	0.27	11
M	-0.70	0.41	-0.26	-0.19	-0.66	-10.73	3.23	3.38	11
M	-0.75	0.41	-0.26	-0.32	-1.47	-12.36	4.22	0.33	11
M	-0.72	0.49	-0.27	-0.15	0.21	-9.88	0.41	2.89	11
N	0.17	0.84	0.12	-0.14	35.45	-1.21	6.70	-4.54	12
N	0.14	0.80	0.10	-0.13	33.19	-1.61	6.90	-3.66	12
N	0.22	0.82	0.10	-0.14	33.83	-0.70	6.57	-4.25	12
N	0.14	0.84	0.10	-0.08	34.14	-0.79	5.20	-3.28	12

N	0.24	0.83	0.09	-0.05	33.84	0.38	5.37	-2.29	12
N	0.13	0.81	0.08	0.00	33.17	-0.48	4.91	-0.75	12
P	-0.65	0.43	-0.42	0.08	-11.39	-6.55	-4.77	10.30	13
P	-0.68	0.43	-0.42	0.07	-11.47	-6.97	-4.64	10.11	13
P	-0.67	0.42	-0.43	0.05	-11.78	-7.03	-4.33	9.87	13
P	-0.64	0.43	-0.43	0.04	-11.63	-6.71	-4.59	9.41	13
P	-0.59	0.42	-0.43	0.07	-11.65	-6.14	-4.44	10.23	13
P	-0.67	0.42	-0.42	0.07	-11.36	-6.93	-4.44	10.33	13
Q	-0.49	0.81	-0.27	0.19	6.24	-2.19	-10.17	5.74	14
Q	-0.54	0.75	-0.28	0.19	4.63	-2.92	-9.29	6.92	14
Q	-0.52	0.78	-0.30	0.17	2.97	-2.55	-10.62	5.96	14
Q	-0.54	0.78	-0.30	0.16	2.94	-2.81	-10.61	5.67	14
Q	-0.53	0.75	-0.29	0.21	3.53	-2.64	-9.90	7.34	14
Q	-0.47	0.80	-0.31	0.19	3.06	-1.78	-11.05	6.17	14
R	1.22	0.77	0.10	0.23	36.05	11.77	7.87	5.61	15
R	1.25	0.76	0.10	0.28	36.13	12.38	7.77	7.00	15
R	1.15	0.78	0.07	0.26	33.80	11.71	6.14	6.33	15
R	1.16	0.75	0.10	0.31	36.47	11.58	7.80	7.74	15
R	0.88	0.76	0.11	0.27	36.60	8.61	7.03	6.68	15
R	1.20	0.75	0.09	0.28	35.62	11.89	7.59	7.12	15
S	-0.68	0.71	0.17	-0.30	36.43	-12.32	10.07	-6.95	16
S	-0.67	0.73	0.10	-0.33	31.34	-11.82	7.87	-7.57	16
S	-0.68	0.73	0.14	-0.31	34.01	-12.03	8.90	-7.19	16
S	-0.68	0.70	0.15	-0.32	35.22	-12.46	10.28	-7.00	16
S	-0.68	0.68	0.17	-0.30	36.11	-12.65	11.17	-6.35	16
S	-0.66	0.69	0.15	-0.31	34.47	-12.27	10.27	-6.55	16
T	-0.53	0.79	0.23	-0.31	42.66	-10.84	10.79	-8.80	17
T	-0.53	0.78	0.23	-0.30	41.98	-10.79	10.91	-8.36	17
T	-0.56	0.78	0.23	-0.30	42.71	-11.13	10.84	-8.38	17
T	-0.55	0.77	0.22	-0.30	41.33	-10.96	10.59	-8.15	17
T	-0.59	0.79	0.24	-0.30	43.58	-11.32	10.76	-8.59	17
T	-0.59	0.84	0.22	-0.31	41.76	-10.82	8.71	-9.61	17
V	-0.59	0.73	-0.38	0.04	-4.69	-4.14	-10.73	4.33	18
V	-0.64	0.73	-0.38	0.07	-4.44	-4.34	-11.31	4.94	18
V	-0.63	0.73	-0.40	0.07	-5.64	-4.15	-11.66	5.17	18
V	-0.65	0.73	-0.40	-0.03	-6.77	-5.21	-10.85	2.79	18
V	-0.68	0.76	-0.40	0.04	-5.73	-4.52	-12.49	3.97	18
V	-0.63	0.74	-0.40	0.01	-6.15	-4.53	-11.50	3.34	18
W	-0.94	-0.64	-0.94	-0.97	-72.08	-23.07	15.31	6.41	19
W	-0.94	-0.65	-0.94	-0.96	-72.25	-23.14	15.67	6.85	19
W	-0.94	-0.64	-0.95	-0.97	-72.23	-23.06	15.45	6.49	19
W	-0.93	-0.65	-0.95	-0.96	-72.21	-22.93	15.52	6.73	19
W	-0.94	-0.64	-0.95	-0.96	-72.23	-23.04	15.48	6.71	19
W	-0.94	-0.64	-0.94	-0.97	-71.96	-23.07	15.47	6.43	19
Y	-0.51	-0.46	-0.50	-0.86	-33.78	-19.91	25.32	3.27	20
Y	-0.51	-0.44	-0.50	-0.86	-33.75	-19.78	24.91	3.02	20
Y	-0.55	-0.45	-0.49	-0.84	-32.61	-20.21	25.31	3.50	20
Y	-0.54	-0.44	-0.49	-0.86	-32.95	-20.15	24.89	3.01	20
Y	-0.54	-0.43	-0.49	-0.85	-32.61	-20.01	24.86	3.04	20
Y	-0.48	-0.44	-0.50	-0.86	-33.82	-19.52	24.91	3.12	20

Table 18. LDA jackknifed classification matrix table obtained from an array of **P5**-Fe^{2+} (pH 10, buffered), **P5**-Cu^{2+} (pH 10, buffered), **P5**-Co^{2+} (pH 7 and 13, buffered) against 20 amino acids. The jackknifed classification matrix with cross-validation reveals a 99% accuracy.

	A	C	D	E	F	G	H	I	K	L	M	N	P	Q	R	S	T	V	W	Y	%correct
A	6	0	0	0	0	0	0	0	0	0	0	0	0	0	0	0	0	0	0	0	100
C	0	6	0	0	0	0	0	0	0	0	0	0	0	0	0	0	0	0	0	0	100
D	0	0	6	0	0	0	0	0	0	0	0	0	0	0	0	0	0	0	0	0	100
E	0	0	0	6	0	0	0	0	0	0	0	0	0	0	0	0	0	0	0	0	100
F	0	0	0	0	6	0	0	0	0	0	0	0	0	0	0	0	0	0	0	0	100
G	0	0	0	0	0	6	0	0	0	0	0	0	0	0	0	0	0	0	0	0	100
H	0	0	0	0	0	0	6	0	0	0	0	0	0	0	0	0	0	0	0	0	100
I	0	0	0	0	0	0	0	5	0	0	0	0	0	0	0	0	0	1	0	0	83
K	0	0	0	0	0	0	0	0	6	0	0	0	0	0	0	0	0	0	0	0	100
L	0	0	0	0	0	0	0	0	0	6	0	0	0	0	0	0	0	0	0	0	100
M	0	0	0	0	0	0	0	0	0	0	6	0	0	0	0	0	0	0	0	0	100
N	0	0	0	0	0	0	0	0	0	0	0	6	0	0	0	0	0	0	0	0	100
P	0	0	0	0	0	0	0	0	0	0	0	0	6	0	0	0	0	0	0	0	100
Q	0	0	0	0	0	0	0	0	0	0	0	0	0	6	0	0	0	0	0	0	100
R	0	0	0	0	0	0	0	0	0	0	0	0	0	0	6	0	0	0	0	0	100
S	0	0	0	0	0	0	0	0	0	0	0	0	0	0	0	6	0	0	0	0	100
T	0	0	0	0	0	0	0	0	0	0	0	0	0	0	0	0	6	0	0	0	100
V	0	0	0	0	0	0	0	0	0	0	0	0	0	0	0	0	0	6	0	0	100
W	0	0	0	0	0	0	0	0	0	0	0	0	0	0	0	0	0	0	6	0	100
Y	0	0	0	0	0	0	0	0	0	0	0	0	0	0	0	0	0	0	0	6	100
Total	6	6	6	6	6	6	6	5	6	6	6	6	6	6	6	6	6	7	6	6	**99**

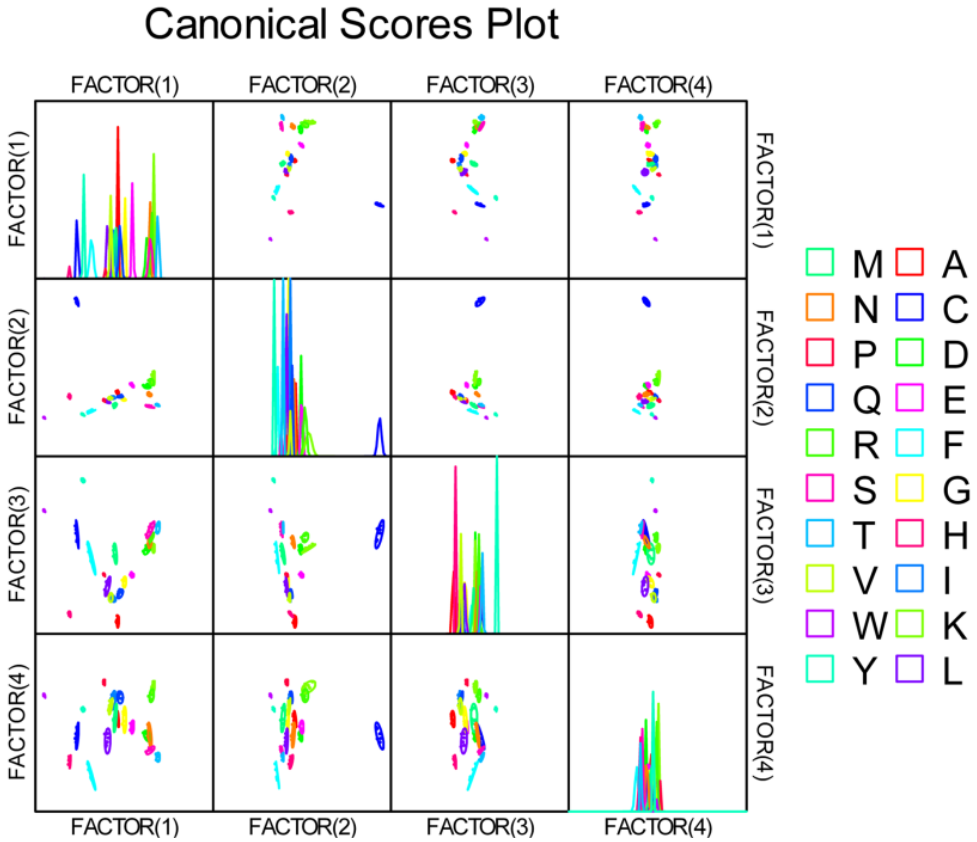

Figure 98. Correlations of canonical fluorescence response patterns from **P5**-Fe^{2+} (pH 10, buffered), **P5**-Cu^{2+} (pH 10, buffered), **P5**-Co^{2+} (pH 7 and 13, buffered) against 20 amino acids. The 95% confidence ellipses for the individual acids are shown.

Table 19. Detection and identification of unknown amino acids samples using LDA from the optimized PPE tongue (Fe^{2+}-pH 10, Cu^{2+}-pH 10, Co^{2+}-pH 7 and Co^{2+}-pH 13). According to the verification, 62 among 80 unknown sample were correctly identified, representing an accuracy of 77.5%.

Analyte	Fluorescence response pattern				Results LDA						
Unknown samples	Fe^{2+} (pH10)	Cu^{2+} (pH10)	Co^{2+} (pH7)	Co^{2+} (pH13)	Factor 1	Factor 2	Factor 3	Factor 4	Group	Identifi ca-tion	Verifica-tion
1	2.03	0.88	0.24	0.12	23.39	1.36	5.18	2.33	9	K	K
2	-0.13	0.59	0.34	-0.28	4.12	-9.26	0.90	-1.12	16	S	T
3	-0.43	0.37	-0.35	-0.57	-14.33	0.05	-1.08	-2.63	10	L	L
4	0.32	0.52	-0.78	-0.69	-20.28	8.45	0.04	-6.89	7	H	H
5	-0.40	0.55	0.28	-0.26	3.59	-8.35	-0.45	-0.08	16	S	S
6	0.35	0.53	-0.77	-0.71	-20.94	7.93	0.37	-7.55	7	H	H
7	1.63	0.81	0.30	0.10	21.98	-0.86	4.32	2.97	15	R	E
8	-0.44	0.88	-0.27	-0.02	8.94	6.76	-6.17	-0.33	1	A	A
9	0.05	0.60	0.41	-0.32	3.82	-10.96	2.17	-2.18	17	T	T
10	-0.28	0.42	0.22	-0.28	1.89	-7.54	0.27	1.76	16	S	S
11	5.26	0.46	-0.87	-0.59	-8.32	17.42	18.64	-3.22	2	C	C
12	-0.87	-0.28	-0.36	-0.95	-32.57	-6.90	1.88	0.25	5	F	F
13	-0.42	0.49	-0.13	-0.09	5.59	1.92	-3.56	4.42	6	G	G
14	-0.58	0.80	-0.26	-0.01	8.71	6.39	-6.48	1.15	1	A	A
15	-0.23	0.18	-0.37	-0.61	-16.84	-0.40	0.55	-0.35	10	L	L
16	1.03	0.42	0.24	-0.17	8.65	-4.89	4.74	3.98	12	N	D
17	-0.40	0.52	-0.39	-0.37	-6.57	3.74	-3.02	-1.16	8	I	I
18	-0.88	-0.19	-0.41	-0.96	-32.71	-5.89	1.39	-1.17	5	F	F
19	3.27	0.40	-0.87	-0.52	-10.00	15.68	10.52	-1.19	2	C	C
20	0.14	0.50	-0.81	-0.66	-20.22	8.97	-0.87	-6.15	7	H	H
21	1.58	0.46	0.22	0.02	16.43	-1.36	5.42	7.07	4	E	R
22	-0.17	0.60	0.30	-0.33	2.05	-9.10	0.79	-2.16	16	S	T
23	-0.37	0.90	-0.09	0.08	14.48	4.62	-5.77	1.24	14	Q	Q
24	-0.42	-0.04	-0.20	-0.56	-14.90	-3.95	1.02	3.95	11	M	M
25	-0.50	0.84	-0.25	0.04	10.81	6.97	-6.58	1.51	1	A	V
26	-0.41	0.89	-0.07	0.09	14.70	4.20	-5.81	1.43	14	Q	Q
27	0.56	0.78	0.46	-0.14	12.83	-8.53	2.58	-1.35	3	D	R
28	-0.21	0.50	-0.39	-0.41	-7.81	3.51	-1.95	-1.56	8	I	I
29	0.63	0.50	0.25	-0.22	6.56	-5.90	3.29	1.77	12	N	D
30	1.23	0.49	0.20	-0.09	11.77	-2.75	4.60	4.40	3	D	E
31	-0.44	-0.49	-0.41	-0.83	-28.92	-4.45	3.24	6.11	20	Y	Y
32	-0.45	0.59	-0.38	-0.11	3.00	6.92	-5.14	2.72	18	V	V
33	-0.37	0.59	-0.39	-0.09	3.60	7.54	-5.01	3.11	18	V	V
34	-0.60	-0.14	-0.25	-0.58	-16.85	-3.72	0.53	5.23	11	M	M
35	4.23	0.40	-0.87	-0.56	-9.73	16.41	14.61	-1.77	2	C	C
36	-0.39	-0.51	-0.44	-0.84	-29.80	-3.94	3.43	6.34	20	Y	Y
37	-0.23	-0.48	-0.48	-0.86	-30.10	-3.14	3.87	5.61	20	Y	Y
38	-0.87	-0.76	-0.95	-0.98	-41.58	3.24	0.75	7.94	19	W	W
39	-0.18	0.75	0.06	-0.04	10.87	-0.17	-2.89	1.16	6	G	G
40	1.42	0.46	0.23	-0.12	11.11	-3.47	5.79	4.36	3	D	K
41	-0.22	-0.51	-0.47	-0.85	-29.83	-3.37	4.03	6.14	20	Y	Y
42	-0.71	-0.30	-0.45	-0.96	-33.30	-5.12	2.19	0.67	5	F	F
43	1.14	0.53	0.27	-0.15	10.25	-4.78	4.87	2.58	3	D	D
44	-0.38	0.51	-0.35	-0.60	-14.45	0.11	-1.16	-5.51	10	L	L
45	0.38	0.74	0.36	-0.19	9.51	-7.59	1.90	-1.76	12	N	N
46	-0.49	0.44	-0.39	-0.03	4.86	7.79	-5.42	6.60	13	P	P
47	-0.38	0.43	-0.41	-0.02	5.14	8.39	-5.10	7.03	13	P	P

48	2.27	0.59	0.19	0.04	18.98	0.88	7.38	5.55	9	K	K
49	-0.23	0.58	-0.39	-0.39	-6.95	3.90	-2.39	-2.64	8	I	I
50	-0.42	0.73	-0.36	0.01	8.23	8.49	-6.20	2.67	18	V	A
51	-0.13	0.56	0.27	-0.30	2.72	-8.22	0.78	-0.92	16	S	S
52	-0.31	0.43	-0.36	-0.35	-6.04	3.20	-2.32	0.64	8	I	I
53	2.11	0.53	0.25	0.04	18.83	-0.87	7.31	6.34	15	R	R
54	1.64	0.81	0.30	0.10	21.97	-0.79	4.35	2.97	15	R	E
55	-0.93	-0.77	-0.95	-0.98	-41.76	3.13	0.54	8.12	19	W	W
56	0.49	0.71	0.26	-0.24	7.00	-6.06	2.21	-2.06	12	N	N
57	-0.45	-0.05	-0.13	-0.57	-14.73	-5.69	1.38	3.82	11	M	M
58	1.66	0.47	0.29	-0.02	16.08	-2.95	6.29	6.28	4	E	R
59	4.64	0.38	-0.87	-0.63	-11.38	15.81	16.77	-2.80	2	C	C
60	-0.29	0.51	-0.37	-0.66	-16.62	-0.28	-0.45	-6.67	10	L	L
61	-0.36	0.56	-0.08	-0.12	5.43	0.92	-3.16	2.77	6	G	G
62	-0.46	1.33	-0.43	-0.07	8.00	10.55	-8.19	-8.37	1	A	P
63	-0.90	-0.77	-0.95	-0.98	-41.72	3.15	0.69	8.12	19	W	W
64	-0.37	0.46	-0.37	-0.03	5.50	7.70	-4.95	6.40	13	P	A
65	0.44	0.67	0.34	-0.21	8.42	-7.43	2.34	-0.83	12	N	N
66	-0.40	0.85	0.02	0.08	15.06	2.19	-5.12	1.87	14	Q	Q
67	-0.75	-0.38	-0.37	-0.95	-32.94	-7.00	2.72	1.92	5	F	F
68	1.33	0.53	0.22	-0.13	11.22	-3.26	5.19	3.15	3	D	E
69	0.64	0.79	0.36	-0.12	12.89	-6.09	2.20	-1.02	3	D	D
70	-0.42	0.75	0.10	-0.05	10.62	-1.31	-3.60	1.05	6	G	G
71	2.04	0.88	0.25	0.12	23.53	1.11	5.29	2.32	9	K	K
72	-0.56	0.74	0.29	-0.25	4.77	-7.96	-1.81	-2.91	16	S	S
73	-0.87	-0.78	-0.95	-0.97	-41.51	3.35	0.77	8.37	19	W	W
74	-0.65	0.68	-0.33	0.08	10.38	8.37	-7.28	4.82	13	P	P
75	-0.62	0.75	0.01	-0.06	9.00	-0.09	-4.72	0.81	6	G	Q
76	0.48	0.71	0.40	-0.22	8.61	-8.65	2.78	-1.83	12	N	N
77	-0.50	0.73	-0.30	-0.01	7.88	7.02	-6.08	2.22	18	V	V
78	-0.46	-0.18	-0.24	-0.61	-17.80	-4.19	1.43	5.36	11	M	M
79	-0.02	0.44	-0.83	-0.70	-22.26	8.71	-1.23	-5.88	7	H	H
80	-0.30	0.48	0.14	-0.37	-1.86	-6.95	0.19	-1.10	16	S	T

Table 20. Training matrix of fluorescence response pattern from an array of **GFP-K72** (pH 7, buffered) with Fe^{2+}, Cu^{2+} and Co^{2+} against 20 amino acids. LDA was carried out as described above resulting in the three factors of the canonical scores and group generation.

Analyte	Fluorescence response pattern			Results LDA			
Amino acids	Fe^{2+} (pH7)	Cu^{2+} (pH7)	Co^{2+} (pH7)	Factor 1	Factor 2	Factor 3	Group
A	0.24	0.91	-0.09	-21.17	2.53	-0.70	1
A	0.23	0.87	-0.07	-20.98	1.98	-0.62	1
A	0.23	0.87	-0.04	-20.56	1.96	-0.74	1
A	0.10	0.93	-0.04	-20.68	2.62	-2.05	1
A	0.19	0.93	-0.07	-20.93	2.84	-1.27	1
A	0.13	0.91	-0.05	-20.80	2.43	-1.77	1
C	0.26	1.01	0.11	-18.67	3.86	-0.96	2
C	0.21	1.03	0.13	-18.35	4.04	-1.47	2
C	0.18	1.00	0.18	-17.86	3.52	-1.72	2
C	0.23	1.03	0.10	-18.71	4.21	-1.27	2
C	0.20	1.03	0.13	-18.46	4.13	-1.59	2
C	0.25	1.02	0.19	-17.64	3.94	-1.13	2
D	0.80	1.06	4.12	32.76	0.59	1.56	3
D	0.63	1.03	4.32	35.11	-0.43	0.01	3

D	0.64	1.00	4.38	35.91	-0.97	0.11	3
D	0.61	1.05	4.25	34.22	-0.08	-0.25	3
D	0.36	0.98	4.38	35.63	-1.62	-2.45	3
D	0.39	1.06	4.41	36.04	-0.40	-2.45	3
E	0.52	1.13	4.05	31.56	1.29	-1.22	4
E	0.41	1.10	4.05	31.48	0.73	-2.13	4
E	0.65	1.16	4.17	33.26	1.72	-0.23	4
E	0.53	1.11	4.05	31.64	0.98	-1.04	4
E	0.41	1.13	3.99	30.68	1.24	-2.21	4
E	0.39	1.13	4.20	33.30	0.86	-2.53	4
F	0.13	0.22	-0.09	-21.24	-7.99	0.60	5
F	0.17	0.07	-0.09	-21.23	-10.20	1.48	5
F	0.14	0.20	-0.14	-21.88	-8.19	0.76	5
F	0.12	-0.16	-0.13	-21.80	-13.66	1.85	5
F	0.15	-0.06	-0.13	-21.73	-12.03	1.78	5
F	0.11	-0.20	-0.14	-21.95	-14.22	1.90	5
G	0.18	0.95	0.23	-17.13	2.74	-1.58	6
G	0.13	0.82	0.23	-17.25	0.66	-1.57	6
G	0.13	0.92	0.23	-17.25	2.16	-1.93	6
G	0.14	0.92	0.13	-18.55	2.37	-1.82	6
G	0.15	0.91	0.18	-17.90	2.08	-1.67	6
G	0.14	0.91	0.18	-17.91	2.06	-1.78	6
H	0.88	1.13	1.14	-4.85	5.34	3.78	7
H	0.76	1.14	1.19	-4.44	5.31	2.57	7
H	0.71	1.07	1.12	-5.34	4.25	2.44	7
H	0.76	1.10	1.08	-5.72	4.71	2.81	7
H	0.77	1.13	1.09	-5.69	5.31	2.83	7
H	0.68	1.06	1.15	-5.02	3.94	2.13	7
I	0.55	0.98	-0.08	-20.69	4.06	1.95	8
I	0.46	0.97	-0.08	-20.80	3.79	1.16	8
I	0.45	1.02	-0.12	-21.35	4.58	0.85	8
I	0.36	0.98	-0.06	-20.72	3.79	0.13	8
I	0.43	1.00	-0.10	-21.07	4.29	0.76	8
I	0.39	0.99	-0.13	-21.56	4.11	0.46	8
K	1.32	1.18	3.84	29.83	3.44	6.14	9
K	1.00	1.07	3.80	28.93	1.43	3.58	9
K	0.98	1.13	3.78	28.75	2.24	3.19	9
K	1.01	1.12	3.86	29.70	2.06	3.45	9
K	0.85	1.16	3.71	27.61	2.63	1.89	9
K	0.95	1.09	3.80	28.93	1.64	3.04	9
L	0.49	0.29	-0.10	-21.02	-6.34	3.73	10
L	0.51	0.68	-0.09	-20.85	-0.53	2.64	10
L	0.40	0.62	-0.14	-21.55	-1.49	1.80	10
L	0.46	0.67	-0.10	-21.10	-0.66	2.12	10
L	0.36	0.29	-0.07	-20.81	-6.59	2.45	10
L	0.35	0.35	-0.13	-21.55	-5.70	2.23	10
M	0.48	0.50	0.13	-18.05	-3.44	2.81	11
M	0.42	0.47	0.14	-18.07	-4.09	2.32	11
M	0.39	0.49	0.03	-19.45	-3.62	2.05	11
M	0.33	0.50	0.04	-19.34	-3.56	1.44	11
M	0.33	0.41	0.01	-19.79	-4.93	1.78	11
M	0.32	0.52	0.05	-19.31	-3.32	1.29	11

N	1.46	1.15	4.06	32.73	2.95	7.42	12
N	1.34	1.21	4.12	33.44	3.60	6.02	12
N	1.22	1.14	4.12	33.21	2.41	5.22	12
N	1.05	1.22	4.14	33.31	3.23	3.30	12
N	0.81	1.22	4.18	33.61	2.89	1.10	12
N	0.80	1.17	4.16	33.26	2.20	1.18	12
P	0.29	0.82	-0.16	-21.95	1.39	0.13	13
P	0.17	0.82	-0.16	-22.08	1.19	-1.04	13
P	0.26	0.79	-0.19	-22.39	0.94	-0.03	13
P	0.13	0.85	-0.18	-22.45	1.69	-1.43	18
P	0.24	0.82	-0.15	-21.94	1.24	-0.36	13
P	0.21	0.80	-0.15	-21.94	0.92	-0.55	13
Q	0.30	0.88	-0.02	-20.26	2.08	-0.07	14
Q	0.22	0.84	-0.03	-20.45	1.46	-0.70	14
Q	0.27	0.88	-0.05	-20.64	2.20	-0.34	14
Q	0.24	0.86	-0.06	-20.72	1.80	-0.51	14
Q	0.41	0.87	-0.05	-20.43	2.20	0.98	14
Q	0.39	0.86	-0.08	-20.92	2.10	0.85	14
R	0.58	1.02	3.91	29.96	-0.13	-0.25	15
R	0.58	1.03	3.78	28.30	0.12	-0.13	15
R	0.41	1.04	3.86	29.11	-0.01	-1.84	15
R	0.33	1.03	3.83	28.63	-0.20	-2.53	15
R	0.24	1.04	3.88	29.11	-0.24	-3.47	15
R	0.20	1.03	3.78	27.88	-0.46	-3.73	15
S	0.28	0.90	1.66	1.07	0.38	-1.31	16
S	0.20	0.90	1.34	-3.08	0.59	-1.85	16
S	0.23	0.86	1.31	-3.40	0.11	-1.44	16
S	0.10	0.85	1.06	-6.69	0.02	-2.40	16
S	0.11	0.84	1.23	-4.57	-0.23	-2.46	16
S	0.12	0.88	1.01	-7.40	0.71	-2.32	16
T	0.17	0.88	3.21	20.56	-2.01	-3.19	17
T	0.15	0.88	3.46	23.70	-2.25	-3.48	17
T	0.14	0.83	3.34	22.19	-2.97	-3.32	17
T	0.07	0.82	3.47	23.77	-3.29	-4.01	17
T	0.07	0.86	3.33	21.95	-2.57	-4.03	17
T	0.11	0.85	3.19	20.29	-2.56	-3.59	17
V	0.12	0.86	-0.17	-22.27	1.73	-1.56	18
V	0.15	0.91	-0.17	-22.27	2.49	-1.51	18
V	0.18	0.86	-0.17	-22.21	1.88	-1.03	18
V	0.16	0.86	-0.17	-22.25	1.76	-1.25	18
V	0.06	0.87	-0.18	-22.49	1.77	-2.19	18
V	0.12	0.85	-0.18	-22.46	1.67	-1.60	18
W	0.34	0.72	2.55	12.42	-3.37	-0.61	19
W	0.33	0.75	2.56	12.53	-2.93	-0.80	19
W	0.23	0.73	2.65	13.57	-3.46	-1.80	19
W	0.20	0.74	2.64	13.38	-3.31	-2.03	19
W	0.21	0.77	2.57	12.57	-2.78	-2.03	19
W	0.20	0.82	2.88	16.42	-2.49	-2.45	19
Y	0.61	0.69	3.16	20.46	-4.20	1.65	20
Y	0.64	0.67	3.04	18.98	-4.32	2.00	20
Y	0.50	0.66	3.19	20.71	-4.85	0.72	20
Y	0.47	0.73	3.18	20.60	-3.76	0.19	20

Y	0.45	0.77	3.21	20.94	-3.27	-0.21	20
Y	0.33	0.70	3.15	20.03	-4.43	-1.03	20

Table 21. LDA jackknifed classification matrix table obtained from an array of **GFP-K72** (pH 7, buffered) with Fe^{2+} Cu^{2+} and Co^{2+} against 20 amino acids. The jackknifed classification matrix with cross-validation reveals a 92% accuracy.

	A	C	D	E	F	G	H	I	K	L	M	N	P	Q	R	S	T	V	W	Y	%correct
A	4	0	0	0	0	0	0	0	0	0	0	0	0	2	0	0	0	0	0	0	67
C	0	6	0	0	0	0	0	0	0	0	0	0	0	0	0	0	0	0	0	0	100
D	0	0	5	1	0	0	0	0	0	0	0	0	0	0	0	0	0	0	0	0	83
E	0	0	0	6	0	0	0	0	0	0	0	0	0	0	0	0	0	0	0	0	100
F	0	0	0	0	6	0	0	0	0	0	0	0	0	0	0	0	0	0	0	0	100
G	0	0	0	0	0	6	0	0	0	0	0	0	0	0	0	0	0	0	0	0	100
H	0	0	0	0	0	0	6	0	0	0	0	0	0	0	0	0	0	0	0	0	100
I	0	0	0	0	0	0	0	6	0	0	0	0	0	0	0	0	0	0	0	0	100
K	0	0	0	0	0	0	0	0	6	0	0	0	0	0	0	0	0	0	0	0	100
L	0	0	0	0	0	0	0	0	0	2	2	0	1	1	0	0	0	0	0	0	33
M	0	0	0	0	0	0	0	0	0	0	6	0	0	0	0	0	0	0	0	0	100
N	0	0	0	2	0	0	0	0	0	0	0	4	0	0	0	0	0	0	0	0	67
P	0	0	0	0	0	0	0	0	0	0	0	0	5	0	0	0	0	1	0	0	83
Q	0	0	0	0	0	0	0	0	0	0	0	0	0	6	0	0	0	0	0	0	100
R	0	0	0	0	0	0	0	0	0	0	0	0	0	0	6	0	0	0	0	0	100
S	0	0	0	0	0	0	0	0	0	0	0	0	0	0	0	6	0	0	0	0	100
T	0	0	0	0	0	0	0	0	0	0	0	0	0	0	0	0	6	0	0	0	100
V	0	0	0	0	0	0	0	0	0	0	0	0	0	0	0	0	0	6	0	0	100
W	0	0	0	0	0	0	0	0	0	0	0	0	0	0	0	0	0	0	6	0	100
Y	0	0	0	0	0	0	0	0	0	0	0	0	0	0	0	0	0	0	0	6	100
Total	4	6	5	9	6	6	6	6	6	2	8	4	6	9	6	6	6	7	6	6	**92**

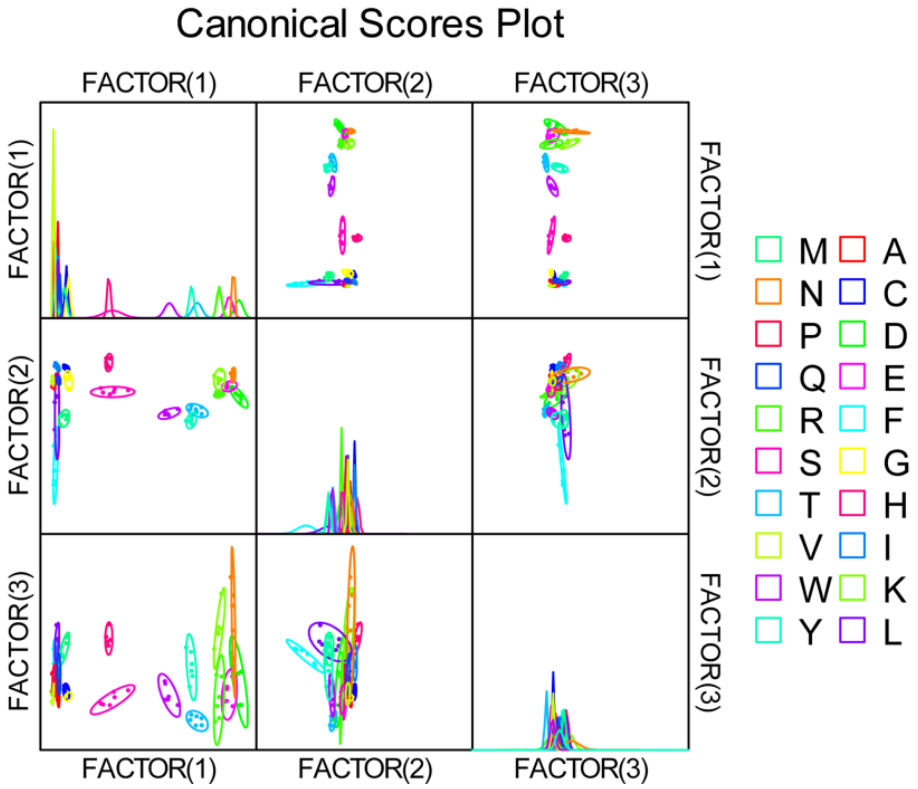

Figure 99. Correlations of canonical fluorescence response patterns from an array of **GFP-K72** (pH 7, buffered) with Fe^{2+}, Cu^{2+} and Co^{2+} against 20 amino acids. The 95% confidence ellipses for the individual acids are shown.

Table 22. Training matrix of fluorescence response pattern from combined tongue consisted of the optimized PPE tongue (Fe^{2+}-pH 10, Cu^{2+}-pH 10, Co^{2+}-pH 7 and Co^{2+}-pH 13) and GFP tongue (Fe^{2+}-pH 7, Cu^{2+}-pH 7 and Co^{2+}-pH 7) against 20 amino acids. LDA was carried out as described above resulting in the seven factors of the canonical scores and group generation.

Analyte	Fluorescence response pattern							Results LDA (the first three scores)			
	PPE tongue				GFP tongue						
Amino acids	Fe^{2+} (pH10)	Cu^{2+} (pH10)	Co^{2+} (pH7)	Co^{2+} (pH13)	Fe^{2+} (pH7)	Cu^{2+} (pH7)	Co^{2+} (pH7)	Factor 1	Factor 2	Factor 3	Group
A	-0.40	1.05	-0.36	0.15	0.24	0.91	-0.09	6.03	9.43	-26.01	1
A	-0.50	1.06	-0.36	0.17	0.23	0.87	-0.07	6.80	7.88	-26.04	1
A	-0.51	1.06	-0.36	0.15	0.23	0.87	-0.04	6.42	7.64	-25.88	1
A	-0.39	1.07	-0.37	0.12	0.10	0.93	-0.04	6.56	9.51	-25.56	1
A	-0.35	1.04	-0.35	0.09	0.19	0.93	-0.07	5.43	9.41	-25.66	1
A	-0.33	1.10	-0.35	0.10	0.13	0.91	-0.05	5.63	9.96	-26.25	1
C	8.87	0.82	-0.83	-0.55	0.26	1.01	0.11	45.72	84.56	21.86	2
C	8.93	0.78	-0.84	-0.55	0.21	1.03	0.13	46.38	84.54	23.23	2
C	8.62	0.79	-0.83	-0.54	0.18	1.00	0.18	45.09	81.90	22.20	2
C	8.78	0.81	-0.84	-0.47	0.23	1.03	0.10	46.44	83.74	21.92	2
C	8.31	0.83	-0.84	-0.38	0.20	1.03	0.13	46.34	79.35	20.46	2
C	8.42	0.83	-0.83	-0.40	0.25	1.02	0.19	45.65	80.17	21.27	2
D	0.73	0.93	0.05	-0.04	0.80	1.06	4.12	-41.85	-0.79	14.99	3
D	0.77	0.91	0.07	-0.05	0.63	1.03	4.32	-44.12	-0.90	16.84	3
D	0.79	0.90	0.01	-0.05	0.64	1.00	4.38	-40.42	-0.54	18.92	3
D	0.93	0.94	0.06	-0.07	0.61	1.05	4.25	-42.49	0.38	16.76	3
D	0.78	0.89	0.05	-0.06	0.36	0.98	4.38	-42.59	-1.17	18.34	3
D	0.78	0.94	0.05	-0.08	0.39	1.06	4.41	-43.39	-0.18	17.82	3
E	0.66	0.93	-0.16	0.02	0.52	1.13	4.05	-27.99	2.57	18.03	4
E	0.71	0.94	-0.15	-0.03	0.41	1.10	4.05	-29.26	3.35	17.59	4
E	0.73	0.95	-0.15	0.03	0.65	1.16	4.17	-29.75	3.04	19.04	4
E	0.62	0.94	-0.15	0.03	0.53	1.11	4.05	-29.17	2.21	17.49	4
E	0.54	0.94	-0.14	0.01	0.41	1.13	3.99	-29.08	1.55	16.40	4
E	0.75	0.96	-0.16	-0.03	0.39	1.13	4.20	-28.92	3.48	19.40	4
F	-0.87	0.50	-0.50	-0.94	0.13	0.22	-0.09	32.96	-12.84	-11.40	5
F	-0.89	0.49	-0.51	-0.95	0.17	0.07	-0.09	33.48	-13.04	-11.27	5
F	-0.89	0.36	-0.52	-0.95	0.14	0.20	-0.14	36.05	-14.34	-9.16	5
F	-0.88	0.27	-0.52	-0.95	0.12	-0.16	-0.13	35.89	-15.16	-8.20	5
F	-0.87	0.52	-0.50	-0.95	0.15	-0.06	-0.13	32.93	-12.55	-12.34	5
F	-0.89	0.48	-0.51	-0.94	0.11	-0.20	-0.14	33.58	-13.02	-11.96	5
G	-0.61	0.76	-0.22	0.03	0.18	0.95	0.23	1.20	-1.53	-20.17	6
G	-0.68	0.80	-0.23	0.03	0.13	0.82	0.23	2.01	-2.51	-20.92	6
G	-0.64	0.78	-0.21	0.01	0.13	0.92	0.23	1.23	-2.38	-20.59	6
G	-0.63	0.80	-0.22	-0.05	0.14	0.92	0.13	2.23	-2.23	-21.73	6
G	-0.63	0.79	-0.23	-0.09	0.15	0.91	0.18	3.00	-2.38	-20.74	6
G	-0.55	0.80	-0.21	-0.09	0.14	0.91	0.18	0.49	-0.96	-21.51	6
H	-0.21	0.71	-0.85	-0.75	0.88	1.13	1.14	42.06	1.50	6.21	7
H	-0.25	0.70	-0.84	-0.75	0.76	1.14	1.19	41.32	1.09	6.41	7
H	-0.18	0.69	-0.84	-0.71	0.71	1.07	1.12	42.03	1.61	6.04	7
H	-0.19	0.70	-0.85	-0.72	0.76	1.10	1.08	42.38	1.67	5.71	7
H	-0.18	0.70	-0.85	-0.67	0.77	1.13	1.09	42.60	1.71	5.84	7
H	-0.09	0.72	-0.85	-0.68	0.68	1.06	1.15	42.26	2.58	6.30	7
I	-0.64	0.75	-0.36	0.13	0.55	0.98	-0.08	19.62	-7.84	-17.52	8
I	-0.67	0.77	-0.36	0.17	0.46	0.97	-0.08	19.68	-7.63	-17.94	8
I	-0.64	0.76	-0.38	0.06	0.45	1.02	-0.12	21.70	-7.41	-17.51	8

I	-0.66	0.77	-0.37	0.08	0.36	0.98	-0.06	19.75	-6.98	-17.74	8
I	-0.66	0.75	-0.38	0.11	0.43	1.00	-0.10	21.94	-8.04	-17.08	8
I	-0.63	0.74	-0.38	0.15	0.39	0.99	-0.13	21.89	-7.66	-17.38	8
K	1.74	0.86	0.10	0.47	1.32	1.18	3.84	-57.73	21.38	10.59	9
K	1.50	0.87	0.08	0.41	1.00	1.07	3.80	-57.42	20.57	9.04	9
K	1.33	0.86	0.10	0.44	0.98	1.13	3.78	-58.07	19.11	8.22	9
K	1.02	0.85	0.10	0.45	1.01	1.12	3.86	-58.55	15.73	8.20	9
K	1.12	0.86	0.10	0.40	0.85	1.16	3.71	-56.80	16.64	7.06	9
K	1.00	0.84	0.09	0.41	0.95	1.09	3.80	-57.72	16.09	7.72	9
L	-0.63	0.74	-0.39	-0.36	0.49	0.29	-0.10	21.67	-7.49	-17.52	10
L	-0.64	0.71	-0.38	-0.33	0.51	0.68	-0.09	21.52	-8.36	-16.78	10
L	-0.62	0.72	-0.40	-0.41	0.40	0.62	-0.14	22.99	-7.69	-16.96	10
L	-0.61	0.79	-0.42	-0.38	0.46	0.67	-0.10	23.38	-6.29	-17.46	10
L	-0.62	0.73	-0.43	-0.29	0.36	0.29	-0.07	23.78	-7.00	-16.46	10
L	-0.58	0.69	-0.39	-0.30	0.35	0.35	-0.13	22.40	-7.92	-16.81	10
M	-0.74	0.48	-0.28	-0.26	0.48	0.50	0.13	16.49	-14.31	-12.94	11
M	-0.70	0.50	-0.27	-0.30	0.42	0.47	0.14	15.57	-13.87	-13.33	11
M	-0.77	0.44	-0.27	-0.30	0.39	0.49	0.03	16.47	-14.61	-13.68	11
M	-0.70	0.41	-0.26	-0.19	0.33	0.50	0.04	16.19	-14.39	-12.98	11
M	-0.75	0.41	-0.26	-0.32	0.33	0.41	0.01	16.25	-14.82	-13.66	11
M	-0.72	0.49	-0.27	-0.15	0.32	0.52	0.05	15.78	-13.54	-14.32	11
N	0.17	0.84	0.12	-0.14	1.46	1.15	4.06	-42.91	-10.59	13.96	12
N	0.14	0.80	0.10	-0.13	1.34	1.21	4.12	-41.19	-11.12	15.75	12
N	0.22	0.82	0.10	-0.14	1.22	1.14	4.12	-42.02	-9.70	15.11	12
N	0.14	0.84	0.10	-0.08	1.05	1.22	4.14	-41.34	-10.49	15.08	12
N	0.24	0.83	0.09	-0.05	0.81	1.22	4.18	-42.30	-8.29	15.60	12
N	0.13	0.81	0.08	0.00	0.80	1.17	4.16	-41.01	-9.81	15.63	12
P	-0.65	0.43	-0.42	0.08	0.29	0.82	-0.16	16.46	0.29	-15.72	13
P	-0.68	0.43	-0.42	0.07	0.17	0.82	-0.16	16.47	0.19	-15.81	13
P	-0.67	0.42	-0.43	0.05	0.26	0.79	-0.19	16.23	0.67	-16.14	13
P	-0.64	0.43	-0.43	0.04	0.13	0.85	-0.18	16.08	1.37	-16.28	13
P	-0.59	0.42	-0.43	0.07	0.24	0.82	-0.15	16.13	1.26	-15.57	13
P	-0.67	0.42	-0.42	0.07	0.21	0.80	-0.15	15.74	0.62	-15.86	13
Q	-0.49	0.81	-0.27	0.19	0.30	0.88	-0.02	-1.16	7.12	-24.52	14
Q	-0.54	0.75	-0.28	0.19	0.22	0.84	-0.03	1.24	5.32	-23.24	14
Q	-0.52	0.78	-0.30	0.17	0.27	0.88	-0.05	2.74	6.00	-23.35	14
Q	-0.54	0.78	-0.30	0.16	0.24	0.86	-0.06	2.53	6.07	-23.58	14
Q	-0.53	0.75	-0.29	0.21	0.41	0.87	-0.05	1.52	6.06	-23.23	14
Q	-0.47	0.80	-0.31	0.19	0.39	0.86	-0.08	1.47	7.94	-24.17	14
R	1.22	0.77	0.10	0.23	0.58	1.02	3.91	-56.31	15.28	11.02	15
R	1.25	0.76	0.10	0.28	0.58	1.03	3.78	-54.91	15.29	10.18	15
R	1.15	0.78	0.07	0.26	0.41	1.04	3.86	-54.75	16.41	10.44	15
R	1.16	0.75	0.10	0.31	0.33	1.03	3.83	-57.47	16.70	9.65	15
R	0.88	0.76	0.11	0.27	0.24	1.04	3.88	-57.69	14.03	9.07	15
R	1.20	0.75	0.09	0.28	0.20	1.03	3.78	-55.80	16.81	9.56	15
S	-0.68	0.71	0.17	-0.30	0.28	0.90	1.66	-31.77	-11.70	-13.01	16
S	-0.67	0.73	0.10	-0.33	0.20	0.90	1.34	-25.45	-10.08	-15.11	16
S	-0.68	0.73	0.14	-0.31	0.23	0.86	1.31	-27.35	-10.70	-15.97	16
S	-0.68	0.70	0.15	-0.32	0.10	0.85	1.06	-26.89	-10.52	-18.50	16
S	-0.68	0.68	0.17	-0.30	0.11	0.84	1.23	-29.37	-10.59	-17.00	16
S	-0.66	0.69	0.15	-0.31	0.12	0.88	1.01	-26.75	-9.43	-18.93	16
T	-0.53	0.79	0.23	-0.31	0.17	0.88	3.21	-47.18	-12.63	-0.12	17

T	-0.53	0.78	0.23	-0.30	0.15	0.88	3.46	-47.71	-13.57	2.92	17
T	-0.56	0.78	0.23	-0.30	0.14	0.83	3.34	-47.32	-13.99	1.40	17
T	-0.55	0.77	0.22	-0.30	0.07	0.82	3.47	-46.31	-14.61	3.41	17
T	-0.59	0.79	0.24	-0.30	0.07	0.86	3.33	-48.05	-13.86	0.76	17
T	-0.59	0.84	0.22	-0.31	0.11	0.85	3.19	-45.52	-12.97	-0.71	17
V	-0.59	0.73	-0.38	0.04	0.12	0.86	-0.17	15.26	0.09	-20.11	18
V	-0.64	0.73	-0.38	0.07	0.15	0.91	-0.17	14.94	0.02	-20.42	18
V	-0.63	0.73	-0.40	0.07	0.18	0.86	-0.17	15.85	0.16	-20.04	18
V	-0.65	0.73	-0.40	-0.03	0.16	0.86	-0.17	16.72	-0.43	-19.81	18
V	-0.68	0.76	-0.40	0.04	0.06	0.87	-0.18	16.29	0.04	-20.67	18
V	-0.63	0.74	-0.40	0.01	0.12	0.85	-0.18	16.28	0.27	-20.29	18
W	-0.94	-0.64	-0.94	-0.97	0.34	0.72	2.55	57.54	-28.44	43.92	19
W	-0.94	-0.65	-0.94	-0.96	0.33	0.75	2.56	57.69	-28.62	44.33	19
W	-0.94	-0.64	-0.95	-0.97	0.23	0.73	2.65	57.16	-28.54	45.05	19
W	-0.93	-0.65	-0.95	-0.96	0.20	0.74	2.64	57.27	-28.42	45.01	19
W	-0.94	-0.64	-0.95	-0.96	0.21	0.77	2.57	57.67	-28.34	44.35	19
W	-0.94	-0.64	-0.94	-0.97	0.20	0.82	2.88	55.80	-29.11	47.34	19
Y	-0.51	-0.46	-0.50	-0.86	0.61	0.69	3.16	22.23	-29.05	39.10	20
Y	-0.51	-0.44	-0.50	-0.86	0.64	0.67	3.04	22.92	-28.65	37.71	20
Y	-0.55	-0.45	-0.49	-0.84	0.50	0.66	3.19	21.12	-29.35	38.83	20
Y	-0.54	-0.44	-0.49	-0.86	0.47	0.73	3.18	21.56	-29.11	38.75	20
Y	-0.54	-0.43	-0.49	-0.85	0.45	0.77	3.21	21.20	-29.04	38.97	20
Y	-0.48	-0.44	-0.50	-0.86	0.33	0.70	3.15	22.50	-28.24	38.82	20

Table 23. LDA jackknifed classification matrix table obtained from combined tongue consisted of the optimized PPE tongue (Fe^{2+}-pH 10, Cu^{2+}-pH 10, Co^{2+}-pH 7 and Co^{2+}-pH 13) and GFP tongue (Fe^{2+}-pH 7, Cu^{2+}-pH 7 and Co^{2+}-pH 7) against 20 amino acids. The jackknifed classification matrix with cross-validation reveals a 92% accuracy.

	A	C	D	E	F	G	H	I	K	L	M	N	P	Q	R	S	T	V	W	Y	%correct
A	6	0	0	0	0	0	0	0	0	0	0	0	0	0	0	0	0	0	0	0	100
C	0	6	0	0	0	0	0	0	0	0	0	0	0	0	0	0	0	0	0	0	100
D	0	0	6	0	0	0	0	0	0	0	0	0	0	0	0	0	0	0	0	0	100
E	0	0	0	6	0	0	0	0	0	0	0	0	0	0	0	0	0	0	0	0	100
F	0	0	0	0	6	0	0	0	0	0	0	0	0	0	0	0	0	0	0	0	100
G	0	0	0	0	0	6	0	0	0	0	0	0	0	0	0	0	0	0	0	0	100
H	0	0	0	0	0	0	6	0	0	0	0	0	0	0	0	0	0	0	0	0	100
I	0	0	0	0	0	0	0	6	0	0	0	0	0	0	0	0	0	0	0	0	100
K	0	0	0	0	0	0	0	0	6	0	0	0	0	0	0	0	0	0	0	0	100
L	0	0	0	0	0	0	0	0	0	6	0	0	0	0	0	0	0	0	0	0	100
M	0	0	0	0	0	0	0	0	0	0	6	0	0	0	0	0	0	0	0	0	100
N	0	0	0	0	0	0	0	0	0	0	0	6	0	0	0	0	0	0	0	0	100
P	0	0	0	0	0	0	0	0	0	0	0	0	6	0	0	0	0	0	0	0	100
Q	0	0	0	0	0	0	0	0	0	0	0	0	0	6	0	0	0	0	0	0	100
R	0	0	0	0	0	0	0	0	0	0	0	0	0	0	6	0	0	0	0	0	100
S	0	0	0	0	0	0	0	0	0	0	0	0	0	0	0	6	0	0	0	0	100
T	0	0	0	0	0	0	0	0	0	0	0	0	0	0	0	0	6	0	0	0	100
V	0	0	0	0	0	0	0	0	0	0	0	0	0	0	0	0	0	6	0	0	100
W	0	0	0	0	0	0	0	0	0	0	0	0	0	0	0	0	0	0	6	0	100
Y	0	0	0	0	0	0	0	0	0	0	0	0	0	0	0	0	0	0	0	6	100
Total	6	6	6	6	6	6	6	6	6	6	6	6	6	6	6	6	6	6	6	6	**100**

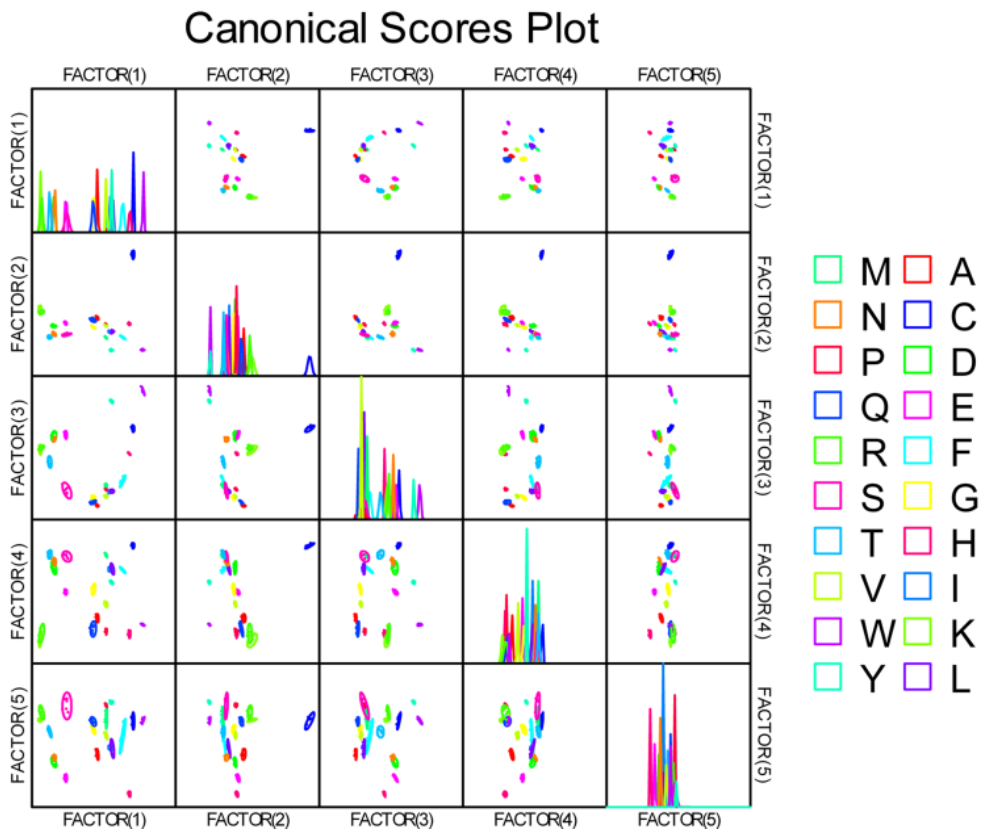

Figure 100. Correlations of canonical fluorescence response patterns from combined tongue consisted of the optimized PPE tongue (Fe^{2+}-pH 10, Cu^{2+}-pH 10, Co^{2+}-pH 7 and Co^{2+}-pH 13) and GFP tongue (Fe^{2+}-pH 7, Cu^{2+}-pH 7 and Co^{2+}-pH 7) against 20 amino acids. The 95% confidence ellipses for the individual acids are shown.

Table 24. Detection and identification of unknown amino acids samples using LDA from combined tongue consisted of the optimized PPE tongue (Fe^{2+}-pH 10, Cu^{2+}-pH 10, Co^{2+}-pH 7 and Co^{2+}-pH 13) and GFP tongue (Fe^{2+}-pH 7, Cu^{2+}-pH 7 and Co^{2+}-pH 7) against 20 amino acids. According to the verification, 69 among 80 unknown samples were correctly identified, representing an accuracy of 86.3%.

Analyte	Fluorescence response pattern							Results LDA (the first three scores)					
Unknown samples	PPE tongue				GFP tongue								
	Fe^{2+}-pH10	Cu^{2+}-pH10	Co^{2+}-pH7	Co^{2+}-pH13	Fe^{2+}-pH7	Cu^{2+}-pH7	Co^{2+}-pH7	Factor 1	Factor 2	Factor 3	Group	Identification	Verification
1	2.03	0.88	0.24	0.12	1.00	1.07	3.80	31.73	16.59	4.60	9	K	K
2	-0.13	0.59	0.34	-0.28	0.05	0.97	3.57	27.35	-1.88	-3.82	17	T	T
3	-0.43	0.37	0.35	-0.57	0.11	0.62	0.12	22.92	-9.50	-2.60	10	L	L
4	0.32	0.52	0.78	-0.69	0.31	0.99	0.63	16.00	16.53	8.34	7	H	H
5	-0.40	0.55	0.28	-0.26	0.10	0.89	2.27	10.63	1.52	-5.57	16	S	S
6	0.35	0.53	0.77	-0.71	0.31	1.06	0.67	15.45	17.34	8.40	7	H	H
7	1.63	0.81	0.30	0.10	0.86	1.16	3.71	30.53	15.51	3.09	9	K	E
8	-0.44	0.88	0.27	-0.02	0.13	0.92	0.05	21.82	15.07	1.28	1	A	A
9	0.05	0.60	0.41	-0.32	0.11	0.98	3.36	25.58	-2.09	-5.42	17	T	T
10	-0.28	0.42	0.22	-0.28	0.16	0.87	1.68	3.17	1.01	-5.93	16	S	S
11	5.26	0.46	0.87	-0.59	0.01	0.93	0.30	25.04	-0.09	21.64	2	C	C
12	-0.87	-0.28	0.36	-0.95	0.01	0.35	0.11	23.31	28.83	-6.97	5	F	F
13	-0.42	0.49	0.13	-0.09	0.05	0.96	0.18	18.34	10.72	-0.65	6	G	G
14	-0.58	0.80	0.26	-0.01	0.10	0.93	0.04	21.85	14.88	1.09	1	A	A
15	-0.23	0.18	0.37	-0.61	0.14	0.72	0.15	23.52	11.92	-1.60	10	L	L
16	1.03	0.42	0.24	-0.17	0.23	0.90	3.65	28.41	2.84	1.03	4	E	D
17	-0.40	0.52	0.39	-0.37	0.14	0.87	0.08	22.87	-1.03	0.76	8	I	I
18	-0.88	-0.19	0.41	-0.96	0.01	0.44	0.09	23.39	28.85	-5.87	5	F	F
19	3.27	0.40	0.87	-0.52	0.09	1.07	0.22	25.72	-2.13	17.99	2	C	C

20	0.14	0.50	0.81	-0.66	0.21	1.02	0.73	15.28	16.38	9.09	7	H	H
21	1.58	0.46	0.22	0.02	0.14	0.95	3.64	28.22	11.59	4.56	15	R	R
22	-0.17	0.60	0.30	-0.33	0.07	1.00	3.74	29.19	-4.46	-3.24	17	T	T
23	-0.37	0.90	0.09	0.08	0.39	0.87	0.08	20.67	19.85	-1.90	14	Q	Q
24	-0.42	-0.04	0.20	-0.56	0.08	0.29	0.02	20.36	11.02	-6.18	11	M	M
25	-0.50	0.84	0.25	0.04	0.24	0.91	0.09	22.20	16.92	0.89	1	A	V
26	-0.41	0.89	0.07	0.09	0.41	0.87	0.05	20.09	19.88	-2.27	14	Q	Q
27	0.56	0.78	0.46	-0.14	0.36	0.98	4.38	39.11	4.09	-2.68	3	D	R
28	-0.21	0.50	0.39	-0.41	0.11	0.93	0.13	23.47	-2.10	1.27	8	I	I
29	0.63	0.50	0.25	-0.22	0.04	0.84	3.85	30.60	0.34	0.05	3	D	D
30	1.23	0.49	0.20	-0.09	0.17	1.14	3.61	27.60	6.73	4.01	4	E	E
31	-0.44	-0.49	0.41	-0.83	0.03	0.77	3.01	14.52	32.56	3.52	20	Y	Y
32	-0.45	0.59	0.38	-0.11	0.05	0.92	0.12	23.69	9.60	2.74	18	V	V
33	-0.37	0.59	0.39	-0.09	0.03	0.94	0.12	23.89	10.51	3.62	18	V	V
34	-0.60	-0.14	0.25	-0.58	0.01	0.38	0.01	21.16	12.59	-5.16	11	M	M
35	4.23	0.40	0.87	-0.56	0.04	1.00	0.32	26.21	-1.51	19.74	2	C	C
36	-0.39	-0.51	0.44	-0.84	0.08	0.67	2.80	11.64	32.73	3.46	20	Y	Y
37	-0.23	-0.48	0.48	-0.86	0.06	0.62	2.73	10.76	32.85	3.85	20	Y	Y
38	-0.87	-0.76	0.95	-0.98	0.20	0.77	2.20	0.00	41.42	10.08	19	W	W
39	-0.18	0.75	0.06	-0.04	0.13	0.92	0.23	15.93	15.21	-3.44	6	G	G
40	1.42	0.46	0.23	-0.12	0.26	1.14	3.62	28.10	5.73	3.62	4	E	K
41	-0.22	-0.51	0.47	-0.85	0.07	0.66	2.82	12.00	32.81	4.13	20	Y	Y
42	-0.71	-0.30	0.45	-0.96	0.04	0.22	0.16	24.02	29.51	-8.01	5	F	F
43	1.14	0.53	0.27	-0.15	0.39	0.90	4.04	33.76	3.00	1.14	3	D	D
44	-0.38	0.51	0.35	-0.60	0.04	0.70	0.08	22.36	-9.63	-2.22	10	L	L
45	0.38	0.74	0.36	-0.19	0.80	1.17	4.16	35.87	0.69	-2.30	12	N	N
46	-0.49	0.44	0.39	-0.03	0.07	0.71	0.11	23.77	11.52	2.49	13	P	P
47	-0.38	0.43	0.41	-0.02	0.11	0.87	0.15	24.42	12.06	3.83	13	P	P
48	2.27	0.59	0.19	0.04	0.61	0.98	3.51	27.48	13.75	5.74	15	R	K
49	-0.23	0.58	0.39	-0.39	0.04	0.83	0.13	23.47	-1.12	0.97	8	I	I
50	-0.42	0.73	0.36	0.01	0.13	0.86	0.17	24.00	15.01	2.66	18	V	A
51	-0.13	0.56	0.27	-0.30	0.01	0.93	0.80	-7.34	4.43	-7.49	16	S	S
52	-0.31	0.43	0.36	-0.35	0.04	0.92	0.09	23.04	-0.22	1.09	8	I	I
53	2.11	0.53	0.25	0.04	0.27	0.93	3.82	31.33	13.21	5.30	15	R	R
54	1.64	0.81	0.30	0.10	0.85	1.16	3.71	30.50	15.53	3.19	9	K	E
55	-0.93	-0.77	0.95	-0.98	0.05	0.79	1.90	-3.46	41.32	8.93	19	W	W
56	0.49	0.71	0.26	-0.24	1.46	1.15	4.06	34.72	-2.80	-2.50	12	N	N
57	-0.45	-0.05	0.13	-0.57	0.06	0.35	0.00	20.21	10.73	-7.04	11	M	M
58	1.66	0.47	0.29	-0.02	0.21	0.97	3.84	31.43	10.25	3.65	15	R	R
59	4.64	0.38	0.87	-0.63	0.04	1.02	0.20	24.39	-3.45	20.55	2	C	C
60	-0.29	0.51	0.37	-0.66	0.03	0.75	0.17	23.45	11.63	-2.07	10	L	L
61	-0.36	0.56	0.08	-0.12	0.08	0.88	0.01	20.11	10.69	-2.36	6	G	G
62	-0.46	1.33	0.43	-0.07	0.06	0.80	0.19	24.21	14.82	2.57	1	A	P
63	-0.90	-0.77	0.95	-0.98	0.00	0.72	2.00	-2.21	41.50	8.92	19	W	W
64	-0.37	0.46	0.37	-0.03	0.08	0.81	0.23	25.22	12.87	3.20	13	P	A
65	0.44	0.67	0.34	-0.21	0.81	1.22	4.18	35.99	-0.40	-1.54	12	N	N
66	-0.40	0.85	0.02	0.08	0.25	0.86	0.06	19.73	20.28	-3.53	14	Q	Q
67	-0.75	-0.38	0.37	-0.95	0.17	0.10	0.15	23.87	28.86	-7.49	5	F	F
68	1.33	0.53	0.22	-0.13	0.01	0.94	3.40	25.18	6.82	2.69	4	E	E
69	0.64	0.79	0.36	-0.12	0.64	1.00	4.43	39.29	3.82	-1.10	3	D	D
70	-0.42	0.75	0.10	-0.05	0.13	0.82	0.23	15.74	14.71	-5.26	6	G	G
71	2.04	0.88	0.25	0.12	1.00	1.06	3.80	31.84	16.69	4.34	9	K	K

72	-0.56	0.74	0.29	-0.25	0.11	0.84	1.23	-1.90	4.99	-8.63	16	S	S
73	-0.87	-0.78	0.95	-0.97	0.04	0.77	1.83	-4.47	40.66	9.17	19	W	W
74	-0.65	0.68	0.33	0.08	0.13	0.85	0.18	24.25	17.28	2.10	13	P	P
75	-0.62	0.75	0.01	-0.06	0.15	0.91	0.18	17.14	13.44	-4.11	6	G	Q
76	0.48	0.71	0.40	-0.22	1.22	1.14	4.12	36.14	-1.22	-4.14	12	N	N
77	-0.50	0.73	0.30	-0.01	0.06	0.87	0.18	23.86	14.61	1.56	18	V	V
78	-0.46	-0.18	0.24	-0.61	0.04	0.24	0.04	21.44	13.71	-6.07	11	M	M
79	-0.02	0.44	0.83	-0.70	0.00	0.94	0.72	15.81	18.06	9.01	7	H	H
80	-0.30	0.48	0.14	-0.37	0.03	0.85	2.98	18.55	-5.87	-2.77	17	T	T

Table 25. Training matrix of fluorescence response pattern from array 4 PPE-CB[7]-AO tongue against 20 amino acids (25 mM). LDA was carried out and resulting in 10 factors of the canonical scores (the first three scores were shown here) and group generation.

Analytes	Fluorescence Response Pattern										Results LDA (the first three scores)			
Amino acids	**P5**-CB7-AO (460 nm)	**P5**-CB7-AO (510 nm)	**P15**-CB7-AO (460 nm)	**P15**-CB7-AO (510 nm)	**P6**-CB7-AO (460 nm)	**P6**-CB7-AO (510 nm)	**P7**-CB7-AO (460 nm)	**P7**-CB7-AO (510 nm)	**P8**-CB7-AO (460 nm)	**P8**-CB7-AO (510 nm)	Factor 1	Factor 2	Factor 3	Gr.
A	0.03	0.01	0.13	0.07	0.25	0.04	0.02	0.01	0.04	0.01	47.05	0.97	10.98	1
A	0.03	0.01	0.11	0.06	0.22	0.02	0.02	0.02	0.05	0.02	48.35	-0.26	10.64	1
A	0.03	0.01	0.11	0.06	0.19	0.02	0.01	0.02	0.05	0.02	47.51	0.09	10.23	1
A	0.03	0.01	0.08	0.03	0.19	0.00	0.01	0.01	0.05	0.02	47.22	-1.12	10.32	1
A	0.02	0.00	0.06	0.02	0.12	-0.02	0.01	0.01	0.05	0.02	46.06	-1.09	10.41	1
A	0.02	0.00	0.12	0.06	0.10	-0.04	0.01	0.01	0.04	0.02	46.16	0.15	11.01	1
C	0.06	-0.10	0.14	-0.06	0.04	-0.16	0.04	-0.04	0.15	-0.07	18.90	14.76	-2.37	2
C	0.06	-0.10	0.11	-0.06	0.01	-0.17	0.06	-0.03	0.16	-0.08	17.93	15.87	-1.63	2
C	0.06	-0.10	0.13	-0.06	-0.10	-0.20	0.06	-0.03	0.18	-0.07	17.82	16.38	-1.76	2
C	0.06	-0.10	0.13	-0.07	-0.08	-0.16	0.06	-0.03	0.18	-0.07	19.33	15.97	-2.41	2
C	0.07	-0.10	0.15	-0.06	-0.06	-0.20	0.05	-0.03	0.16	-0.06	19.29	15.24	-1.72	2
C	0.06	-0.10	0.15	-0.06	-0.05	-0.22	0.05	-0.04	0.15	-0.08	16.94	16.08	-1.75	2
D	0.01	-0.25	0.00	-0.23	-0.30	-0.51	-0.48	-0.33	-0.13	-0.30	14.13	11.64	22.52	3
D	-0.04	-0.26	-0.20	-0.35	-0.20	-0.48	-0.43	-0.29	-0.13	-0.30	13.41	14.17	19.06	3
D	-0.07	-0.22	-0.27	-0.31	-0.33	-0.52	-0.41	-0.28	-0.13	-0.29	10.25	14.86	17.60	3
D	0.01	-0.21	-0.15	-0.38	-0.26	-0.50	-0.43	-0.28	-0.19	-0.32	11.10	15.14	22.45	3
D	-0.06	-0.26	-0.27	-0.22	-0.16	-0.47	-0.47	-0.29	-0.15	-0.30	11.38	17.18	21.44	3
D	-0.07	-0.27	-0.22	-0.35	-0.33	-0.52	-0.49	-0.32	-0.16	-0.33	15.64	18.28	22.45	3
E	0.04	-0.18	-0.20	-0.32	-0.09	-0.42	-0.42	-0.29	-0.12	-0.28	8.09	12.17	19.99	4
E	0.05	-0.18	-0.22	-0.34	-0.03	-0.41	-0.40	-0.27	-0.11	-0.27	7.25	11.65	20.05	4
E	-0.05	-0.24	-0.10	-0.26	-0.21	-0.44	-0.40	-0.27	-0.14	-0.29	9.04	12.29	17.39	4
E	0.04	-0.18	-0.24	-0.34	-0.18	-0.46	-0.39	-0.26	-0.12	-0.28	8.63	11.01	20.45	4
E	0.06	-0.17	0.01	-0.20	-0.18	-0.46	-0.45	-0.30	-0.15	-0.29	6.08	11.63	22.37	4
E	-0.03	-0.22	-0.16	-0.31	-0.23	-0.49	-0.46	-0.31	-0.16	-0.29	10.66	15.60	18.12	4
F	-0.08	-0.48	-0.13	-0.50	-0.22	-0.74	-0.11	-0.40	-0.09	-0.52	84.27	41.97	-1.29	5
F	-0.06	-0.49	-0.13	-0.50	-0.24	-0.74	-0.08	-0.38	-0.07	-0.52	85.11	44.52	0.14	5
F	-0.07	-0.48	-0.14	-0.51	-0.27	-0.75	-0.11	-0.41	-0.08	-0.52	85.49	43.15	-0.83	5
F	-0.08	-0.49	-0.13	-0.50	-0.32	-0.76	-0.10	-0.39	-0.08	-0.53	84.72	42.55	0.57	5
F	-0.08	-0.49	-0.14	-0.50	-0.26	-0.74	-0.09	-0.39	-0.09	-0.53	84.52	42.67	-0.35	5
F	-0.07	-0.49	-0.10	-0.49	-0.43	-0.77	-0.11	-0.40	-0.08	-0.53	84.33	42.62	0.79	5
G	0.00	-0.02	0.05	0.03	0.13	-0.04	0.01	0.01	0.00	0.00	45.19	-2.50	11.13	6
G	-0.01	-0.02	0.06	0.03	0.13	-0.05	0.01	0.02	0.03	0.01	45.46	-2.62	-9.95	6
G	0.00	-0.01	0.07	0.04	0.09	-0.08	0.02	0.02	0.02	0.00	44.86	-1.49	-9.79	6
G	-0.01	-0.01	0.09	0.05	0.04	-0.07	0.01	0.01	0.03	0.02	46.04	-1.90	12.05	6
G	0.00	-0.02	0.04	0.03	0.07	-0.04	0.00	0.01	0.01	0.00	44.61	-2.22	10.87	6

G	0.00	-0.01	0.04	0.02	0.14	-0.01	0.01	0.01	0.01	0.01	45.79	-1.94	12.44	6
H	-0.11	-0.28	-0.16	-0.29	-0.29	-0.44	-0.13	-0.19	0.01	-0.25	16.55	8.69	0.86	7
H	-0.12	-0.29	-0.15	-0.28	-0.30	-0.47	-0.12	-0.19	-0.02	-0.25	17.78	9.36	-0.56	7
H	-0.12	-0.29	-0.14	-0.28	-0.30	-0.46	-0.12	-0.18	0.01	-0.25	16.62	9.02	0.93	7
H	-0.12	-0.30	-0.16	-0.29	-0.29	-0.43	-0.12	-0.19	-0.01	-0.26	17.91	9.50	0.09	7
H	-0.12	-0.28	-0.14	-0.29	-0.31	-0.45	-0.13	-0.19	-0.10	-0.29	17.79	7.46	0.81	7
H	-0.14	-0.30	-0.13	-0.28	-0.32	-0.44	-0.13	-0.20	-0.05	-0.27	18.49	8.87	-1.13	7
I	0.00	-0.11	-0.01	-0.11	-0.03	-0.14	-0.02	-0.04	0.03	-0.12	19.63	5.89	-1.96	8
I	-0.01	-0.11	-0.01	-0.10	-0.05	-0.14	-0.02	-0.04	0.03	-0.12	19.79	6.02	-2.55	8
I	-0.02	-0.12	-0.02	-0.08	-0.04	-0.14	-0.01	-0.04	0.03	-0.12	19.50	5.79	-2.94	8
I	-0.02	-0.12	-0.01	-0.10	-0.05	-0.14	-0.01	-0.04	0.02	-0.12	18.47	6.56	-2.71	8
I	-0.02	-0.12	0.01	-0.09	-0.05	-0.15	-0.01	-0.05	0.01	-0.12	19.05	6.18	-2.95	8
I	-0.02	-0.12	0.01	-0.09	-0.16	-0.16	-0.01	-0.04	0.02	-0.12	18.99	6.05	-2.63	8
K	-0.07	-0.17	-0.15	-0.20	-0.29	-0.31	-0.45	-0.28	-0.04	-0.16	-9.81	19.95	8.78	9
K	-0.05	-0.17	-0.24	-0.26	-0.20	-0.33	-0.41	-0.25	-0.04	-0.17	-7.67	18.26	8.98	9
K	-0.06	-0.18	-0.18	-0.22	-0.23	-0.31	-0.44	-0.27	-0.11	-0.20	-6.60	19.39	9.47	9
K	-0.08	-0.18	-0.24	-0.25	-0.11	-0.32	-0.42	-0.26	-0.04	-0.18	-6.58	18.67	8.41	9
K	-0.10	-0.19	-0.23	-0.23	-0.27	-0.32	-0.37	-0.23	-0.14	-0.22	-6.68	18.37	7.86	9
K	-0.08	-0.17	-0.26	-0.26	-0.31	-0.33	-0.37	-0.23	-0.12	-0.22	-5.57	17.04	8.94	9
L	0.08	-0.19	0.15	-0.17	-0.04	-0.37	0.02	-0.12	0.02	-0.26	13.74	25.64	5.85	10
L	0.08	-0.19	0.16	-0.16	-0.04	-0.37	0.02	-0.12	0.03	-0.26	13.57	25.56	5.99	10
L	0.09	-0.19	0.16	-0.15	-0.04	-0.38	0.02	-0.12	0.02	-0.26	13.50	25.89	7.19	10
L	0.08	-0.20	0.17	-0.15	-0.08	-0.39	0.02	-0.12	0.03	-0.26	14.48	26.01	7.16	10
L	0.10	-0.19	0.15	-0.16	-0.07	-0.38	0.02	-0.12	0.03	-0.27	14.37	26.19	7.73	10
L	0.08	-0.20	0.15	-0.15	-0.12	-0.38	0.03	-0.12	0.03	-0.27	14.77	26.53	7.28	10
M	-0.08	-0.32	-0.05	-0.29	-0.27	-0.50	-0.03	-0.19	-0.01	-0.32	31.19	22.80	1.38	11
M	-0.09	-0.31	-0.09	-0.31	-0.26	-0.52	-0.03	-0.18	0.01	-0.33	32.35	23.01	2.21	11
M	-0.09	-0.32	-0.06	-0.30	-0.27	-0.51	-0.04	-0.20	0.01	-0.30	30.94	22.39	-1.39	11
M	-0.08	-0.32	-0.06	-0.30	-0.26	-0.49	-0.05	-0.19	-0.01	-0.31	30.09	20.90	1.15	11
M	-0.07	-0.31	-0.08	-0.31	-0.30	-0.51	-0.05	-0.19	-0.01	-0.32	31.11	21.06	2.30	11
M	-0.09	-0.32	-0.06	-0.30	-0.29	-0.50	-0.05	-0.20	0.00	-0.32	31.59	21.98	0.84	11
N	-0.17	-0.32	-0.10	-0.25	-0.07	-0.48	-0.51	-0.32	-0.23	-0.32	11.73	23.25	16.87	12
N	-0.13	-0.29	-0.10	-0.25	-0.11	-0.47	-0.58	-0.38	-0.21	-0.32	13.65	22.92	16.47	12
N	-0.12	-0.29	-0.09	-0.23	-0.10	-0.47	-0.49	-0.32	-0.27	-0.33	10.56	21.24	16.33	12
N	-0.18	-0.33	-0.10	-0.25	-0.11	-0.48	-0.55	-0.36	-0.24	-0.33	14.08	24.01	15.17	12
N	-0.14	-0.30	-0.10	-0.24	-0.10	-0.47	-0.50	-0.32	-0.22	-0.32	12.11	20.82	16.73	12
N	-0.19	-0.32	-0.03	-0.21	-0.13	-0.48	-0.50	-0.32	-0.28	-0.34	10.81	23.33	14.94	12
P	0.06	-0.02	0.05	-0.03	-0.19	-0.08	-0.01	-0.02	0.01	-0.05	36.21	2.53	-5.41	13
P	0.07	-0.02	0.05	-0.01	-0.17	-0.08	-0.02	-0.02	0.01	-0.03	38.21	1.44	-5.13	13
P	0.07	-0.03	0.08	0.00	-0.35	-0.09	0.00	-0.01	0.02	-0.03	38.21	2.91	-5.99	13
P	0.06	-0.02	0.06	-0.02	-0.23	-0.10	-0.01	-0.02	0.00	-0.05	36.32	2.47	-5.12	13
P	0.05	-0.03	0.06	-0.03	-0.16	-0.11	-0.01	-0.02	0.00	-0.05	35.57	1.81	-5.05	13
P	0.04	-0.03	0.07	-0.02	-0.25	-0.11	-0.01	-0.02	0.01	-0.04	36.31	2.08	-6.29	13
Q	0.09	0.02	0.17	0.05	0.02	-0.01	0.02	0.00	0.01	0.00	45.57	2.77	-8.53	14
Q	0.10	0.02	0.20	0.07	0.25	-0.01	0.02	0.00	0.02	0.00	44.19	4.39	-8.22	14
Q	0.10	0.01	0.24	0.09	0.22	-0.05	0.02	0.00	0.02	0.00	43.80	3.98	-6.68	14
Q	0.08	0.01	0.21	0.08	0.03	-0.03	0.02	0.01	0.03	0.00	45.31	3.44	-7.80	14
Q	0.09	0.01	0.16	0.06	0.04	-0.05	0.02	0.00	0.02	-0.01	42.58	4.46	-7.91	14
Q	0.08	0.01	0.20	0.08	0.04	-0.06	0.02	0.00	0.01	-0.01	43.63	3.79	-8.12	14
R	-0.11	-0.18	-0.05	-0.13	-0.33	-0.27	-0.46	-0.25	-0.30	-0.24	15.53	27.04	7.63	15
R	-0.05	-0.14	-0.07	-0.13	-0.43	-0.30	-0.49	-0.28	-0.29	-0.24	14.93	26.75	11.41	15
R	-0.08	-0.15	-0.07	-0.12	-0.41	-0.27	-0.45	-0.25	-0.27	-0.23	15.70	24.53	9.04	15

R	-0.08	-0.16	-0.03	-0.14	-0.41	-0.30	-0.47	-0.25	-0.31	-0.25	15.86	27.63	11.91	15
R	-0.08	-0.16	-0.01	-0.11	-0.32	-0.28	-0.47	-0.26	-0.29	-0.23	15.81	26.34	9.87	15
R	-0.07	-0.16	-0.12	-0.15	-0.45	-0.30	-0.48	-0.27	-0.33	-0.24	14.82	28.42	10.35	15
S	0.01	-0.02	0.10	0.04	0.13	0.01	0.00	0.00	0.01	0.01	45.82	-1.03	12.08	16
S	0.02	0.00	0.08	0.04	0.20	0.00	0.02	0.01	0.02	0.01	45.98	-0.24	12.11	16
S	0.03	-0.01	0.09	0.05	0.26	0.02	0.02	0.01	0.02	0.00	44.74	0.91	11.03	16
S	0.02	0.00	0.15	0.08	0.09	0.00	0.00	0.00	0.01	0.00	46.26	0.31	12.04	16
S	0.01	-0.01	0.12	0.06	-0.02	-0.01	0.01	0.00	0.01	0.00	45.72	-0.21	11.95	16
S	0.00	-0.01	0.12	0.07	0.09	-0.01	0.00	0.00	0.02	0.00	44.48	0.20	11.89	16
T	0.10	0.01	0.26	0.09	0.21	-0.03	0.02	0.01	-0.01	-0.04	42.90	3.92	-3.57	17
T	0.10	0.01	0.29	0.12	0.09	-0.04	0.03	0.01	0.00	-0.04	42.62	5.93	-3.76	17
T	0.10	0.01	0.29	0.11	0.12	-0.02	0.02	0.01	-0.01	-0.04	43.60	4.37	-3.65	17
T	0.10	0.01	0.27	0.10	0.19	-0.04	0.02	0.01	0.00	-0.03	42.44	4.79	-4.21	17
T	0.10	0.01	0.26	0.09	0.10	-0.06	0.03	0.01	0.00	-0.04	41.37	5.18	-3.55	17
T	0.09	0.01	0.30	0.09	0.13	-0.06	0.02	0.00	-0.01	-0.04	42.50	4.43	-4.99	17
V	0.15	-0.10	0.34	-0.05	-0.18	-0.23	0.00	-0.08	-0.03	-0.22	-6.20	19.70	8.64	18
V	0.15	-0.10	0.35	-0.04	-0.26	-0.28	0.02	-0.06	-0.02	-0.23	-6.71	19.36	12.34	18
V	0.14	-0.11	0.33	-0.04	-0.11	-0.25	0.01	-0.07	-0.01	-0.22	-6.02	19.78	10.25	18
V	0.13	-0.11	0.32	-0.05	-0.27	-0.26	0.01	-0.06	-0.01	-0.23	-6.04	18.82	10.87	18
V	0.12	-0.11	0.32	-0.05	-0.13	-0.27	0.01	-0.08	0.00	-0.23	-4.28	19.81	9.15	18
V	0.13	-0.12	0.32	-0.06	-0.16	-0.26	0.01	-0.07	-0.02	-0.23	-4.83	19.37	9.21	18
W	-0.83	-0.74	-0.83	-0.76	-0.58	-0.74	-0.71	-0.63	-0.43	-0.54	75.40	31.03	22.15	19
W	-0.83	-0.75	-0.80	-0.74	-0.63	-0.73	-0.71	-0.63	-0.39	-0.52	74.46	29.71	23.30	19
W	-0.84	-0.76	-0.81	-0.75	-0.62	-0.74	-0.70	-0.62	-0.40	-0.53	75.38	29.69	23.10	19
W	-0.84	-0.75	-0.84	-0.77	-0.67	-0.75	-0.65	-0.60	-0.38	-0.52	74.35	28.08	23.77	19
W	-0.83	-0.75	-0.83	-0.76	-0.67	-0.76	-0.65	-0.60	-0.40	-0.53	75.75	27.28	23.41	19
W	-0.83	-0.75	-0.84	-0.77	-0.68	-0.76	-0.71	-0.63	-0.39	-0.52	75.20	30.35	22.73	19
Y	-0.77	-0.72	-0.77	-0.75	-0.38	-0.70	-0.62	-0.55	-0.29	-0.51	71.97	24.89	15.56	20
Y	-0.76	-0.72	-0.78	-0.75	-0.40	-0.70	-0.60	-0.54	-0.28	-0.51	71.52	24.42	14.07	20
Y	-0.76	-0.72	-0.76	-0.73	-0.28	-0.68	-0.58	-0.52	-0.32	-0.52	70.79	23.97	14.74	20
Y	-0.77	-0.73	-0.78	-0.75	-0.42	-0.71	-0.61	-0.54	-0.31	-0.51	71.95	25.27	15.07	20
Y	-0.78	-0.73	-0.77	-0.75	-0.35	-0.70	-0.58	-0.52	-0.30	-0.52	71.81	23.89	15.55	20
Y	-0.78	-0.73	-0.78	-0.75	-0.40	-0.71	-0.59	-0.53	-0.28	-0.50	71.50	24.54	15.44	20

Table 26. LDA jackknifed classification matrix table obtained from array 4 PPE-CB[7]-AO tongue against 20 amino acids (25 mM). The jackknifed classification matrix with cross-validation reveals a 93% accuracy.

	A	C	D	E	F	G	H	I	K	L	M	N	P	Q	R	S	T	V	W	Y	%correct
A	4	0	0	0	0	2	0	0	0	0	0	0	0	0	0	0	0	0	0	0	67
C	0	6	0	0	0	0	0	0	0	0	0	0	0	0	0	0	0	0	0	0	100
D	0	0	2	3	0	0	0	0	0	0	0	1	0	0	0	0	0	0	0	0	33
E	0	0	2	4	0	0	0	0	0	0	0	0	0	0	0	0	0	0	0	0	67
F	0	0	0	0	6	0	0	0	0	0	0	0	0	0	0	0	0	0	0	0	100
G	0	0	0	0	0	6	0	0	0	0	0	0	0	0	0	0	0	0	0	0	100
H	0	0	0	0	0	0	6	0	0	0	0	0	0	0	0	0	0	0	0	0	100
I	0	0	0	0	0	0	0	6	0	0	0	0	0	0	0	0	0	0	0	0	100
K	0	0	0	0	0	0	0	0	6	0	0	0	0	0	0	0	0	0	0	0	100
L	0	0	0	0	0	0	0	0	0	6	0	0	0	0	0	0	0	0	0	0	100
M	0	0	0	0	0	0	0	0	0	0	6	0	0	0	0	0	0	0	0	0	100
N	0	0	0	0	0	0	0	0	0	0	0	6	0	0	0	0	0	0	0	0	100
P	0	0	0	0	0	0	0	0	0	0	0	0	6	0	0	0	0	0	0	0	100
Q	0	0	0	0	0	0	0	0	0	0	0	0	0	6	0	0	0	0	0	0	100
R	0	0	0	0	0	0	0	0	0	0	0	0	0	0	6	0	0	0	0	0	100

S	1	0	0	0	0	0	0	0	0	0	0	0	0	0	0	5	0	0	0	0	83
T	0	0	0	0	0	0	0	0	0	0	0	0	0	0	0	0	6	0	0	0	100
V	0	0	0	0	0	0	0	0	0	0	0	0	0	0	0	0	0	6	0	0	100
W	0	0	0	0	0	0	0	0	0	0	0	0	0	0	0	0	0	0	6	0	100
Y	0	0	0	0	0	0	0	0	0	0	0	0	0	0	0	0	0	0	0	6	100
Total	5	6	4	7	6	8	6	6	6	6	6	7	6	6	6	5	6	6	6	6	**93**

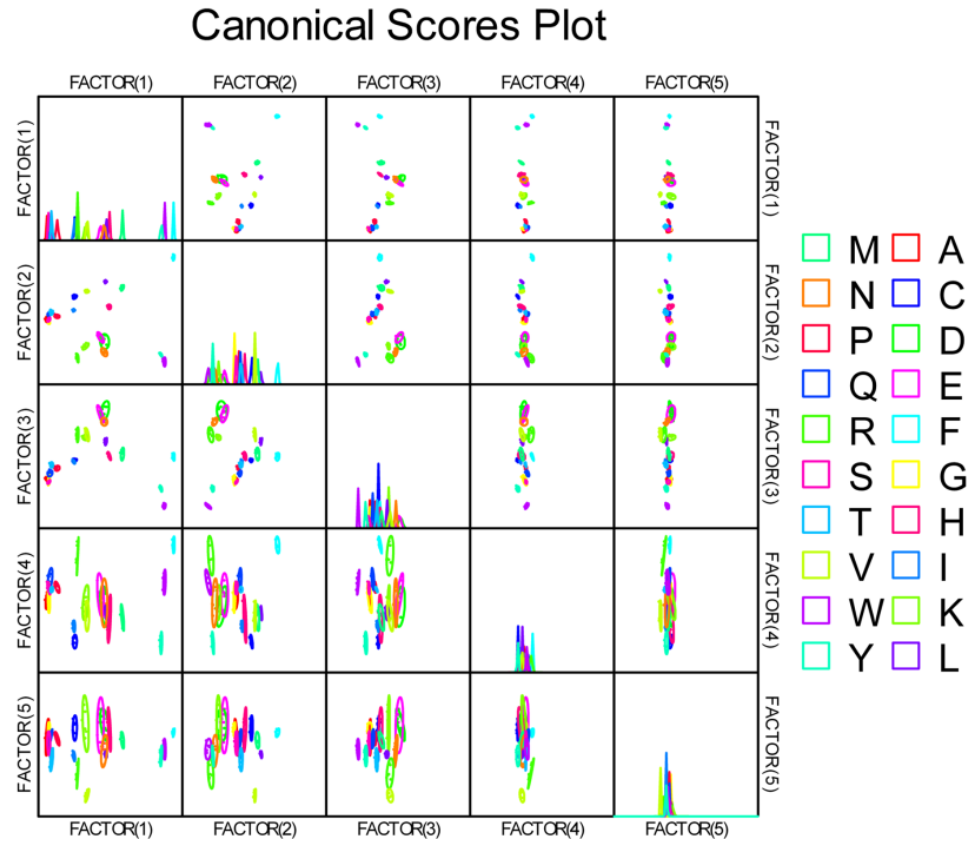

Figure 101. Correlations of canonical fluorescence response patterns from array 4 PPE-CB[7]-AO tongue against 20 amino acids (25 mM). The 95% confidence ellipses for the individual analytes are shown.

Table 27. Factor loadings of fluorescence response pattern from four arrays against 20 amino acids (25 mM). PCA was carried out and resulting in 28 factors of the canonical scores (the first ten scores were shown here).

	F1	F2	F3	F4	F5	F6	F7	F8	F9	F10
GFP-Fe(pH7)	-0.128	0.729	0.129	0.188	-0.171	-0.368	-0.334	0.159	0.294	-0.059
GFP-Cu(pH7)	0.275	0.586	-0.457	0.509	-0.235	0.004	-0.058	0.023	-0.114	0.081
GFP-Co(pH7)	-0.277	0.843	-0.185	0.029	0.225	0.231	-0.077	0.126	-0.129	-0.049
P7-CB8(pH3)	0.757	0.036	0.516	0.053	-0.304	0.152	0.011	0.077	-0.001	-0.015
P13-CB8(pH3)	0.823	0.051	0.446	-0.054	-0.273	0.059	-0.034	0.075	0.024	-0.029
P14-CB8(pH3)	0.716	0.132	0.343	-0.013	-0.259	0.450	0.020	0.234	-0.045	0.011
P7-CB8(pH13)	0.725	0.027	0.449	0.141	0.243	0.148	-0.281	-0.162	-0.004	-0.164
P13-CB8(pH13)	0.855	0.221	0.262	-0.284	-0.076	-0.203	-0.005	-0.031	-0.032	0.071
P14-CB8(pH13)	0.783	0.095	0.409	0.120	0.356	-0.118	-0.045	-0.034	-0.060	-0.016
P5-Fe(pH7)	0.137	0.886	0.191	0.177	0.070	-0.019	-0.008	-0.270	-0.024	0.038
P5-Fe(pH10)	0.138	0.012	0.145	0.862	0.298	0.161	0.210	0.097	0.184	-0.002
P5-Fe(pH13)	0.096	0.771	0.166	-0.133	0.012	-0.293	0.403	0.148	-0.204	-0.178
P5-Cu(pH7)	0.834	0.316	-0.237	0.288	-0.010	-0.069	0.015	-0.092	-0.123	0.112
P5-Cu(pH10)	0.897	0.282	0.130	0.082	0.076	-0.098	0.060	0.025	0.007	0.226
P5-Cu(pH13)	0.803	0.300	-0.278	-0.070	-0.157	-0.096	-0.284	-0.043	-0.128	-0.050

P5-Co(pH7)	0.464	0.598	-0.191	-0.438	0.320	0.196	-0.085	0.059	0.083	-0.100
P5-Co(pH10)	0.684	0.265	-0.090	-0.615	0.148	0.063	0.092	0.015	0.140	0.072
P5-Co(pH13)	0.679	0.442	-0.277	-0.097	-0.182	0.020	0.285	-0.161	0.306	-0.037
P5-CB7-AO(460nm)	0.954	-0.023	0.218	-0.032	0.063	-0.046	0.107	-0.052	-0.028	0.057
P5-CB7-AO(510nm)	0.967	-0.041	-0.206	0.034	-0.018	0.044	0.078	-0.040	-0.019	-0.044
P15-CB7-AO(460nm)	0.930	-0.203	0.085	-0.053	0.058	0.057	-0.038	-0.061	0.012	0.121
P15-CB7-AO(510nm)	0.949	-0.129	-0.237	0.019	-0.018	0.102	-0.033	-0.036	0.016	0.002
P6-CB7-AO(460nm)	0.764	-0.218	-0.329	-0.068	0.258	-0.138	-0.108	0.335	0.014	0.141
P6-CB7-AO(510nm)	0.832	-0.192	-0.483	0.067	-0.040	0.086	-0.003	-0.014	0.013	-0.111
P7-CB7-AO(460nm)	0.735	-0.645	0.089	-0.035	0.023	-0.139	-0.038	-0.031	-0.029	-0.053
P7-CB7-AO(510nm)	0.909	-0.330	-0.212	0.054	-0.023	-0.056	-0.005	-0.049	-0.015	-0.063
P8-CB7-AO(460nm)	0.762	-0.484	0.113	0.184	0.066	-0.291	0.080	0.095	0.012	-0.120
P8-CB7-AO(510nm)	0.843	-0.180	-0.439	0.138	-0.054	0.036	0.029	0.038	0.000	-0.143

Table 28. Training matrix of fluorescence response pattern from eight optimized sensor elements tongue against 20 amino acids (25 mM). LDA was carried out and resulting in 8 factors of the canonical scores (the first three scores were shown here) and group generation.

Analytes	Fluorescence Response Pattern								Results LDA (the first three scores)			
Amino acids	GFP-Cu (pH7)	GFP-Co (pH7)	**P5**-Fe (pH7)	**P5**-Fe (pH10)	**P5**-Co (pH7)	**P5**-Co (pH13)	**P7**-CB7-AO (460nm)	**P7**-CB7-AO (510nm)	Factor 1	Factor 2	Factor 3	Gr.
A	0.91	-0.09	-0.41	-0.40	-0.36	0.15	0.02	0.01	10.12	23.83	18.52	1
A	0.87	-0.07	-0.39	-0.50	-0.36	0.17	0.02	0.02	9.64	23.84	19.15	1
A	0.87	-0.04	-0.41	-0.51	-0.36	0.15	0.01	0.02	9.42	23.16	19.17	1
A	0.93	-0.04	-0.39	-0.39	-0.37	0.12	0.01	0.01	9.91	23.76	17.98	1
A	0.93	-0.07	-0.41	-0.35	-0.35	0.09	0.01	0.01	9.10	23.70	18.41	1
A	0.91	-0.05	-0.42	-0.33	-0.35	0.10	0.01	0.01	9.87	22.98	17.89	1
C	1.01	0.11	-0.19	8.87	-0.83	-0.55	0.04	-0.04	46.56	65.29	-63.06	2
C	1.03	0.13	-0.24	8.93	-0.84	-0.55	0.06	-0.03	46.85	66.02	-63.50	2
C	1.00	0.18	-0.31	8.62	-0.83	-0.54	0.06	-0.03	46.22	63.38	-61.14	2
C	1.03	0.10	-0.32	8.78	-0.84	-0.47	0.06	-0.03	47.19	65.81	-62.17	2
C	1.03	0.13	-0.31	8.31	-0.84	-0.38	0.05	-0.03	46.35	63.58	-58.92	2
C	1.02	0.19	-0.31	8.42	-0.83	-0.40	0.05	-0.04	46.33	63.09	-60.16	2
D	1.06	4.12	1.40	0.73	0.05	-0.04	-0.48	-0.33	44.00	-12.62	-17.55	3
D	1.03	4.32	1.27	0.77	0.07	-0.05	-0.43	-0.29	46.54	-11.54	-17.64	3
D	1.00	4.38	1.12	0.79	0.01	-0.05	-0.41	-0.28	43.11	-11.31	-18.93	3
D	1.05	4.25	1.10	0.93	0.06	-0.07	-0.43	-0.28	45.54	-9.70	-18.03	3
D	0.98	4.38	1.16	0.78	0.05	-0.06	-0.47	-0.29	47.01	-11.27	-18.22	3
D	1.06	4.41	1.41	0.78	0.05	-0.08	-0.49	-0.32	47.01	-12.69	-19.55	3
E	1.13	4.05	0.49	0.66	-0.16	0.02	-0.42	-0.29	28.08	-11.24	-18.65	4
E	1.10	4.05	0.49	0.71	-0.15	-0.03	-0.40	-0.27	28.93	-10.53	-18.32	4
E	1.16	4.17	0.43	0.73	-0.15	0.03	-0.40	-0.27	29.26	-10.92	-19.38	4
E	1.11	4.05	0.53	0.62	-0.15	0.03	-0.39	-0.26	29.14	-10.34	-17.77	4
E	1.13	3.99	0.64	0.54	-0.14	0.01	-0.45	-0.30	29.57	-12.20	-17.43	4
E	1.13	4.20	0.48	0.75	-0.16	-0.03	-0.46	-0.31	28.41	-13.87	-20.75	4
F	0.22	-0.09	-0.29	-0.87	-0.50	-0.94	-0.11	-0.40	47.15	-32.42	9.84	5
F	0.07	-0.09	-0.36	-0.89	-0.51	-0.95	-0.08	-0.38	48.14	-32.31	10.19	5
F	0.20	-0.14	-0.34	-0.89	-0.52	-0.95	-0.11	-0.41	49.45	-32.84	9.81	5
F	-0.16	-0.13	-0.38	-0.88	-0.52	-0.95	-0.10	-0.39	48.78	-32.96	9.99	5
F	-0.06	-0.13	-0.36	-0.87	-0.50	-0.95	-0.09	-0.39	47.65	-32.33	10.31	5
F	-0.20	-0.14	-0.36	-0.89	-0.51	-0.94	-0.11	-0.40	48.12	-33.18	10.22	5

G	0.95	0.23	-0.37	-0.61	-0.22	0.03	0.01	0.01	-0.75	19.98	21.28	6
G	0.82	0.23	-0.39	-0.68	-0.23	0.03	0.01	0.02	-0.84	19.98	21.90	6
G	0.92	0.23	-0.40	-0.64	-0.21	0.01	0.02	0.02	-1.21	19.84	21.90	6
G	0.92	0.13	-0.42	-0.63	-0.22	-0.05	0.01	0.01	0.15	19.08	22.32	6
G	0.91	0.18	-0.43	-0.63	-0.23	-0.09	0.00	0.01	0.64	18.63	21.80	6
G	0.91	0.18	-0.36	-0.55	-0.21	-0.09	0.01	0.01	-0.84	19.28	21.68	6
H	1.13	1.14	0.68	-0.21	-0.85	-0.75	-0.13	-0.19	43.36	-6.06	-7.83	7
H	1.14	1.19	0.66	-0.25	-0.84	-0.75	-0.12	-0.19	43.14	-6.92	-7.59	7
H	1.07	1.12	0.45	-0.18	-0.84	-0.71	-0.12	-0.18	43.52	-5.51	-7.08	7
H	1.10	1.08	0.45	-0.19	-0.85	-0.72	-0.12	-0.19	44.21	-5.88	-7.01	7
H	1.13	1.09	0.73	-0.18	-0.85	-0.67	-0.13	-0.19	43.13	-4.68	-7.89	7
H	1.06	1.15	0.58	-0.09	-0.85	-0.68	-0.13	-0.20	43.90	-6.10	-8.84	7
I	0.98	-0.08	-0.26	-0.64	-0.36	0.13	-0.02	-0.04	11.90	17.85	18.89	8
I	0.97	-0.08	-0.30	-0.67	-0.36	0.17	-0.02	-0.04	12.13	17.92	18.99	8
I	1.02	-0.12	-0.31	-0.64	-0.38	0.06	-0.01	-0.04	14.17	17.46	18.83	8
I	0.98	-0.06	-0.29	-0.66	-0.37	0.08	-0.01	-0.04	13.05	16.93	18.78	8
I	1.00	-0.10	-0.33	-0.66	-0.38	0.11	-0.01	-0.05	14.12	17.27	18.71	8
I	0.99	-0.13	-0.29	-0.63	-0.38	0.15	-0.01	-0.04	13.71	18.40	18.74	8
K	1.18	3.84	1.14	1.74	0.10	0.47	-0.45	-0.28	49.40	5.41	-20.88	9
K	1.07	3.80	0.94	1.50	0.08	0.41	-0.41	-0.25	47.29	3.67	-18.19	9
K	1.13	3.78	0.92	1.33	0.10	0.44	-0.44	-0.27	48.04	2.20	-16.92	9
K	1.12	3.86	0.94	1.02	0.10	0.45	-0.42	-0.26	48.89	0.57	-14.84	9
K	1.16	3.71	1.04	1.12	0.10	0.40	-0.37	-0.23	48.23	3.91	-14.18	9
K	1.09	3.80	0.98	1.00	0.09	0.41	-0.37	-0.23	47.80	1.97	-14.09	9
L	0.29	-0.10	-0.27	-0.63	-0.39	-0.36	0.02	-0.12	23.79	1.15	16.26	10
L	0.68	-0.09	-0.27	-0.64	-0.38	-0.33	0.02	-0.12	22.39	2.59	16.74	10
L	0.62	-0.14	-0.33	-0.62	-0.40	-0.41	0.02	-0.12	24.25	2.18	16.74	10
L	0.67	-0.10	-0.23	-0.61	-0.42	-0.38	0.02	-0.12	25.29	2.42	15.69	10
L	0.29	-0.07	-0.23	-0.62	-0.43	-0.29	0.02	-0.12	25.23	1.93	15.14	10
L	0.35	-0.13	-0.30	-0.58	-0.39	-0.30	0.03	-0.12	23.21	2.75	16.43	10
M	0.50	0.13	-0.30	-0.74	-0.28	-0.26	-0.03	-0.19	16.87	-4.27	16.82	11
M	0.47	0.14	-0.30	-0.70	-0.27	-0.30	-0.03	-0.18	16.11	-4.28	16.81	11
M	0.49	0.03	-0.31	-0.77	-0.27	-0.30	-0.04	-0.20	17.45	-5.40	17.73	11
M	0.50	0.04	-0.33	-0.70	-0.26	-0.19	-0.05	-0.19	15.52	-2.71	17.45	11
M	0.41	0.01	-0.30	-0.75	-0.26	-0.32	-0.05	-0.19	16.16	-4.43	18.14	11
M	0.52	0.05	-0.32	-0.72	-0.27	-0.15	-0.05	-0.20	16.08	-3.22	17.24	11
N	1.15	4.06	0.61	0.17	0.12	-0.14	-0.51	-0.32	47.73	-15.58	-9.15	12
N	1.21	4.12	0.65	0.14	0.10	-0.13	-0.58	-0.38	45.59	-19.97	-11.17	12
N	1.14	4.12	0.42	0.22	0.10	-0.14	-0.49	-0.32	45.73	-16.57	-9.91	12
N	1.22	4.14	0.63	0.14	0.10	-0.08	-0.55	-0.36	46.35	-17.94	-10.79	12
N	1.22	4.18	0.57	0.24	0.09	-0.05	-0.50	-0.32	46.31	-15.77	-11.22	12
N	1.17	4.16	0.53	0.13	0.08	0.00	-0.50	-0.32	46.03	-15.61	-10.30	12
P	0.82	-0.16	-0.27	-0.65	-0.42	0.08	-0.01	-0.02	15.60	19.73	18.40	13
P	0.82	-0.16	-0.32	-0.68	-0.42	0.07	-0.02	-0.02	15.29	19.78	18.82	13
P	0.79	-0.19	-0.30	-0.67	-0.43	0.05	0.00	-0.01	15.96	19.77	18.91	13
P	0.85	-0.18	-0.28	-0.64	-0.43	0.04	-0.01	-0.02	15.93	19.90	18.62	13
P	0.82	-0.15	-0.32	-0.59	-0.43	0.07	-0.01	-0.02	15.83	19.78	18.06	13
P	0.80	-0.15	-0.33	-0.67	-0.42	0.07	-0.01	-0.02	15.71	18.94	18.62	13
Q	0.88	1.70	-0.28	-0.49	-0.27	0.19	0.02	0.00	-6.43	11.33	9.25	14
Q	0.84	1.66	-0.28	-0.54	-0.28	0.19	0.02	0.00	-4.88	10.62	9.39	14
Q	0.88	1.74	-0.33	-0.52	-0.30	0.17	0.02	0.00	-3.78	10.06	8.39	14
Q	0.86	1.67	-0.30	-0.54	-0.30	0.16	0.02	0.01	-3.81	11.13	9.16	14

Q	0.87	1.70	-0.33	-0.53	-0.29	0.21	0.02	0.00	-4.00	10.42	8.82	14
Q	0.86	1.69	-0.30	-0.47	-0.31	0.19	0.02	0.00	-3.35	10.72	8.17	14
R	1.02	3.91	1.13	1.22	0.10	0.23	-0.46	-0.25	51.04	1.49	-16.62	15
R	1.03	3.78	1.09	1.25	0.10	0.28	-0.49	-0.28	50.35	1.95	-16.34	15
R	1.04	3.86	1.20	1.15	0.07	0.26	-0.45	-0.25	48.76	1.95	-16.64	15
R	1.03	3.83	1.06	1.16	0.10	0.31	-0.47	-0.25	51.60	3.12	-15.35	15
R	1.04	3.88	1.27	0.88	0.11	0.27	-0.47	-0.26	51.97	0.38	-14.13	15
R	1.03	3.78	1.39	1.20	0.09	0.28	-0.48	-0.27	51.12	3.15	-16.54	15
S	0.90	1.66	-0.25	-0.68	0.17	-0.30	0.00	0.00	33.56	7.04	21.47	16
S	0.90	1.34	-0.27	-0.67	0.10	-0.33	0.02	0.01	27.06	8.90	22.16	16
S	0.86	1.31	-0.24	-0.68	0.14	-0.31	0.02	0.01	29.18	9.20	23.04	16
S	0.85	1.06	-0.27	-0.68	0.15	-0.32	0.00	0.00	28.76	10.00	24.93	16
S	0.84	1.23	-0.25	-0.68	0.17	-0.30	0.01	0.00	30.97	9.51	24.23	16
S	0.88	1.01	-0.28	-0.66	0.15	-0.31	0.00	0.00	27.86	10.61	25.04	16
T	0.88	3.21	-0.29	-0.53	0.23	-0.31	0.02	0.01	46.79	-2.17	12.15	17
T	0.88	3.46	-0.33	-0.53	0.23	-0.30	0.03	0.01	47.37	-3.95	10.41	17
T	0.83	3.34	-0.31	-0.56	0.23	-0.30	0.02	0.01	47.68	-3.24	11.58	17
T	0.82	3.47	-0.31	-0.55	0.22	-0.30	0.02	0.01	46.98	-4.61	10.17	17
T	0.86	3.33	-0.34	-0.59	0.24	-0.30	0.03	0.01	47.70	-3.72	12.02	17
T	0.85	3.19	-0.32	-0.59	0.22	-0.31	0.02	0.00	44.82	-3.45	12.10	17
V	0.86	-0.17	-0.20	-0.59	-0.38	0.04	0.00	-0.08	17.62	13.02	17.41	18
V	0.91	-0.17	-0.19	-0.64	-0.38	0.07	0.02	-0.06	16.54	15.21	18.30	18
V	0.86	-0.17	-0.28	-0.63	-0.40	0.07	0.01	-0.07	18.22	14.04	17.84	18
V	0.86	-0.17	-0.23	-0.65	-0.40	-0.03	0.01	-0.06	18.48	13.31	17.94	18
V	0.87	-0.18	-0.24	-0.68	-0.40	0.04	0.01	-0.08	19.04	12.61	17.84	18
V	0.85	-0.18	-0.24	-0.63	-0.40	0.01	0.01	-0.07	18.97	12.82	17.62	18
W	0.72	2.55	-0.86	-0.94	-0.94	-0.97	-0.71	-0.63	51.37	-53.70	-18.60	19
W	0.75	2.56	-0.86	-0.94	-0.94	-0.96	-0.71	-0.63	51.62	-53.91	-18.72	19
W	0.73	2.65	-0.87	-0.94	-0.95	-0.97	-0.70	-0.62	51.10	-54.04	-19.15	19
W	0.74	2.64	-0.86	-0.93	-0.95	-0.96	-0.65	-0.60	51.15	-52.48	-18.69	19
W	0.77	2.57	-0.87	-0.94	-0.95	-0.96	-0.65	-0.60	51.86	-52.40	-18.25	19
W	0.82	2.88	-0.86	-0.94	-0.94	-0.97	-0.71	-0.63	49.51	-55.65	-20.66	19
Y	0.69	3.16	-0.27	-0.51	-0.50	-0.86	-0.62	-0.55	15.10	-46.85	-15.37	20
Y	0.67	3.04	-0.22	-0.51	-0.50	-0.86	-0.60	-0.54	15.35	-44.77	-14.40	20
Y	0.66	3.19	-0.27	-0.55	-0.49	-0.84	-0.58	-0.52	13.58	-45.19	-14.39	20
Y	0.73	3.18	-0.34	-0.54	-0.49	-0.86	-0.61	-0.54	14.36	-46.41	-14.68	20
Y	0.77	3.21	-0.33	-0.54	-0.49	-0.85	-0.58	-0.52	14.03	-45.51	-14.55	20
Y	0.70	3.15	-0.20	-0.48	-0.50	-0.86	-0.59	-0.53	14.86	-45.09	-15.29	20

Table 29. LDA jackknifed classification matrix table obtained from eight optimized sensor elements tongue against 20 amino acids (25 mM). The jackknifed classification matrix with cross-validation reveals a 100% accuracy.

	A	C	D	E	F	G	H	I	K	L	M	N	P	Q	R	S	T	V	W	Y	%correct
A	6	0	0	0	0	0	0	0	0	0	0	0	0	0	0	0	0	0	0	0	100
C	0	6	0	0	0	0	0	0	0	0	0	0	0	0	0	0	0	0	0	0	100
D	0	0	6	0	0	0	0	0	0	0	0	0	0	0	0	0	0	0	0	0	100
E	0	0	0	6	0	0	0	0	0	0	0	0	0	0	0	0	0	0	0	0	100
F	0	0	0	0	6	0	0	0	0	0	0	0	0	0	0	0	0	0	0	0	100
G	0	0	0	0	0	6	0	0	0	0	0	0	0	0	0	0	0	0	0	0	100
H	0	0	0	0	0	0	6	0	0	0	0	0	0	0	0	0	0	0	0	0	100
I	0	0	0	0	0	0	0	6	0	0	0	0	0	0	0	0	0	0	0	0	100
K	0	0	0	0	0	0	0	0	6	0	0	0	0	0	0	0	0	0	0	0	100
L	0	0	0	0	0	0	0	0	0	6	0	0	0	0	0	0	0	0	0	0	100

M	0	0	0	0	0	0	0	0	0	0	6	0	0	0	0	0	0	0	0	0	100
N	0	0	0	0	0	0	0	0	0	0	0	6	0	0	0	0	0	0	0	0	100
P	0	0	0	0	0	0	0	0	0	0	0	0	6	0	0	0	0	0	0	0	100
Q	0	0	0	0	0	0	0	0	0	0	0	0	0	6	0	0	0	0	0	0	100
R	0	0	0	0	0	0	0	0	0	0	0	0	0	0	6	0	0	0	0	0	100
S	0	0	0	0	0	0	0	0	0	0	0	0	0	0	0	6	0	0	0	0	100
T	0	0	0	0	0	0	0	0	0	0	0	0	0	0	0	0	6	0	0	0	100
V	0	0	0	0	0	0	0	0	0	0	0	0	0	0	0	0	0	6	0	0	100
W	0	0	0	0	0	0	0	0	0	0	0	0	0	0	0	0	0	0	6	0	100
Y	0	0	0	0	0	0	0	0	0	0	0	0	0	0	0	0	0	0	0	6	100
Total	6	6	6	6	6	6	6	6	6	6	6	6	6	6	6	6	6	6	6	6	**100**

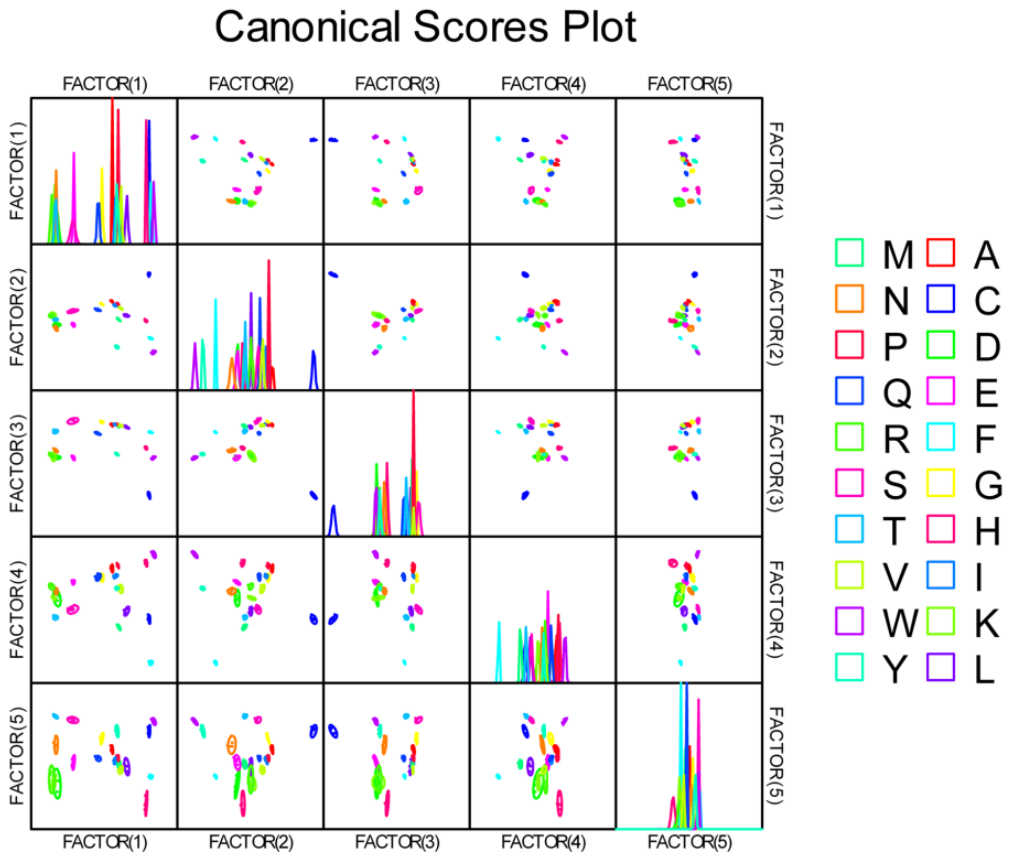

Figure 102. Correlations of canonical fluorescence response patterns from eight optimized sensor elements tongue against 20 amino acids. The 95% confidence ellipses for the individual analytes are shown.

Table 30. Training matrix of fluorescence response pattern from the eight optimized sensor elements tongue against 20 amino acids (10 mM). LDA was carried out and resulted in 8 canonical scores (the first three scores were shown here) and group generation.

Analytes	Fluorescence Response Pattern								Results LDA (the first three scores)			
Amino acids	GFP-Cu (pH7)	GFP-Co (pH7)	**P5**-Fe (pH7)	**P5**-Fe (pH10)	**P5**-Co (pH7)	**P5**-Co (pH13)	**P7**-CB7-AO (460nm)	**P7**-CB7-AO (510nm)	Factor 1	Factor 2	Factor 3	Gr.
A	0.29	0.05	-0.25	-0.49	-0.43	0.07	0.04	0.02	-7.28	-22.44	9.34	1
A	0.29	0.06	-0.22	-0.55	-0.43	0.08	0.04	0.03	-7.05	-23.27	9.71	1
A	0.30	0.07	-0.28	-0.53	-0.43	0.06	0.03	0.02	-7.12	-21.99	8.89	1
A	0.30	0.07	-0.16	-0.53	-0.43	0.08	0.04	0.02	-7.46	-22.41	9.52	1
A	0.29	0.06	-0.22	-0.50	-0.42	0.06	0.03	0.01	-6.40	-21.41	9.00	1
A	0.25	0.06	-0.21	-0.50	-0.43	0.04	0.02	0.01	-6.83	-21.00	9.44	1
C	0.41	-0.68	-0.12	-0.26	-0.84	-0.65	0.05	-0.01	-30.05	1.74	1.16	2

C	0.42	-0.70	-0.20	0.00	-0.83	-0.56	0.06	0.00	-27.66	1.18	4.10	2
C	0.39	-0.70	-0.14	-0.16	-0.85	-0.63	0.05	0.00	-29.56	1.76	2.30	2
C	0.35	-0.70	-0.13	-0.21	-0.85	-0.58	0.06	-0.01	-30.24	-0.29	1.99	2
C	0.38	-0.72	-0.21	-0.16	-0.85	-0.62	0.07	0.01	-29.67	0.18	2.08	2
C	0.39	-0.70	-0.22	-0.17	-0.86	-0.68	0.08	0.02	-30.92	1.18	2.10	2
D	0.40	0.12	0.34	-0.24	0.42	-0.59	-0.34	-0.16	52.12	8.03	-24.73	3
D	0.41	0.12	0.35	-0.27	0.42	-0.60	-0.34	-0.16	52.26	8.21	-25.43	3
D	0.39	0.12	0.31	-0.25	0.41	-0.60	-0.34	-0.16	51.52	8.17	-25.31	3
D	0.37	0.14	0.26	-0.30	0.48	-0.60	-0.35	-0.17	55.29	6.96	-28.28	3
D	0.35	0.12	0.28	-0.34	0.46	-0.60	-0.34	-0.17	53.60	6.40	-27.87	3
D	0.34	0.12	0.26	-0.30	0.44	-0.63	-0.36	-0.17	53.42	8.37	-26.77	3
E	0.39	0.07	0.46	0.21	-0.37	-0.14	-0.34	-0.16	12.69	14.40	18.75	4
E	0.40	0.09	0.34	0.22	-0.36	-0.18	-0.34	-0.17	12.51	15.22	17.53	4
E	0.34	0.11	0.50	0.27	-0.35	-0.19	-0.34	-0.16	13.95	15.05	18.37	4
E	0.40	0.09	0.41	0.27	-0.34	-0.19	-0.33	-0.16	13.95	15.08	17.09	4
E	0.35	0.09	0.35	0.25	-0.37	-0.18	-0.34	-0.16	12.79	15.10	18.12	4
E	0.31	0.10	0.34	0.24	-0.36	-0.17	-0.34	-0.16	13.27	14.20	17.95	4
F	0.28	0.05	0.01	-0.77	-0.41	-0.94	0.03	-0.32	-28.72	14.06	-38.33	5
F	0.28	0.04	-0.03	-0.78	-0.41	-0.94	0.03	-0.31	-28.46	13.57	-38.60	5
F	0.30	0.03	-0.04	-0.80	-0.41	-0.94	0.03	-0.32	-28.83	13.61	-39.04	5
F	0.27	0.02	-0.01	-0.78	-0.42	-0.94	0.04	-0.31	-29.21	13.06	-38.37	5
F	0.26	0.02	0.00	-0.79	-0.41	-0.94	0.02	-0.32	-28.44	13.87	-38.21	5
F	0.27	-0.01	-0.07	-0.78	-0.43	-0.94	0.03	-0.32	-29.72	14.05	-38.18	5
G	0.31	0.00	-0.28	-0.52	-0.35	0.02	0.02	0.00	-2.68	-20.94	3.78	6
G	0.30	0.03	-0.27	-0.50	-0.36	-0.10	0.02	0.00	-3.85	-18.13	2.47	6
G	0.35	0.02	-0.31	-0.56	-0.35	-0.14	0.01	0.00	-3.02	-17.04	1.13	6
G	0.27	0.02	-0.28	-0.52	-0.37	-0.13	0.02	0.00	-4.39	-17.45	1.46	6
G	0.31	0.01	-0.32	-0.57	-0.36	-0.11	0.02	0.00	-4.16	-18.42	1.75	6
G	0.36	-0.01	-0.34	-0.53	-0.36	0.02	0.01	0.01	-3.10	-20.74	5.00	6
H	0.37	-0.50	0.46	-0.45	-0.72	-0.72	-0.02	-0.04	-20.89	5.82	0.09	7
H	0.35	-0.49	0.33	-0.42	-0.72	-0.75	-0.04	-0.04	-20.02	7.12	0.44	7
H	0.32	-0.52	0.19	-0.46	-0.72	-0.70	-0.04	-0.05	-20.73	5.50	0.15	7
H	0.33	-0.53	0.25	-0.47	-0.72	-0.70	-0.06	-0.05	-20.06	6.31	0.52	7
H	0.33	-0.49	0.20	-0.46	-0.73	-0.72	-0.06	-0.04	-20.26	6.44	1.99	7
H	0.34	-0.51	0.20	-0.43	-0.73	-0.73	-0.06	-0.04	-19.85	7.17	1.25	7
I	0.32	0.05	-0.35	-0.58	-0.42	-0.04	0.01	-0.02	-8.68	-17.74	4.00	8
I	0.34	0.05	-0.38	-0.56	-0.41	0.02	0.01	-0.03	-8.42	-18.18	4.21	8
I	0.33	0.03	-0.32	-0.62	-0.42	0.00	0.01	-0.03	-8.39	-18.32	4.00	8
I	0.33	0.03	-0.33	-0.57	-0.42	0.06	0.01	-0.03	-8.67	-19.27	5.36	8
I	0.32	0.03	-0.43	-0.62	-0.41	-0.01	0.00	-0.04	-8.57	-17.55	3.07	8
I	0.31	0.02	-0.32	-0.60	-0.41	0.00	0.01	-0.04	-8.03	-18.22	2.87	8
K	0.40	0.06	0.50	1.41	-0.20	0.30	-0.34	-0.17	29.01	12.59	26.76	9
K	0.43	0.07	0.45	1.34	-0.20	0.29	-0.36	-0.15	31.05	12.41	29.32	9
K	0.41	0.07	0.49	1.20	-0.19	0.34	-0.41	-0.19	31.26	13.81	28.67	9
K	0.42	0.08	0.39	1.11	-0.21	0.32	-0.42	-0.21	29.45	15.03	27.39	9
K	0.40	0.02	0.50	1.18	-0.22	0.27	-0.36	-0.17	27.77	12.16	26.32	9
K	0.40	0.05	0.44	1.15	-0.22	0.21	-0.37	-0.20	26.54	15.21	23.73	9
L	0.28	0.01	-0.31	-0.56	-0.43	-0.57	0.01	-0.09	-13.56	-2.44	-10.90	10
L	0.28	0.03	-0.30	-0.57	-0.42	-0.56	0.01	-0.10	-13.75	-2.19	-11.57	10
L	0.32	0.03	-0.17	-0.56	-0.43	-0.57	0.01	-0.10	-14.03	-1.52	-11.01	10
L	0.33	0.03	-0.19	-0.60	-0.42	-0.54	0.00	-0.10	-13.01	-1.87	-10.28	10
L	0.29	0.02	-0.26	-0.61	-0.43	-0.53	0.02	-0.09	-14.53	-4.25	-10.64	10

L	0.24	-0.03	-0.17	-0.61	-0.43	-0.57	0.00	-0.10	-13.62	-2.16	-11.54	10
M	0.19	0.01	-0.18	-0.58	-0.36	-0.34	0.03	-0.09	-10.19	-10.36	-11.01	11
M	0.04	0.02	-0.16	-0.59	-0.35	-0.33	0.04	-0.09	-9.45	-12.21	-11.40	11
M	0.14	0.02	-0.15	-0.62	-0.34	-0.36	0.04	-0.09	-9.38	-11.36	-11.93	11
M	0.01	0.01	-0.20	-0.61	-0.33	-0.36	0.04	-0.09	-8.63	-12.46	-12.83	11
M	-0.01	-0.03	-0.17	-0.62	-0.35	-0.37	0.03	-0.10	-8.99	-11.87	-12.26	11
M	0.08	-0.01	-0.16	-0.59	-0.37	-0.33	0.01	-0.10	-9.35	-10.12	-9.95	11
N	0.26	0.00	-0.06	-0.19	0.41	-0.27	-0.36	-0.16	54.14	0.16	-19.35	12
N	0.42	0.04	-0.11	-0.17	0.42	-0.27	-0.38	-0.18	54.08	3.11	-20.33	12
N	0.42	0.07	-0.04	-0.24	0.43	-0.21	-0.39	-0.19	54.28	1.76	-19.70	12
N	0.41	0.08	-0.08	-0.21	0.43	-0.24	-0.34	-0.15	53.49	-1.41	-19.43	12
N	0.38	0.07	-0.13	-0.25	0.42	-0.28	-0.34	-0.15	52.95	-0.57	-20.16	12
N	0.26	-0.04	-0.11	-0.26	0.35	-0.28	-0.38	-0.17	50.86	1.93	-18.26	12
P	0.32	0.02	-0.15	-0.52	-0.46	-0.03	0.02	0.01	-8.82	-18.40	7.94	13
P	0.33	0.01	-0.19	-0.54	-0.46	-0.03	0.01	0.00	-8.63	-17.73	8.04	13
P	0.27	0.03	-0.15	-0.53	-0.45	-0.03	0.00	-0.01	-7.80	-17.21	7.86	13
P	0.29	0.02	-0.11	-0.53	-0.45	-0.04	0.01	0.00	-7.65	-17.85	8.39	13
P	0.20	0.05	-0.09	-0.46	-0.46	-0.05	0.00	0.00	-7.29	-17.00	9.66	13
P	0.27	0.00	-0.06	-0.43	-0.45	-0.03	-0.01	-0.01	-5.90	-15.64	9.55	13
Q	0.32	0.05	-0.29	-0.37	-0.39	0.09	0.06	0.03	-5.11	-23.60	8.15	14
Q	0.32	0.02	-0.30	-0.40	-0.39	0.08	0.04	0.01	-4.95	-22.35	6.62	14
Q	0.33	0.04	-0.19	-0.45	-0.39	0.08	0.04	0.03	-4.04	-22.93	8.25	14
Q	0.22	0.06	-0.20	-0.45	-0.38	0.08	0.04	0.02	-3.99	-23.16	7.69	14
Q	0.21	0.03	-0.27	-0.47	-0.38	0.10	0.03	0.01	-3.97	-24.01	7.20	14
Q	0.25	0.03	-0.18	-0.43	-0.39	0.09	0.03	0.01	-4.44	-22.58	7.26	14
R	0.42	0.14	0.82	0.76	-0.22	0.02	-0.31	-0.12	25.05	10.91	21.83	15
R	0.43	0.17	0.86	0.75	-0.22	0.05	-0.31	-0.13	25.25	11.00	23.05	15
R	0.41	0.16	0.87	0.77	-0.22	0.05	-0.29	-0.12	24.77	9.65	22.76	15
R	0.42	0.17	0.89	0.59	-0.21	0.03	-0.30	-0.12	24.81	8.50	21.28	15
R	0.37	0.18	0.84	0.69	-0.20	0.02	-0.33	-0.14	25.62	11.62	20.98	15
R	0.34	0.16	0.74	0.58	-0.20	0.02	-0.33	-0.14	25.48	9.79	20.24	15
S	0.38	0.15	-0.26	-0.58	-0.30	-0.26	0.03	0.02	-1.87	-15.93	-1.06	16
S	0.37	0.14	-0.26	-0.55	-0.30	-0.26	0.03	0.01	-2.07	-15.22	-1.67	16
S	0.37	0.16	-0.23	-0.52	-0.30	-0.26	0.01	0.01	-0.49	-14.24	0.54	16
S	0.34	0.15	-0.17	-0.56	-0.31	-0.28	0.02	0.01	-1.55	-15.04	-0.47	16
S	0.37	0.16	-0.26	-0.57	-0.31	-0.26	0.02	0.01	-1.68	-15.09	0.04	16
S	0.35	0.16	-0.24	-0.55	-0.28	-0.26	0.02	0.01	-0.36	-15.40	-1.35	16
T	0.37	0.06	-0.21	-0.49	-0.20	-0.31	0.03	0.01	4.43	-15.84	-6.85	17
T	0.40	0.06	-0.16	-0.52	-0.19	-0.30	0.02	0.02	5.28	-16.10	-6.85	17
T	0.38	0.05	-0.09	-0.48	-0.19	-0.30	-0.01	0.00	7.10	-14.06	-5.69	17
T	0.36	0.04	-0.14	-0.48	-0.23	-0.32	-0.01	-0.01	4.01	-12.55	-5.80	17
T	0.37	0.04	-0.17	-0.50	-0.22	-0.30	0.02	0.00	3.84	-15.00	-6.29	17
T	0.33	0.04	-0.26	-0.51	-0.26	-0.28	0.02	0.00	1.21	-15.15	-5.52	17
V	0.37	0.05	-0.16	-0.55	-0.43	0.05	0.04	-0.04	-11.30	-18.98	3.94	18
V	0.36	0.04	-0.18	-0.55	-0.44	0.08	0.02	-0.04	-10.40	-19.00	5.34	18
V	0.38	0.05	-0.17	-0.55	-0.43	0.08	0.03	-0.03	-10.81	-19.19	4.86	18
V	0.33	0.03	-0.15	-0.49	-0.43	0.08	0.01	-0.05	-9.89	-17.59	5.05	18
V	0.32	0.02	-0.16	-0.49	-0.42	0.05	0.03	-0.04	-9.89	-18.38	3.57	18
V	0.31	0.04	-0.27	-0.56	-0.43	0.10	0.03	-0.04	-10.26	-20.45	4.71	18
W	0.10	-0.08	-0.55	-0.78	-0.86	-0.97	-0.59	-0.46	-24.98	51.86	4.51	19
W	0.16	-0.07	-0.56	-0.78	-0.86	-0.97	-0.58	-0.45	-25.66	51.43	4.43	19
W	0.14	-0.10	-0.54	-0.79	-0.87	-0.97	-0.57	-0.45	-26.39	50.47	4.43	19

W	0.17	-0.10	-0.54	-0.78	-0.87	-0.97	-0.57	-0.45	-26.17	50.95	3.98	19
W	0.16	-0.08	-0.56	-0.78	-0.88	-0.97	-0.59	-0.46	-26.61	52.14	4.87	19
W	0.11	-0.11	-0.55	-0.79	-0.88	-0.97	-0.59	-0.47	-26.33	52.02	4.01	19
Y	0.30	0.05	0.28	-0.12	-0.59	-0.77	-0.49	-0.39	-7.07	44.50	4.91	20
Y	0.39	0.06	0.30	-0.13	-0.57	-0.77	-0.44	-0.35	-7.26	41.06	4.06	20
Y	0.38	0.06	0.27	-0.20	-0.57	-0.78	-0.45	-0.36	-7.47	41.61	2.55	20
Y	0.40	0.05	0.29	-0.18	-0.60	-0.77	-0.45	-0.36	-9.47	42.31	3.91	20
Y	0.43	0.04	0.28	-0.16	-0.51	-0.79	-0.46	-0.37	-4.03	42.22	-0.10	20
Y	0.34	0.05	0.28	-0.13	-0.59	-0.78	-0.46	-0.37	-8.60	43.22	3.73	20

Table 31. Detection and identification of unknown samples using LDA from an array of 6 metals-based selected elements tongue against 20 amino acids (25 mM). According to the verification, 72 among 80 unknown samples were correctly identified, representing an accuracy of 90%.

Analyte	Fluorescence response pattern						Results LDA (the first three scores)					
Unknown samples	**P5**-Fe (PH7)	**P5**-Co (PH7)	**P5**-Fe (PH10)	**P5**-Co (PH13)	GFP-Co (PH7)	GFP-Cu (PH7)	Factor 1	Factor 2	Factor 3	Group	Identification	Verification
1	-0.20	-0.20	-0.72	-0.86	0.00	-0.07	-14.15	1.92	6.53	11	M	M
2	1.16	0.25	1.61	-0.29	0.09	0.21	16.68	4.75	12.41	4	E	E
3	-0.31	-0.43	-0.88	-0.97	-0.13	0.16	-20.95	-4.31	5.03	5	F	F
4	-0.20	-0.39	-0.66	-0.76	0.05	0.33	-16.12	-2.14	2.22	8	I	I
5	-0.27	0.40	-0.41	-0.06	0.19	0.33	9.62	15.98	-7.60	17	T	T
6	-0.31	0.28	-0.56	-0.16	0.19	0.21	5.41	14.42	-6.33	16	S	S
7	-0.21	-0.37	-0.89	-0.97	0.01	0.14	-20.16	-1.82	7.16	5	F	F
8	-0.15	-0.40	-0.62	-0.83	0.05	0.02	-16.67	-1.61	5.02	5	F	L
9	-0.37	-0.52	-0.62	-0.12	0.08	0.22	-6.85	0.80	-13.74	13	P	P
10	-0.18	-0.87	6.08	-0.69	-0.71	0.35	11.01	-46.56	-3.89	2	C	C
11	0.73	-0.77	-0.14	-0.65	-0.52	0.34	-13.16	-12.78	5.60	7	H	H
12	-0.35	-0.11	-0.57	-0.22	-0.06	0.17	-1.17	5.65	-9.06	6	G	G
13	-0.11	-0.85	5.90	-0.71	-0.80	0.49	10.49	-46.82	-3.28	2	C	C
14	-0.26	-0.36	-0.63	-0.15	-0.03	0.42	-4.58	1.53	-11.80	1	A	A
15	0.57	0.30	0.39	-0.40	0.09	0.51	7.97	8.10	7.45	12	N	N
16	0.77	-0.39	-0.07	-0.91	-0.07	0.35	-13.26	-5.36	15.74	20	Y	Y
17	-0.16	0.35	-0.52	0.02	0.12	0.34	10.54	16.01	-8.85	17	T	T
18	-0.35	-0.36	-0.63	-0.13	0.08	0.32	-4.49	3.00	-12.57	1	A	A
19	-0.26	-0.41	-0.54	-0.24	0.04	0.20	-6.35	1.25	-9.34	18	V	V
20	0.71	0.26	0.28	-0.37	-0.10	0.42	8.54	7.16	7.71	12	N	D
21	0.91	0.24	2.10	0.03	0.04	0.41	23.65	3.00	2.17	15	R	K
22	-0.31	-0.30	-0.42	0.14	0.05	0.22	2.64	5.25	-17.38	14	Q	Q
23	-0.77	-0.98	-0.88	-0.98	-0.13	0.27	-31.22	-14.57	-3.89	19	W	W
24	-0.30	-0.40	-0.51	-0.22	0.05	0.18	-5.87	1.51	-10.05	18	V	V
25	-0.78	-0.98	-0.90	-0.98	-0.14	0.24	-31.21	-14.52	-4.02	19	W	W
26	1.25	0.44	2.93	0.07	0.19	0.63	31.17	3.37	6.34	9	K	K
27	-0.30	-0.42	-0.55	-0.12	0.03	0.37	-4.76	1.07	-13.02	1	A	A
28	0.31	0.28	0.44	-0.38	0.06	0.41	7.79	7.27	4.17	12	N	N
29	-0.27	-0.38	-0.68	-0.84	-0.01	-0.09	-16.70	-1.17	4.24	5	F	L
30	0.39	-0.76	-0.24	-0.67	-0.56	0.44	-14.85	-13.82	1.80	7	H	H
31	-0.17	-0.31	-0.63	-0.83	0.20	0.36	-16.37	-0.35	4.97	10	L	L
32	-0.49	-0.34	-0.62	-0.77	-0.03	0.23	-15.55	-2.25	-0.42	8	I	I
33	-0.38	-0.28	-0.40	0.25	0.13	0.29	4.29	6.47	-20.27	14	Q	Q
34	0.37	0.29	1.30	0.09	-0.04	0.29	21.00	6.94	-4.90	15	R	R
35	0.53	-0.42	0.09	-0.91	-0.22	0.25	-12.86	-7.78	12.71	20	Y	Y
36	-0.34	-0.52	-0.65	-0.15	0.02	0.20	-7.08	0.34	-12.99	13	P	P

37	-0.38	-0.27	-0.88	-0.97	-0.05	0.10	-18.73	-0.83	5.82	5	F	F
38	0.86	0.37	0.58	-0.43	0.20	0.33	10.04	10.23	12.67	3	D	D
39	-0.27	-0.05	-0.70	-0.88	0.00	-0.10	-12.17	4.17	7.24	11	M	M
40	-0.38	-0.27	-0.42	0.26	0.14	0.26	4.53	6.94	-20.20	14	Q	Q
41	0.96	0.31	1.62	-0.27	0.12	0.39	17.04	4.87	9.78	4	E	E
42	0.69	0.35	0.59	-0.32	0.14	0.43	11.22	9.38	7.88	3	D	D
43	-0.18	-0.34	-0.65	-0.80	-0.03	0.31	-15.58	-2.12	3.46	10	L	I
44	0.66	0.42	0.53	-0.46	0.05	0.45	9.77	8.93	10.70	12	N	N
45	0.79	-0.76	-0.14	-0.65	-0.54	0.38	-12.93	-12.93	6.09	7	H	H
46	-0.21	0.40	-0.35	0.06	0.04	0.18	13.19	16.18	-9.69	17	T	T
47	-0.40	-0.52	-0.61	-0.14	0.03	0.16	-6.96	0.36	-13.69	13	P	P
48	-0.26	0.37	-0.54	-0.16	0.09	0.39	7.20	14.36	-6.11	16	S	S
49	-0.20	-0.86	5.62	-0.66	-0.71	0.41	9.46	-44.39	-4.71	2	C	C
50	-0.35	0.02	-0.54	-0.33	0.06	0.40	-1.70	6.83	-5.99	6	G	G
51	-0.28	-0.23	-0.43	0.19	0.05	0.21	4.78	7.01	-17.64	14	Q	Q
52	-0.73	-0.98	-0.81	-0.97	-0.12	0.19	-30.67	-14.47	-3.34	19	W	W
53	-0.09	-0.38	-0.91	-0.97	-0.10	0.16	-19.58	-2.57	7.79	5	F	F
54	1.22	0.25	2.16	0.20	0.04	0.45	27.90	4.44	1.68	15	R	K
55	-0.26	-0.39	-0.60	-0.24	-0.01	0.34	-6.37	0.86	-9.73	18	V	A
56	0.80	-0.76	-0.26	-0.67	-0.57	0.33	-13.57	-12.53	6.43	7	H	H
57	-0.27	-0.41	-0.52	-0.22	0.08	0.20	-6.13	1.60	-9.75	18	V	V
58	0.88	0.29	1.46	0.10	0.14	0.18	22.77	9.06	1.49	15	R	R
59	-0.72	-0.98	-0.89	-0.97	-0.10	0.20	-31.03	-13.97	-3.22	19	W	W
60	-0.29	0.37	-0.53	-0.17	0.21	0.33	6.56	15.39	-5.50	16	S	S
61	-0.19	-0.32	-0.62	-0.84	0.14	0.29	-16.43	-0.85	4.85	10	L	L
62	0.81	-0.39	0.56	-0.91	-0.06	0.29	-10.13	-7.86	16.46	20	Y	Y
63	-0.12	-0.36	0.00	-0.75	-0.01	0.23	-11.78	-4.43	3.33	8	I	I
64	1.16	0.38	3.24	0.08	0.19	0.43	31.95	1.92	5.34	9	K	K
65	-0.16	-0.16	-0.66	-0.88	-0.01	-0.09	-13.49	2.22	7.81	11	M	M
66	-0.37	-0.06	-0.49	-0.31	0.07	0.33	-2.34	5.73	-6.99	6	G	G
67	-0.13	-0.11	-0.66	-0.88	0.06	-0.08	-13.05	3.54	8.74	11	M	M
68	-0.35	-0.41	-0.50	-0.22	0.05	0.18	-6.20	1.14	-10.63	18	V	V
69	1.11	0.34	1.24	0.18	0.21	0.30	24.08	11.80	2.33	15	R	R
70	-0.31	-0.07	-0.53	-0.30	0.04	0.37	-2.38	5.47	-6.87	6	G	G
71	0.83	0.22	1.50	0.16	0.19	0.17	22.46	8.36	-0.61	15	R	R
72	-0.31	-0.51	-0.61	-0.16	0.01	0.13	-6.76	0.45	-12.37	13	P	P
73	1.16	0.35	1.85	-0.24	0.13	0.36	19.74	5.24	11.71	4	E	E
74	0.70	-0.42	0.05	-0.90	-0.09	0.25	-12.84	-6.11	14.82	20	Y	Y
75	0.14	0.36	0.32	-0.31	-0.09	0.19	10.14	9.16	1.53	12	N	N
76	1.18	0.38	2.30	-0.28	0.19	0.37	21.42	3.91	13.43	4	E	E
77	-0.24	0.31	-0.50	-0.11	-0.16	0.06	8.87	13.05	-7.49	16	S	T
78	0.90	0.40	0.51	-0.46	0.26	0.38	9.37	11.14	14.25	3	D	D
79	-0.35	0.22	-0.51	-0.08	0.15	0.36	5.79	12.66	-9.60	16	S	S
80	-0.31	-0.85	4.29	-0.68	-0.81	0.19	3.76	-38.16	-5.68	2	C	C

Table 32. Detection and identification of unknown samples using LDA from an array of eight optimized sensor elements tongue against 20 amino acids (25 mM). According to the verification, all of the 80 unknown samples were correctly identified, representing an accuracy of 100%.

Analyte	Fluorescence response pattern								Results LDA (the first three scores)					
Unknown samples	**P5**-Fe (PH 7)	**P5**-Co (PH 7)	**P5**-Fe (PH 10)	**P5**-Co (PH 13)	GFP-Co (PH7)	GFP-Cu (PH7)	**P7**-CB7-AO (460 nm)	**P7**-CB7-AO (510 nm)	Factor 1	Factor 2	Factor 3	Group	Identification	Verification

1	0.20	0.20	0.72	0.86	0.00	-0.07	0.02	-0.17	18.47	4.54	4.23	11	M	M
2	1.16	0.25	1.61	0.29	0.09	0.21	-0.29	-0.20	25.10	14.00	6.32	4	E	E
3	0.31	0.43	0.88	0.97	-0.13	0.16	-0.04	-0.39	34.27	13.11	-0.97	5	F	F
4	0.20	0.39	0.66	0.76	0.05	0.33	0.01	-0.04	11.06	0.57	0.94	8	I	I
5	0.27	0.40	0.41	0.06	0.19	0.33	0.38	0.16	1.41	26.00	8.98	17	T	T
6	0.31	0.28	0.56	0.16	0.19	0.21	0.38	0.15	-2.58	24.19	8.40	16	S	S
7	0.21	0.37	0.89	0.97	0.01	0.14	-0.05	-0.40	32.96	14.12	1.72	5	F	F
8	0.15	0.40	0.62	0.83	0.05	0.02	0.04	-0.12	17.57	3.43	1.34	10	L	L
9	0.37	0.52	0.62	0.12	0.08	0.22	0.37	0.14	12.90	22.28	-3.09	13	P	P
10	0.18	0.87	6.08	0.69	-0.71	0.35	0.10	-0.02	4.62	0.14	48.29	2	C	C
11	0.73	0.77	0.14	0.65	-0.52	0.34	-0.09	-0.18	-8.58	11.69	-8.02	7	H	H
12	0.35	0.11	0.57	0.22	-0.06	0.17	0.05	0.02	0.93	11.19	3.78	6	G	G
13	0.11	0.85	5.90	0.71	-0.80	0.49	0.15	0.02	4.76	-1.63	48.62	2	C	C
14	0.26	0.36	0.63	0.15	-0.03	0.42	0.02	0.00	-1.28	-9.51	0.50	1	A	A
15	0.57	0.30	0.39	0.40	0.09	0.51	-0.37	-0.22	19.25	13.41	10.72	12	N	N
16	0.77	0.39	0.07	0.91	-0.07	0.35	-0.43	-0.45	-6.67	30.60	2.86	20	Y	Y
17	0.16	0.35	0.52	0.02	0.12	0.34	0.07	0.02	9.56	14.92	11.41	17	T	T
18	0.35	0.36	0.63	0.13	0.08	0.32	0.03	0.02	-1.23	10.80	1.69	1	A	A
19	0.26	0.41	0.54	0.24	0.04	0.20	0.31	0.06	14.02	16.63	-1.87	18	V	V
20	0.71	0.26	0.28	0.37	-0.10	0.42	-0.37	-0.25	17.85	14.40	9.64	3	D	D
21	0.91	0.24	2.10	0.03	0.04	0.41	-0.36	-0.21	31.92	10.40	2.51	9	K	K
22	0.31	0.30	0.42	0.14	0.05	0.22	0.41	0.16	-6.88	27.75	-1.48	14	Q	Q
23	0.77	0.98	0.88	0.98	-0.13	0.27	-0.61	-0.60	27.29	31.72	-5.16	19	W	W
24	0.30	0.40	0.51	0.22	0.05	0.18	0.31	0.05	14.54	16.78	-1.87	18	V	V
25	0.78	0.98	0.90	0.98	-0.14	0.24	-0.64	-0.62	27.33	32.97	-4.94	19	W	W
26	1.25	0.44	2.93	0.07	0.19	0.63	-0.26	-0.13	39.27	6.97	1.58	9	K	K
27	0.30	0.42	0.55	0.12	0.03	0.37	0.00	-0.02	-1.76	-8.90	0.06	1	A	A
28	0.31	0.28	0.44	0.38	0.06	0.41	-0.39	-0.24	17.33	12.32	9.33	12	N	N
29	0.27	0.38	0.68	0.84	-0.01	-0.09	0.04	-0.12	18.17	2.59	1.52	10	L	L
30	0.39	0.76	0.24	0.67	-0.56	0.44	-0.11	-0.20	11.23	10.59	-9.35	7	H	H
31	0.17	0.31	0.63	0.83	0.20	0.36	0.06	-0.12	17.58	2.46	2.34	10	L	L
32	0.49	0.34	0.62	0.77	-0.03	0.23	0.03	-0.03	11.96	-2.09	-0.02	8	I	I
33	0.38	0.28	0.40	0.25	0.13	0.29	0.45	0.19	-6.16	31.32	-1.32	14	Q	Q
34	0.37	0.29	1.30	0.09	-0.04	0.29	-0.48	-0.27	29.37	9.97	6.22	15	R	R
35	0.53	0.42	0.09	0.91	-0.22	0.25	-0.47	-0.48	-7.65	30.86	0.07	20	Y	Y
36	0.34	0.52	0.65	0.15	0.02	0.20	0.38	0.17	11.65	22.68	-3.33	13	P	P
37	0.38	0.27	0.88	0.97	-0.05	0.10	-0.05	-0.41	33.54	13.07	1.97	5	F	F
38	0.86	0.37	0.58	0.43	0.20	0.33	-0.31	-0.21	20.06	13.77	12.75	3	D	D
39	0.27	0.05	0.70	0.88	0.00	-0.10	0.03	-0.16	17.11	3.35	5.92	11	M	M
40	0.38	0.27	0.42	0.26	0.14	0.26	0.42	0.18	-5.15	30.42	-0.65	14	Q	Q
41	0.96	0.31	1.62	0.27	0.12	0.39	-0.34	-0.24	24.41	14.55	6.16	4	E	E
42	0.69	0.35	0.59	0.32	0.14	0.43	-0.38	-0.27	19.60	14.51	11.36	3	D	D
43	0.18	0.34	0.65	0.80	-0.03	0.31	0.06	-0.01	10.90	-1.22	0.63	8	I	I
44	0.66	0.42	0.53	0.46	0.05	0.45	-0.43	-0.27	20.99	16.98	11.98	12	N	N
45	0.79	0.76	0.14	0.65	-0.54	0.38	-0.06	-0.18	-9.60	11.19	-8.39	7	H	H
46	0.21	0.40	0.35	0.06	0.04	0.18	0.11	0.04	9.81	17.32	10.48	17	T	T
47	0.40	0.52	0.61	0.14	0.03	0.16	0.33	0.14	10.89	21.19	-3.07	13	P	P
48	0.26	0.37	0.54	0.16	0.09	0.39	0.10	0.04	6.23	14.66	10.41	16	S	S
49	0.20	0.86	5.62	0.66	-0.71	0.41	0.16	0.02	2.39	-2.90	46.53	2	C	C
50	0.35	0.02	0.54	0.33	0.06	0.40	0.08	0.04	0.16	11.30	5.12	6	G	G
51	0.28	0.23	0.43	0.19	0.05	0.21	0.43	0.19	-4.62	29.58	-0.32	14	Q	Q
52	0.73	0.98	0.81	0.97	-0.12	0.19	-0.64	-0.62	26.59	33.22	-4.86	19	W	W

53	0.09	0.38	0.91	0.97	-0.10	0.16	-0.07	-0.41	31.80	15.44	1.21	5	F	F
54	1.22	0.25	2.16	0.20	0.04	0.45	-0.39	-0.23	36.75	11.27	3.56	9	K	K
55	0.26	0.39	0.60	0.24	-0.01	0.34	0.02	0.01	-1.66	-8.27	0.56	1	A	A
56	0.80	0.76	0.26	0.67	-0.57	0.33	-0.14	-0.21	-8.11	14.17	-7.18	7	H	H
57	0.27	0.41	0.52	0.22	0.08	0.20	0.33	0.06	14.54	17.54	-1.81	18	V	V
58	0.88	0.29	1.46	0.10	0.14	0.18	-0.15	-0.06	29.29	-0.35	6.75	15	R	R
59	0.72	0.98	0.89	0.97	-0.10	0.20	-0.65	-0.63	26.76	33.83	-4.20	19	W	W
60	0.29	0.37	0.53	0.17	0.21	0.33	0.38	0.17	-0.86	24.73	9.23	16	S	S
61	0.19	0.32	0.62	0.84	0.14	0.29	0.03	-0.13	17.39	3.35	2.02	10	L	L
62	0.81	0.39	0.56	0.91	-0.06	0.29	-0.45	-0.48	-5.32	32.92	0.13	20	Y	Y
63	0.12	0.36	0.00	0.75	-0.01	0.23	0.07	0.00	-8.24	-1.43	-2.33	8	I	I
64	1.16	0.38	3.24	0.08	0.19	0.43	-0.28	-0.14	39.43	7.70	0.01	9	K	K
65	0.16	0.16	0.66	0.88	-0.01	-0.09	0.07	-0.15	18.59	3.20	4.21	11	M	M
66	0.37	0.06	0.49	0.31	0.07	0.33	0.07	0.03	-0.14	10.84	4.19	6	G	G
67	0.13	0.11	0.66	0.88	0.06	-0.08	0.05	-0.17	18.26	4.65	5.69	11	M	M
68	0.35	0.41	0.50	0.22	0.05	0.18	0.27	0.02	14.81	15.28	-2.01	18	V	V
69	1.11	0.34	1.24	0.18	0.21	0.30	-0.11	-0.02	31.49	-2.23	9.18	15	R	R
70	0.31	0.07	0.53	0.30	0.04	0.37	0.04	0.02	0.50	-9.51	4.24	6	G	G
71	0.83	0.22	1.50	0.16	0.19	0.17	-0.23	-0.10	30.36	2.17	6.54	15	R	R
72	0.31	0.51	0.61	0.16	0.01	0.13	0.33	0.15	10.21	20.77	-2.81	13	P	P
73	1.16	0.35	1.85	0.24	0.13	0.36	-0.31	-0.21	28.17	13.76	6.30	4	E	E
74	0.70	0.42	0.05	0.90	-0.09	0.25	-0.47	-0.48	-6.98	32.17	2.14	20	Y	Y
75	0.14	0.36	0.32	0.31	-0.09	0.19	-0.36	-0.22	17.88	8.88	9.94	12	N	N
76	1.18	0.38	2.30	0.28	0.19	0.37	-0.31	-0.20	30.23	14.37	5.00	4	E	E
77	0.24	0.31	0.50	0.11	-0.16	0.06	0.08	0.02	6.75	14.19	8.73	17	T	T
78	0.90	0.40	0.51	0.46	0.26	0.38	-0.33	-0.21	20.29	15.01	14.12	3	D	D
79	0.35	0.22	0.51	0.08	0.15	0.36	0.35	0.15	-1.39	24.99	6.43	16	S	S
80	0.31	0.85	4.29	0.68	-0.81	0.19	0.11	-0.01	-1.96	-2.22	39.43	2	C	C

5.3.3 LDA Calculation of Teas (Chapter 4)

Table 33. Training matrix of fluorescence response pattern from an array of **P7**/CB[8], **P13**/CB[8] and **P14**/CB[8] (each at pH 3 and 13, buffered) against 12 analytes. LDA was carried out and resulting in 6 factors of the canonical scores (the first three scores were shown here) and group generation.

Analytes	Fluorescence Response Pattern						Results LDA (the first three scores)			
	P7/CB[8] (pH3)	**P13**/CB[8] (pH3)	**P14**/CB[8] (pH3)	**P7**/CB[8] (pH13)	**P13**/CB[8] (pH13)	**P14**/CB[8] (pH13)	Factor 1	Factor 2	Factor 3	Group
Asp	-0.10	-0.04	0.05	0.12	0.08	0.10	-3.65	-15.79	-2.64	3
Asp	-0.10	-0.04	0.05	0.10	0.08	0.08	-4.13	-15.92	-3.41	3
Asp	-0.09	-0.04	0.05	0.10	0.08	0.07	-3.91	-15.79	-3.78	3
Asp	-0.10	-0.05	0.04	0.12	0.07	0.07	-4.37	-16.87	-3.27	3
Asp	-0.06	-0.04	0.07	0.10	0.08	0.10	-3.69	-14.37	-1.84	3
Asp	-0.06	-0.05	0.05	0.16	0.09	0.08	-3.50	-15.70	-2.55	3
Glu	0.03	0.10	0.10	0.30	0.22	0.21	4.98	-3.05	-1.42	7
Glu	0.01	0.12	0.09	0.28	0.22	0.21	5.06	-2.53	-2.41	7
Glu	0.01	0.10	0.08	0.24	0.22	0.21	4.87	-3.92	-1.46	7
Glu	0.00	0.08	0.07	0.28	0.20	0.17	3.48	-5.72	-2.77	7
Glu	-0.03	0.10	0.09	0.23	0.21	0.17	3.68	-4.45	-4.45	7
Glu	-0.01	0.08	0.10	0.30	0.22	0.21	4.79	-5.04	-1.68	7
Phe	0.07	0.12	0.07	0.39	0.13	0.27	2.34	-1.49	2.42	8
Phe	0.06	0.08	0.07	0.37	0.19	0.25	4.88	-3.75	2.44	8
Phe	0.07	0.10	0.09	0.36	0.18	0.24	4.10	-2.22	1.26	8

Phe	0.05	0.09	0.07	0.31	0.18	0.24	4.23	-3.46	1.40	8
Phe	0.06	0.10	0.08	0.33	0.16	0.23	3.26	-2.71	0.86	8
Phe	0.05	0.12	0.09	0.35	0.12	0.25	1.31	-1.93	1.54	8
Asn	0.02	0.09	0.13	0.26	0.13	0.09	-1.30	-4.19	-6.19	2
Asn	0.02	0.08	0.13	0.31	0.10	0.08	-2.69	-4.77	-6.13	2
Asn	0.01	0.10	0.13	0.28	0.12	0.06	-2.13	-3.71	-7.93	2
Asn	0.02	0.10	0.12	0.29	0.11	0.07	-2.25	-3.65	-7.49	2
Asn	-0.01	0.10	0.11	0.26	0.07	0.08	-4.24	-4.48	-6.68	2
Asn	0.01	0.10	0.13	0.24	0.09	0.07	-3.51	-3.52	-7.03	2
Gln	0.09	0.12	0.17	0.34	0.25	0.21	6.26	0.71	-1.57	6
Gln	0.10	0.11	0.18	0.40	0.22	0.18	4.65	0.20	-2.08	6
Gln	0.08	0.12	0.15	0.34	0.24	0.16	5.23	0.04	-3.74	6
Gln	0.07	0.12	0.16	0.38	0.26	0.20	6.63	0.52	-3.05	6
Gln	0.07	0.11	0.14	0.30	0.24	0.21	6.15	-0.36	-1.06	6
Gln	0.09	0.10	0.15	0.32	0.29	0.21	8.05	-0.46	-1.41	6
Arg	0.08	0.14	0.15	0.37	0.03	0.05	-6.24	0.24	-7.77	1
Arg	0.11	0.14	0.17	0.40	0.04	0.04	-5.64	1.08	-7.54	1
Arg	0.11	0.11	0.14	0.37	0.07	0.05	-4.39	-1.05	-6.46	1
Arg	0.07	0.10	0.14	0.31	0.07	0.07	-4.05	-2.42	-5.93	1
Arg	0.10	0.12	0.15	0.39	0.06	0.04	-4.80	-0.53	-7.35	1
Arg	0.11	0.11	0.14	0.29	0.00	0.06	-7.26	-1.27	-5.15	1
Ser	0.07	0.02	0.14	0.27	0.34	0.22	10.71	-5.64	1.31	9
Ser	0.06	0.00	0.14	0.27	0.33	0.19	9.51	-7.26	0.83	9
Ser	0.06	0.02	0.12	0.19	0.32	0.20	9.56	-6.59	1.18	9
Ser	0.06	0.00	0.11	0.20	0.33	0.20	9.91	-7.81	1.52	9
Ser	0.05	0.01	0.12	0.19	0.37	0.20	11.51	-7.12	0.63	9
Ser	0.05	0.00	0.13	0.25	0.35	0.24	11.21	-7.08	2.52	9
GABA	0.16	0.06	0.18	0.32	0.32	0.30	11.49	-0.45	5.80	5
GABA	0.18	0.04	0.17	0.32	0.33	0.31	11.92	-1.58	7.38	5
GABA	0.16	0.03	0.22	0.28	0.33	0.27	10.75	-1.53	5.08	5
GABA	0.17	0.05	0.17	0.27	0.27	0.26	8.19	-1.47	5.24	5
GABA	0.16	0.04	0.14	0.29	0.31	0.28	10.49	-2.59	6.03	5
GABA	0.16	0.03	0.18	0.30	0.28	0.30	9.40	-2.54	7.63	5
Thea	0.19	0.05	0.21	0.30	0.39	0.38	15.55	0.74	9.77	11
Thea	0.19	0.04	0.22	0.29	0.32	0.41	13.20	0.18	12.59	11
Thea	0.18	0.05	0.20	0.32	0.37	0.40	15.06	0.22	10.90	11
Thea	0.20	0.03	0.22	0.30	0.36	0.35	14.02	-0.31	9.65	11
Thea	0.15	0.02	0.18	0.32	0.32	0.40	12.89	-2.49	11.70	11
Thea	0.12	0.05	0.14	0.29	0.39	0.36	15.58	-2.35	8.00	11
Caff	0.21	0.32	0.33	0.43	0.69	0.37	28.65	21.12	-4.35	4
Caff	0.23	0.35	0.34	0.43	0.67	0.39	28.22	23.48	-3.61	4
Caff	0.26	0.34	0.31	0.39	0.68	0.37	28.55	22.92	-3.67	4
Caff	0.27	0.35	0.32	0.38	0.68	0.38	28.73	24.31	-3.15	4
Caff	0.24	0.33	0.33	0.36	0.72	0.38	30.29	22.45	-3.71	4
Caff	0.21	0.32	0.29	0.39	0.72	0.36	30.04	20.66	-4.89	4
Tbro	0.21	0.07	0.28	0.23	-0.29	0.13	-19.94	0.25	5.02	10
Tbro	0.22	0.10	0.27	0.23	-0.28	0.11	-20.03	2.33	3.22	10
Tbro	0.16	0.09	0.29	0.20	-0.27	0.13	-19.60	0.88	2.64	10
Tbro	0.20	0.10	0.32	0.23	-0.29	0.13	-20.10	2.49	3.71	10
Tbro	0.21	0.08	0.29	0.21	-0.29	0.10	-20.91	0.76	3.09	10
Tbro	0.20	0.09	0.28	0.24	-0.29	0.08	-21.11	0.98	1.57	10
Tphy	0.26	0.29	0.35	0.41	-0.84	0.07	-46.12	13.52	0.86	12

Tphy	0.24	0.29	0.35	0.41	-0.83	0.09	-45.33	13.49	1.18	12
Tphy	0.29	0.26	0.38	0.36	-0.84	0.08	-45.93	13.05	2.87	12
Tphy	0.31	0.23	0.40	0.40	-0.85	0.06	-47.02	11.93	3.41	12
Tphy	0.29	0.26	0.35	0.38	-0.82	0.08	-45.07	12.81	2.82	12
Tphy	0.24	0.26	0.32	0.38	-0.85	0.07	-46.43	10.60	1.57	12

Table 34. LDA jackknifed classification matrix table obtained from an array of **P7**/CB[8], **P13**/CB[8] and **P14**/CB[8] (each at pH 3 and 13, buffered) against 12 analytes. The jackknifed classification matrix with cross-validation reveals a 99% accuracy.

	Arg	Asn	Asp	Caff	GABA	Gln	Glu	Phe	Ser	Tbro	Thea	Tphy	%correct
Arg	5	1	0	0	0	0	0	0	0	0	0	0	83
Asn	0	6	0	0	0	0	0	0	0	0	0	0	100
Asp	0	0	6	0	0	0	0	0	0	0	0	0	100
Caff	0	0	0	6	0	0	0	0	0	0	0	0	100
GABA	0	0	0	0	6	0	0	0	0	0	0	0	100
Gln	0	0	0	0	0	6	0	0	0	0	0	0	100
Glu	0	0	0	0	0	0	6	0	0	0	0	0	100
Phe	0	0	0	0	0	0	0	6	0	0	0	0	100
Ser	0	0	0	0	0	0	0	0	6	0	0	0	100
Tbro	0	0	0	0	0	0	0	0	0	6	0	0	100
Thea	0	0	0	0	0	0	0	0	0	0	6	0	100
Tphy	0	0	0	0	0	0	0	0	0	0	0	6	100
Total	5	7	6	6	6	6	6	6	6	6	6	6	**99**

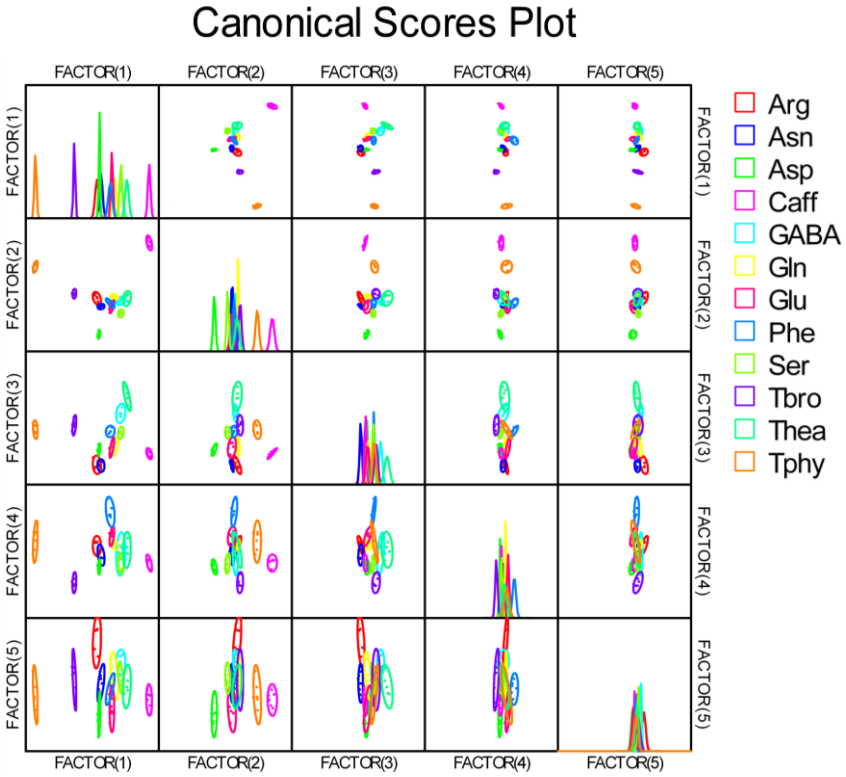

Figure 103. Correlations of canonical fluorescence response patterns from an array of **P7**/CB[8], **P13**/CB[8] and **P14**/CB[8] (each at pH 3 and 13, buffered) against 12 analytes. The 95% confidence ellipses for the individual analytes are shown.

Table 35. Detection and identification of unknown samples using LDA from an array of **P7**/CB[8], **P13**/CB[8] and **P14**/CB[8] (each at pH 3 and 13, buffered). According to the verification, 46 among 48 unknown samples were correctly identified, representing an accuracy of 95.8%.

Unknown samples	Fluorescence Response Pattern						Results LDA (the first three scores)					
	P7/ CB[8] (pH3)	**P13**/ CB[8] (pH3)	**P14**/ CB[8] (pH3)	**P7**/ CB[8] (pH13)	**P13**/ CB[8] (pH13)	**P14**/ CB[8] (pH13)	Factor 1	Factor 2	Factor 3	Group	Identification	Verification
1	-0.01	0.09	0.08	0.19	0.21	0.19	4.18	-4.90	-2.35	7	Glu	Glu
2	-0.07	-0.03	0.07	0.12	0.10	0.09	-3.05	-13.99	-3.04	3	Asp	Asp
3	0.05	0.10	0.09	0.27	0.12	0.22	0.70	-3.27	0.95	8	Phe	Phe
4	0.01	0.08	0.12	0.22	0.08	0.07	-4.11	-4.92	-6.37	2	Asn	Asn
5	0.05	0.04	0.13	0.21	0.37	0.24	12.10	-4.82	1.08	9	Ser	Ser
6	-0.07	-0.03	0.05	0.12	0.09	0.07	-3.40	-14.68	-3.44	3	Asp	Asp
7	-0.03	0.09	0.08	0.17	0.20	0.21	3.68	-5.29	-1.38	7	Glu	Glu
8	0.06	0.10	0.08	0.28	0.12	0.25	1.29	-2.92	2.55	8	Phe	Phe
9	0.03	0.07	0.11	0.24	0.12	0.07	-1.95	-5.34	-6.14	2	Asn	Asn
10	0.10	0.09	0.11	0.33	0.03	0.06	-5.66	-3.04	-4.77	1	Arg	Arg
11	0.24	0.36	0.33	0.44	0.73	0.36	30.62	24.58	-6.23	4	Caff	Caff
12	0.15	0.03	0.14	0.29	0.33	0.27	11.41	-3.54	5.65	5	GABA	GABA
13	0.06	0.02	0.11	0.21	0.34	0.22	10.82	-6.65	1.66	9	Ser	Ser
14	0.24	0.32	0.34	0.38	0.69	0.37	28.70	21.82	-3.28	4	Caff	Caff
15	0.19	0.08	0.31	0.20	-0.29	0.13	-20.41	1.26	4.16	10	Tbro	Tbro
16	0.12	0.04	0.14	0.31	0.36	0.41	15.17	-2.76	10.37	11	Thea	Thea
17	0.17	0.10	0.31	0.22	-0.31	0.14	-20.87	1.63	3.78	10	Tbro	Tbro
18	0.07	0.12	0.10	0.29	0.03	0.05	-6.15	-2.25	-6.57	1	Arg	Arg
19	0.16	0.06	0.14	0.30	0.30	0.29	10.34	-1.07	5.80	5	GABA	GABA
20	0.22	0.33	0.37	0.37	0.73	0.40	30.85	23.02	-3.50	4	Caff	Caff
21	0.05	0.11	0.14	0.26	0.26	0.21	6.58	-1.01	-1.68	6	Gln	Gln
22	0.06	0.09	0.13	0.28	0.22	0.22	5.35	-2.07	0.30	7	Glu	Gln
23	0.10	0.14	0.12	0.32	0.06	0.05	-4.71	0.09	-7.05	1	Arg	Arg
24	0.19	0.25	0.28	0.31	-0.84	0.04	-46.62	8.09	0.06	12	Tphy	Tphy
25	0.12	0.05	0.14	0.30	0.33	0.39	13.17	-2.44	10.13	11	Thea	Thea
26	0.09	0.13	0.11	0.31	0.02	0.07	-6.27	-1.05	-5.77	1	Arg	Arg
27	0.22	0.07	0.30	0.22	-0.30	0.13	-20.52	0.75	5.09	10	Tbro	Tbro
28	0.23	0.26	0.28	0.32	-0.83	0.08	-45.22	9.66	2.27	12	Tphy	Tphy
29	0.03	0.10	0.08	0.24	0.14	0.23	1.65	-3.93	0.90	8	Phe	Phe
30	0.02	0.07	0.15	0.23	0.10	0.05	-3.28	-4.86	-6.91	2	Asn	Asn
31	0.12	0.02	0.14	0.28	0.35	0.40	14.16	-3.84	11.24	11	Thea	Thea
32	0.11	0.04	0.15	0.29	0.38	0.40	15.75	-2.71	9.71	11	Thea	Thea
33	0.00	0.07	0.11	0.21	0.07	0.08	-4.40	-5.98	-5.22	2	Asn	Asn
34	0.04	0.11	0.14	0.25	0.23	0.18	4.86	-1.57	-3.03	7	Glu	Gln
35	0.06	0.09	0.13	0.28	0.24	0.18	5.47	-2.46	-1.90	6	Gln	Gln
36	0.16	0.08	0.28	0.18	-0.30	0.11	-21.31	-0.25	2.88	10	Tbro	Tbro
37	0.23	0.23	0.30	0.34	-0.83	0.07	-45.67	8.32	2.82	12	Tphy	Tphy
38	0.22	0.24	0.27	0.34	-0.84	0.04	-46.23	8.15	0.67	12	Tphy	Tphy
39	-0.10	-0.03	0.05	0.08	0.07	0.07	-4.45	-15.71	-3.60	3	Asp	Asp
40	0.00	0.13	0.12	0.20	0.21	0.18	4.02	-1.57	-4.02	7	Glu	Glu
41	0.05	0.01	0.11	0.21	0.34	0.24	11.01	-6.80	2.58	9	Ser	Ser
42	0.16	0.03	0.18	0.28	0.28	0.30	9.42	-2.23	7.39	5	GABA	GABA
43	0.21	0.33	0.32	0.41	0.67	0.40	28.22	21.45	-2.98	4	Caff	Caff
44	0.05	0.00	0.12	0.22	0.36	0.23	11.71	-7.17	2.11	9	Ser	Ser
45	0.16	0.03	0.18	0.27	0.35	0.31	12.74	-2.30	7.47	5	GABA	GABA

46	0.06	0.10	0.08	0.28	0.15	0.20	1.81	-3.01	0.03	8	Phe	Phe
47	0.00	0.07	0.10	0.20	0.21	0.17	3.66	-5.34	-2.47	7	Glu	Glu
48	-0.07	-0.05	0.07	0.12	0.10	0.10	-2.68	-15.20	-1.58	3	Asp	Asp

Table 36. Training matrix of fluorescence response pattern from an array of **P7**/CB[8], **P13**/CB[8] and **P14**/CB[8] (each at pH 3, 7 and 13, buffered) against 22 teas. LDA was carried out and resulting in 9 factors of the canonical scores (the first three scores were shown here) and group generation. The jackknifed classification matrix with cross-validation reveals a 100% accuracy.

Analytes	Fluorescence Response Pattern									Results LDA(the first three scores)			
	P7/ CB[8] (pH3)	**P13**/ CB[8] (pH3)	**P14**/ CB[8] (pH3)	**P7**/ CB[8] (pH7)	**P13**/ CB[8] (pH7)	**P14**/ CB[8] (pH7)	**P7**/ CB[8] (pH13)	**P13**/ CB[8] (pH13)	**P14**/ CB[8] (pH13)	Factor 1	Factor 2	Factor 3	Group
B1	-0.98	-0.95	-0.89	-0.73	-0.64	-0.43	-0.44	-0.97	-0.78	-47.36	-0.06	3.41	1
B1	-0.98	-0.93	-0.90	-0.73	-0.64	-0.45	-0.45	-0.97	-0.78	-46.63	-0.35	3.40	1
B1	-0.99	-0.95	-0.90	-0.73	-0.63	-0.46	-0.44	-0.97	-0.80	-47.89	0.22	2.30	1
B1	-0.99	-0.95	-0.90	-0.74	-0.63	-0.45	-0.45	-0.97	-0.79	-47.36	-0.13	2.06	1
B1	-0.99	-0.95	-0.91	-0.73	-0.63	-0.43	-0.45	-0.97	-0.79	-47.64	-0.64	3.44	1
B1	-0.99	-0.95	-0.90	-0.74	-0.63	-0.42	-0.45	-0.97	-0.78	-47.55	-0.53	3.09	1
B2	-0.99	-0.96	-0.92	-0.93	-0.77	-0.62	-0.44	-0.97	-0.78	-54.76	19.57	1.75	2
B2	-0.98	-0.97	-0.92	-0.93	-0.77	-0.62	-0.44	-0.97	-0.78	-55.29	19.57	1.82	2
B2	-0.99	-0.96	-0.93	-0.93	-0.77	-0.61	-0.45	-0.97	-0.78	-54.87	19.10	1.40	2
B2	-0.99	-0.97	-0.92	-0.93	-0.76	-0.63	-0.42	-0.97	-0.78	-55.31	19.70	2.37	2
B2	-0.99	-0.96	-0.93	-0.94	-0.77	-0.63	-0.44	-0.97	-0.78	-55.09	19.62	2.29	2
B2	-0.99	-0.96	-0.92	-0.94	-0.77	-0.63	-0.45	-0.97	-0.77	-54.86	19.25	2.25	2
B3	-0.99	-0.94	-0.92	-0.75	-0.63	-0.43	-0.43	-0.98	-0.75	-48.16	0.71	3.81	3
B3	-0.98	-0.95	-0.93	-0.75	-0.63	-0.45	-0.44	-0.98	-0.75	-48.23	0.81	2.76	3
B3	-0.99	-0.94	-0.93	-0.76	-0.63	-0.46	-0.42	-0.97	-0.76	-48.20	1.37	2.63	3
B3	-0.99	-0.96	-0.93	-0.75	-0.63	-0.46	-0.41	-0.98	-0.78	-49.07	1.16	2.14	3
B3	-0.99	-0.95	-0.94	-0.77	-0.63	-0.45	-0.40	-0.97	-0.76	-48.51	1.30	2.06	3
B3	-0.99	-0.96	-0.93	-0.77	-0.63	-0.45	-0.48	-0.98	-0.77	-49.07	0.71	2.25	3
B4	-0.94	-0.82	-0.67	-0.90	-0.73	-0.58	-0.47	-0.98	-0.76	-39.00	22.11	1.02	4
B4	-0.95	-0.82	-0.68	-0.89	-0.73	-0.61	-0.47	-0.98	-0.76	-39.82	22.18	1.80	4
B4	-0.94	-0.82	-0.68	-0.90	-0.73	-0.63	-0.48	-0.98	-0.76	-39.43	22.42	2.59	4
B4	-0.95	-0.82	-0.69	-0.90	-0.73	-0.59	-0.48	-0.98	-0.76	-39.55	21.78	1.07	4
B4	-0.95	-0.83	-0.66	-0.90	-0.73	-0.59	-0.48	-0.98	-0.77	-39.29	21.36	2.28	4
B4	-0.95	-0.82	-0.66	-0.91	-0.74	-0.59	-0.49	-0.98	-0.77	-39.22	22.50	1.82	4
B5	-0.96	-0.86	-0.74	-0.65	-0.51	-0.30	-0.48	-0.98	-0.77	-34.23	-9.01	4.79	5
B5	-0.96	-0.85	-0.74	-0.64	-0.53	-0.33	-0.48	-0.98	-0.77	-34.83	-7.23	4.87	5
B5	-0.96	-0.85	-0.75	-0.64	-0.51	-0.32	-0.48	-0.98	-0.76	-33.71	-9.13	4.79	5
B5	-0.97	-0.86	-0.74	-0.65	-0.50	-0.34	-0.48	-0.98	-0.77	-34.97	-8.24	3.27	5
B5	-0.96	-0.86	-0.75	-0.64	-0.53	-0.31	-0.47	-0.98	-0.77	-35.45	-7.33	5.63	5
B5	-0.96	-0.86	-0.74	-0.66	-0.52	-0.32	-0.50	-0.98	-0.76	-34.92	-7.81	4.39	5
B6	-0.69	-0.64	-0.38	-0.72	-0.53	-0.36	-0.48	-0.97	-0.71	-3.07	7.76	8.00	6
B6	-0.69	-0.66	-0.39	-0.73	-0.55	-0.36	-0.48	-0.97	-0.70	-5.11	9.21	7.93	6
B6	-0.69	-0.66	-0.40	-0.75	-0.54	-0.38	-0.49	-0.97	-0.71	-4.78	8.66	9.26	6
B6	-0.70	-0.66	-0.39	-0.72	-0.57	-0.37	-0.49	-0.97	-0.71	-6.54	9.28	6.82	6
B6	-0.68	-0.66	-0.40	-0.74	-0.57	-0.41	-0.47	-0.97	-0.71	-6.08	11.69	9.32	6
B6	-0.68	-0.63	-0.40	-0.76	-0.57	-0.40	-0.48	-0.97	-0.72	-4.25	12.11	8.38	6
B7	-0.65	-0.64	-0.34	-0.71	-0.55	-0.35	-0.48	-0.97	-0.71	-1.16	9.25	8.86	7
B7	-0.66	-0.63	-0.33	-0.75	-0.55	-0.32	-0.50	-0.97	-0.71	-1.15	10.59	8.35	7
B7	-0.68	-0.63	-0.36	-0.74	-0.55	-0.39	-0.50	-0.97	-0.70	-2.04	10.05	8.79	7
B7	-0.66	-0.63	-0.36	-0.76	-0.56	-0.36	-0.50	-0.97	-0.72	-2.08	12.00	8.39	7
B7	-0.66	-0.64	-0.37	-0.75	-0.57	-0.38	-0.50	-0.96	-0.71	-2.41	11.64	9.48	7
B7	-0.68	-0.63	-0.38	-0.75	-0.58	-0.40	-0.50	-0.96	-0.72	-2.91	11.80	8.39	7
B8	-0.63	-0.61	-0.31	-0.72	-0.54	-0.37	-0.49	-0.97	-0.69	2.72	10.38	10.66	8

B8	-0.63	-0.62	-0.32	-0.72	-0.54	-0.39	-0.49	-0.96	-0.69	1.88	10.18	11.50	8
B8	-0.65	-0.61	-0.31	-0.73	-0.54	-0.38	-0.50	-0.97	-0.72	2.00	10.51	10.61	8
B8	-0.64	-0.62	-0.32	-0.73	-0.55	-0.38	-0.50	-0.96	-0.71	1.39	10.56	10.58	8
B8	-0.63	-0.61	-0.34	-0.73	-0.55	-0.40	-0.50	-0.96	-0.70	2.13	10.09	11.11	8
B8	-0.66	-0.61	-0.34	-0.74	-0.55	-0.40	-0.51	-0.96	-0.71	1.07	10.27	10.46	8
G1	-0.52	-0.27	-0.16	-0.64	-0.58	-0.27	-0.45	-0.98	-0.60	25.49	21.88	6.69	9
G1	-0.55	-0.26	-0.19	-0.65	-0.58	-0.28	-0.43	-0.98	-0.61	25.09	21.78	-7.96	9
G1	-0.58	-0.27	-0.20	-0.67	-0.58	-0.31	-0.45	-0.98	-0.63	22.23	22.46	7.46	9
G1	-0.60	-0.30	-0.24	-0.66	-0.58	-0.29	-0.45	-0.98	-0.62	19.60	19.99	8.71	9
G1	-0.57	-0.29	-0.20	-0.66	-0.59	-0.30	-0.46	-0.98	-0.62	21.35	21.89	7.72	9
G1	-0.56	-0.29	-0.26	-0.67	-0.59	-0.30	-0.41	-0.98	-0.62	20.89	22.03	7.38	9
G2	-0.66	-0.34	-0.37	-0.71	-0.58	-0.31	-0.51	-0.98	-0.64	12.10	17.80	10.37	10
G2	-0.68	-0.35	-0.38	-0.73	-0.58	-0.30	-0.50	-0.98	-0.67	10.33	18.20	10.36	10
G2	-0.64	-0.38	-0.38	-0.69	-0.60	-0.30	-0.54	-0.98	-0.68	10.28	16.90	9.75	10
G2	-0.68	-0.30	-0.37	-0.73	-0.60	-0.33	-0.55	-0.98	-0.68	12.86	19.51	12.69	10
G2	-0.67	-0.29	-0.36	-0.72	-0.61	-0.34	-0.53	-0.98	-0.68	13.48	20.37	12.42	10
G2	-0.67	-0.32	-0.39	-0.72	-0.61	-0.33	-0.55	-0.98	-0.67	11.47	18.96	12.47	10
G3	-0.47	-0.28	-0.29	-0.33	-0.36	-0.09	-0.36	-0.98	-0.59	34.97	-8.82	9.15	11
G3	-0.51	-0.25	-0.29	-0.33	-0.37	-0.08	-0.37	-0.98	-0.60	34.55	-8.31	13.83	11
G3	-0.48	-0.26	-0.32	-0.34	-0.38	-0.07	-0.37	-0.98	-0.59	34.84	-8.14	12.87	11
G3	-0.53	-0.28	-0.26	-0.33	-0.38	-0.11	-0.37	-0.98	-0.58	32.94	-8.27	11.12	11
G3	-0.47	-0.26	-0.28	-0.31	-0.38	-0.13	-0.39	-0.98	-0.59	35.78	-7.54	9.90	11
G3	-0.51	-0.28	-0.27	-0.34	-0.37	-0.13	-0.38	-0.98	-0.61	33.64	-7.69	9.66	11
G4	-0.54	-0.30	-0.25	-0.64	-0.53	-0.25	-0.37	-0.98	-0.64	24.15	16.52	4.75	12
G4	-0.53	-0.29	-0.27	-0.65	-0.53	-0.23	-0.37	-0.98	-0.65	24.73	16.46	5.27	12
G4	-0.55	-0.32	-0.22	-0.64	-0.54	-0.25	-0.40	-0.98	-0.65	22.85	16.06	4.31	12
G4	-0.50	-0.29	-0.25	-0.66	-0.56	-0.25	-0.40	-0.97	-0.65	25.48	18.93	4.36	12
G4	-0.54	-0.31	-0.25	-0.66	-0.57	-0.26	-0.40	-0.97	-0.65	23.03	18.36	5.02	12
G4	-0.55	-0.31	-0.22	-0.66	-0.54	-0.28	-0.40	-0.97	-0.66	23.68	17.47	2.75	12
G5	-0.39	-0.36	-0.31	-0.70	-0.55	-0.32	-0.40	-0.98	-0.63	23.65	23.05	3.92	13
G5	-0.40	-0.39	-0.32	-0.69	-0.54	-0.29	-0.35	-0.98	-0.64	22.23	21.65	4.33	13
G5	-0.46	-0.36	-0.34	-0.68	-0.52	-0.33	-0.38	-0.98	-0.64	21.88	19.54	1.77	13
G5	-0.42	-0.33	-0.33	-0.73	-0.53	-0.33	-0.39	-0.98	-0.66	24.44	23.25	3.07	13
G5	-0.47	-0.33	-0.37	-0.72	-0.54	-0.36	-0.39	-0.98	-0.65	21.44	22.24	0.79	13
G5	-0.46	-0.33	-0.32	-0.70	-0.55	-0.34	-0.41	-0.98	-0.65	22.74	21.65	1.19	13
G6	-0.45	-0.27	-0.16	-0.60	-0.49	-0.27	-0.40	-0.98	-0.68	31.81	16.80	0.15	14
G6	-0.46	-0.30	-0.16	-0.61	-0.48	-0.28	-0.39	-0.98	-0.67	30.49	16.29	1.63	14
G6	-0.45	-0.29	-0.15	-0.62	-0.48	-0.26	-0.40	-0.98	-0.68	31.89	16.45	2.29	14
G6	-0.47	-0.29	-0.18	-0.63	-0.49	-0.26	-0.41	-0.98	-0.68	30.40	15.90	1.08	14
G6	-0.45	-0.28	-0.20	-0.64	-0.48	-0.28	-0.39	-0.97	-0.68	31.48	16.58	1.82	14
G6	-0.46	-0.30	-0.27	-0.66	-0.49	-0.29	-0.41	-0.97	-0.68	28.75	16.25	1.27	14
O1	-0.34	-0.28	-0.17	-0.35	-0.34	-0.12	-0.28	-0.97	-0.56	44.51	-5.42	1.50	15
O1	-0.33	-0.29	-0.17	-0.35	-0.36	-0.12	-0.28	-0.97	-0.55	43.35	-4.00	1.53	15
O1	-0.35	-0.30	-0.16	-0.35	-0.35	-0.11	-0.32	-0.97	-0.54	42.78	-5.84	1.32	15
O1	-0.35	-0.30	-0.17	-0.36	-0.36	-0.12	-0.32	-0.97	-0.54	42.30	-4.22	1.54	15
O1	-0.32	-0.30	-0.18	-0.37	-0.36	-0.13	-0.30	-0.97	-0.53	43.24	-4.37	3.52	15
O1	-0.34	-0.27	-0.18	-0.36	-0.35	-0.12	-0.31	-0.97	-0.53	44.61	-5.41	1.15	15
O2	-0.27	-0.21	-0.10	-0.36	-0.37	-0.14	-0.29	-0.97	-0.49	52.57	-1.43	3.27	16
O2	-0.27	-0.23	-0.11	-0.37	-0.38	-0.13	-0.30	-0.97	-0.52	50.87	-0.94	2.98	16
O2	-0.28	-0.25	-0.09	-0.34	-0.38	-0.12	-0.29	-0.96	-0.51	50.03	-2.78	3.36	16
O2	-0.30	-0.24	-0.13	-0.40	-0.38	-0.15	-0.30	-0.97	-0.48	48.44	0.46	3.00	16
O2	-0.29	-0.24	-0.13	-0.40	-0.38	-0.15	-0.31	-0.96	-0.50	50.14	-1.10	4.33	16

O2	-0.29	-0.23	-0.11	-0.39	-0.38	-0.14	-0.30	-0.96	-0.49	50.71	-0.56	3.38	16
O3	-0.75	-0.69	-0.46	-0.32	-0.34	-0.13	-0.43	-0.96	-0.64	1.72	-31.29	0.03	17
O3	-0.76	-0.69	-0.47	-0.35	-0.35	-0.13	-0.45	-0.95	-0.63	1.33	-31.21	0.08	17
O3	-0.74	-0.68	-0.47	-0.31	-0.34	-0.14	-0.44	-0.95	-0.63	2.41	-32.17	0.19	17
O3	-0.74	-0.69	-0.48	-0.32	-0.34	-0.14	-0.45	-0.96	-0.64	1.69	-31.55	0.21	17
O3	-0.75	-0.69	-0.45	-0.32	-0.36	-0.15	-0.44	-0.95	-0.64	1.84	-31.93	0.54	17
O3	-0.75	-0.69	-0.49	-0.33	-0.35	-0.15	-0.45	-0.95	-0.66	1.22	-32.11	0.37	17
O4	-0.66	-0.65	-0.39	-0.30	-0.34	-0.19	-0.38	-0.94	-0.60	11.73	-31.03	7.60	18
O4	-0.65	-0.63	-0.37	-0.32	-0.33	-0.16	-0.38	-0.95	-0.59	11.35	-28.21	5.20	18
O4	-0.68	-0.64	-0.39	-0.31	-0.33	-0.19	-0.40	-0.95	-0.61	10.28	-29.92	6.07	18
O4	-0.66	-0.66	-0.39	-0.33	-0.35	-0.18	-0.40	-0.95	-0.59	9.80	-28.75	7.08	18
O4	-0.65	-0.65	-0.42	-0.34	-0.34	-0.18	-0.39	-0.94	-0.61	10.50	-28.96	7.05	18
O4	-0.68	-0.63	-0.41	-0.33	-0.34	-0.19	-0.40	-0.94	-0.60	11.24	-30.25	5.79	18
O5	-0.91	-0.78	-0.64	-0.45	-0.46	-0.20	-0.45	-0.96	-0.71	-19.34	-24.02	6.32	19
O5	-0.91	-0.81	-0.65	-0.45	-0.47	-0.19	-0.48	-0.96	-0.73	-21.67	-24.05	6.23	19
O5	-0.91	-0.80	-0.64	-0.48	-0.47	-0.19	-0.48	-0.96	-0.72	-20.95	-22.47	5.64	19
O5	-0.92	-0.81	-0.65	-0.49	-0.46	-0.18	-0.46	-0.96	-0.73	-21.99	-22.79	5.24	19
O5	-0.92	-0.80	-0.61	-0.50	-0.48	-0.18	-0.49	-0.96	-0.72	-20.62	-21.52	5.48	19
O5	-0.91	-0.82	-0.61	-0.49	-0.48	-0.20	-0.48	-0.96	-0.72	-21.75	-21.09	3.79	19
O6	-0.79	-0.72	-0.46	-0.34	-0.39	-0.13	-0.44	-0.96	-0.69	-4.23	-28.35	2.95	20
O6	-0.81	-0.73	-0.48	-0.33	-0.40	-0.13	-0.44	-0.96	-0.69	-6.91	-28.41	3.73	20
O6	-0.80	-0.74	-0.50	-0.31	-0.40	-0.12	-0.46	-0.95	-0.70	-5.62	-32.63	3.08	20
O6	-0.79	-0.74	-0.50	-0.35	-0.40	-0.15	-0.45	-0.96	-0.69	-6.12	-28.20	2.08	20
O6	-0.81	-0.73	-0.45	-0.38	-0.41	-0.15	-0.45	-0.95	-0.69	-4.47	-28.42	0.26	20
O6	-0.81	-0.72	-0.47	-0.36	-0.40	-0.15	-0.47	-0.95	-0.70	-4.61	-28.71	1.09	20
O7	-0.75	-0.71	-0.48	-0.47	-0.48	-0.22	-0.46	-0.96	-0.69	-6.25	-14.67	0.32	21
O7	-0.75	-0.70	-0.48	-0.47	-0.46	-0.20	-0.46	-0.96	-0.69	-5.17	-16.49	0.06	21
O7	-0.75	-0.71	-0.46	-0.47	-0.46	-0.19	-0.45	-0.96	-0.70	-5.18	-16.53	0.24	21
O7	-0.75	-0.71	-0.46	-0.48	-0.47	-0.23	-0.46	-0.96	-0.69	-5.18	-15.22	1.93	21
O7	-0.76	-0.68	-0.46	-0.47	-0.48	-0.21	-0.46	-0.96	-0.70	-4.43	-14.39	0.88	21
O7	-0.76	-0.71	-0.46	-0.50	-0.48	-0.22	-0.47	-0.95	-0.71	-5.51	-14.84	1.83	21
O8	-0.62	-0.59	-0.42	-0.42	-0.42	-0.16	-0.37	-0.95	-0.65	9.99	-17.04	2.06	22
O8	-0.63	-0.62	-0.42	-0.42	-0.40	-0.16	-0.38	-0.95	-0.65	10.24	-21.03	5.21	22
O8	-0.64	-0.63	-0.40	-0.43	-0.40	-0.19	-0.41	-0.95	-0.65	9.53	-19.82	6.07	22
O8	-0.64	-0.63	-0.42	-0.46	-0.42	-0.19	-0.40	-0.95	-0.67	7.91	-17.72	6.27	22
O8	-0.65	-0.59	-0.44	-0.45	-0.42	-0.19	-0.42	-0.95	-0.67	8.73	-17.20	2.64	22
O8	-0.68	-0.61	-0.39	-0.47	-0.42	-0.20	-0.43	-0.94	-0.69	8.63	-18.85	5.30	22

Table 37. Training matrix of fluorescence response pattern from an array of **P7**, **P13** and **P14** (each at pH 3, 7 and 13, buffered) against 22 teas. LDA was carried out and resulting in 9 factors of the canonical scores (the first three scores were shown here) and group generation. The jackknifed classification matrix with cross-validation reveals a 100% accuracy.

Analytes	Fluorescence Response Pattern									Results LDA (the first three scores)			
	P7 (pH3)	**P13** (pH3)	**P14** (pH3)	**P7** (pH7)	**P13** (pH7)	**P14** (pH7)	**P7** (pH13)	**P13** (pH13)	**P14** (pH13)	Factor 1	Factor 2	Factor 3	Group
B1	-0.99	-0.95	-0.97	-0.57	-0.69	-0.50	-0.60	-0.98	-0.74	-57.03	12.88	5.73	1
B1	-0.99	-0.96	-0.97	-0.58	-0.69	-0.50	-0.60	-0.98	-0.76	-58.29	14.39	7.27	1
B1	-0.98	-0.94	-0.97	-0.59	-0.70	-0.51	-0.60	-0.98	-0.75	-56.42	14.54	5.59	1
B1	-0.99	-0.96	-0.97	-0.61	-0.69	-0.51	-0.60	-0.99	-0.77	-58.77	14.97	7.53	1
B1	-0.98	-0.97	-0.96	-0.60	-0.70	-0.50	-0.60	-0.98	-0.75	-58.38	15.35	6.79	1
B1	-0.99	-0.96	-0.97	-0.61	-0.69	-0.52	-0.61	-0.99	-0.77	-58.12	15.59	6.57	1
B2	-0.99	-0.98	-0.98	-0.80	-0.79	-0.64	-0.61	-0.98	-0.75	-60.81	25.96	-8.87	2
B2	-0.99	-0.97	-0.98	-0.81	-0.79	-0.68	-0.61	-0.98	-0.76	-59.71	26.39	-8.82	2
B2	-0.99	-0.97	-0.98	-0.81	-0.80	-0.68	-0.62	-0.98	-0.77	-59.37	26.66	-10.38	2
B2	-0.99	-0.98	-0.98	-0.81	-0.80	-0.69	-0.61	-0.99	-0.78	-60.36	30.21	-7.96	2

B2	-0.99	-0.97	-0.98	-0.82	-0.80	-0.66	-0.61	-0.99	-0.78	-60.59	29.85	-8.47	2
B2	-0.99	-0.98	-0.97	-0.82	-0.80	-0.69	-0.62	-0.99	-0.76	-60.04	30.37	-8.43	2
B3	-0.99	-0.97	-0.97	-0.62	-0.67	-0.49	-0.57	-0.99	-0.75	-59.89	13.33	8.87	3
B3	-0.99	-0.97	-0.98	-0.63	-0.68	-0.54	-0.58	-0.99	-0.76	-59.71	14.92	8.01	3
B3	-0.99	-0.96	-0.97	-0.63	-0.68	-0.52	-0.58	-0.99	-0.78	-59.08	14.69	8.34	3
B3	-0.99	-0.96	-0.97	-0.65	-0.68	-0.51	-0.58	-0.99	-0.76	-59.29	14.96	8.07	3
B3	-0.99	-0.98	-0.97	-0.63	-0.68	-0.52	-0.59	-0.99	-0.77	-60.48	15.24	8.59	3
B3	-0.99	-0.96	-0.97	-0.65	-0.69	-0.55	-0.58	-0.99	-0.76	-58.41	15.70	6.31	3
B4	-0.97	-0.91	-0.76	-0.73	-0.77	-0.62	-0.34	-0.98	-0.74	-46.21	22.37	-4.05	4
B4	-0.97	-0.91	-0.75	-0.74	-0.78	-0.64	-0.36	-0.98	-0.74	-44.83	24.05	-5.00	4
B4	-0.97	-0.90	-0.77	-0.74	-0.77	-0.64	-0.35	-0.98	-0.76	-46.06	23.14	-4.51	4
B4	-0.97	-0.90	-0.77	-0.76	-0.78	-0.65	-0.34	-0.98	-0.74	-45.83	24.04	-5.31	4
B4	-0.97	-0.87	-0.76	-0.76	-0.77	-0.63	-0.34	-0.98	-0.75	-44.01	23.60	-6.18	4
B4	-0.97	-0.90	-0.76	-0.76	-0.78	-0.64	-0.34	-0.98	-0.74	-45.56	23.95	-5.27	4
B5	-0.97	-0.90	-0.80	-0.57	-0.61	-0.43	-0.35	-0.98	-0.73	-47.49	3.26	14.78	5
B5	-0.97	-0.85	-0.77	-0.58	-0.61	-0.41	-0.35	-0.98	-0.75	-44.11	4.15	13.95	5
B5	-0.97	-0.86	-0.80	-0.57	-0.62	-0.42	-0.34	-0.98	-0.75	-45.71	5.40	14.11	5
B5	-0.95	-0.89	-0.79	-0.58	-0.61	-0.43	-0.34	-0.98	-0.74	-46.30	4.47	15.92	5
B5	-0.97	-0.89	-0.77	-0.57	-0.62	-0.44	-0.35	-0.98	-0.75	-45.63	5.10	14.59	5
B5	-0.95	-0.85	-0.79	-0.58	-0.62	-0.43	-0.33	-0.98	-0.74	-43.46	5.65	14.02	5
B6	-0.93	-0.86	-0.49	-0.59	-0.64	-0.45	-0.46	-0.98	-0.70	-23.95	8.14	7.16	6
B6	-0.94	-0.84	-0.51	-0.59	-0.64	-0.42	-0.47	-0.98	-0.70	-24.96	7.85	6.69	6
B6	-0.93	-0.86	-0.50	-0.60	-0.64	-0.43	-0.46	-0.98	-0.71	-24.70	8.97	6.71	6
B6	-0.92	-0.87	-0.50	-0.59	-0.65	-0.47	-0.47	-0.98	-0.71	-24.02	9.56	6.26	6
B6	-0.93	-0.86	-0.49	-0.61	-0.65	-0.46	-0.46	-0.98	-0.70	-23.92	9.54	5.47	6
B6	-0.94	-0.86	-0.49	-0.62	-0.64	-0.47	-0.45	-0.98	-0.70	-24.56	8.82	5.95	6
B7	-0.80	-0.70	-0.34	-0.59	-0.66	-0.38	-0.42	-0.97	-0.62	0.53	7.91	1.45	7
B7	-0.80	-0.69	-0.33	-0.58	-0.65	-0.43	-0.43	-0.97	-0.62	3.18	7.82	0.47	7
B7	-0.80	-0.68	-0.31	-0.59	-0.65	-0.44	-0.42	-0.97	-0.61	5.36	8.71	0.40	7
B7	-0.80	-0.71	-0.31	-0.62	-0.66	-0.46	-0.42	-0.97	-0.63	2.73	8.73	-0.01	7
B7	-0.80	-0.70	-0.31	-0.62	-0.66	-0.44	-0.42	-0.97	-0.62	3.23	8.91	-0.86	7
B7	-0.79	-0.71	-0.31	-0.66	-0.66	-0.43	-0.43	-0.97	-0.62	2.20	9.97	0.03	7
B8	-0.83	-0.73	-0.35	-0.58	-0.64	-0.41	-0.39	-0.97	-0.63	-3.07	7.08	5.06	8
B8	-0.82	-0.72	-0.37	-0.57	-0.63	-0.41	-0.40	-0.97	-0.63	-2.91	6.49	5.65	8
B8	-0.83	-0.73	-0.37	-0.58	-0.63	-0.44	-0.41	-0.97	-0.65	-3.48	6.89	4.92	8
B8	-0.84	-0.74	-0.38	-0.59	-0.64	-0.46	-0.40	-0.97	-0.62	-4.73	7.66	4.75	8
B8	-0.84	-0.74	-0.35	-0.59	-0.64	-0.46	-0.40	-0.97	-0.64	-3.88	8.23	4.65	8
B8	-0.84	-0.74	-0.37	-0.60	-0.64	-0.47	-0.41	-0.97	-0.64	-4.99	8.19	4.36	8
G1	-0.48	-0.37	-0.22	-0.65	-0.73	-0.52	-0.49	-0.96	-0.58	47.89	18.21	-11.28	9
G1	-0.49	-0.37	-0.20	-0.64	-0.71	-0.52	-0.52	-0.97	-0.59	48.63	18.19	-10.25	9
G1	-0.49	-0.38	-0.20	-0.61	-0.71	-0.52	-0.53	-0.96	-0.58	49.01	17.38	-9.73	9
G1	-0.50	-0.38	-0.19	-0.62	-0.71	-0.53	-0.50	-0.96	-0.59	48.34	16.60	-10.16	9
G1	-0.47	-0.38	-0.19	-0.66	-0.72	-0.53	-0.49	-0.96	-0.61	48.99	17.91	-9.44	9
G1	-0.45	-0.35	-0.21	-0.63	-0.71	-0.51	-0.49	-0.97	-0.59	51.19	17.93	-7.80	9
G2	-0.65	-0.45	-0.28	-0.65	-0.73	-0.49	-0.58	-0.96	-0.58	31.23	14.78	-17.84	10
G2	-0.66	-0.44	-0.25	-0.65	-0.73	-0.50	-0.58	-0.96	-0.60	32.56	15.23	-17.43	10
G2	-0.68	-0.44	-0.26	-0.66	-0.72	-0.51	-0.58	-0.96	-0.59	31.45	13.76	-17.30	10
G2	-0.69	-0.45	-0.28	-0.65	-0.73	-0.51	-0.59	-0.96	-0.59	29.43	15.17	-18.80	10
G2	-0.64	-0.45	-0.28	-0.67	-0.75	-0.51	-0.59	-0.96	-0.59	32.70	16.92	-19.15	10
G2	-0.68	-0.44	-0.31	-0.65	-0.73	-0.52	-0.58	-0.96	-0.58	29.29	13.93	-18.65	10
G3	-0.53	-0.37	-0.29	-0.40	-0.54	-0.28	-0.48	-0.96	-0.60	41.47	-6.16	10.75	11
G3	-0.56	-0.38	-0.26	-0.39	-0.54	-0.30	-0.50	-0.96	-0.61	41.15	-5.78	11.05	11

G3	-0.58	-0.38	-0.29	-0.42	-0.55	-0.30	-0.51	-0.96	-0.60	37.87	-3.70	9.05	11
G3	-0.54	-0.38	-0.31	-0.43	-0.54	-0.32	-0.49	-0.96	-0.63	38.41	-5.78	10.31	11
G3	-0.54	-0.39	-0.27	-0.41	-0.55	-0.28	-0.49	-0.96	-0.59	39.98	-3.46	10.87	11
G3	-0.59	-0.38	-0.26	-0.42	-0.55	-0.33	-0.50	-0.96	-0.63	39.14	-4.36	8.51	11
G4	-0.61	-0.53	-0.31	-0.60	-0.72	-0.50	-0.49	-0.97	-0.67	25.68	17.49	-4.87	12
G4	-0.61	-0.54	-0.33	-0.59	-0.72	-0.51	-0.50	-0.97	-0.68	23.97	18.23	-4.02	12
G4	-0.60	-0.54	-0.31	-0.60	-0.72	-0.51	-0.52	-0.97	-0.68	25.39	18.03	-4.24	12
G4	-0.63	-0.55	-0.32	-0.58	-0.71	-0.50	-0.50	-0.97	-0.68	23.02	17.35	-3.52	12
G4	-0.60	-0.54	-0.35	-0.58	-0.72	-0.49	-0.52	-0.97	-0.68	23.48	17.72	-4.04	12
G4	-0.58	-0.54	-0.33	-0.60	-0.71	-0.49	-0.50	-0.97	-0.69	24.87	17.19	-2.89	12
G5	-0.62	-0.33	-0.13	-0.65	-0.71	-0.55	-0.56	-0.97	-0.59	48.71	21.92	-12.33	13
G5	-0.62	-0.32	-0.10	-0.65	-0.70	-0.56	-0.51	-0.97	-0.59	50.93	21.19	-11.82	13
G5	-0.60	-0.33	-0.13	-0.65	-0.70	-0.58	-0.50	-0.97	-0.60	49.16	21.33	-11.38	13
G5	-0.62	-0.34	-0.08	-0.68	-0.71	-0.58	-0.50	-0.97	-0.60	50.23	22.16	-12.82	13
G5	-0.61	-0.33	-0.11	-0.66	-0.70	-0.59	-0.47	-0.97	-0.61	49.30	21.87	-10.90	13
G5	-0.59	-0.32	-0.14	-0.66	-0.71	-0.58	-0.50	-0.97	-0.61	49.76	22.07	-11.64	13
G6	-0.43	-0.37	-0.21	-0.59	-0.66	-0.49	-0.53	-0.97	-0.60	51.87	15.96	0.18	14
G6	-0.41	-0.34	-0.21	-0.61	-0.68	-0.51	-0.52	-0.97	-0.63	54.09	17.32	-1.84	14
G6	-0.44	-0.35	-0.19	-0.63	-0.67	-0.51	-0.52	-0.97	-0.62	53.17	17.20	-1.76	14
G6	-0.39	-0.36	-0.23	-0.63	-0.66	-0.52	-0.54	-0.97	-0.64	53.11	17.32	1.00	14
G6	-0.40	-0.36	-0.22	-0.61	-0.66	-0.53	-0.52	-0.97	-0.64	53.41	17.47	1.66	14
G6	-0.42	-0.37	-0.23	-0.62	-0.67	-0.53	-0.52	-0.97	-0.65	51.04	16.67	-0.14	14
O1	-0.37	-0.40	-0.28	-0.42	-0.51	-0.31	-0.29	-0.97	-0.65	45.60	-6.01	24.07	15
O1	-0.36	-0.40	-0.27	-0.42	-0.51	-0.31	-0.29	-0.97	-0.65	46.46	-5.90	24.54	15
O1	-0.37	-0.39	-0.26	-0.41	-0.51	-0.31	-0.33	-0.97	-0.65	47.15	-5.62	23.45	15
O1	-0.37	-0.41	-0.28	-0.42	-0.52	-0.33	-0.33	-0.97	-0.66	45.19	-4.87	23.37	15
O1	-0.35	-0.40	-0.29	-0.42	-0.54	-0.32	-0.31	-0.97	-0.66	46.04	-3.24	22.69	15
O1	-0.37	-0.40	-0.30	-0.42	-0.54	-0.33	-0.32	-0.97	-0.66	44.82	-2.83	20.79	15
O2	-0.30	-0.32	-0.18	-0.45	-0.56	-0.36	-0.30	-0.96	-0.56	61.32	-4.82	12.67	16
O2	-0.30	-0.31	-0.19	-0.43	-0.55	-0.34	-0.31	-0.96	-0.55	61.81	-4.78	14.33	16
O2	-0.31	-0.30	-0.18	-0.47	-0.57	-0.36	-0.30	-0.96	-0.55	61.48	-2.65	10.93	16
O2	-0.32	-0.33	-0.18	-0.46	-0.56	-0.36	-0.31	-0.96	-0.54	59.13	-3.88	12.52	16
O2	-0.32	-0.31	-0.21	-0.43	-0.57	-0.34	-0.32	-0.96	-0.55	59.66	-3.42	11.31	16
O2	-0.31	-0.33	-0.20	-0.44	-0.57	-0.37	-0.30	-0.96	-0.54	59.07	-3.19	12.09	16
O3	-0.78	-0.61	-0.47	-0.41	-0.51	-0.31	-0.53	-0.93	-0.65	4.90	-28.75	-0.92	17
O3	-0.80	-0.61	-0.44	-0.43	-0.52	-0.31	-0.52	-0.93	-0.65	4.75	-26.42	-1.61	17
O3	-0.80	-0.60	-0.44	-0.41	-0.52	-0.31	-0.53	-0.93	-0.65	6.22	-27.17	-1.50	17
O3	-0.79	-0.61	-0.44	-0.43	-0.51	-0.33	-0.54	-0.93	-0.60	6.99	-27.84	-2.37	17
O3	-0.80	-0.61	-0.44	-0.41	-0.50	-0.32	-0.52	-0.93	-0.63	5.31	-28.25	0.02	17
O3	-0.80	-0.61	-0.47	-0.43	-0.52	-0.32	-0.56	-0.93	-0.62	4.40	-27.23	-2.64	17
O4	-0.72	-0.71	-0.60	-0.41	-0.48	-0.28	-0.51	-0.91	-0.67	-6.26	-40.47	1.97	18
O4	-0.71	-0.70	-0.61	-0.41	-0.47	-0.28	-0.52	-0.92	-0.69	-5.53	-39.47	4.17	18
O4	-0.72	-0.71	-0.61	-0.41	-0.46	-0.32	-0.50	-0.92	-0.70	-6.24	-39.45	5.37	18
O4	-0.75	-0.70	-0.62	-0.41	-0.47	-0.31	-0.52	-0.92	-0.67	-7.22	-38.48	2.86	18
O4	-0.75	-0.70	-0.60	-0.41	-0.47	-0.31	-0.52	-0.91	-0.68	-6.21	-40.89	1.09	18
O4	-0.73	-0.71	-0.61	-0.40	-0.47	-0.32	-0.52	-0.91	-0.67	-6.34	-39.82	2.28	18
O5	-0.96	-0.74	-0.64	-0.46	-0.58	-0.32	-0.44	-0.91	-0.61	-23.76	-33.46	-14.68	19
O5	-0.97	-0.76	-0.64	-0.48	-0.57	-0.32	-0.45	-0.90	-0.63	-24.72	-36.71	-17.41	19
O5	-0.96	-0.75	-0.64	-0.46	-0.58	-0.34	-0.46	-0.91	-0.60	-23.52	-33.73	-15.93	19
O5	-0.93	-0.76	-0.65	-0.47	-0.58	-0.32	-0.47	-0.90	-0.61	-23.15	-36.31	-16.72	19
O5	-0.94	-0.76	-0.64	-0.47	-0.58	-0.34	-0.47	-0.90	-0.61	-22.52	-35.96	-18.24	19
O5	-0.95	-0.76	-0.64	-0.46	-0.57	-0.34	-0.46	-0.91	-0.60	-23.15	-33.36	-14.64	19

O6	-0.77	-0.74	-0.63	-0.41	-0.52	-0.29	-0.36	-0.94	-0.68	-14.72	-23.56	12.32	20
O6	-0.76	-0.73	-0.63	-0.40	-0.52	-0.29	-0.37	-0.94	-0.66	-14.19	-22.10	12.71	20
O6	-0.79	-0.73	-0.60	-0.39	-0.52	-0.28	-0.39	-0.94	-0.66	-13.25	-22.85	11.83	20
O6	-0.79	-0.74	-0.60	-0.42	-0.52	-0.28	-0.41	-0.94	-0.66	-13.87	-22.99	10.56	20
O6	-0.77	-0.73	-0.63	-0.40	-0.52	-0.29	-0.40	-0.95	-0.66	-14.38	-22.04	12.88	20
O6	-0.78	-0.74	-0.62	-0.43	-0.52	-0.30	-0.40	-0.94	-0.66	-14.14	-23.49	10.47	20
O7	-0.91	-0.68	-0.57	-0.47	-0.62	-0.38	-0.44	-0.93	-0.58	-12.75	-19.68	-13.05	21
O7	-0.95	-0.67	-0.57	-0.50	-0.61	-0.38	-0.46	-0.92	-0.57	-14.21	-20.76	-15.22	21
O7	-0.94	-0.68	-0.56	-0.50	-0.61	-0.38	-0.48	-0.93	-0.56	-13.43	-19.71	-14.79	21
O7	-0.93	-0.66	-0.56	-0.50	-0.61	-0.36	-0.46	-0.93	-0.56	-12.88	-18.83	-13.64	21
O7	-0.93	-0.68	-0.55	-0.50	-0.61	-0.38	-0.47	-0.92	-0.56	-12.41	-20.45	-15.25	21
O7	-0.95	-0.67	-0.55	-0.48	-0.61	-0.36	-0.46	-0.93	-0.56	-13.47	-19.20	-13.71	21
O8	-0.79	-0.67	-0.60	-0.45	-0.53	-0.32	-0.38	-0.90	-0.67	-8.87	-43.13	-11.57	22
O8	-0.80	-0.68	-0.56	-0.46	-0.54	-0.30	-0.39	-0.90	-0.68	-7.84	-40.34	-11.50	22
O8	-0.80	-0.66	-0.56	-0.46	-0.53	-0.32	-0.39	-0.90	-0.67	-6.53	-41.90	-11.35	22
O8	-0.81	-0.68	-0.56	-0.48	-0.52	-0.30	-0.42	-0.90	-0.68	-7.78	-42.52	-11.59	22
O8	-0.79	-0.69	-0.57	-0.47	-0.53	-0.34	-0.43	-0.90	-0.65	-7.13	-41.91	-11.95	22
O8	-0.80	-0.68	-0.58	-0.47	-0.53	-0.34	-0.42	-0.90	-0.67	-7.89	-39.47	-9.24	22

Table 38. Training matrix of fluorescence response pattern from an array of **P7**/CB[8], **P13**/CB[8] and **P14**/CB[8] (each at pH 3 and 13, buffered) against different concentrations of caffeine (0-10 mM) in three kinds of teas (B-black tea, G-green tea and O-oolong tea). LDA was carried out and resulting in 6 factors of the canonical scores (the first three scores were shown here) and group generation. The jackknifed classification matrix with cross-validation reveals a 96% accuracy.

Analytes	Fluorescence Response Pattern						Results LDA (the first three scores)			
	P7/CB[8] (pH3)	**P13**/CB[8] (pH3)	**P14**/CB[8] (pH3)	**P7**/CB[8] (pH13)	**P13**/CB[8] (pH13)	**P14**/CB[8] (pH13)	Factor 1	Factor 2	Factor 3	Group
Control	0.07	0.00	0.04	0.04	0.10	0.08	53.95	-75.72	1.00	9
Control	0.03	0.03	0.00	-0.03	0.05	-0.03	58.53	-70.48	-3.55	9
Control	-0.01	0.00	0.02	-0.04	-0.03	-0.03	55.32	-65.24	-2.38	9
Control	0.04	0.00	0.06	0.03	-0.03	0.04	55.53	-64.84	3.24	9
Control	-0.04	-0.01	-0.04	-0.01	-0.01	-0.02	52.54	-68.20	-2.39	9
Control	-0.10	-0.01	-0.07	0.00	-0.08	-0.05	52.90	-64.74	-2.27	9
B-0mM	-0.97	-0.86	-0.67	-0.48	-0.99	-0.70	-48.82	-0.98	-8.05	3
B-0mM	-0.97	-0.86	-0.68	-0.48	-0.99	-0.70	-48.64	-1.10	-8.08	3
B-0mM	-0.97	-0.88	-0.68	-0.48	-0.99	-0.71	-50.21	-1.03	-7.73	3
B-0mM	-0.97	-0.87	-0.67	-0.48	-0.99	-0.71	-49.62	-0.94	-7.79	3
B-0mM	-0.97	-0.87	-0.67	-0.47	-0.99	-0.72	-49.15	-1.18	-7.53	3
B-0mM	-0.97	-0.87	-0.67	-0.47	-0.99	-0.71	-49.17	-1.17	-7.60	3
B-0.2mM	-0.97	-0.83	-0.65	-0.46	-0.98	-0.70	-45.29	-1.82	-7.73	2
B-0.2mM	-0.97	-0.84	-0.67	-0.47	-0.99	-0.69	-46.17	-1.53	-8.05	1
B-0.2mM	-0.97	-0.84	-0.67	-0.47	-0.99	-0.71	-46.24	-1.51	-7.93	1
B-0.2mM	-0.97	-0.84	-0.67	-0.47	-0.99	-0.71	-45.74	-1.33	-8.33	1
B-0.2mM	-0.97	-0.85	-0.66	-0.48	-0.99	-0.71	-47.32	-1.18	-8.08	1
B-0.2mM	-0.97	-0.85	-0.66	-0.47	-0.99	-0.69	-47.05	-1.39	-7.98	1
B-0.5mM	-0.97	-0.83	-0.65	-0.45	-0.98	-0.68	-45.18	-2.00	-7.23	2
B-0.5mM	-0.97	-0.84	-0.66	-0.45	-0.98	-0.68	-46.55	-2.02	-7.19	2
B-0.5mM	-0.97	-0.84	-0.67	-0.46	-0.98	-0.69	-45.75	-1.93	-7.65	2
B-0.5mM	-0.97	-0.83	-0.66	-0.46	-0.98	-0.68	-44.41	-1.80	-8.21	2
B-0.5mM	-0.97	-0.83	-0.66	-0.46	-0.99	-0.68	-45.43	-1.71	-7.91	2
B-0.5mM	-0.97	-0.83	-0.65	-0.46	-0.98	-0.70	-45.30	-1.74	-8.05	2
B-1.0mM	-0.97	-0.83	-0.63	-0.27	-0.98	-0.64	-49.16	-6.36	1.65	4
B-1.0mM	-0.97	-0.84	-0.64	-0.26	-0.98	-0.65	-50.01	-6.49	2.18	4
B-1.0mM	-0.97	-0.84	-0.65	-0.28	-0.98	-0.65	-49.92	-6.25	1.11	4
B-1.0mM	-0.97	-0.83	-0.64	-0.28	-0.98	-0.65	-49.06	-6.10	1.07	4

B-1.0mM	-0.97	-0.84	-0.65	-0.27	-0.98	-0.64	-50.38	-6.28	1.78	4
B-1.0mM	-0.97	-0.84	-0.64	-0.28	-0.98	-0.65	-49.93	-6.20	1.35	4
B-2.0mM	-0.95	-0.77	-0.57	-0.22	-0.97	-0.59	-41.75	-7.73	2.77	6
B-2.0mM	-0.96	-0.78	-0.57	-0.23	-0.98	-0.60	-42.95	-7.39	2.49	6
B-2.0mM	-0.96	-0.78	-0.57	-0.23	-0.98	-0.61	-42.83	-7.44	2.44	6
B-2.0mM	-0.96	-0.78	-0.57	-0.23	-0.98	-0.61	-42.93	-7.54	2.76	6
B-2.0mM	-0.96	-0.77	-0.58	-0.25	-0.97	-0.59	-41.68	-7.35	1.53	6
B-2.0mM	-0.96	-0.78	-0.59	-0.25	-0.98	-0.60	-42.38	-7.14	1.43	6
B-5.0mM	-0.92	-0.72	-0.53	-0.19	-0.97	-0.54	-35.39	-8.05	4.21	7
B-5.0mM	-0.93	-0.72	-0.54	-0.20	-0.97	-0.57	-35.87	-8.08	3.58	7
B-5.0mM	-0.92	-0.72	-0.54	-0.19	-0.97	-0.56	-36.24	-8.04	4.07	7
B-5.0mM	-0.92	-0.72	-0.52	-0.20	-0.97	-0.57	-36.15	-7.66	3.86	7
B-5.0mM	-0.93	-0.71	-0.53	-0.22	-0.97	-0.55	-33.86	-7.65	2.48	7
B-5.0mM	-0.93	-0.72	-0.54	-0.23	-0.97	-0.56	-35.27	-7.27	1.92	7
B-8.0mM	-0.88	-0.63	-0.48	-0.15	-0.96	-0.49	-24.84	-8.58	5.11	8
B-8.0mM	-0.88	-0.63	-0.49	-0.18	-0.96	-0.52	-24.66	-7.97	3.64	8
B-8.0mM	-0.88	-0.64	-0.49	-0.18	-0.96	-0.52	-25.60	-7.65	4.01	8
B-8.0mM	-0.88	-0.64	-0.49	-0.18	-0.96	-0.52	-25.48	-7.94	3.95	8
B-8.0mM	-0.88	-0.63	-0.51	-0.18	-0.96	-0.50	-23.91	-8.02	3.14	8
B-8.0mM	-0.88	-0.64	-0.51	-0.17	-0.97	-0.54	-25.81	-7.50	4.30	8
B-10.0mM	-0.84	-0.58	-0.50	-0.16	-0.96	-0.49	-17.12	-7.68	4.08	5
B-10.0mM	-0.85	-0.58	-0.47	-0.16	-0.96	-0.51	-18.08	-7.88	4.16	5
B-10.0mM	-0.85	-0.58	-0.48	-0.16	-0.96	-0.51	-18.11	-7.78	3.88	5
B-10.0mM	-0.85	-0.58	-0.47	-0.18	-0.96	-0.49	-17.23	-7.27	2.88	5
B-10.0mM	-0.85	-0.57	-0.47	-0.18	-0.96	-0.49	-16.02	-7.37	2.82	5
B-10.0mM	-0.85	-0.58	-0.47	-0.18	-0.96	-0.51	-17.30	-7.38	2.72	5
G-0mM	-0.68	-0.33	-0.38	-0.53	-0.98	-0.68	23.32	7.58	-14.83	12
G-0mM	-0.66	-0.33	-0.38	-0.52	-0.98	-0.63	23.67	7.91	-13.55	12
G-0mM	-0.65	-0.33	-0.37	-0.52	-0.99	-0.65	24.04	8.47	-13.25	12
G-0mM	-0.66	-0.33	-0.35	-0.53	-0.98	-0.67	23.73	8.29	-13.68	12
G-0mM	-0.67	-0.33	-0.37	-0.52	-0.99	-0.65	23.64	7.69	-14.30	12
G-0mM	-0.70	-0.33	-0.42	-0.53	-0.98	-0.67	23.10	6.79	-16.33	12
G-0.2mM	-0.67	-0.28	-0.42	-0.53	-0.98	-0.53	30.44	6.34	-16.59	10
G-0.2mM	-0.67	-0.28	-0.38	-0.50	-0.98	-0.53	30.19	6.14	-14.93	10
G-0.2mM	-0.64	-0.28	-0.35	-0.51	-0.98	-0.54	30.55	7.47	-13.90	10
G-0.2mM	-0.65	-0.28	-0.38	-0.51	-0.98	-0.57	30.36	7.29	-14.68	10
G-0.2mM	-0.65	-0.28	-0.37	-0.51	-0.98	-0.54	29.71	7.11	-14.50	10
G-0.2mM	-0.67	-0.28	-0.32	-0.51	-0.98	-0.53	30.15	6.24	-14.94	10
G-0.5mM	-0.67	-0.26	-0.42	-0.49	-0.98	-0.52	31.35	5.32	-15.09	11
G-0.5mM	-0.64	-0.26	-0.40	-0.49	-0.98	-0.51	32.82	6.40	-14.11	11
G-0.5mM	-0.65	-0.27	-0.38	-0.50	-0.98	-0.49	31.95	6.45	-14.58	11
G-0.5mM	-0.66	-0.26	-0.34	-0.51	-0.98	-0.50	31.79	6.21	-14.62	11
G-0.5mM	-0.63	-0.26	-0.40	-0.51	-0.98	-0.50	32.50	7.02	-14.67	11
G-0.5mM	-0.66	-0.26	-0.41	-0.51	-0.98	-0.50	32.81	6.21	-15.95	11
G-1.0mM	-0.56	-0.21	-0.28	-0.41	-0.97	-0.51	38.93	7.21	-8.07	13
G-1.0mM	-0.54	-0.21	-0.35	-0.40	-0.96	-0.53	39.17	6.67	-8.03	13
G-1.0mM	-0.54	-0.21	-0.29	-0.40	-0.97	-0.54	39.12	7.33	-7.38	13
G-1.0mM	-0.54	-0.21	-0.31	-0.41	-0.97	-0.52	38.67	7.48	-7.95	13
G-1.0mM	-0.54	-0.22	-0.33	-0.41	-0.97	-0.53	38.33	7.48	-7.85	13
G-1.0mM	-0.57	-0.22	-0.39	-0.39	-0.97	-0.58	37.35	6.85	-8.38	13
G-2.0mM	-0.47	-0.21	-0.18	-0.38	-0.96	-0.48	40.18	8.77	-2.91	15
G-2.0mM	-0.45	-0.21	-0.18	-0.36	-0.96	-0.47	40.41	8.98	-1.62	15

G-2.0mM	-0.45	-0.21	-0.22	-0.38	-0.96	-0.48	40.29	9.31	-2.58	15
G-2.0mM	-0.44	-0.21	-0.29	-0.35	-0.96	-0.46	39.98	9.36	-1.48	15
G-2.0mM	-0.45	-0.22	-0.22	-0.36	-0.96	-0.42	39.32	8.56	-1.84	15
G-2.0mM	-0.49	-0.21	-0.24	-0.36	-0.96	-0.50	38.71	8.00	-3.31	15
G-5.0mM	-0.41	-0.20	-0.07	-0.32	-0.95	-0.54	40.31	9.08	1.88	16
G-5.0mM	-0.34	-0.20	-0.02	-0.33	-0.95	-0.39	42.13	10.83	4.70	16
G-5.0mM	-0.37	-0.21	-0.04	-0.34	-0.96	-0.49	41.32	11.00	2.86	16
G-5.0mM	-0.39	-0.21	-0.19	-0.33	-0.96	-0.40	41.00	10.11	2.06	16
G-5.0mM	-0.43	-0.21	-0.12	-0.33	-0.96	-0.46	40.11	9.01	0.96	16
G-5.0mM	-0.40	-0.21	-0.13	-0.33	-0.96	-0.52	40.82	10.36	1.65	16
G-8.0mM	-0.28	-0.20	0.02	-0.29	-0.95	-0.37	42.93	11.63	8.90	17
G-8.0mM	-0.27	-0.20	0.02	-0.26	-0.94	-0.39	42.75	10.98	10.08	17
G-8.0mM	-0.30	-0.20	0.05	-0.26	-0.95	-0.44	42.16	11.32	9.96	17
G-8.0mM	-0.33	-0.20	-0.04	-0.28	-0.95	-0.45	41.96	10.75	6.98	17
G-8.0mM	-0.31	-0.21	-0.03	-0.28	-0.95	-0.43	41.47	11.33	8.15	17
G-8.0mM	-0.29	-0.20	-0.08	-0.29	-0.95	-0.38	42.58	11.76	7.49	17
G-10.0mM	-0.28	-0.20	0.08	-0.25	-0.93	-0.31	42.59	9.69	10.82	14
G-10.0mM	-0.24	-0.19	0.12	-0.24	-0.94	-0.35	43.37	11.41	13.12	14
G-10.0mM	-0.23	-0.20	0.10	-0.23	-0.94	-0.38	42.75	12.22	13.98	14
G-10.0mM	-0.22	-0.20	0.06	-0.23	-0.95	-0.37	43.54	12.55	13.65	14
G-10.0mM	-0.26	-0.20	0.05	-0.25	-0.93	-0.39	42.97	10.85	11.39	14
G-10.0mM	-0.27	-0.21	0.06	-0.25	-0.94	-0.33	41.62	10.36	11.40	14
O-0mM	-0.64	-0.60	-0.42	-0.46	-0.97	-0.68	-9.83	7.62	-2.35	20
O-0mM	-0.64	-0.62	-0.42	-0.46	-0.98	-0.69	-11.80	8.35	-2.11	20
O-0mM	-0.65	-0.62	-0.41	-0.46	-0.97	-0.70	-13.04	7.85	-1.91	20
O-0mM	-0.65	-0.63	-0.42	-0.47	-0.97	-0.67	-13.91	8.15	-2.23	20
O-0mM	-0.64	-0.60	-0.41	-0.45	-0.97	-0.70	-10.46	7.91	-2.04	20
O-0mM	-0.64	-0.61	-0.42	-0.48	-0.97	-0.70	-10.94	8.15	-3.36	20
O-0.2mM	-0.62	-0.57	-0.40	-0.40	-0.97	-0.66	-7.00	7.17	0.17	19
O-0.2mM	-0.62	-0.61	-0.40	-0.41	-0.97	-0.66	-11.85	7.67	1.52	18
O-0.2mM	-0.62	-0.62	-0.39	-0.42	-0.97	-0.68	-13.16	7.78	1.03	18
O-0.2mM	-0.62	-0.61	-0.39	-0.43	-0.97	-0.66	-11.02	7.74	0.15	18
O-0.2mM	-0.62	-0.60	-0.40	-0.41	-0.97	-0.68	-10.44	7.44	0.59	18
O-0.2mM	-0.62	-0.61	-0.40	-0.42	-0.97	-0.67	-11.55	7.85	0.50	18
O-0.5mM	-0.60	-0.59	-0.36	-0.39	-0.97	-0.67	-8.89	7.49	2.35	19
O-0.5mM	-0.61	-0.57	-0.38	-0.37	-0.97	-0.67	-7.80	7.03	2.12	19
O-0.5mM	-0.61	-0.60	-0.36	-0.40	-0.97	-0.67	-10.82	7.65	2.00	19
O-0.5mM	-0.61	-0.60	-0.39	-0.40	-0.97	-0.65	-10.24	7.03	1.36	19
O-0.5mM	-0.60	-0.60	-0.38	-0.42	-0.97	-0.65	-10.44	8.29	1.31	18
O-0.5mM	-0.61	-0.60	-0.40	-0.42	-0.97	-0.64	-9.43	8.06	0.74	19
O-1.0mM	-0.60	-0.59	-0.37	-0.33	-0.95	-0.57	-10.93	4.52	5.10	21
O-1.0mM	-0.61	-0.60	-0.39	-0.34	-0.95	-0.58	-11.68	4.42	3.99	21
O-1.0mM	-0.60	-0.58	-0.37	-0.33	-0.95	-0.61	-9.18	4.92	4.55	21
O-1.0mM	-0.62	-0.59	-0.34	-0.36	-0.95	-0.53	-10.02	3.77	2.91	21
O-1.0mM	-0.60	-0.58	-0.36	-0.34	-0.95	-0.61	-9.33	4.97	3.92	21
O-1.0mM	-0.60	-0.59	-0.36	-0.36	-0.95	-0.54	-10.44	4.86	3.83	21
O-2.0mM	-0.55	-0.55	-0.27	-0.29	-0.95	-0.52	-5.68	4.49	8.17	23
O-2.0mM	-0.57	-0.55	-0.32	-0.28	-0.95	-0.52	-6.30	3.52	7.13	23
O-2.0mM	-0.55	-0.55	-0.31	-0.29	-0.94	-0.55	-6.06	4.33	7.63	23
O-2.0mM	-0.57	-0.55	-0.28	-0.32	-0.95	-0.51	-5.67	4.25	6.04	23
O-2.0mM	-0.57	-0.54	-0.30	-0.27	-0.94	-0.53	-5.32	3.36	7.86	23
O-2.0mM	-0.56	-0.55	-0.31	-0.34	-0.95	-0.53	-3.98	5.38	5.05	23

O-5.0mM	-0.54	-0.51	-0.24	-0.27	-0.94	-0.46	-0.84	3.49	8.13	24
O-5.0mM	-0.54	-0.51	-0.27	-0.26	-0.94	-0.53	-1.41	3.76	8.54	24
O-5.0mM	-0.53	-0.50	-0.25	-0.27	-0.94	-0.49	0.82	3.92	8.24	24
O-5.0mM	-0.55	-0.51	-0.25	-0.27	-0.94	-0.49	-1.48	2.56	7.63	24
O-5.0mM	-0.54	-0.51	-0.24	-0.27	-0.94	-0.52	-0.55	3.97	8.29	24
O-5.0mM	-0.55	-0.52	-0.28	-0.27	-0.94	-0.53	-2.29	3.23	7.49	24
O-8.0mM	-0.50	-0.46	-0.19	-0.23	-0.93	-0.44	5.07	2.54	9.89	25
O-8.0mM	-0.48	-0.45	-0.21	-0.21	-0.93	-0.39	6.93	2.32	11.05	25
O-8.0mM	-0.49	-0.47	-0.19	-0.22	-0.93	-0.43	4.57	2.64	10.91	25
O-8.0mM	-0.50	-0.45	-0.18	-0.19	-0.93	-0.45	5.17	2.25	12.23	25
O-8.0mM	-0.50	-0.46	-0.21	-0.23	-0.93	-0.46	4.73	3.06	10.30	25
O-8.0mM	-0.50	-0.45	-0.24	-0.19	-0.93	-0.47	6.20	2.26	11.04	25
O-10.0mM	-0.47	-0.40	-0.18	-0.15	-0.92	-0.43	11.27	1.17	12.99	22
O-10.0mM	-0.46	-0.42	-0.20	-0.16	-0.91	-0.42	9.10	1.18	13.35	22
O-10.0mM	-0.47	-0.44	-0.19	-0.20	-0.92	-0.37	7.74	2.04	11.54	22
O-10.0mM	-0.48	-0.42	-0.17	-0.23	-0.92	-0.44	10.06	2.63	9.27	22
O-10.0mM	-0.49	-0.44	-0.18	-0.23	-0.93	-0.44	8.26	3.08	10.09	22
O-10.0mM	-0.49	-0.44	-0.24	-0.24	-0.93	-0.44	8.12	3.29	8.96	22

Table 39. Training matrix of fluorescence response pattern from an array of **P7**, **P13** and **P14** (each at pH 3, 7 and 13, buffered) against different concentrations of caffeine (0-10 mM) in three kinds of teas (B-black tea, G-green tea and O-oolong tea). LDA was carried out and resulting in 6 factors of the canonical scores (the first three scores were shown here) and group generation. The jackknifed classification matrix with cross-validation reveals a 91% accuracy.

Analytes	Fluorescence Response Pattern						Results LDA(the first three scores)			
	P7(pH3)	**P13**(pH3)	**P14**(pH3)	**P7**(pH13)	**P13**(pH13)	**P14**(pH13)	Factor 1	Factor 2	Factor 3	Group
Control	0.00	0.04	0.03	0.03	-0.01	0.02	294.80	5.75	1.48	9
Control	0.00	0.01	0.02	0.02	0.01	0.03	298.80	1.83	2.19	9
Control	0.00	-0.01	0.02	-0.01	0.01	0.02	298.55	1.05	3.06	9
Control	0.00	-0.01	-0.01	-0.02	-0.02	-0.04	289.48	1.01	5.68	9
Control	-0.01	0.02	0.00	-0.04	0.01	-0.03	299.51	0.99	4.61	9
Control	-0.03	0.01	-0.01	-0.02	0.00	0.00	296.15	0.86	2.72	9
B-0mM	-0.88	-0.87	-0.74	-0.20	-0.92	-0.55	-13.30	-42.64	-0.78	3
B-0mM	-0.88	-0.87	-0.75	-0.20	-0.92	-0.55	-13.04	-43.01	-0.76	3
B-0mM	-0.89	-0.87	-0.76	-0.22	-0.92	-0.56	-13.26	-43.53	-0.59	3
B-0mM	-0.89	-0.87	-0.76	-0.22	-0.92	-0.56	-13.66	-43.31	-0.55	3
B-0mM	-0.91	-0.87	-0.73	-0.22	-0.93	-0.55	-14.57	-42.26	-1.80	3
B-0mM	-0.91	-0.88	-0.73	-0.23	-0.93	-0.56	-14.04	-42.94	-0.72	3
B-0.2mM	-0.87	-0.86	-0.72	-0.20	-0.92	-0.53	-10.96	-40.59	-1.54	1
B-0.2mM	-0.87	-0.86	-0.72	-0.19	-0.92	-0.55	-11.51	-41.04	-0.67	1
B-0.2mM	-0.89	-0.85	-0.72	-0.20	-0.92	-0.54	-11.44	-40.74	-1.89	1
B-0.2mM	-0.87	-0.86	-0.73	-0.21	-0.92	-0.55	-11.27	-41.54	-0.64	1
B-0.2mM	-0.90	-0.86	-0.72	-0.21	-0.92	-0.54	-12.05	-41.58	-1.82	1
B-0.2mM	-0.90	-0.86	-0.73	-0.20	-0.92	-0.56	-12.19	-41.87	-1.07	1
B-0.5mM	-0.84	-0.85	-0.72	-0.19	-0.91	-0.52	-9.37	-39.82	-0.83	2
B-0.5mM	-0.84	-0.85	-0.70	-0.20	-0.91	-0.54	-9.16	-39.20	0.49	2
B-0.5mM	-0.84	-0.85	-0.73	-0.22	-0.92	-0.52	-10.84	-39.78	-1.46	2
B-0.5mM	-0.84	-0.85	-0.71	-0.17	-0.91	-0.54	-7.77	-39.81	0.36	2
B-0.5mM	-0.88	-0.85	-0.71	-0.20	-0.92	-0.52	-10.61	-39.65	-2.35	1
B-0.5mM	-0.87	-0.85	-0.71	-0.20	-0.92	-0.54	-11.28	-39.61	-0.95	1
B-1.0mM	-0.85	-0.83	-0.70	-0.20	-0.91	-0.50	-9.46	-37.53	-2.97	4
B-1.0mM	-0.85	-0.84	-0.70	-0.22	-0.91	-0.53	-8.02	-38.64	-1.11	4
B-1.0mM	-0.86	-0.83	-0.69	-0.21	-0.91	-0.52	-7.98	-37.84	-1.88	4
B-1.0mM	-0.86	-0.84	-0.71	-0.19	-0.91	-0.52	-8.86	-39.08	-2.29	4

B-1.0mM	-0.85	-0.84	-0.70	-0.20	-0.91	-0.53	-9.61	-38.86	-1.25	2
B-1.0mM	-0.87	-0.83	-0.71	-0.17	-0.91	-0.50	-9.31	-38.46	-3.79	4
B-2.0mM	-0.80	-0.78	-0.70	-0.17	-0.90	-0.47	-6.09	-33.08	-4.57	6
B-2.0mM	-0.79	-0.79	-0.63	-0.17	-0.90	-0.47	-5.25	-31.09	-2.74	6
B-2.0mM	-0.79	-0.78	-0.66	-0.17	-0.90	-0.48	-5.05	-31.20	-3.12	6
B-2.0mM	-0.80	-0.78	-0.64	-0.16	-0.90	-0.49	-5.18	-31.23	-2.51	6
B-2.0mM	-0.82	-0.78	-0.63	-0.20	-0.91	-0.49	-6.42	-30.68	-2.93	6
B-2.0mM	-0.80	-0.75	-0.66	-0.14	-0.90	-0.47	-5.30	-30.08	-4.21	6
B-5.0mM	-0.69	-0.71	-0.63	-0.16	-0.89	-0.44	-0.54	-24.04	-3.27	7
B-5.0mM	-0.72	-0.75	-0.62	-0.19	-0.90	-0.42	-2.56	-25.89	-4.33	7
B-5.0mM	-0.71	-0.71	-0.60	-0.17	-0.89	-0.44	0.17	-23.16	-3.12	7
B-5.0mM	-0.71	-0.71	-0.60	-0.14	-0.89	-0.45	-0.16	-22.99	-3.00	7
B-5.0mM	-0.75	-0.71	-0.62	-0.13	-0.89	-0.46	-0.13	-25.15	-3.84	7
B-5.0mM	-0.72	-0.71	-0.63	-0.19	-0.89	-0.44	-1.64	-24.10	-3.82	7
B-8.0mM	-0.64	-0.63	-0.53	-0.13	-0.88	-0.38	3.58	-13.21	-5.70	8
B-8.0mM	-0.67	-0.66	-0.55	-0.10	-0.88	-0.37	4.51	-16.70	-6.71	8
B-8.0mM	-0.64	-0.62	-0.49	-0.13	-0.88	-0.40	4.19	-11.18	-4.26	8
B-8.0mM	-0.64	-0.62	-0.51	-0.09	-0.88	-0.40	3.52	-12.34	-4.18	8
B-8.0mM	-0.68	-0.64	-0.53	-0.11	-0.88	-0.37	3.47	-15.05	-6.99	8
B-8.0mM	-0.63	-0.62	-0.53	-0.19	-0.88	-0.44	3.87	-12.99	-1.54	8
B-10.0mM	-0.58	-0.59	-0.45	-0.07	-0.85	-0.18	13.24	-5.73	-15.06	5
B-10.0mM	-0.62	-0.62	-0.45	-0.11	-0.85	-0.19	14.28	-9.36	-14.38	5
B-10.0mM	-0.58	-0.58	-0.43	-0.04	-0.85	-0.20	13.87	-4.90	-13.65	5
B-10.0mM	-0.60	-0.60	-0.43	-0.07	-0.85	-0.19	13.49	-5.66	-13.96	5
B-10.0mM	-0.64	-0.58	-0.46	-0.09	-0.85	-0.19	13.62	-6.76	-16.43	5
B-10.0mM	-0.59	-0.55	-0.49	-0.14	-0.85	-0.23	13.96	-5.92	-13.36	5
G-0mM	-0.48	-0.49	-0.24	-0.29	-0.96	-0.54	-20.31	16.18	7.77	12
G-0mM	-0.48	-0.48	-0.23	-0.29	-0.96	-0.55	-19.83	16.79	8.66	12
G-0mM	-0.46	-0.50	-0.24	-0.29	-0.97	-0.55	-20.51	15.96	9.53	12
G-0mM	-0.47	-0.50	-0.25	-0.32	-0.96	-0.56	-19.90	14.97	9.71	12
G-0mM	-0.49	-0.49	-0.24	-0.30	-0.97	-0.57	-20.87	15.99	9.34	12
G-0mM	-0.48	-0.49	-0.22	-0.33	-0.97	-0.56	-20.48	16.80	9.37	12
G-0.2mM	-0.46	-0.48	-0.22	-0.29	-0.96	-0.54	-18.71	17.67	8.43	10
G-0.2mM	-0.46	-0.48	-0.22	-0.30	-0.96	-0.54	-19.11	18.08	8.27	10
G-0.2mM	-0.45	-0.49	-0.23	-0.31	-0.96	-0.53	-18.97	16.65	8.56	10
G-0.2mM	-0.47	-0.48	-0.22	-0.31	-0.96	-0.54	-18.96	17.17	8.56	10
G-0.2mM	-0.46	-0.48	-0.23	-0.32	-0.96	-0.56	-19.19	17.60	9.49	10
G-0.2mM	-0.48	-0.48	-0.24	-0.34	-0.96	-0.55	-18.81	16.48	8.33	10
G-0.5mM	-0.44	-0.46	-0.20	-0.26	-0.96	-0.52	-18.07	20.41	7.71	11
G-0.5mM	-0.45	-0.47	-0.21	-0.26	-0.96	-0.52	-18.37	19.43	7.43	11
G-0.5mM	-0.45	-0.46	-0.22	-0.26	-0.96	-0.52	-18.61	19.14	7.65	11
G-0.5mM	-0.44	-0.46	-0.21	-0.27	-0.96	-0.53	-17.76	19.72	8.18	11
G-0.5mM	-0.44	-0.45	-0.22	-0.29	-0.96	-0.51	-18.47	20.72	6.88	11
G-0.5mM	-0.45	-0.46	-0.22	-0.30	-0.96	-0.52	-18.40	19.28	7.13	11
G-1.0mM	-0.44	-0.43	-0.20	-0.25	-0.96	-0.50	-17.58	22.43	5.88	13
G-1.0mM	-0.42	-0.43	-0.21	-0.24	-0.96	-0.51	-17.57	22.69	6.63	13
G-1.0mM	-0.44	-0.44	-0.19	-0.25	-0.96	-0.50	-17.72	22.73	5.95	13
G-1.0mM	-0.44	-0.42	-0.20	-0.26	-0.96	-0.51	-17.25	22.91	6.33	13
G-1.0mM	-0.42	-0.42	-0.21	-0.26	-0.96	-0.50	-17.21	23.06	6.31	13
G-1.0mM	-0.45	-0.44	-0.20	-0.28	-0.96	-0.50	-17.07	21.94	5.86	13
G-2.0mM	-0.39	-0.39	-0.13	-0.20	-0.95	-0.42	-15.59	29.97	2.49	15
G-2.0mM	-0.37	-0.38	-0.14	-0.22	-0.95	-0.43	-15.14	30.28	3.61	15

G-2.0mM	-0.38	-0.39	-0.13	-0.23	-0.95	-0.42	-14.50	29.85	3.45	15
G-2.0mM	-0.37	-0.37	-0.12	-0.22	-0.95	-0.40	-15.23	32.55	2.04	15
G-2.0mM	-0.38	-0.40	-0.15	-0.23	-0.95	-0.40	-15.60	29.30	1.89	15
G-2.0mM	-0.37	-0.37	-0.15	-0.24	-0.95	-0.40	-15.49	31.15	1.23	15
G-5.0mM	-0.35	-0.31	-0.10	-0.21	-0.95	-0.39	-12.13	37.60	0.38	16
G-5.0mM	-0.37	-0.30	-0.12	-0.21	-0.95	-0.37	-12.46	37.09	-1.97	16
G-5.0mM	-0.36	-0.30	-0.12	-0.22	-0.94	-0.38	-11.80	36.96	-0.65	16
G-5.0mM	-0.36	-0.29	-0.11	-0.22	-0.95	-0.36	-12.88	38.92	-2.05	16
G-5.0mM	-0.32	-0.30	-0.11	-0.21	-0.94	-0.34	-11.68	38.93	-1.74	16
G-5.0mM	-0.35	-0.30	-0.12	-0.23	-0.95	-0.33	-12.74	38.48	-3.61	16
G-8.0mM	-0.31	-0.19	-0.02	-0.19	-0.94	-0.28	-8.61	50.56	-6.32	17
G-8.0mM	-0.31	-0.21	-0.06	-0.18	-0.94	-0.24	-10.26	48.59	-8.94	17
G-8.0mM	-0.31	-0.17	-0.07	-0.19	-0.94	-0.28	-9.52	50.04	-7.11	17
G-8.0mM	-0.29	-0.21	-0.04	-0.20	-0.94	-0.22	-8.43	49.96	-9.27	17
G-8.0mM	-0.27	-0.20	-0.03	-0.21	-0.94	-0.23	-9.31	50.75	-8.06	17
G-8.0mM	-0.29	-0.19	-0.07	-0.20	-0.94	-0.23	-9.20	49.77	-9.44	17
G-10.0mM	-0.31	-0.16	-0.03	-0.17	-0.93	-0.21	-6.60	52.85	-11.56	14
G-10.0mM	-0.29	-0.16	-0.06	-0.16	-0.93	-0.23	-6.86	51.48	-9.74	14
G-10.0mM	-0.33	-0.15	-0.03	-0.16	-0.93	-0.23	-7.38	52.88	-11.02	14
G-10.0mM	-0.30	-0.14	-0.04	-0.17	-0.93	-0.16	-6.23	54.34	-14.31	14
G-10.0mM	-0.30	-0.15	0.01	-0.20	-0.93	-0.20	-6.47	55.73	-11.06	14
G-10.0mM	-0.32	-0.14	-0.05	-0.17	-0.93	-0.18	-6.15	53.34	-14.40	14
O-0mM	-0.61	-0.67	-0.55	-0.14	-0.97	-0.52	-24.78	-11.52	2.31	20
O-0mM	-0.61	-0.69	-0.55	-0.11	-0.97	-0.53	-24.53	-12.97	3.27	20
O-0mM	-0.63	-0.70	-0.52	-0.07	-0.97	-0.53	-25.37	-12.86	3.19	20
O-0mM	-0.63	-0.67	-0.56	-0.08	-0.97	-0.54	-25.49	-12.29	2.26	20
O-0mM	-0.64	-0.67	-0.56	-0.14	-0.97	-0.51	-25.49	-12.38	0.73	20
O-0mM	-0.63	-0.68	-0.53	-0.21	-0.97	-0.53	-25.74	-11.53	2.86	18
O-0.2mM	-0.61	-0.66	-0.54	-0.09	-0.97	-0.52	-24.71	-10.12	2.03	18
O-0.2mM	-0.63	-0.68	-0.54	-0.07	-0.97	-0.52	-24.96	-12.08	2.01	20
O-0.2mM	-0.62	-0.68	-0.51	-0.19	-0.97	-0.53	-25.10	-10.19	3.29	18
O-0.2mM	-0.62	-0.66	-0.51	-0.11	-0.97	-0.53	-24.84	-9.29	2.74	18
O-0.2mM	-0.60	-0.66	-0.53	-0.13	-0.97	-0.52	-25.01	-9.87	2.38	18
O-0.2mM	-0.63	-0.66	-0.53	-0.20	-0.97	-0.52	-24.52	-10.44	2.12	18
O-0.5mM	-0.59	-0.66	-0.55	-0.18	-0.97	-0.53	-23.57	-10.80	3.05	19
O-0.5mM	-0.60	-0.66	-0.56	-0.10	-0.97	-0.53	-23.97	-11.21	2.61	19
O-0.5mM	-0.61	-0.64	-0.55	-0.11	-0.97	-0.53	-23.59	-9.68	2.40	19
O-0.5mM	-0.60	-0.64	-0.56	-0.15	-0.97	-0.54	-23.74	-9.81	3.12	19
O-0.5mM	-0.59	-0.66	-0.57	-0.17	-0.97	-0.53	-24.43	-10.94	3.24	19
O-0.5mM	-0.59	-0.65	-0.55	-0.17	-0.97	-0.54	-23.78	-10.07	3.60	19
O-1.0mM	-0.59	-0.63	-0.49	-0.15	-0.96	-0.51	-22.51	-5.87	2.44	21
O-1.0mM	-0.58	-0.64	-0.49	-0.14	-0.97	-0.53	-23.63	-6.77	3.72	21
O-1.0mM	-0.61	-0.63	-0.49	-0.15	-0.97	-0.51	-23.24	-6.61	1.65	21
O-1.0mM	-0.57	-0.63	-0.51	-0.17	-0.97	-0.54	-23.73	-6.50	4.15	21
O-1.0mM	-0.59	-0.65	-0.49	-0.18	-0.97	-0.53	-23.72	-7.12	3.91	21
O-1.0mM	-0.60	-0.64	-0.51	-0.20	-0.97	-0.53	-23.78	-7.82	3.20	21
O-2.0mM	-0.53	-0.57	-0.44	-0.25	-0.95	-0.52	-17.02	0.68	4.80	23
O-2.0mM	-0.54	-0.57	-0.47	-0.11	-0.95	-0.51	-17.92	-0.70	2.55	23
O-2.0mM	-0.53	-0.57	-0.43	-0.09	-0.95	-0.52	-17.43	0.55	4.09	23
O-2.0mM	-0.52	-0.57	-0.46	-0.11	-0.95	-0.51	-17.71	-0.63	3.79	23
O-2.0mM	-0.54	-0.57	-0.42	-0.11	-0.95	-0.53	-16.92	0.51	4.61	23
O-2.0mM	-0.54	-0.57	-0.44	-0.10	-0.95	-0.53	-17.89	-0.36	4.02	23

O-5.0mM	-0.49	-0.53	-0.43	-0.08	-0.95	-0.48	-16.78	4.85	2.17	24
O-5.0mM	-0.49	-0.54	-0.42	-0.09	-0.95	-0.46	-16.97	4.86	1.12	24
O-5.0mM	-0.51	-0.54	-0.43	-0.08	-0.95	-0.47	-16.79	3.42	1.43	24
O-5.0mM	-0.50	-0.54	-0.41	-0.06	-0.95	-0.48	-16.25	4.23	2.35	24
O-5.0mM	-0.52	-0.52	-0.46	-0.07	-0.95	-0.47	-15.27	3.68	-0.15	24
O-5.0mM	-0.49	-0.51	-0.45	-0.08	-0.95	-0.50	-14.88	4.82	2.40	24
O-8.0mM	-0.45	-0.48	-0.35	-0.08	-0.94	-0.42	-11.75	11.62	0.23	25
O-8.0mM	-0.45	-0.49	-0.36	-0.07	-0.94	-0.44	-12.35	10.86	1.27	25
O-8.0mM	-0.44	-0.48	-0.35	-0.06	-0.94	-0.44	-12.77	11.85	1.40	25
O-8.0mM	-0.45	-0.50	-0.36	-0.05	-0.95	-0.44	-14.76	10.60	1.15	25
O-8.0mM	-0.46	-0.47	-0.37	-0.08	-0.94	-0.46	-14.00	11.46	1.41	25
O-8.0mM	-0.45	-0.47	-0.37	-0.05	-0.94	-0.47	-12.72	11.03	2.08	25
O-10.0mM	-0.42	-0.44	-0.36	-0.01	-0.90	-0.38	0.04	12.76	-1.81	22
O-10.0mM	-0.42	-0.44	-0.33	-0.03	-0.91	-0.36	-2.83	14.47	-2.57	22
O-10.0mM	-0.46	-0.44	-0.36	-0.01	-0.91	-0.41	-3.18	11.92	-1.36	22
O-10.0mM	-0.47	-0.47	-0.35	-0.04	-0.90	-0.40	-0.56	9.97	-1.36	22
O-10.0mM	-0.45	-0.45	-0.36	-0.04	-0.90	-0.40	-0.15	11.50	-1.49	22
O-10.0mM	-0.42	-0.44	-0.35	-0.04	-0.90	-0.39	-0.09	12.94	-1.40	22

5.4 Determination of Binding Constants

All titrations were performed in pH7 buffered solution. The corresponding emission spectra are shown in the inset of the following figures. The molecular structure of the fluorophore, K_{SV}, and log K_{SV} is shown on the right. The fitting of quenching data was performed using the following modified Stern-Volmer equation.

$$I_q = I_0 + \frac{I_{final} - I_0}{2} \times \left\{1 + \frac{[Q]}{[F]} + \frac{1}{K_{SV}[F]} - \left[(1 + \frac{[Q]}{[F]} + \frac{1}{K_{SV}[F]})^2 - 4\frac{[Q]}{[F]}\right]^{1/2}\right\} \quad \textbf{(eq. 1)}$$

Here, I_0 = initial fluorescence intensity of the fluorophore, I_{final} = final fluorescence intensity of the fluorophore, I_q = fluorescence intensity at a given quencher concentration, $[F]$ = concentration of the fluorophore, $[Q]$ = total concentration of the added quencher Q and K_{SV} = Stern-Volmer constant.

5.4.1 Titration Experiments between PPE and Metal Salts (Chapter 3)

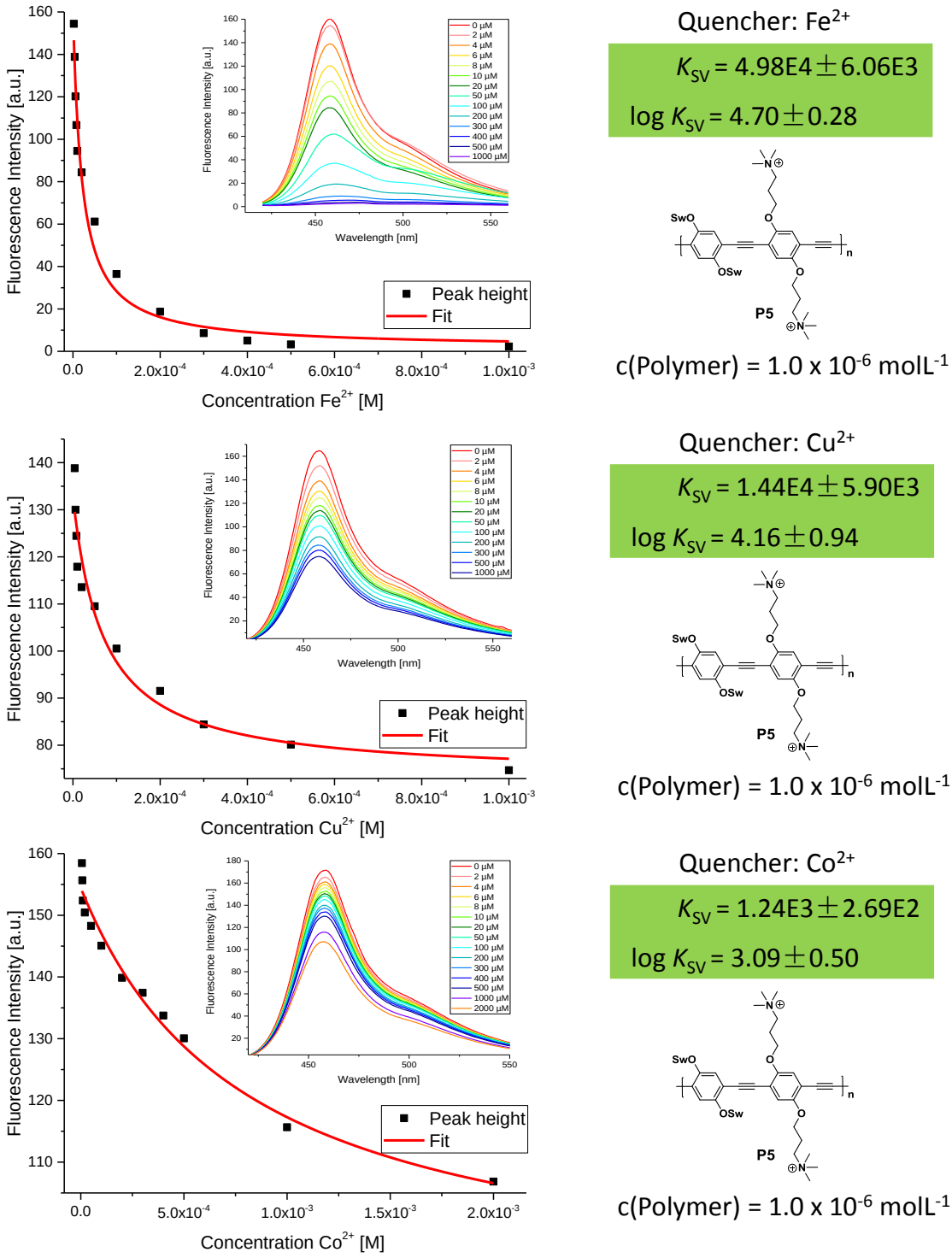

Figure 104. Volmer plots using a modified Stern-Volmer equation for fluorescence quenching of **P5** (1.0×10^{-6} M) with different metal salts. The inset shows the emission quenching data.

5.4.2 Titration Experiments between GFP and Metal Salts (Chapter 3)

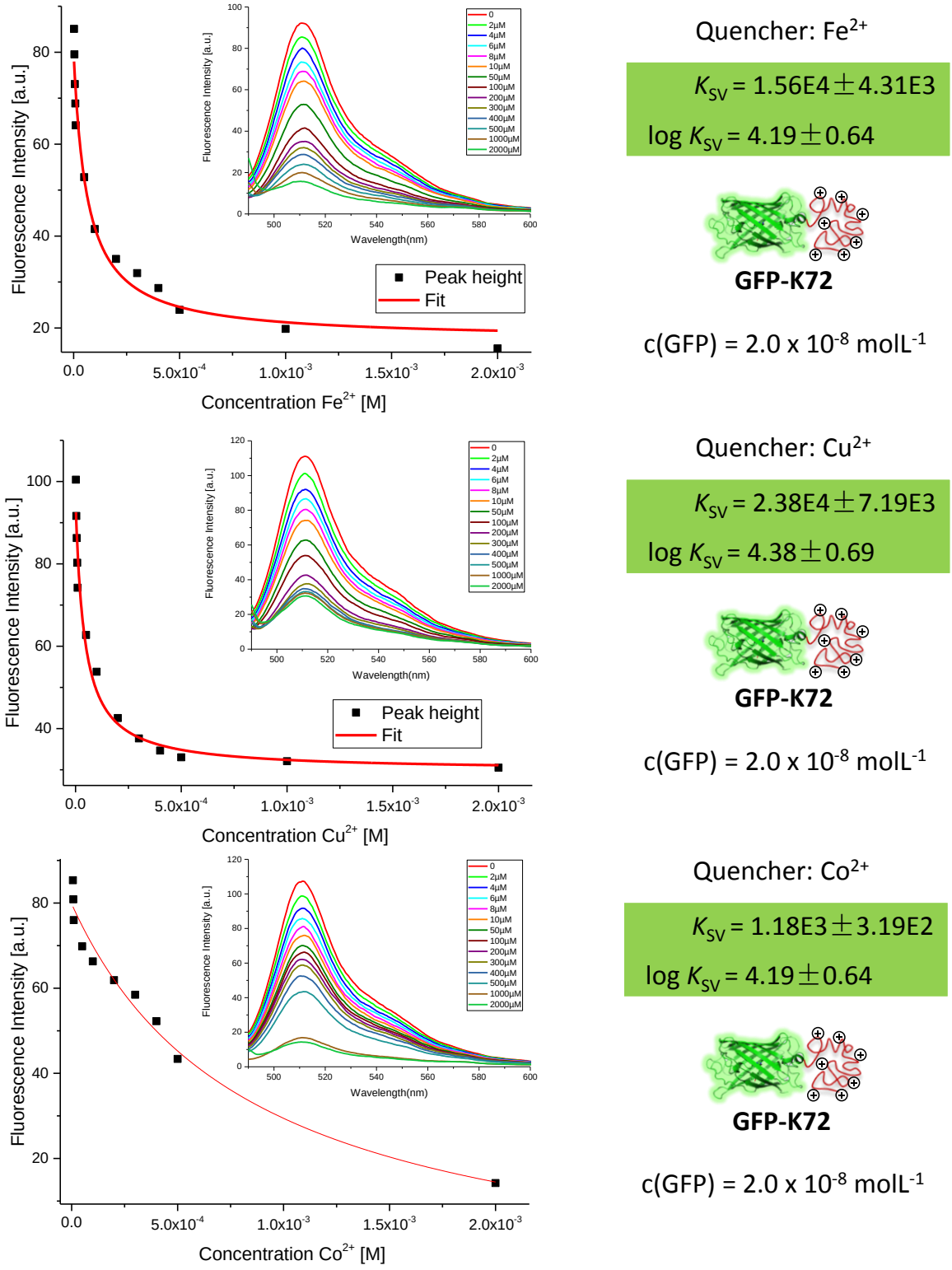

Figure 105. Volmer plots using a modified Stern-Volmer equation for fluorescence quenching of **GFP-K72** (2.0×10^{-8} M) with different metal salts. The inset shows the emission quenching data.

5.4.3 Titration Experiments between PPE and Cucurbit[8] Uril (Chapter 4)

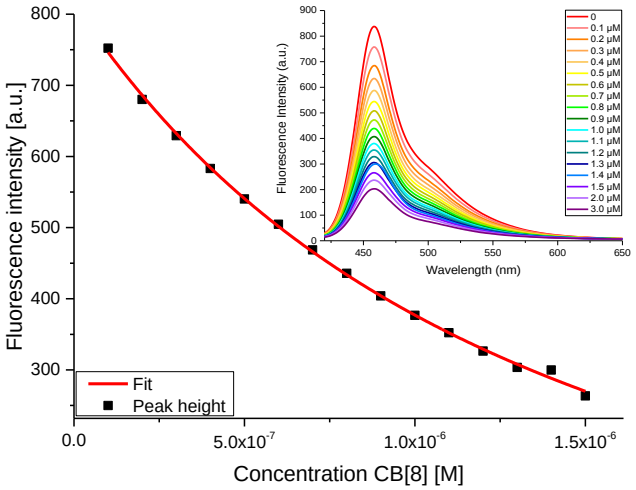

K_{SV} = 8.16E6 ± 6.56E4

log K_{SV} = 5.91 ± 1.09

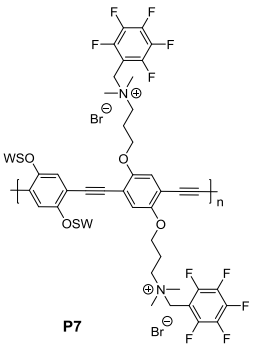

c(Polymer) = 2.0 x 10^{-7} molL^{-1}

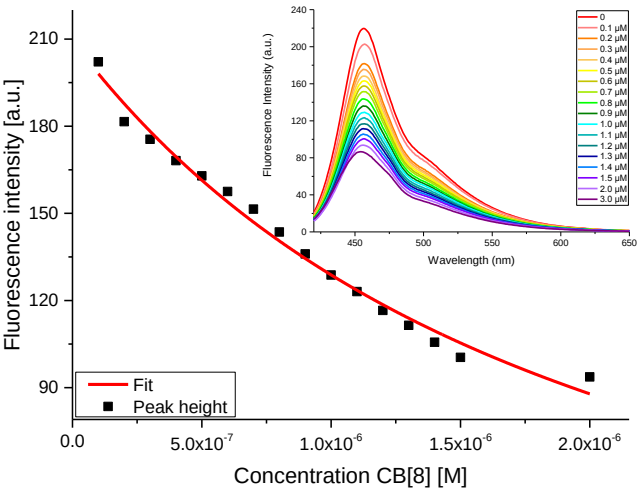

K_{SV} = 5.46E5 ± 1.47E5

log K_{SV} = 5.74 ± 0.62

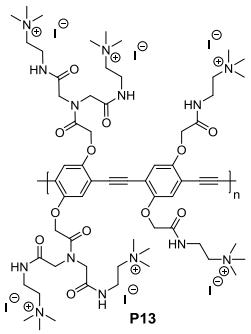

c(Polymer) = 2.0 x 10^{-7} molL^{-1}

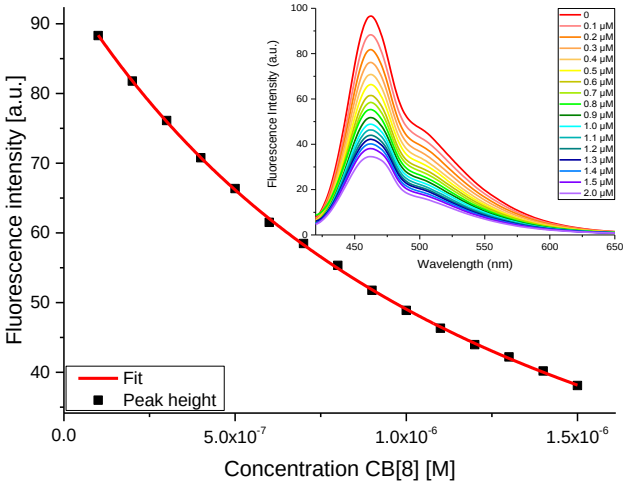

K_{SV} = 9.10E5 ± 3.24E4

log K_{SV} = 5.96 ± 0.08

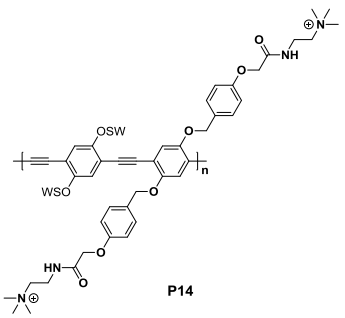

c(Polymer) = 2.0 x 10^{-7} molL^{-1}

Figure 106. Volmer plots using a modified Stern–Volmer equation for fluorescence quenching of **P7**, **P13** and **P14** (2.0×10^{-7} M) with CB[8]. The inset shows the emission quenching data.

References

[1] A. Alvarez, J. M. Costa-Fernández, R. Pereiro, A. Sanz-Medel and A. Salinas-Castillo, *TrAC, Trends Anal. Chem.* **2011**, *30*, 1513-1525.

[2] Y. Liu, K. Ogawa and K. S. Schanze, *J. Photochem. Photobiol., C* **2009**, *10*, 173-190.

[3] U. H. F. Bunz, *Macromol. Rapid Commun.* **2009**, *30*, 772-805.

[4] L. Feng, C. Zhu, H. Yuan, L. Liu, F. Lv and S. Wang, *Chem. Soc. Rev.* **2013**, *42*, 6620-6633.

[5] K. B. Becker, *Synthesis* **1983**, *1983*, 341-368.

[6] H. G. Gilch and W. L. Wheelwright, *J. Polym. Sci., Part A-1: Polym. Chem.* **1966**, *4*, 1337-1349.

[7] H. E. Katz, S. F. Bent, W. L. Wilson, M. L. Schilling and S. B. Ungashe, *J. Am. Chem. Soc.* **1994**, *116*, 6631-6635.

[8] N. Miyaura and A. Suzuki, *Chem. Rev.* **1995**, *95*, 2457-2483.

[9] U. H. F. Bunz, *Chem. Rev.* **2000**, *100*, 1605-1644.

[10] L. Kloppenburg, D. Song and U. H. F. Bunz, *J. Am. Chem. Soc.* **1998**, *120*, 7973-7974.

[11] U. H. F. Bunz, *Acc. Chem. Res.* **2001**, *34*, 998-1010.

[12] T. Dutta, K. B. Woody and M. D. Watson, *J. Am. Chem. Soc.* **2008**, *130*, 452-453.

[13] R. Chinchilla and C. Nájera, *Chem. Rev.* **2007**, *107*, 874-922.

[14] R. Giesa and R. C. Schulz, *Makromol. Chem.* **1990**, *191*, 857-867.

[15] U. H. F. Bunz, K. Seehafer, M. Bender and M. Porz, *Chem. Soc. Rev.* **2015**, *44*, 4322-4336.

[16] H. Jiang, P. Taranekar, J. R. Reynolds and K. S. Schanze, *Angew. Chem. Int. Ed.* **2009**, *48*, 4300-4316.

[17] J. Kim and T. M. Swager, *Nature* **2001**, *411*, 1030-1034.

[18] Q. Zhou and T. M. Swager, *J. Am. Chem. Soc.* **1995**, *117*, 7017-7018.

[19] Q. Zhou and T. M. Swager, *J. Am. Chem. Soc.* **1995**, *117*, 12593-12602.

[20] T. M. Swager, *Acc. Chem. Res.* **1998**, *31*, 201-207.

[21] L.-J. Fan, Y. Zhang, C. B. Murphy, S. E. Angell, M. F. L. Parker, B. R. Flynn and W. E. Jones, *Coord. Chem. Rev.* **2009**, *253*, 410-422.

[22] L. Buck and R. Axel, *Cell 65*, 175-187.

[23] J. R. Askim, M. Mahmoudi and K. S. Suslick, *Chem. Soc. Rev.* **2013**, *42*, 8649-8682.

[24] L. You, D. Zha and E. V. Anslyn, *Chem. Rev.* **2015**, *115*, 7840-7892.

[25] J. J. Lavigne and E. V. Anslyn, *Angew. Chem. Int. Ed.* **2001**, *40*, 3118-3130.

[26] E. V. Anslyn, *J. Org. Chem.* **2007**, *72*, 687-699.

[27] J. J. Lavigne and E. V. Anslyn, *Angew. Chem. Int. Ed.* **1999**, *38*, 3666-3669.

[28] S. L. Tobey and E. V. Anslyn, *J. Am. Chem. Soc.* **2003**, *125*, 14807-14815.

[29] Z. Zhong and E. V. Anslyn, *J. Am. Chem. Soc.* **2002**, *124*, 9014-9015.

[30] A. P. Umali, S. E. LeBoeuf, R. W. Newberry, S. Kim, L. Tran, W. A. Rome, T. Tian, D. Taing, J. Hong, M. Kwan, H. Heymann and E. V. Anslyn, *Chem. Sci.* **2011**, *2*, 439-445.

[31] X. Zhang, E. V. Anslyn and X. Qian, *Supramol. Chem.* **2012**, *24*, 520-525.

[32] N. A. Rakow and K. S. Suslick, *Nature* **2000**, *406*, 710-713.

[33] C. Zhang and K. S. Suslick, *J. Agric. Food Chem.* **2007**, *55*, 237-242.

[34] N. A. Rakow, A. Sen, M. C. Janzen, J. B. Ponder and K. S. Suslick, *Angew. Chem. Int. Ed.* **2005**, *44*, 4528-4532.

[35] M. C. Janzen, J. B. Ponder, D. P. Bailey, C. K. Ingison and K. S. Suslick, *Anal. Chem.* **2006**, *78*, 3591-3600.

[36] H. Lin, M. Jang and K. S. Suslick, *J. Am. Chem. Soc.* **2011**, *133*, 16786-16789.

[37] Z. Li and K. S. Suslick, *ACS Sens.* **2018**, *3*, 121-127.

[38] A. Bajaj, O. R. Miranda, I.-B. Kim, R. L. Phillips, D. J. Jerry, U. H. F. Bunz and V. M. Rotello, *Proc. Natl. Acad. Sci. U. S. A.* **2009**, *106*, 10912-10916.

[39] C.-C. You, O. R. Miranda, B. Gider, P. S. Ghosh, I.-B. Kim, B. Erdogan, S. A. Krovi, U. H. F. Bunz and V. M. Rotello, *Nat. Nanotechnol.* **2007**, *2*, 318-323.

[40] M. De, S. Rana, H. Akpinar, O. R. Miranda, R. R. Arvizo, U. H. F. Bunz and V. M. Rotello, *Nat. Chem.* **2009**, *1*, 461-465.

[41] S. Rana, S. G. Elci, R. Mout, A. K. Singla, M. Yazdani, M. Bender, A. Bajaj, K. Saha, U. H. F. Bunz, F. R. Jirik and V. M. Rotello, *J. Am. Chem. Soc.* **2016**, *138*, 4522-4529.

[42] D. F. Moyano, S. Rana, U. H. F. Bunz and V. M. Rotello, *Faraday Discuss.* **2011**, *152*, 33-42.

[43] R. L. Phillips, O. R. Miranda, C.-C. You, V. M. Rotello and U. H. F. Bunz, *Angew. Chem. Int. Ed.* **2008**, *47*, 2590-2594.

[44] R. L. Phillips, O. R. Miranda, D. E. Mortenson, C. Subramani, V. M. Rotello and U. H. F. Bunz, *Soft Matter* **2009**, *5*, 607-612.

[45] U. H. F. Bunz and V. M. Rotello, *Angew. Chem. Int. Ed.* **2010**, *49*, 3268-3279.

[46] J. Han, M. Bender, K. Seehafer and U. H. F. Bunz, *Angew. Chem. Int. Ed.* **2016**, *55*, 7689-7692.

[47] J. Han, H. Cheng, B. Wang, M. S. Braun, X. Fan, M. Bender, W. Huang, C. Domhan, W. Mier, T. Lindner, K. Seehafer, M. Wink and U. H. F. Bunz, *Angew. Chem. Int. Ed.* **2017**, *56*, 15246-15251.

[48] J. Han, M. Bender, S. Hahn, K. Seehafer and U. H. F. Bunz, *Chem. Eur. J.* **2016**, *22*, 3230-3233.

[49] B. Wang, J. Han, C. Ma, M. Bender, K. Seehafer, A. Herrmann and U. H. F. Bunz, *Chem. Eur. J.* **2017**, *23*, 12471-12474.

[50] C. G. Bangcuyo, M. E. Rampey-Vaughn, L. T. Quan, S. M. Angel, M. D. Smith and U. H. F. Bunz, *Macromolecules* **2002**, *35*, 1563-1568.

[51] S. Stewart, M. A. Ivy and E. V. Anslyn, *Chem. Soc. Rev.* **2014**, *43*, 70-84.

[52] P. C. Jurs, G. A. Bakken and H. E. McClelland, *Chem. Rev.* **2000**, *100*, 2649-2678.

[53] K. L. Diehl and E. V. Anslyn, *Chem. Soc. Rev.* **2013**, *42*, 8596-8611.

[54] K. L. Diehl, M. A. Ivy, S. Rabidoux, S. M. Petry, G. Müller and E. V. Anslyn, *Proc. Natl. Acad. Sci. U. S. A.* **2015**, *112*, 3977-3986.

[55] I.-B. Kim, A. Dunkhorst, J. Gilbert and U. H. F. Bunz, *Macromolecules* **2005**, *38*, 4560-4562.

[56] I.-B. Kim and U. H. F. Bunz, *J. Am. Chem. Soc.* **2006**, *128*, 2818-2819.

[57] Y. Wu, Y. Tan, J. Wu, S. Chen, Y. Z. Chen, X. Zhou, Y. Jiang and C. Tan, *ACS Appl. Mater. Interf.* **2015**, *7*, 6882-6888.

[58] H. Wang, F. He, R. Yan, X. Wang, X. Zhu and L. Li, *ACS Appl. Mater. Interf.* **2013**, *5*, 8254-8259.

[59] S. Hussain, A. H. Malik and P. K. Iyer, *ACS Appl. Mater. Interf.* **2015**, *7*, 3189-3198.

[60] Q. Zhao, Z. Zhang and Y. Tang, *Chem. Commun.* **2017**, *53*, 9414-9417.

[61] Y. Fu, J. Yao, W. Xu, T. Fan, Q. He, D. Zhu, H. Cao and J. Cheng, *Polym. Chem.* **2015**, *6*, 2179-2182.

[62] Y.-J. Zhao, K. Miao, Z. Zhu and L.-J. Fan, *ACS Sens.* **2017**, *2*, 842-847.

[63] C.-G. Qian, S. Zhu, P.-J. Feng, Y.-L. Chen, J.-C. Yu, X. Tang, Y. Liu and Q.-D. Shen, *ACS Appl. Mater. Interf.* **2015**, *7*, 18581-18589.

[64] X. Chen, Y. Zhou, X. Peng and J. Yoon, *Chem. Soc. Rev.* **2010**, *39*, 2120-2135.

[65] J. Li, C. Tian, Y. Yuan, Z. Yang, C. Yin, R. Jiang, W. Song, X. Li, X. Lu, L. Zhang, Q. Fan and W. Huang, *Macromolecules* **2015**, *48*, 1017-1025.

[66] N. Houstis, E. D. Rosen and E. S. Lander, *Nature* **2006**, *440*, 944-948.

[67] F. He, Y. Tang, M. Yu, S. Wang, Y. Li and D. Zhu, *Adv. Funct. Mater.* **2006**, *16*, 91-94.

[68] H.-A. Ho and M. Leclerc, *J. Am. Chem. Soc.* **2004**, *126*, 1384-1387.

[69] H. Bai, H. Yuan, C. Nie, B. Wang, F. Lv, L. Liu and S. Wang, *Angew. Chem. Int. Ed.* **2015**, *54*, 13208-13213.

[70] A. Duarte, A. Chworos, S. F. Flagan, G. Hanrahan and G. C. Bazan, *J. Am. Chem. Soc.* **2010**, *132*, 12562-12564.

[71] H. Yuan, Z. Liu, L. Liu, F. Lv, Y. Wang and S. Wang, *Adv. Mater.* **2014**, *26*, 4333-4338.

[72] C. J. Musto, S. H. Lim and K. S. Suslick, *Anal. Chem.* **2009**, *81*, 6526-6533.

[73] B. A. Suslick, L. Feng and K. S. Suslick, *Anal. Chem.* **2010**, *82*, 2067-2073.

[74] E. Ghanem, S. Afsah, P. N. Fallah, A. Lawrence, E. LeBovidge, S. Raghunathan, D. Rago, M. A. Ramirez, M. Telles, M. Winkler, B. Schumm, K. Makhnejia, D. Portillo, R. C. Vidal, A. Hall, D. Yeh, H. Judkins, A. A. da Silva, D. W. Franco and E. V. Anslyn, *ACS Sens.* **2017**, *2*, 641-647.

[75] E. Ghanem, H. Hopfer, A. Navarro, M. Ritzer, L. Mahmood, M. Fredell, A. Cubley, J. Bolen, R. Fattah, K. Teasdale, L. Lieu, T. Chua, F. Marini, H. Heymann and E. Anslyn, *Molecules* **2015**, *20*, 9170.

[76] J. Han, B. Wang, M. Bender, K. Seehafer and U. H. F. Bunz, *Analyst* **2017**, *142*, 537-543.

[77] B. Wang, J. Han, M. Bender, S. Hahn, K. Seehafer and U. H. F. Bunz, *ACS Sens.* **2018**, *3*, 504-511.

[78] N. M. Bojanowski, F. Hainer, M. Bender, K. Seehafer and U. H. F. Bunz, *Chem. Eur. J.* **2018**, *24*, 4255-4258.

[79] J. Han, C. Ma, B. Wang, M. Bender, M. Bojanowski, M. Hergert, K. Seehafer, A. Herrmann and U. H. F. Bunz, *Chem* **2017**, *2*, 817-824.

[80] B. Wang, J. Han, M. Bender, K. Seehafer and U. H. F. Bunz, *Macromolecules* **2017**, *50*, 4126-4131.

[81] X. Sun, Y. Wang and Y. Lei, *Chem. Soc. Rev.* **2015**, *44*, 8019-8061.

[82] J. M. Sylvia, J. A. Janni, J. D. Klein and K. M. Spencer, *Anal. Chem.* **2000**, *72*, 5834-5840.

[83] D. S. Moore, *Rev. Sci. Instrum.* **2004**, *75*, 2499-2512.

[84] J. S. Caygill, F. Davis and S. P. J. Higson, *Talanta* **2012**, *88*, 14-29.

[85] M. Krausa and K. Schorb, *J. Electroanal. Chem.* **1999**, *461*, 10-13.

[86] N. Pon Saravanan, S. Venugopalan, N. Senthilkumar, P. Santhosh, B. Kavita and H. Gurumallesh Prabu, *Talanta* **2006**, *69*, 656-662.

[87] R. D. Luggar, M. J. Farquharson, J. A. Horrocks and R. J. Lacey, *X-Ray Spectrom.* **1998**, *27*, 87-94.

[88] D. T. McQuade, A. E. Pullen and T. M. Swager, *Chem. Rev.* **2000**, *100*, 2537-2574.

[89] Z. Hu, B. J. Deibert and J. Li, *Chem. Soc. Rev.* **2014**, *43*, 5815-5840.

[90] Y. Salinas, R. Martinez-Manez, M. D. Marcos, F. Sancenon, A. M. Costero, M. Parra and S. Gil, *Chem. Soc. Rev.* **2012**, *41*, 1261-1296.

[91] S. b. Rochat and T. M. Swager, *ACS Appl. Mater. Interf.* **2013**, *5*, 4488-4502.

[92] L. Ding, Y. Bai, Y. Cao, G. Ren, G. J. Blanchard and Y. Fang, *Langmuir* **2014**, *30*, 7645-7653.

[93] S. W. Thomas, G. D. Joly and T. M. Swager, *Chem. Rev.* **2007**, *107*, 1339-1386.

[94] M. S. Meaney and V. L. McGuffin, *Anal. Chim. Acta* **2008**, *610*, 57-67.

[95] Y.-Z. Zhang, X. Xiang, P. Mei, J. Dai, L.-L. Zhang and Y. Liu, *Spectrochim. Acta, Part A* **2009**, *72*, 907-914.

[96] G. He, N. Yan, J. Yang, H. Wang, L. Ding, S. Yin and Y. Fang, *Macromolecules* **2011**, *44*, 4759-4766.

[97] A. Chowdhury and P. S. Mukherjee, *J. Org. Chem.* **2015**, *80*, 4064-4075.

[98] J.-S. Yang and T. M. Swager, *J. Am. Chem. Soc.* **1998**, *120*, 11864-11873.

[99] J. Wu, C. Tan, Z. Chen, Y. Z. Chen, Y. Tan and Y. Jiang, *Analyst* **2016**, *141*, 3242-3245.

[100] W. Huang, E. Smarsly, J. Han, M. Bender, K. Seehafer, I. Wacker, R. R. Schroeder and U. H. F. Bunz, *ACS Appl. Mater. Interf.* **2017**, *9*, 3068-3074.

[101] T. L. Andrew and T. M. Swager, *J. Am. Chem. Soc.* **2007**, *129*, 7254-7255.

[102] S.-W. Zhang and T. M. Swager, *J. Am. Chem. Soc.* **2003**, *125*, 3420-3421.

[103] G. Bunte, J. Hürttlen, H. Pontius, K. Hartlieb and H. Krause, *Anal. Chim. Acta* **2007**, *591*, 49-56.

[104] X. Wang, C. Drew, S.-H. Lee, K. J. Senecal, J. Kumar and L. A. Samuelson, *Nano Lett.* **2002**, *2*, 1273-1275.

[105] S. J. Toal and W. C. Trogler, *J. Mater. Chem.* **2006**, *16*, 2871-2883.

[106] H. Gan, Y. Li, H. Liu, S. Wang, C. Li, M. Yuan, X. Liu, C. Wang, L. Jiang and D. Zhu, *Biomacromolecules* **2007**, *8*, 1723-1729.

[107] A. Khan, S. Muller and S. Hecht, *Chem. Commun.* **2005**, 584-586.

[108] I.-B. Kim, R. Phillips and U. H. F. Bunz, *Macromolecules* **2007**, *40*, 5290-5293.

[109] U. H. F. Bunz, *Macromol. Rapid Commun.* **2009**, *30*, 772-805.

[110] J. H. Liao and T. M. Swager, *Langmuir* **2007**, *23*, 112-115.

[111] T. L. Andrew and T. M. Swager, *J. Polym. Sci., Part B: Polym. Phys.* **2011**, *49*, 476-498.

[112] J. Han, B. Wang, M. Bender, K. Seehafer and U. H. F. Bunz, *ACS Appl. Mater. Interf.* **2016**, *8*, 20415-20421.

[113] R. E. Ionescu, S. Cosnier and R. S. Marks, *Anal. Chem.* **2006**, *78*, 6327-6331.

[114] B. Li and Z. Zhang, *Sens. Actuators, B* **2000**, *69*, 70-74.

[115] M. Friedman, *J. Agric. Food Chem.* **1999**, *47*, 3457-3479.

[116] W. J. M. Underberg and J. C. M. Waterval, *Electrophoresis* **2002**, *23*, 3922-3933.

[117] M. M. Stone, A. H. Franz and C. B. Lebrilla, *J. Am. Soc. Mass Spectrom.* **2002**, *13*, 964-974.

[118] G. L. Luque, N. F. Ferreyra and G. A. Rivas, *Talanta* **2007**, *71*, 1282-1287.

[119] Y. Zhou and J. Yoon, *Chem. Soc. Rev.* **2012**, *41*, 52-67.

[120] J. Wang, H.-B. Liu, Z. Tong and C.-S. Ha, *Coord. Chem. Rev.* **2015**, *303*, 139-184.

[121] A. Buryak and K. Severin, *J. Am. Chem. Soc.* **2005**, *127*, 3700-3701.

[122] J. Freudenberg, F. Hinkel, D. Jänsch and U. H. F. Bunz, *Top. Curr. Chem.* **2017**, *375*, 67.

[123] V. Amendola, D. Esteban-Gómez, L. Fabbrizzi and M. Licchelli, *Acc. Chem. Res.* **2006**, *39*, 343-353.

[124] T. Gunnlaugsson, M. Glynn, G. M. Tocci, P. E. Kruger and F. M. Pfeffer, *Coord. Chem. Rev.* **2006**, *250*, 3094-3117.

[125] S.-H. Li, C.-W. Yu and J.-G. Xu, *Chem. Commun.* **2005**, 450-452.

[126] J. W. Steed, *Chem. Soc. Rev.* **2009**, *38*, 506-519.

[127] M. Qin, F. Li, Y. Huang, W. Ran, D. Han and Y. Song, *Anal. Chem.* **2015**, *87*, 837-842.

[128] L. A. Baumes, M. Buaki, J. Jolly, A. Corma and H. Garcia, *Tetrahedron Lett.* **2011**, *52*, 1418-1421.

[129] B. Aswathy and G. Sony, *J. Lumin.* **2014**, *154*, 541-548.

[130] F. Zhang, C. Lu, M. Wang, X. Yu, W. Wei and Z. Xia, *ACS Sens.* **2018**, *3*, 304-312.

[131] J. Wu, B. Kwon, W. Liu, E. V. Anslyn, P. Wang and J. S. Kim, *Chem. Rev.* **2015**, *115*, 7893-7943.

[132] A. Buryak and K. Severin, *J. Comb. Chem.* **2006**, *8*, 540-543.

[133] B. Lee, S. Chen, C. Heinis, R. Scopelliti and K. Severin, *Org. Lett.* **2013**, *15*, 3456-3459.

[134] F. Zaubitzer, A. Buryak and K. Severin, *Chem. Eur. J.* **2006**, *12*, 3928-3934.

[135] L. T. Gallagher, J. S. Heo, M. A. Lopez, B. M. Ray, J. Xiao, A. P. Umali, A. Zhang, S. Dharmarajan, H. Heymann and E. V. Anslyn, *Supramol. Chem.* **2012**, *24*, 143-148.

[136] J. Han, B. Wang, M. Bender, S. Kushida, K. Seehafer and U. H. F. Bunz, *ACS Appl. Mater. Interf.* **2017**, *9*, 790-797.

[137] J. Han, B. Wang, M. Bender, J. Pfisterer, W. Huang, K. Seehafer, M. Yazdani, V. M. Rotello, C. M. Rotello and U. H. F. Bunz, *Polym. Chem.* **2017**, *8*, 2723-2732.

[138] R. Martínez-Máñez and F. Sancenón, *Chem. Rev.* **2003**, *103*, 4419-4476.

[139] A. P. de Silva, H. Q. N. Gunaratne, T. Gunnlaugsson, A. J. M. Huxley, C. P. McCoy, J. T. Rademacher and T. E. Rice, *Chem. Rev.* **1997**, *97*, 1515-1566.

[140] D. H. Lee, S. Y. Kim and J.-I. Hong, *Angew. Chem. Int. Ed.* **2004**, *43*, 4777-4780.

[141] B. L. Rivas, E. D. Pereira, M. A. Mondaca, R. J. Rivas and M. A. Saavedra, *J. Appl. Polym. Sci.* **2003**, *87*, 452-457.

[142] B. L. Rivas, E. Pereira, C. Guzmán and A. Maureira, *Macromol. Symp.* **2011**, *304*, 46-54.

[143] G. J. d. A. A. Soler-Illia and C. Sanchez, *New J. Chem.* **2000**, *24*, 493-499.

[144] B. Branchi, P. Ceroni, G. Bergamini, V. Balzani, M. Maestri, J. v. Heyst, S. K. Lee, F. Luppertz and F. Vögtle, *Chem. Eur. J.* **2006**, *12*, 8926-8934.

[145] R. De Maesschalck, D. Jouan-Rimbaud and D. L. Massart, *Chemom. Intell. Lab. Syst.* **2000**, *50*, 1-18.

[146] H. L. Mark and D. Tunnell, *Anal. Chem.* **1985**, *57*, 1449-1456.

[147] D. Pesce, Y. Wu, A. Kolbe, T. Weil and A. Herrmann, *Biomaterials* **2013**, *34*, 4360-4367.

[148] P. Yao, P. Chen, L. Jiang, H. Zhao, H. Zhu, D. Zhou, W. Hu, B. H. Han and M. Liu, *Adv. Biomater.* **2010**, *22*, 5008-5012.

[149] K. Liu, D. Pesce, C. Ma, M. Tuchband, M. Shuai, D. Chen, J. Su, Q. Liu, J. Y. Gerasimov, A. Kolbe, W. Zajaczkowski, W. Pisula, K. Müllen, N. A. Clark and A. Herrmann, *Adv. Biomater.* **2015**, *27*, 2459-2465.

[150] R. K. Pathak, K. Tabbasum, A. Rai, D. Panda and C. P. Rao, *Anal. Chem.* **2012**, *84*, 5117-5123.

[151] G. He, N. Yan, H. Cui, T. Liu, L. Ding and Y. Fang, *Macromolecules* **2011**, *44*, 7096-7099.

[152] K. E. S. Dean, G. Klein, O. Renaudet and J.-L. Reymond, *Bioorg. Med. Chem. Lett.* **2003**, *13*, 1653-1656.

[153] B. Wang, J. Han, N. M. Bojanowski, M. Bender, C. Ma, K. Seehafer, A. Herrmann and U. H. F. Bunz, *ACS Sens.* **2018**.

[154] J. Lagona, P. Mukhopadhyay, S. Chakrabarti and L. Isaacs, *Angew. Chem. Int. Ed.* **2005**, *44*, 4844-4870.

[155] A. R. Urbach and V. Ramalingam, *Isr. J. Chem.* **2011**, *51*, 664-678.

[156] D. M. Bailey, A. Hennig, V. D. Uzunova and W. M. Nau, *Chem. Eur. J.* **2008**, *14*, 6069-6077.

[157] M. Shaikh, J. Mohanty, P. K. Singh, W. M. Nau and H. Pal, *Photochem. Photobiol. Sci.* **2008**, *7*, 408-414.

[158] K. Scholtbach, I. Venegas, C. Bohne and D. Fuentealba, *Photochem. Photobiol. Sci.* **2015**, *14*, 842-852.

[159] S. G. Elci, D. F. Moyano, S. Rana, G. Y. Tonga, R. L. Phillips, U. H. F. Bunz and V. M. Rotello, *Chem. Sci.* **2013**, *4*, 2076-2080.

[160] C.-C. You, O. R. Miranda, B. Gider, P. S. Ghosh, I.-B. Kim, B. Erdogan, S. A. Krovi, U. H. F. Bunz and V. M. Rotello, *Nat. Nanotechnol.* **2007**, *2*, 318-323.

[161] L. Wang, R. Xu, B. Hu, W. Li, Y. Sun, Y. Tu and X. Zeng, *Food Chem.* **2010**, *123*, 1259-1266.

[162] D. Huo, Y. Wu, M. Yang, H. Fa, X. Luo and C. Hou, *Food Chem.* **2014**, *145*, 639-645.

[163] A. K. Ghosh, C. Ghosh and A. Gupta, *J. Agric. Food Chem.* **2013**, *61*, 3814-3820.

[164] N. Hayashi, T. Ujihara, R. Chen, K. Irie and H. Ikezaki, *Food Res. Int.* **2013**, *53*, 816-821.

[165] J. Li, B. Fu, D. Huo, C. Hou, M. Yang, C. Shen, H. Luo and P. Yang, *Sens. Actuators, B* **2017**, *240*, 770-778.

[166] N. Ye, L. Zhang and X. Gu, *Food Anal. Methods* **2012**, *5*, 856-860.

[167] S. Baldermann, Z. Yang, T. Katsuno, V. A. Tu, N. Mase, Y. Nakamura and N. Watanabe, *Am. J. Anal. Chem.* **2014**, *5*, 620-632.

[168] Q. Chen, J. Zhao, C. H. Fang and D. Wang, *Spectrochim. Acta, Part A* **2007**, *66*, 568-574.

[169] Y. He, X. Li and X. Deng, *J. Food Eng.* **2007**, *79*, 1238-1242.

[170] L.-F. Wang, J.-Y. Lee, J.-O. Chung, J.-H. Baik, S. So and S.-K. Park, *Food Chem.* **2008**, *109*, 196-206.

[171] H. Yu and J. Wang, *Sens. Actuators, B* **2007**, *122*, 134-140.

[172] P. Ivarsson, S. Holmin, N.-E. Höjer, C. Krantz-Rülcker and F. Winquist, *Sens. Actuators, B* **2001**, *76*, 449-454.

[173] H. Yu, Y. Wang and J. Wang, *Sensors* **2009**, *9*, 8073-8082.

[174] C. Zhang, D. P. Bailey and K. S. Suslick, *J. Agric. Food Chem.* **2006**, *54*, 4925-4931.

[175] C. Hou, J. Li, D. Huo, X. Luo, J. Dong, M. Yang and X. Shi, *Sens. Actuators, B* **2012**, *161*, 244-250.

[176] H. Qin, D. Huo, L. Zhang, L. Yang, S. Zhang, M. Yang, C. Shen and C. Hou, *Food Res. Int.* **2012**, *45*, 45-51.

[177] B. A. Suslick, L. Feng and K. S. Suslick, *Anal. Chem.*, **2010**, *82*, 2067-2073.

[178] L. Liu, Y. Fan, H. Fu, F. Chen, C. Ni, J. Wang, Q. Yin, Q. Mu, T. Yang and Y. She, *Anal. Chim. Acta* **2017**, *963*, 119-128.

[179] O. R. Miranda, C.-C. You, R. Phillips, I.-B. Kim, P. S. Ghosh, U. H. F. Bunz and V. M. Rotello, *J. Am. Chem. Soc.* **2007**, *129*, 9856-9857.

[180] N. D. B. Le, G. Yesilbag Tonga, R. Mout, S.-T. Kim, M. E. Wille, S. Rana, K. A. Dunphy, D. J. Jerry, M. Yazdani, R. Ramanathan, C. M. Rotello and V. M. Rotello, *J. Am. Chem. Soc.* **2017**, *139*, 8008-8012.

[181] J. Liu, Y. Lan, Z. Yu, C. S. Y. Tan, R. M. Parker, C. Abell and O. A. Scherman, *Acc. Chem. Res.* **2017**, *50*, 208-217.

[182] P. J. De Vink, J. M. Briels, T. Schrader, L.-G. Milroy, L. Brunsveld and C. Ottmann, *Angew. Chem. Int. Ed.* **2017**, *56*, 8998-9002.

[183] G. Ghale and W. M. Nau, *Acc. Chem. Res.* **2014**, *47*, 2150-2159.

[184] E. Masson, X. Ling, R. Joseph, L. Kyeremeh-Mensah and X. Lu, *RSC Adv.* **2012**, *2*, 1213-1247.

[185] R. N. Dsouza, U. Pischel and W. M. Nau, *Chem. Rev.* **2011**, *111*, 7941-7980.

[186] S. J. Barrow, S. Kasera, M. J. Rowland, J. del Barrio and O. A. Scherman, *Chem. Rev.* **2015**, *115*, 12320-12406.

[187] G. H. Aryal, L. Huang and K. W. Hunter, *RSC Adv.* **2016**, *6*, 82566-82570.

[188] S. Gurbuz, M. Idris and D. Tuncel, *Org. Biomol. Chem.* **2015**, *13*, 330-347.

[189] Y.-T. Hung, P.-C. Chen, R. L. C. Chen and T.-J. Cheng, *Food Chem.* **2010**, *118*, 876-881.

[190] Y. Liang, J. Lu, L. Zhang, S. Wu and Y. Wu, *Food Chem.* **2003**, *80*, 283-290.

[191] F. Tan, C. Tan, A. Zhao and M. Li, *J. Agric. Food Chem.* **2011**, *59*, 10839-10847.

[192] R. Horanni and U. H. Engelhardt, *J. Food Compos. Anal.* **2013**, *31*, 94-100.

[193] H. Sereshti, M. Khosraviani, S. Samadi and M. S. Amini-Fazl, *RSC Adv.* **2014**, *4*, 47114-47120.

[194] A. Jończyk, M. Ludwikow and M. Mąkosza, *Angew. Chem. Int. Ed.* **1978**, *17*, 62-63.

[195] G. R. Fulmer, A. J. M. Miller, N. H. Sherden, H. E. Gottlieb, A. Nudelman, B. M. Stoltz, J. E. Bercaw and K. I. Goldberg, *Organometallics* **2010**, *29*, 2176-2179.

[196] P. C. DeRose, E. A. Early and G. W. Kramer, *Rev. Sci. Instrum.* **2007**, *78*, 033107.

[197] C. Würth, M. Grabolle, J. Pauli, M. Spieles and U. Resch-Genger, *Nat. Protoc.* **2013**, *8*, 1535-1550.

[198] C. S. Mizuno, A. G. Chittiboyina, F. H. Shah, A. Patny, T. W. Kurtz, H. A. Pershadsingh, R. C. Speth, V. T. Karamyan, P. B. Carvalho and M. A. Avery, *J. Med. Chem.* **2010**, *53*, 1076-1085.

[199] N. M. Bojanowski, M. Bender, K. Seehafer and U. H. F. Bunz, *Chem. Eur. J.* **2017**, *23*, 12253-12258.

[200] A. H. Berrie, G. T. Newbold and F. S. Spring, *J. Chem. Soc.* **1952**, 2042-2046.

Eidesstattliche Versicherung gemäß § 8 der Promotionsordnung der Naturwissenschaftlich-Mathematischen Gesamtfakultät der Universität Heidelberg

Bei der eingereichten Dissertation zu dem Thema

„Fingerprinting Chemical Analytes with Water-Soluble Conjugated Polymer-Based Fluorescent Sensor Arrays “

handelt es sich um meine eigenständig erbrachte Leistung.

Ich habe nur die angegebenen Quellen und Hilfsmittel benutzt und mich keiner unzulässigen Hilfe Dritter bedient. Insbesondere habe ich wörtlich oder sinngemäß aus anderen Werken übernommene Inhalte als solche kenntlich gemacht.

Die Arbeit oder Teile davon habe ich bislang nicht an einer Hochschule des In- oder Auslands als Bestandteil einer Prüfungs- oder Qualifikationsleistung vorgelegt.

Die Richtigkeit der vorstehenden Erklärung bestätige ich.

Die Bedeutung der eidesstaatlichen Versicherung und die strafrechtlichen Folgen einer unrichtigen oder unvollständigen eidesstattlichen Versicherung sind mir bekannt.

Ich versichere an Eides statt, dass ich nach bestem Wissen die reine Wahrheit erklärt und nichts verschwiegen habe.

_____ _____

Ort und Datum Unterschrift